CRANFIELD UNIVERSITY

Anayo Isaac Ogazi

Multiphase Severe Slug Flow Control

School of Engineering
Process Systems Group

PhD Thesis

CRANFIELD UNIVERSITY
School of Engineering, Department of Offshore, Process and Energy Engineering
Process Systems Group

PhD Thesis

Anayo Isaac Ogazi

Multiphase Severe Slug Flow Control

Dr. Yi Cao
Supervisor

January, 2011

This thesis is submitted in fulfilment of the requirements for the degree of Doctor of Philosophy

This thesis is dedicated to the memory of my mother Mrs Maria Ogazi, whose love and sacrifices laid the foundation for these achievements.

Abstract

Severe slug flow is one of the most undesired multiphase flow regimes, due to the associated instability, which imposes major challenges to flow assurance in the oil and gas industry. This thesis presents a comprehensive analysis of the systematic approach to achieving stability and maximum production from an unstable riser-pipeline system. The development of a plant-wide model which comprises an improved simplified riser model (ISRM) required for severe slug controller design and control performance analysis is achieved. The ability of the ISRM to predict nonlinear stability of the unstable riser-pipeline is investigated using an industrial riser and a 4 inch laboratory riser system. Its prediction of the nonlinear stability showed close agreement with experimental and simulation results.

Through controllability analysis of the unstable riser-pipeline system, which is focused on achieving the core operational targets of the riser-pipeline production system, the maximum stable valve opening achievable with each controlled variable considered is predicted and confirmed through the simulation results. The potential to increase oil production through feedback control is presented by analysing the pressure production relationship using a pressure dependent dimensionless variable known as Production Gain Index (PGI).

The performance analyses of three active slug controllers are presented to show that the ability of a slug controller to achieve closed loop stability at large valve opening can be assessed by the analysis of the H_∞ norm of the complementary sensitivity function of the closed loop system, $\|T(s)\|_\infty$. A slug con-

troller which achieves the lowest value of the $\|T(s)\|_\infty$, will achieve closed loop stability at a larger valve opening. Finally, the development of a new improved relay auto-tuned slug controller algorithm based on a perturbed first-order-plus dead-time (FOPDT) model of the riser system is achieved. Its performance showed that it has the ability to stabilise the riser system at a valve opening that is larger than that achieved with the original (conventional) algorithm with about 4% increase in production.

Acknowledgements

It is with great pleasure and thanks to the Almighty God that I write this section to acknowledge many individuals and organisations who have sown their golden treasures, talent and time into me and into this work to make it a success.

Firstly, without any iota of reservation, I am saying a very loud thank you to my able and understanding supervisor, Dr. Yi Cao, whose guidance and encouragement was pivotal to the success of this work. His style of leading the way and at the same time allowing you to lead, made a lot of difference in building my research skills and completing this work. I will not fail to also thank the head of the Process Systems Engineering Group, Prof. Hoi Yeung, whose wealth of experience advice meant a lot to the success of this work. Thank you Prof. Hoi. The entire Process Systems Engineering Group team has been exceptionally fantastic. The likes of Sam Skears (the administrator) whose support and advice was always there will always be appreciated by me. I will not forget to thank the Multiphase flow laboratory technicians, David and Clerve for their support during my experiment periods in the laboratory.

It is important to stress that this work has been undertaken within the Joint Project on Transient Multiphase Flows and Flow Assurance. I wish to acknowledge the contributions made to this project by the UK Engineering and Physical Sciences Research Council (EPSRC) and the following: - Advantica; BP Exploration; CD-adapco; Chevron; ConocoPhillips; ENI; ExxonMobil; FEESA; IFP; Institutt for Energiteknikk; PDVSA (INTEVEP); Petrobras; PETRONAS; Scand-

power PT; Shell; SINTEF; StatoilHydro and TOTAL. I wish to express my sincere gratitude for this support. I also wish to thank SPT Group Ltd for the use of OLGA during this work and for providing an OLGA model of a tie-back system for use in testing the slug control algorithm. OLGA is a registered trademark of SPT Group.

I will like to thank my friends and colleagues in Cranfield University, including Dr. Ogaji Stephen, Dr. Gareth Davis, Tesi Arubi, Ade Lawal, Daniel Kamunge, Patricia Odiowei, Edith Ejikeme and Lanchang. Special thanks to my brother and friend Crispin Alison for his soul motivation and encouragement especially when the going gets though. Thank you all.

With heart full of thanks, I wish to say to the entire Holding Forth the Word Ministry including the Cranfield Pentecostal Assembly that you have given me what money cannot buy, the eternal peace and family to succeed. The heart of love of Pastor Biyi Ajala will always be in my memory.

My entire family has always been there for me in full measure. The love and sacrifice of my wife, Mrs Tina Nkiruka Ogazi and my little daughter Miss Bithiah Chimnechem Ogazi will always be appreciated. The support and prayers of my brother Elder Emeka Ogazi and his family and special cousin Mrs Ede Nwali Elizabeth and her family will always be in my heart. Obviously, words and space may have failed me in expressing my deep held appreciation to many who should be on this page, but in my heart, that which words cannot say is written. Thank you.

Contents

List of Figures

Notation

Table 1: Notation

Symbols	Descriptions	Units
D	Dead time	s
D_u	Maximum allowed input deviation	$\%$
G	Linear riser model	
G_p	Perturbed linear riser model	
J_W	Total well production	kg/day
J_p	Pressure dependent production	kg/s
P_{RB}	Riser base pressure	barg
P_{WHc}	Riser base pressure at unstable equilibrium	barg
P_{RBe}	Riser base pressure at steady state	barg
P_{RBmax}	Maximum riser base pressure	barg
P_{RBmin}	Minimum riser base pressure	barg
P_{RT}	Riser top pressure	barg
P_{res}	Reservoir pressure	barg
P_s	Separator top pressure	barg
P_{WH}	Well head pressure	barg

Table 2: Notation

Symbols	Descriptions	Units
P_{WHe}	Well head pressure at steady state	barg
P_{WHc}	Well head pressure at unstable equilibrium	barg
$\bar{P}_{WH}$	Average pressure over time	barg
Q_{Gouts}	Separator gas volume outlet flow rate	m^3/s
Q_T	Riser top total volumetric flow rate	m3/s
u	Riser top valve position	$\%$
u_g	Separator gas valve position	$\%$
u_c	Riser top valve position at unstable equilibrium	$\%$
u_e	Riser top valve position at steady state	
u_{ge}	Separator gas valve position at steady state	$\%$
u_{min}	Minimum valve opening	$\%$
u_{max}	Maximum valve opening	$\%$
u_r	Reference valve opening	$\%$
S	Sensitivity function	
T	Complementary sensitivity function	
τ	Process time constant	
q_w	Well production rate	kg/s
τ_f	Filter time constant	
ξ	Production Gain Index	

Table 3: Notation - ISRM model

Symbol	Description	Unit
A_s	Separator cross sectional area	m^2
A	Internal gas mass flow area	m^2
A_p	Pipe cross sectional area	m^2
g	Gravity	m/s^2
H_R	Riser height	m
H_s	Separator height	m
H_1	Critical liquid height	m
h_1	Liquid level upstream the riser inlet	m
h_L	Separator liquid height	m
K_1	Valve coefficient	
K_2	Internal gas flow coefficient	
K_3	Entrainment tuning parameter	
L_h	Length of horizontal riser section	m
m_{G1}	Mass of gas in pipeline	kg
m_{G2}	Mass of gas in the riser top	kg
m_L	Mass of liquid in the riser	kg
m_{Lins}	Separator liquid inlet mass flow rate	kg/s
m_{Louts}	Separator liquid outlet mass flow rate	kg/s
m_{mix}	Total fluid mass flow rate at riser top	kg/s
M_G	Molecular weight of gas	kg/K.mol
m_{Gin}	Mass flow rate of gas into the system	kg/s
m_{Lin}	Mass flow rate of liquid into the system	kg/s
m_{Lout}	Mass flow rate of liquid out the riser	kg/s

Table 4: Notation - ISRM model

Symbol	Description	Unit
m_{Gout}	Mass flow rate of gas out the riser	kg/s
m_G	Internal gas mass flow rate	kg/s
P_s	Separator top pressure	barg
P_{RB}	Riser base pressure	barg
P_{RT}	Riser top pressure	barg
Q_{Gins}	Separator gas volume inlet flow rate	m^3/s
Q_{Gouts}	Separator gas volume outlet flow rate	m^3/s
Q_T	Total volumetric flowrate out of the riser	m^3/s
R	Gas constant	J/K/mol
T	System temperature	K
v_{G1}	Internal gas velocity	m/s
V_{G1}	Volume of gas in the pipeline	m^3
V_T	Total riser volume	m^3
α_{LT}	liquid volume fraction at the riser top	
α_G	Gas volume fraction in the pipeline	
α_L^m	Liquid mass fraction	
ρ_{G1}	Pipeline gas density	kg/m^3
ρ_{G2}	Riser top gas density	kg/m^3
ρ_L	Liquid density	kg/m^3
ρ_T	Total fluid density at riser top	kg/m^3
u	Riser top valve position	$\%$

Chapter 1

Introduction

1.1 Background and motivation

In the oil and gas production system, the ability to achieve continuous, safe, economic and uninterrupted flow of oil and gas from the oil reservoir to the point of sale is known as flow assurance. About 35% of the world energy supply is from oil and gas. Recently, the rate of discovery of commercially viable oil fields has been in serious decline, leading to increasing number of deep offshore interests. The reservoir pressure in existing oil fields are known to decline over time, making self lifting of oil to the topside difficult. In the North Sea oil fields for example, production from existing oil fields have seen a decline of about 11% since 1998 [84]. Despite these challenges, efforts are constantly being made to ensure maximum oil recovery. In the drive to recover oil from the reservoirs that are uneconomical to stand alone, production pipelines from different oil fields could be tied in to one existing production platform, sometimes resulting to long distant network of pipelines. Thus, the multiphase fluid has to be transported through long distant horizontal pipelines and high risers, under varying pressure, temperature and fluid composition condition.

With the complex nature of multiphase flow, these conditions can often generate some physical multiphase flow phenomena such as slug flow. Also, physical-chemical phenomena such as wax deposition, emulsion, corrosion, hydrates formation and sand deposition can be initiated in the pipeline. These phenomena have the potential to obstruct the flow of oil and gas in the pipeline.

A competent flow assurance technology should be able to cover the whole range of adequate understanding and knowledge, design tools as well as the professional skills required to manage any form of these flow assurance problems. With the vast amount of work already put into developing these capabilities, there are still wide gaps in the knowledge required to solve these whole range of flow assurance problems.

The motivation for this research is to contribute to the adequate understanding of the fundamental principles for eliminating a form of the slug flow, known as severe slugging and at the same time maximise oil production. Severe slugging is the most undesired flow regime in multiphase flow in the oil and gas industry. It is characterised by intermittent flow of liquid and gas surges, which impose significant challenges to the reservoir structure, the topside processing efficiency and pipeline integrity.

1.1.1 The riser-pipeline system

The riser is a flow pipeline commonly applied in the oil and gas industry to connect the horizontal upstream subsea pipes with the topside (downstream) facilities. The primary function of the riser is to transport produced well fluid (water, oil and gas) to the topside facilities for processing. Consequently, the riser is positioned to connect the subsea pipelines at the sea bed to the topside

facilities. The riser height can vary from a few hundred metres to more than 2000 metres, depending on the sea bed depth from the topside. Also the riser diameter can vary depending on the design it can also be designed into different shapes, like the S-shaped riser.

1.1.2 Severe slugging phenomenon

Severe slugging phenomenon is a four stage cyclic flow condition occurring in the order as shown in Figure 1.1. One major condition for the occurrence of severe slugging is the presence of dips and low points in the pipeline. This causes liquid to accumulate at these dips, due to balance of pressure by opposing gravitational force. Thus, the liquid blocks the flowline (step 1). With the flowline blocked, gas flow into the riser is stopped and further inlet gas is compressed in the pipeline resulting in pipeline pressure build up, with a continuous liquid building up in the riser. This will continue until the pressure drop across the riser overcomes the gravitational hydrostatic head in the riser; pushing the liquid slug out of the riser (step 2). This will result in a pressure drop in the pipeline which allows the gas to expand, penetrate the liquid and increase the flow velocity. With the gas tail entering the riser, the liquid is blown out with a drop both in velocity and pressure (step 3). This causes the liquid to fall back and block the riser base again (step 4). Detailed description of this phenomenon can be found in the literature, e.g. [103]

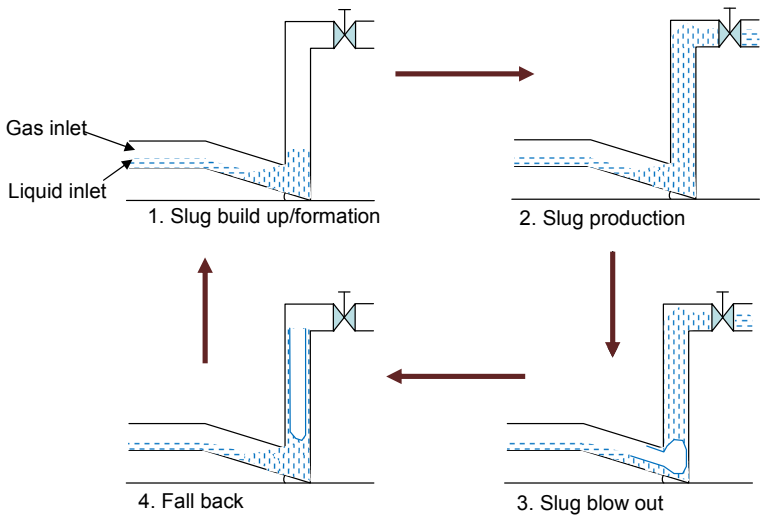

Figure 1.1: Severe slug cycle phenomenon illustrated

1.1.2.1 Typical severe slug profile

A typical severe slug flow differs from an oscillating slug flow condition. It is necessary to specify a common characteristic of the severe slug profile, which can be easily identified. A typical severe slug flow condition can be easily identified using one major characteristic of the pressure profile. This is the differential pressure (DP) across the riser during severe slugging. During the slug production stage as shown in Figure 1.1, the entire riser column is completely filled with liquid, such that the liquid volume fraction (α_L) is equal to 1. This is the prevalent condition before the gas tail penetrates the riser, as shown in stage 2 and 3 of Figure 1.1. Thus, the maximum pressure difference across the riser at this condition will be equal to the gravitational pressure head (P_h), which will be calculated using (1.1), when $\alpha_L = 1$.

$$P_h = \alpha_L \rho_L g H_R \tag{1.1}$$

In (1.1), ρ_L is the liquid density, H_R is the riser height and g is the gravitational acceleration. If the $\alpha_L < 1$ in all stages of the slug cycle, then the condition in which the riser is completely filled with liquid does not occur and the system is not under severe slug flow. Under water-air two phase flow, a typical severe slug flow obtained experimentally from a 4 inch and about 10.5m height riser-pipeline system, which is located in the Cranfield University multiphase flow laboratory (see Chapter 3), has the pressure profile shown in Figure 1.2. The approximate value of P_h when $\alpha_L = 1$ (i.e riser is filled with liquid) is 1.08 barg. This is the maximum pressure difference across the riser as shown in Figure 1.2.

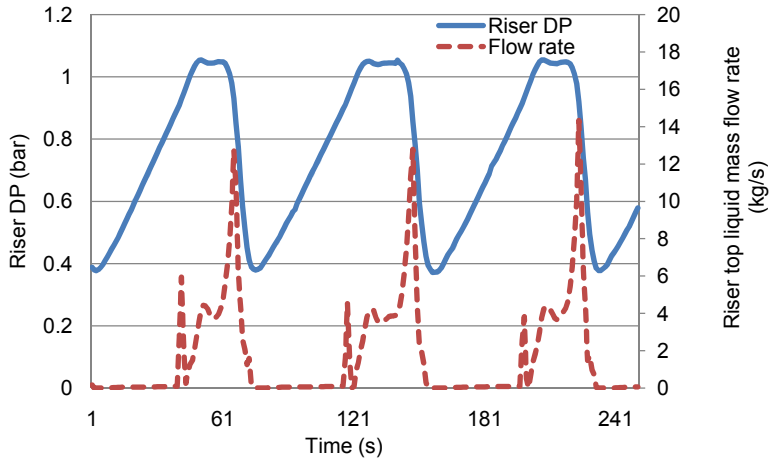

Figure 1.2: Typical severe slug flow profile

A slugging (oscillating) condition in the same system, will have the pressure and flow profile shown in Figure 1.3. The maximum differential pressure across the riser in this case is less than 1.08 barg. This implies that $\alpha_L < 1$ in all stages of the slug cycle, and the condition in which the riser is filled with liquid (production stage) does not occur. Thus, this system can be described to be slugging, but not severe slugging.

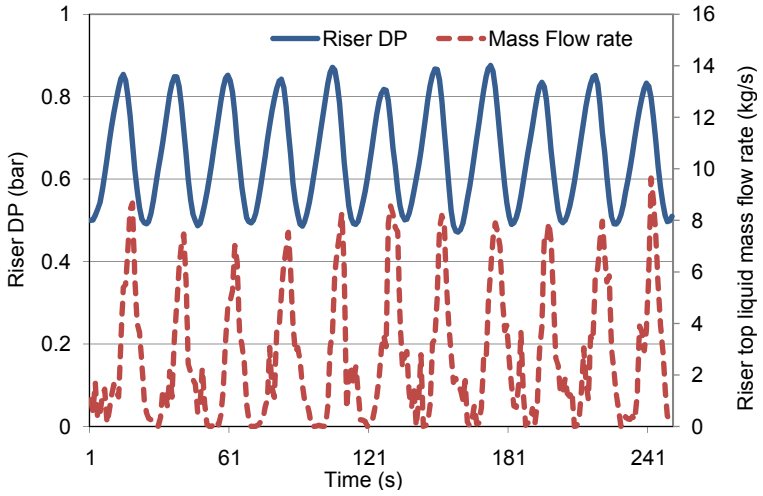

Figure 1.3: Oscillatory slug flow profile

1.2 Project aim and objectives

The aim of this project is to gain fundamental understanding of severe slug control in a plant-wide scale.

The main objectives of this project are to:

1. develop a simplified plant-wide model of the riser-pipeline system for predicting severe slugging and estimating control performance
2. perform controllability analysis of the unstable riser-pipeline system
3. develop a systematic approach to severe slug controller design and implementation in a plant-wide scale
4. develop a systematic approach to production potential analysis of severe slugging control system

5. carry out laboratory demonstrations of severe slug control using designed controllers

1.3 Methodology

In this section, the methodologies applied in this research project are explained. The project adopts model based and experimental analysis methodology. As a result, the methodology involves four major areas which includes: modeling, simulation, experimentation and validation.

Modeling

The accurate prediction of severe slugging characteristics and control performance are key requirements for this project. As a result, the modeling of the riser induced severe slugging is performed using mechanistic modeling of the riser-pipeline system in a plant-wide scale. Using a basic simplified riser model (SRM) which had been developed by Storkaas [102], an improved simplified riser model(ISRM) is developed, with improved performance and more reliable results achieved, when compared to experimental results. The ISRM is programmed in the Matlab/Simulink software. The 2 inch, 4 inch and the industrial riser-pipeline systems used in the project are all modeled using the ISRM. These systems are described in Chapter 3. It should be mentioned here that in order to simulate the real field behaviour of these systems, a linear well model and a two phase separator model have also been developed and linked with the ISRM.

Simulation

Software simulations are carried out using the commercial multiphase flow simulator, OLGA, which is developed by the SPT Group [37]. Two riser-pipeline systems are modeled in the OLGA software. These two riser systems include, an industrial riser-pipeline system and the 4 inch riser-pipeline system which is used in the experimental studies. The industrial riser-pipeline system is a standard system which was provided by the SPT Group. The configuration and operating conditions of the industrial riser system is described in section 3.5.

Experiment

In this project, experimental studies have been carried out on two riser-pipeline systems. The two riser-pipeline systems are the 2 inch and the 4 inch riser-pipeline systems, which are flow loops in the multiphase flow laboratory at Cranfield University. The configuration and operating conditions of these systems are described in Chapter 3.

Analyses and validation

Various analyses are performed for understanding of the system and validation. These analyses include, severe slug characteristics, controllability, controller design, control performance, control impact and production analysis.

1.4 Thesis outline and contributions

The work presented in this thesis is outlined according to the chapters as follows:

Chapter 2

In this chapter, a review of multiphase slug flow and the current severe slugging control technologies and their applications is presented. Firstly, a general overview of multiphase flow and slug flow is presented. This is followed by detailed discussions of the underlying principles of operation of severe slugging control technologies. Their limitations and challenges are also discussed.

Chapter 3

In this chapter, the description of the experimental facility and the industrial riser system used in this work is presented. The description of the relevant operating conditions and the pipeline dimensions are also presented.

Chapter 4

In this chapter, the modeling of the major system units of the riser-pipeline system to develop the plant-wide model, which is required for severe slug flow prediction and control performance analysis is presented. The modeling of the riser-pipeline system and its integration with the model of the two phase separator system and the pressure dependent well model is achieved. Through the development of the plant-wide model, an improved simplified riser model (ISRM) is developed to eliminate some assumptions and limitations of an original simplified riser model (SRM) in predicting severe slugging. The ability of the ISRM to predict nonlinear stability of the system is investigated using the indus-

trial riser system and a 4 inch laboratory riser system. The ISRM prediction of these nonlinear stabilities showed close agreement with experimental results, than the SRM.

Chapter 5

In this chapter, the controllability analysis of the unstable riser-pipeline system which is focused on the ability to achieve stable operation and maximise production is presented. A more appropriate slug control strategy is implemented to show that some controlled variables which had been considered unsuitable for slug control can in practice be used to stabilise the unstable riser-pipeline system. In this control strategy, the perfect tracking of controlled variable set point ideology is neglected and the unstable riser system is stabilised at a reference valve opening using a derivative controller, whose control input is the controlled variable. The lower bound of the control input magnitude required to stabilise the system at the open-loop unstable operating points is evaluated as a function of the Hankel singular value of the system's linear model transfer function. This controllability analysis reveals the ability of various controlled variable to stabilise the unstable riser-pipeline system at relatively large valve opening.

Chapter 6

In this chapter, a new concept known as the production gain index (PGI) analysis, which is used for the systematic analysis of the potential of the slug control system to maximise production in an unstable riser-pipeline system is presented. This systematic method, which is based on the pressure bifurcation map of a riser system is applied to analyse the production and pressure loss relationship at the different operating points. This analysis has been successfully applied to an industrial riser system, which was modeled in the commer-

cial multiphase flow simulator, OLGA. The prediction of production gain or loss using the PGI agrees with actual simulated production. This result is very significant in planning and implementing suitable control strategy for stabilising unstable riser-pipeline production systems with the aim of achieving stability and ensuring increased productivity, especially for brown fields.

Chapter 7

In this chapter, the design, characterisation, implementation and the performance analysis of three active slug controllers for maximising oil production is presented. The three active slug controllers namely: the relay auto-tuned controller, the robust PID controller and the H_∞ robust controller are designed, characterised and implemented under the same operating condition for two controlled variables; P_{RB} and Q_T. A principle for characterising the ability of a slug controller to achieve closed-loop stability at large valve opening in the open-loop unstable operating point, using the $\|T\|_\infty$ is presented. It is shown that the H_∞ robust slug controller which achieved the lowest value of the $\|T\|_\infty$, achieved closed-loop stability at a larger valve opening than the relay auto-tuned slug controller, which achieved the highest value of the $\|T\|_\infty$.

Chapter 8

In this chapter, the development of an improved relay auto-tuned slug controller algorithm is achieved to improve the poor performance of the relay auto-tuned slug controller in Chapter 6. The developed controller algorithm is based on a perturbed FOPDT model of the riser system, obtained through relay shape factor analysis. The developed controller algorithm is implemented on the industrial riser system to show that it has the ability to stabilise the unstable riser system at a valve opening that is larger than that achieved with the original (conventional) design algorithm with about 4% increase in production.

Chapter 9

The conclusion and summary of the work and results presented in the thesis are presented in this chapter.

1.5 Publications

The following publications have resulted from this work.

1.5.1 Conference papers

Chapter 3 and 6

Ogazi, A. I., Ogunkolade, S., Cao, Y., Lao, L., and Yeung, H. Severe slugging control through open-loop unstable PID tuning to increase oil production. In 14th International Conference on Multiphase Technology (Cannes, France, June 2009), BHR Group, pp. 17-32.

Chapter 6

Ogazi, A.I., Cao, Y., Yeung, H., and Lao, L. . Slug control with large valve opening to maximise oil production. In SPE Offshore Europe Conference, SPE 124883,(2009)

Ogazi, A.I., Cao, Y., Yeung, H., and Lao, L. Robust Control of severe slugging to maximise oil production. In International Conference on System Engineering, 2009 Conference, (Conventry, UK, 2009).

Chapter 5

Ogazi, A.I., Cao, Y., Yeung, H., and Lao, L. Production potential of a severe slugging control system. IFAC World Congress (Milan Italy, September, 2011) (to be presented).

1.5.2 Journal paper

Chapter 6

Ogazi, A.I., Cao, Y., Yeung, H., and Lao, L. . Slug control with large valve opening to maximise oil production. SPE Journal, SPE 124883,(2010), 15(3), 812-821.

Chapter 2

Literature review

2.1 Introduction

In this Chapter, the review of the relevant literatures on severe slugging control is presented. Firstly, a general overview of multiphase flow is presented with the relevant literatures. This is followed by a review of the flow regime maps, and then slug flow. A review of the current severe slugging control technologies and their applications is then presented. This begins with classification of pipeline slugging and detailed description of the slug control techniques and the underlying technology is then provided. The hierarchal structure for the literature review is laid out in Figure 2.1 for clarity.

2.2 Multiphase flow

As the name implies, a flow is said to be a multiphase flow when it contains more than one fluid phase, which are flowing simultaneously in the same conduit or an enclosure, such as a pipe [16, 13]. A multiphase flow containing any

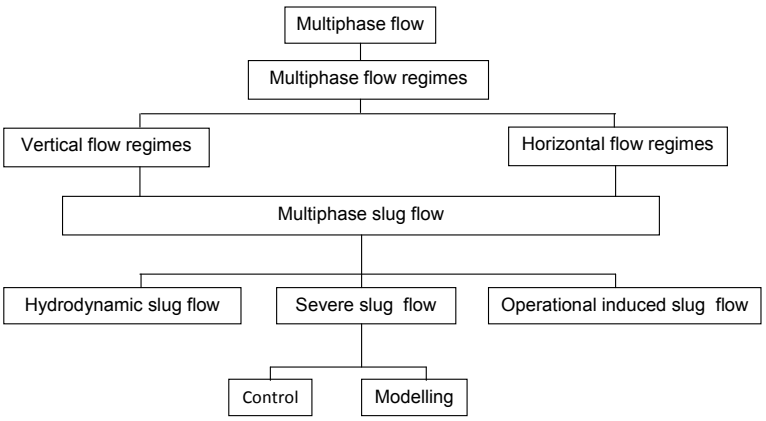

Figure 2.1: Diagram showing hierarchy of literature review structure

three components is referred to as three-phase flow, while a flow containing only two components is referred to as two-phase flow. In the oil gas industry, three major fluid components namely: oil, water and gas are the focus of the multiphase flow concept. However, other possible components such as sand and dissolved salt which come from the oil reservoir can become part of the multiphase flow. One important characteristic of multiphase flow is its ability to exist in different flow patterns, which is the physical distribution of the phases within the flow enclosure or pipe. Thus, multiphase flows can been classified according to the different flow patterns known as the flow regime.

2.2.1 Multiphase flow regimes

Multiphase flow regime is a term popularly used in multiphase flow studies to classify the different flow patterns, which occur during multiphase flow through pipes [5]. The complex interaction between the phases often result to a distribution of the gas and liquid in the pipe in such a pattern that is observable and

can be represented using a flow map known as flow regime map. In generating the flow regime map, a good number of investigation is carried out to determine the dependency of flow patterns on the volume fraction of the components of the multiphase flow [17]. Although multiphase flow regimes can be studied for two-phase gas-liquid flows and for three-phase oil-water-gas flows, this review will focus mainly on the two-phase gas-liquid flow.

One of the limitation of flow regime maps is that they are only relevant to the system (pipeline dimension, operating condition and fluid type) applied in generating it [13]. This implies that no one flow regime can be applied to interpret flow pattern in all flow systems. Previous works such as that by Schicht [87], Weisman and Kang [115], which was aimed at generalising flow regime map coordinates has not been successful because the transition in most flow regime maps and the corresponding instabilities depend on different properties of the fluid.

The flow pattern predominant in a vertical pipeline vary from that of the horizontal pipeline [115]. For example, while a stratified flow pattern observed in the horizontal pipe flow is not observed in the vertical pipe flow, the churn flow observed in the vertical pipe flow is not observed in the horizontal pipe flow. Thus, the flow regime in the vertical and horizontal pipe are discussed.

2.2.1.1 Multiphase two-phase gas-liquid flow regimes in horizontal pipe

The flow patterns generated during multiphase flow through horizontal pipes has been studies in reasonable details over the years. One of the earliest study on flow regime in horizontal pipes was reported by Baker [5] and Hoogendoorn [45]. Recently, a number of other studies on two-phase gas-liquid hor-

izontal pipe flow regimes have been reported [2, 35, 64, 108, 107, 113]. Figure 2.2 shows a typical flow regime map obtained through experimental studies on a 2.5cm diameter pipe, which was reported by Taitel et al [107]. From

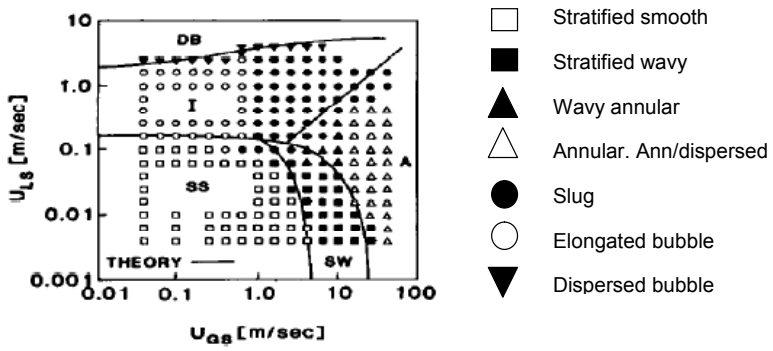

Figure 2.2: Two-phase gas-liquid flow regime, [107]

this flow regime map, the typical flow regimes prevalent in the two-phase gas-liquid horizontal flow can be classified as shown in Figure 2.3. Weisman [114],

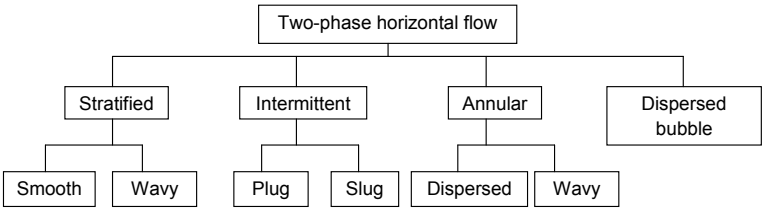

Figure 2.3: Hierarchial diagram showing flow regime in two-phase flow

provided a pictorial representation of the two-phase flow patterns, which is obtained from a 5.1cm diameter horizontal pipe. This pictorial representation is shown in Figure 2.4.

In the stratified flow condition, the liquid flows at the bottom of the liquid while the gas is at the top of the liquid. The interface of between the liquid and the gas can be smooth or wavy [53]. In the intermittent flow pattern, the liquid body,

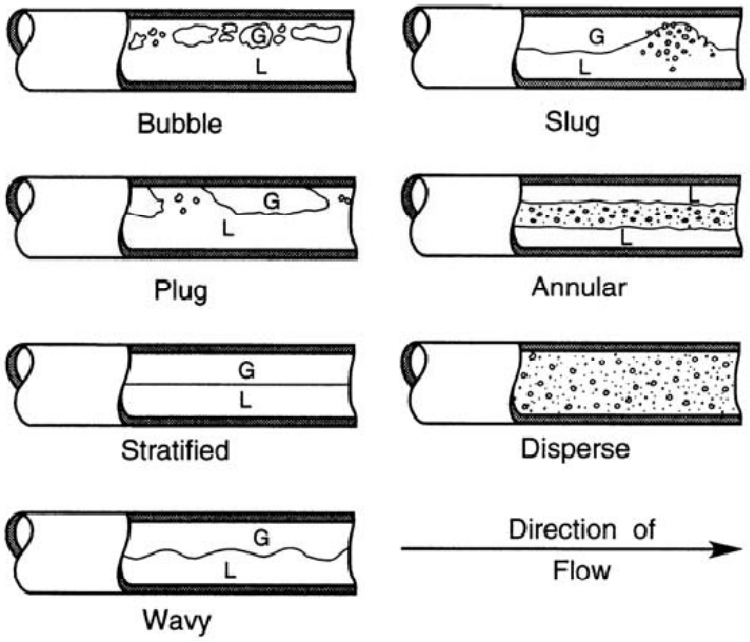

Figure 2.4: Flow pattern for two-phase gas-liquid flow, [114]

which fill the pipe are usually separated by gas pockets, which at the bottom of the pipe, contains a stratified liquid layer flowing along the gas pocket. The intermittent slow pattern is usually divided into slug and elongated bubble (plug) flow patterns. In the annular flow pattern, the liquid in the pipe flows as a film around the wall of the pipe. This type of flow pattern is often observed under high gas flow velocity. The gas, which may contain some liquid droplets flows through the core center and it is surrounded by the liquid film. The wavy annular flow pattern is observed during the transition from slug flow to the annular flow. In the dispersed bubble flow, the gas phase flows as a distributed discrete bubbles within the liquid body, which is continuous. Detailed description of these flow patterns can be found the literature [61, 62, 106].

Taitel and Dukler [108] developed a model for predicting flow regime transition in

horizontal and nearly horizontal pipe with two-phase gas-liquid flow. In a later work by Taitel et al [107], the model result was compared with experimental results and good agreement between the two was concluded. A model for predicting pressure distribution for two-phase flow through inclined, vertical and curved pipes was also developed by Gould et al [34].

Further studies has also been carried out on the effect of pipeline inclination on flow regime of two-phase flow in horizontal pipes [8, 11, 34, 36, 93, 107]. The work by Taitel et al [107] reported the effect of pipe inclination on the flow regime map. They showed that small deviation (inclination) from the horizontal have significant effect on the flow regime map. The effect of pipe inclination on the liquid holdup and the pressure loss across the pipe was investigated by Beggs and Brill [8]. Gould et al [34] also reported flow pattern maps for horizontal and vertical flows with pipe inclination for upflow at 45^o.

2.2.1.2 Multiphase two-phase flow regimes in vertical pipe

The flow regimes identified in vertical pipelines are often different from that of the horizontal pipeline [115]. The challenge of the lack of a universal flow regime map for interpreting two-phase flow in the vertical pipes still exist. This is due to the significant effect of phase properties and the pipe diameters on multiphase flow regimes [96]. Despite these limitations, the main types of flow regimes, which are identified in the vertical pipeline include the bubbly flow, the slug flow, the churn flow and the annular flow [66]. Figure 2.5 shows typical flow patterns and the flow regime map obtained from a 72mm diameter vertical pipe, reported by Guet and Ooms [38].

The modeling and experimental work to predict and describe these flow regimes

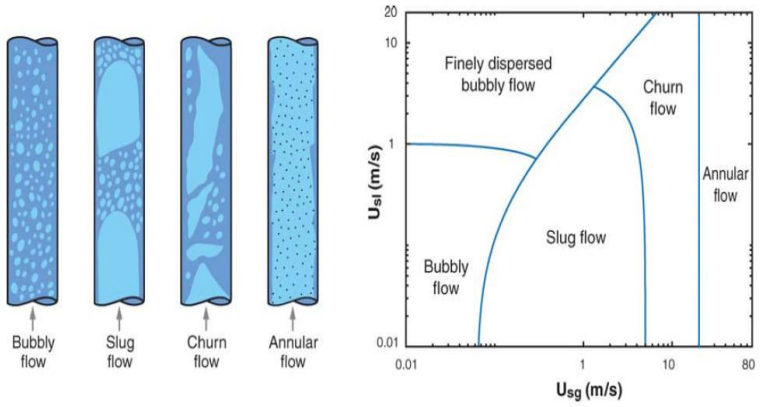

Figure 2.5: Flow pattern for two-phase gas-liquid vertical flow, [38]

can be found in many literatures [66, 68, 73, 96, 105, 115]. The bubble flow represents a flow pattern in which the gas phase flows as a small discrete bubbles in a continuous liquid phase [115]. The slug flow pattern occur due to the coalescence of the gas bubbles at increased gas flowrate, which results to bullet type gas pocket, known as Taylor bubbles [96]. The Taylor bubble is usually separated by liquid slug, which often contain some gas bubbles in the liquid body. The diameter of the Taylor bubble often correspond to the diameter of the pipe, but the Taylor bubble is usually surrounded by a thin of liquid film, which flows vertically downwards. The churn flow is formed due to the break up of Taylor bubble into the liquid body as the gas flowrate increases [52]. The churn flow is predominantly a disorderly flow regime, in which the liquid is observed to flow vertically upwards in an oscillatory motion. The annular flow regime occurs when the gas flowrate is further increased such that the gas flows in the core of the pipe and the liquid flows around the pipe walls [66]. The gas flowing through the pipe core can also carry liquid droplets, which are dispersed in it.

2.3 Multiphase slug Flow

Slug flow is one of the most undesired multiphase flow regimes, due to the associated instability which imposes a major challenge to flow assurance in the oil and gas industry. The oil and gas industry encounters slug flow in the course of their production activities. As was discussed in sections 2.2.1.1 and 2.2.1.2, slug flow occur both in horizontal and vertical pipes. Thus, there are different types of slugs, which can be distinguished from each other by mechanism of formation. Thus, the multiphase slug flow can be classified into three different types, based on the formation mechanism [91, 32]. The three types include:

1. hydrodynamic slugging
2. operation induced slugging
3. severe slugging

2.3.1 Hydrodynamic slugging

Hydrodynamic slug flow, which occur mainly in horizontal pipes is initiated from stratified flow due to two broad hydrodynamic mechanisms, namely: the natural growth of hydrodynamic wave instabilities generated on the gas-liquid interface, and the accumulation of liquid caused by sudden pressure and gravitational force imbalance, due to undulation in the pipeline geometry [47]. The growth of hydrodynamic wave instabilities has been described to depend on the classical KelvinHelmholtz (KH) instability mechanism [27, 28, 56, 60]. Arnaud et al investigated the effects of wave interaction on the formation of hydrodynamic slugs in two-phase pipe flow at relatively low gas and liquid superficial veloci-

ties. They conducted their experiments in a horizontal pipe, which is 31m long, 10cm internal diameter at atmospheric pressure. They found that the formation of hydrodynamic slugs due to wave interaction differs from predictions for slug formation using long wavelength stability theory.

The study of hydrodynamic slug flow has resulted to the development of a number of transient and steady state models. Isaa and Kempf [47] suggested the classification of the transient models into three categories namely: empirical slug specification, slug tracking, and slug capturing models. While the empirical slug specification models are used to describe various stages of slug development including slug formation, growth, decay and slug shape [108, 25], the slug tracking models are used to track the movement, the growth and the dissipation of individual slugs in the slug flow [9]. A slug tracking technique, which is capable of predicting slug generation, slug growth, and slug dissipation was also developed by Zheng et al [117]. The capturing models are developed to predict slug flow regimes using mechanistic and automatic results of the hydrodynamic growth instabilities [48].

2.3.2 Operation induced slug

This type of slug is induced due to certain operations performed during production. Operations such as ramp-up (increasing production), pigging and depressurisation can generate a huge number of liquid slugs.

2.3.3 Severe slugging

This type of slug flow is caused by the undulations and dips in the pipeline geometry, topography and network [82]. Towards the end of the operational life of an oil reservoir, the reservoir pressure can become depleted or the Gas-to-liquid ratio (GLR) can become very low. In such conditions, the gravitational pressure dominates the flow resistance, and liquid accumulates at the pipe dips, thereby blocking the flow channel and preventing gas flow. This process results to intermittent flow condition. This intermittent flow condition, which is characterised by pockets of liquid and gas flow followed by no liquid and gas flow out of the riser is referred to as severe slugging [70, 72]. The severe slug cycle process, which was discussed in section 1.1.2 has been described in many literatures [7, 18, 43, 59, 70].

The slug lenght produced in a typical severe slug flow is usually equal to or greater than one riser height [72, 89]. One major challenge associated with severe slugging is that it is characterized by large pressure and flowrate fluctuations [86]. The associated fluctuations in pressure and flowrate can damage downstream processing equipment, increase pipeline stress, reduce productivity and shorten the reservoir operation life [44].

2.3.3.1 Severe slug models

A number of steady state models [33, 82, 108, 103] and transient models [26, 69, 85, 89, 104] have been developed to predict the occurrence of severe slugging in a riser-pipeline system. The severe slug models are often developed to answer some basic questions associated with severe slug flow, such as:

1. at what condition does severe slugging occur and

2. what will be the characteristics of the severe slugging when it occurs?

One of the models reported to predict at what condition severe slugging will occur was developed to show that a stratified flow regime in the pipeline is a condition for severe slugging to occur [89]. Taitel and Dukler [108] first developed a criterion to predict stratified flow regime in horizontal and near horizontal pipelines. By applying the inviscid Kelvin- Helmholtz theory in which shear stress is neglected [56], the condition given in (2.1) was developed. In (2.1), U_G is the superficial gas velocity, h_G is height occupied by the gas phase, ρ is density and the subscripts G and L refer to the gas and liquid phases respectively.

$$U_G > \left[\frac{g(\rho_L - \rho_G)h_G}{\rho_G}\right]^{\frac{1}{2}} \tag{2.1}$$

When the superficial gas velocity, U_G, is lower than that obtained by evaluating the right-hand-side (RHS) of (2.1), then a stratified flow regime is obtained in the pipeline and severe slugging can occur in the riser-pipeline system. A plot of this criterion as presented by Taitel and Dukler [108], is shown in Figure 2.6. Below the transition line in Figure 2.6 is the region were stratified flow occur in the pipeline.

Base on the Taitel and Dukler criterion, Goldzberg and McKee [33] also developed a criterion for the formation of slug in a pipe dip, by the sweeping out of the accumulated liquid in the pipe dip. The resulting criterion obtained by Goldzberg and McKee, which was achieved by analysing the Bernoulli equation over the liquid surface is given in (2.8), where θ is the angle of inclination of the pipeline, A_L is the liquid flow area, A_G is the gas flow area and C_2 is

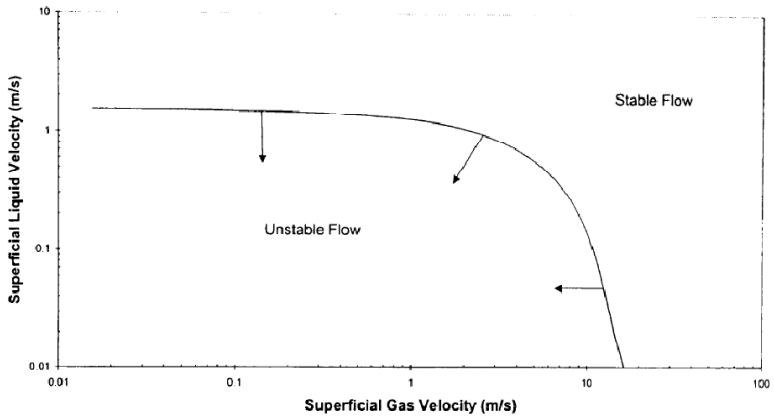

Figure 2.6: Stratified flow criterion [108]

approximately equal to the ratio of A_G to A_L.

$$U_G < C_2 \left[\frac{g(\rho_L - \rho_G)\cos\theta A_G}{\rho_G \frac{dA_L}{dh_{LP}}} \right]^{\frac{1}{2}} \tag{2.2}$$

Another criterion for severe slugging, which is based on the rate of pressure head accumulation at the riser base to the rate of pipeline gas pressure increase was developed by Bøe [10]. This criterion is summarised as shown in (2.3).

$$\frac{\partial(\triangle P_{HYD})}{\partial t} > \frac{\partial(P_p)}{\partial t} \tag{2.3}$$

In (2.3), P in the pressure and the subscripts HYD and P are the hydrostatic and pipeline pressures respectively, while t is time. The analysis of (2.3) under constant inlet fluid flowrate, for the mass balance of gas in the pipeline and the riser pressure balance resulted in the criterion given in (2.4).

$$U_L \geq \frac{P_p}{\rho_L(1-\alpha_L)\sin\theta} U_G \tag{2.4}$$

In (2.4), θ is the pipeline angle of inclination, P_p is the pipeline pressure, U_L is the superficial liquid velocity and α_L is the liquid hold-up, which is obtained

assuming no slip condition as given in (2.5). For severe slugging to occur, the condition in (2.4) must be satisfied.

$$\alpha_L = \frac{U_L}{U_L + U_G} \tag{2.5}$$

Pots et al [82] also developed another criterion for predicting the occurrence of severe slugging. Similar to the Bøe's [10] criterion, the criterion developed by Pots et al [82] considered the balance between the rate of hydrostatic pressure head build up across the riser and the rate of gas pressure build up in the pipeline. In the development of the Pots et al criterion given in (2.6), it is considered that for severe slugging to occur, the rate of hydrostatic pressure head build up across the riser must be greater than the rate of accumulation of gas pressure in the pipeline. The analysis of this criterion shows that severe slugging will occur if $\Pi_{ss} < 1$. The criterion was developed assuming that there is no mass transfer between the liquid and gas phase, the riser is vertical and there is no liquid fall back.

$$\Pi_{ss} = \frac{ZRT/M_G m_G}{g\alpha_L L m_L} \tag{2.6}$$

In (2.6), Z is the gas compressibility, M_G is the gas molecular weight, m_L and m_G is the mass flowrate of liquid and gas respectively.

Another criterion for severe slugging to occur was developed by Taitel [103]. The Taitel's criterion considered the blow-out stage of the severe cycle process and the net force across the riser during the blow-out stage. In the Taitel's criterion, the condition for severe slugging to occur is given by (2.7). Thus, severe slugging will occur is $\triangle F$ increases y, where $\triangle F$ is the net force over the riser column, when the gas tail penetrates into the riser at the base, y is the height of the gas bubble penetrating into the riser.

$$\frac{\partial(\triangle F)}{\partial y} > 0 \tag{2.7}$$

The $\triangle F$ is given by (2.8),

$$\triangle F = \left[(P_s + \rho_L g H_R)\frac{\alpha_G L}{\alpha_G L + y\alpha_G^{'}}\right] - [P_s + \rho_L g(H_R - y)] \tag{2.8}$$

where P_s is the topside separator pressure, H_R is the riser height, α_G is the gas hold-up in the pipeline, L is the length of the pipeline and $\alpha_G^{'}$ is the gas hold-up in the gas bubble penetrating the riser. By combining (2.7) and (2.8), (2.9), which is the final form of the criterion, considering the atmospheric pressure is obtained. Thus, severe slugging will occur if the condition in (2.9) is satisfied.

$$\frac{P_s}{P_0} < \frac{\left(\frac{\alpha_G}{\alpha_G^{'}}\right) L - H_R}{P_0/\rho_L g} \tag{2.9}$$

The analysis of this criterion shows that it depends on the riser-pipeline operating condition and geometry. The gas hold-up, $\alpha_G^{'}$, is assumed to be equal to a constant value of 0.89. Fuchs [30] also developed a severe slug criterion model, which was based on the slug blow out stage analysis.

Schmidt et al [89] with focus on the liquid build up stage developed a transient model based on mass and pressure balances on the riser-pipeline system. The purpose of their model was to predict the time for slug build up and the slug length. Although the model prediction showed good agreement with their experimental result, the model's ability to be generalised was very limited due to the closure model, which was developed as empirical correlations generated from their experimental facility.

Another transient model for predicting severe slugging was developed by Schmidt et al [90]. This model was developed with focus on predicting all the stages in the severe slugging cycle (see section 1.1.2). Similar to the model of Schmidt et al [89], the model was developed using the mass and pressure balances on the riser-pipeline system for each stage in the cycle. The gas-liquid interface were used to define the transition between the stages in the slug cycle. The

simulation results obtained from this model was reported to agree closely from their experimental result. This model developed by Schmidt et al [90] has been used in subsequent work by Hill [43]. A comprehensive review of transient slug model was reported by Ozawa and Sakaguchi [79]. They explained that while slug transport was dominated by gravity in the vertical pipe, in the horizontal pipe, it was dominated by momentum flux of the liquid at the back of the slug.

2.4 Severe slugging control techniques and technologies

Severe slugging has become a major challenge to gathering crude oil from the fast depleting oil reservoirs. With deepwater exploration up to 2000m becoming common, many risers will be required in the coming decade, all of which will become vulnerable to severe slugging if a sustainable solution is not found. A number of severe slugging control techniques have been proposed based on experimental, theoretical and field studies. This section reviews these severe slugging control techniques and their objectives based on the underlying technologies. The current control techniques can be classified into two, based on the underlying scientific and/or technological principles employed. The two classifications are:

1. changing flow condition

2. riser outlet downstream adjustment

2.4.1 Changing flow condition

This approach focuses on altering the flow, pressure conditions and the structure of the flowline upstream (sub-sea) of the riser. Current practical approaches include:

1. design modification of upstream facilities
2. riser base gas lift
3. gas re-injection (self-lifting)
4. homogenising the multiphase flow
5. subsea separation and processing

2.4.1.1 Design modification of upstream facilities

This method involves applying changes to the existing facilities upstream of the riser. The common concepts are: changing flowline internal diameter and changing pipeline layout structure.

Changing flowline internal diameter

In order to mitigate the severe slugging occurring in a production system, the pipeline size can be changed with targets on increasing or reducing the internal pipe diameter, depending on the type of slug prevalent in the system. Reducing the pipe diameter, will reduce the cross sectional area of the pipe thereby increasing the fluid velocity. This concept generates a flow regime with low gravitational pressure drop in the riser, a condition necessary for avoiding liquid

accumulation at the riser base which is prevalent in low velocity terrain induced severe slugging. Increasing the pipe diameter increases the cross sectional area of the pipe. This may produce a low velocity stratified flow in the flowline, a condition necessary for avoiding hydrodynamic slug. This implies that while increasing pipe diameter may remove hydrodynamic slug, it may initiate terrain induced slug and vice versa.

Fargharly [29] concluded in a study of severe slugging in the Upper Zakum oil field that optimum sizing may alleviate (mitigate) the severe slugging problem but it will not eliminate severe slugging completely. However, optimal sizing will depend on other production factors which could be difficult to determine precisely. One disadvantage of this method is that changing flowline diameter is capital intensive and it may introduce other operational problems. This reduces the chances of implementing this strategy.

Changing pipeline geometry

Makogan and Brook [63] of BP patented a slug mitigation device which they claim can inhibit severe slugs. The device is a specially designed pipe which has an upward inclined part, a horizontal part and a downward inclined part. The device is positioned immediately upstream of the riser as shown in Figure 2.7. They claim that the device inhibits severe slugging by reducing the length of the liquid slugs as well as increasing the frequency of the discrete liquid slugs. This enables the gas pressure behind the slug to be sufficient enough to drive the slug through the riser. As a result, plug (intermittent) flow regime is generated. It is claimed that the produced intermittent flow can be handled by the topside facilities.

There is no field or experimental results reported on the effectiveness of this device. The device, on examination can be considered as a mini-riser which may

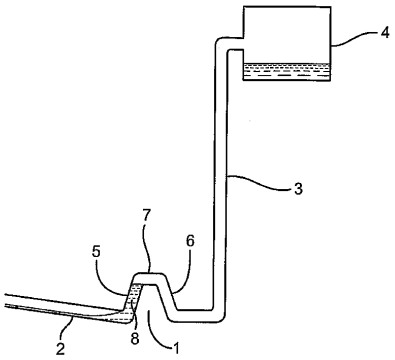

1. Slug inhibitor device
2. Pipeline
3. Riser
4. Separator
5. Upward inclined part
6. Downward inclined part
7. Horizontal part

Figure 2.7: Device for slug inhibition, [63]

increase pressure drop along the main riser, more significantly if the reservoir pressure is low.

2.4.1.2 Riser base gas lift

Riser base gas lift system is a slug attenuation strategy in which compressed gas is injected into the riser base to lift the liquid. Riser base gas injection can attenuate slug formation by the following interrelated fluid, flow and pressure mechanisms:

1. decreasing the pressure in the flowline
2. increasing the flowrate and changing the flow regime in the riser
3. decreasing the pressure in the riser

Alvarez and Al-Malki [3] reported the attenuation of a hilly terrain induced slugging encountered in an 11.4km long large diameter pipeline by increasing GOR

through riser base gas injection. Meng and Zhang [67] also discussed the possibility of attenuating severe slugging by increasing GOR through increased well gas injection. Jansen and Shoham [50] showed through experimental studies conducted using a 9.1m pipeline and 3m higher riser system that it is possible to stabilize severe slugging by gas injection. However, riser base gas injection is not a straight forward process as it requires accurate flow regime assessment. Introducing riser base gas injection into a stratified flow regime can cause flow instability. There have been industrial reports of riser base gas injection introducing or even aggravating severe slugging. Al-Kandari and Koleshwar [1] reported the occurrence of excessive severe slugging in an onshore multiphase pipeline in Kuwait. This platform had no slugging problem until riser base gas injection was introduced. It can be explained that the riser base gas injection changed the flow regime from stratified flow to slug flow.

Another crucial issue is the trade off between the optimum point for gas injection and the amount of gas required to stabilise the system as shown in differing reports by Jansen and Shoham [50], Pots et al [83], Schmidt et al [89] and Meng and Zhang [67]. Jansen and Shoham [50] concluded through their experiment that a high amount of gas is required to eliminate severe slugging in just a 3m high riser. Pots et al [83] also reported that an unrealistically large volume of gas is required to achieve stability by riser base gas injection in about 400m water depth. An unrealistic gas injection implies an unrealistic cost of gas compression for injection. Schmidt et al [89] also discouraged the idea of riser base gas injection due to this cost of gas compression.

However, Meng and Zhang [67] in their report investigating severe slugging in a 2.5km downward sloping tieback in about 700m water depth, stated that only one third of the injected gas was required if the gas is injected closer to the individual well formation rather than at the riser base. Obviously, only distance

has changed. Thus, there is a requirement for accurate assessment of flow condition and estimation of optimal gas injection points to achieve economical gas injection operation.

A patented gas injection technique invented by Duret and Tran [24], claimed to neutralise slugging by computerised control of the gas injection rate. The patent explained that gas injection is optimised through this controlled rate. However, how this optimization is achieved is not demonstrated and not very explicit. No laboratory, experiment or field use of this system is mentioned even in the literature.

Cousins and Johal [19] reported a patented device which they called a multipurpose riser. They claimed that this system is capable of performing three important functions at the same time, namely: a slug catcher, a multiphase flow meter and a riser base gas lift. The schematic of the system is shown in Figure 2.8.

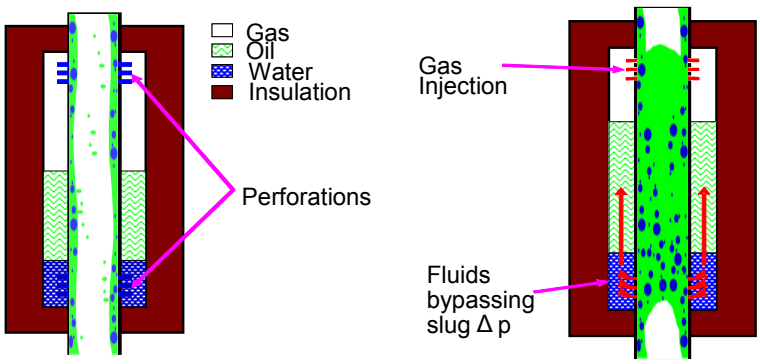

Figure 2.8: Multi-purpose riser for slug control [19]

The system consists of two concentric pipes in which the inner one is the riser while the outer one is flanged off at the bottom to create an annulus in-between the two pipes. The inner pipe connects to the outer one through a number

of perforations at the bottom and the top. The topside of the outer pipe is connected to a compressed gas inlet source with an isolation valve.

As a riser base gas lift system, the system provides a route for injection of compressed gas into the annulus during start up operation. Due to differential pressure between the annulus and the inner pipe, the gas then penetrates into the riser (inner pipe) through the bottom perforations. This gas penetration reduces the fluid density and the gravitational pressure drop thereby easing the lifting of the liquid. The injection is continued until steady state operation is reached. The operation of this system has not been reported in any literature.

2.4.1.3 Gas re-injection

This technique primarily focuses on achieving a self stabilizing system [110]. The compressed gas in the pipeline, upstream of the riser base is separated and re-injected into the riser, as shown in Figure 2.9. The injected gas bubbles help break up the liquid slugs and reduce the static pressure of the liquid in the riser. Thus, slug formation is inhibited.

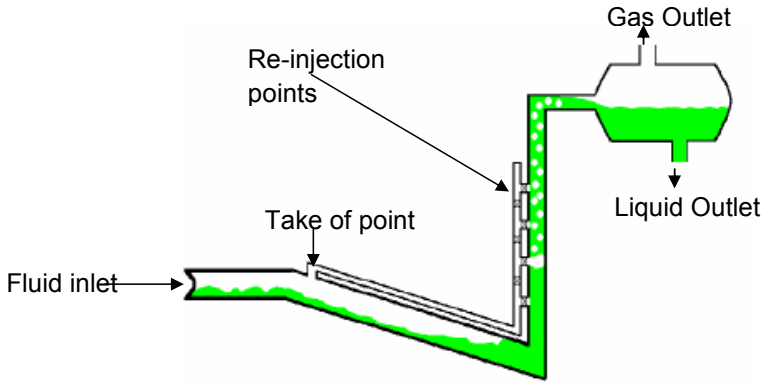

Figure 2.9: Gas re-injection system for riser slug control, [110]

Further studies have considered different locations for gas re-injection and a basic regulatory control is included to manipulate the gas re-injection for optimisation [110]. Tengesdal et al [110] reported various experimental results focused on identifying the optimal injection point. He concluded that the ideal injection point is at the same level or slightly higher than the take off point. The pressure drop in the by-pass system must be higher than the static head above the injection point, less liquid would block the injection pipe. To achieve this, a ball valve is installed at the injection line for backpressure build up when throttled. Another location considered is the gas bypass as shown in Figure 2.10.

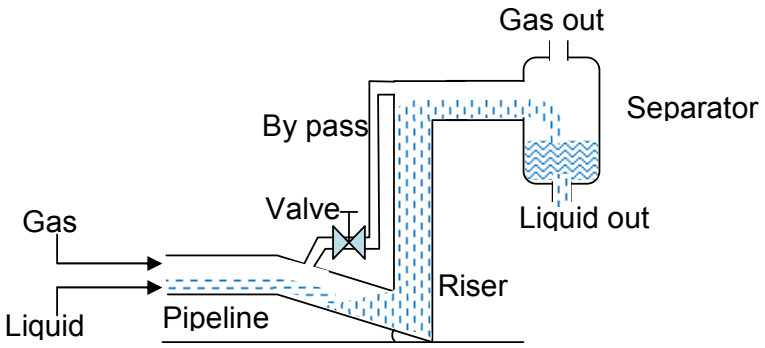

Figure 2.10: Gas by-pass method

The major advantage of this process is that it can prevent slug formation without an additional gas supply. However, the provision of additional control for the ball valves could be a limitation. Modification to an existing platform (well) can be expensive as it may involve major structural changes.

2.4.1.4 Homogenising the multiphase flow

Another method of attenuating slug formation is homogenising the mixture. The objective would be to force the gas and liquid into a homogeneous fluid. This will eliminate the intermittent flow regime associated with non-homogeneous multiphase flow. Hassanein and Fairhurst [39] suggested that this can be achieved by reducing the surface tension of the fluid by injecting a surface tension reducing surfactant into the flowline. This will change the fluid into foam, making the fluid homogeneous. The limitation with this method is that it would increase separation difficulty at the topside and reduce product quality. Another method would be the use of intrusive inline mixer in the flow line. This method would avoid the separation problems but may increase pressure drop and cause pigging problems.

2.4.1.5 Sub-sea separation of multiphase fluid

This method employs sub-sea separation facilities to separate the fluid into single phase, liquid and gas. Thus, two separate pipelines for gas and liquid are required. A subsea pump is also required to provide the pressure head needed to deliver the liquid to the topside. Consequently, this method avoids multiphase flow and severe slugging is prevented.

2.4.2 Riser outlet downstream adjustment

This approach focuses on altering the flowrate, flow regime, pressure and structure of the downstream (topside) system. Practical approaches include:

1. design modification of processing facilities
2. topside choke manipulation
   - **i** fixed choking
   - **ii** dynamic choking

2.4.2.1 Design modification of processing facilities

Modifying the system with the installation of slug catcher(s) is one way to mitigate the effect of severe slugging. Slug catchers are enclosed vessels specially designed and installed at the end of a riser or a pipeline to receive and buffer liquid slugs. They also provide the first stage of separation and are often referred to as pre-separators. A schematic diagram of a horizontal slug catcher is shown in Figure 2.11. They are designed with the capacity to receive and dampen slug surges thereby protecting the downstream systems. As a slug mitigation system, slug catchers do not inhibit slug formation.

The addition of control systems to the slug catcher can improve or reduce its performance. A slug catcher with controlled liquid level would pass the high liquid surge to the processing facility in order to maintain set liquid level. This makes the slug catcher ineffective. On the other hand, a slug catcher with a controlled liquid drain rate will protect the downstream equipment, but such a slug catcher must have a volume large enough to contain the accumulated

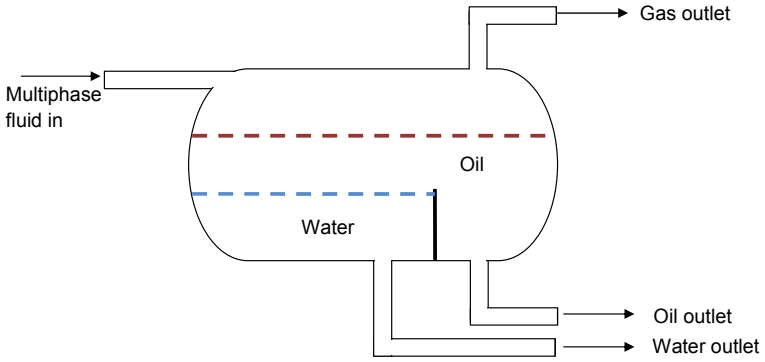

Figure 2.11: Schematic diagram of a horizontal slug catcher

liquid. These uncertainties make the basic slug catcher unsuitable for severe slug control, unless other control methods are incorporated.

2.4.2.2 Topside choke control

The concept of choking the flow line to suppress severe slugging has become an established methodology with advancing improvements. This method was first suggested by Schmidt et al [88]. Choking transforms the unstable flow in the riser to stable flow by inducing a minimum excessive back pressure on the pipeline. This condition results in a considerable increase in pressure drop across the choke at constant gas mass flowrate. This will reduce the gas velocity in the riser, eliminating slip and inhibiting the gas tail from penetrating the riser base [29].

Fargharly [29] reported his experimental work at the upper Zakum field to show that fixed but manually manipulated riser topside valve increased the back pressure in the system, thereby suppressing severe slugging. Molyneux and Kinvig [71] patented a controlled system for choking the topside separator gas outlet

valve to stabilise severe slugging in a vertical riser. Choking can be broadly divided into two categories namely: fixed choking and dynamic (controlled) choking.

Fixed choke

Taitel [103] used stability criteria to define a theoretical severe slugging control law which relates the back pressure to the slug tail propagation into the riser. With a good approximation, the position of the valve required to stabilize the system can be pre-calculated and little movement of the valve is required to maintain quasi-equilibrium in the system. Due to the non-linear nature of multiphase flow, the application of fixed choke to eliminate severe slugging may have severe consequences during sudden operational changes. Sudden operational changes can cause the system to become either stable or unstable, depending on the nature of the changes occurring in the system. While an unstable system condition is obviously unacceptable and would require immediate control action, a stable system condition may also require control action. This is because the operating condition of such stable system may occur at a valve opening that is lower than necessarily required to achieve the same stable condition. Thus, in order to stabilise the system at the best possible valve opening, transient flow instabilities require dynamic choke adjustment. Without this, unnecessary high flowline pressure can occur in the system. This could lead to losses in production and increased pipeline stress. Dynamic choking is therefore preferred as an efficient option to controlling slugging problems in riser-pipeline systems.

Dynamic choke

Dynamic choke is a choke manipulated by active control based on real time changes of system variables. The choking position is not fixed but adjusted based on a measured variable for achieving stability. Riser base pressure, riser top pressure and flow rate are commonly adopted control variables. Current applications of these controlled variables are discussed below.

Riser base pressure control

Many reports on using the riser base pressure as a control variable have shown its suitability in slug control. Storkaas and Skogestad [101], Drengstig and Magndal [23], Molyneux and Kinvig [71] and Henriot et al [42] all described severe slugging suppression using the riser base pressure measurement.

Storkaas and Skogestad [99] applied a systematic analysis of the riser-pipeline system using control theories. The analysis also included the assessment of the stability characteristics of the system using the riser top valve opening as the manipulated variable. Based on their analysis, they identified the riser base pressure as the best variable for stabilizing riser-pipeline system. This is because the corresponding transfer function has no right half plane zero which limits control performance.

Drengstig and Magndal [23] implemented a simple PI controller by measuring both the riser base and the riser top pressure and the using the pressure difference as the controlled variable while the riser top valve opening as the manipulated variable. Their report also pointed out that the riser base pressure is the optimum variable for the slug control.

Molyneux and Kinvig [71] reported a difference in the performance observed in

the application of their patented slug control system in a transient multiphase flow simulation software to that obtained from a test rig. While the controller achieved only 50% reduction in test rig pressure fluctuation, the simulation stabilised the system. They attributed this difference to the incompleteness of the transient model used.

Henriot et al [42] reported the simulation studies performed on the Dunbar-Alwyn pipeline using TACITE multiphase simulator. Having considered various options to control flow instabilities in the riser, the riser base pressure was considered most appropriate and used as the controlled variable while the riser topside valve opening was used as the manipulated variable. When there is a pressure build up at the riser base, the control system reduces the valve opening to stabilize the system. This controller action presents a different approach to that reported by Molyneux and Kinvig [71], in which the valve opening is increased periodically in order to achieve stability. This implies that systems may respond differently to increased riser base pressure condition. However, the controller action based on pressure measurement only may not present a sufficient judgement. The analysis of the GLR in the system is also very important. Consequently, the difference in the controller action in the above reports may be due to the GLR ratio in the system. While the Dunbar-Alwyn [42] may be a low GLR system, the one reported by Molyneux and Kinvig [71] may be a high GLR system.

The SlugCon is a slug suppression system developed by ABB to control terrain induced slug [41, 40]. The schematic diagram of the system is shown in Figure 2.12.

This system is configured such that the controlled variable is a pressure measurement at a point close to the well. Thus the set point for the controlled

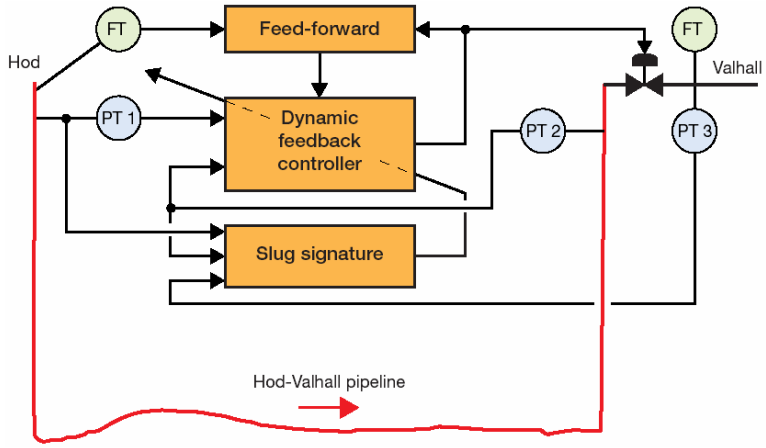

Figure 2.12: Schematic diagram of the ABB SlugCon Control System, [40]

pressure is determined based on the inlet condition of flow rate and pressure.

Riser top pressure control

The use of riser topside pressure measurement as a variable for severe slugging control has been reported with diverging views. The controllability analysis reported by Storkaas and Skogestad [100] showed that the riser top pressure alone is not a good variable for riser-pipeline instability control. This is based on the fact that the zeros of the corresponding transfer function are in the right-half-plane (RHP) of the complex plane. They proposed a cascade control configuration, which implements two controllers as shown in Figure 2.13.

For a normal operation, the outer loop can be configured for riser top pressure control while the inner loop is configured for riser top total volumetric flowrate control. This cascade control structure was developed due to the control limitations associated with implementing slug control with riser top pressure as the controlled variable in a single feedback control loop.

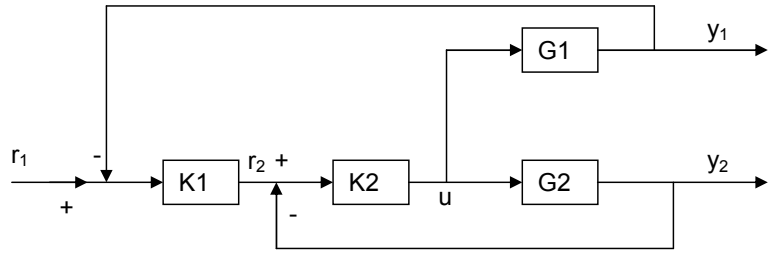

Figure 2.13: Cascade control configuration for severe slug control

However, Cao et al [15] reported the development of a slug control system which achieves stability using only topside variables such as the riser top pressure (P_{RT}), total volumetric flow rate at the riser top (Q_T) and total fluid density (ρ_T). The control system operates with an automated topside valve and uses its controller output to manipulate the valve at the exit of the riser. This ensures that the system fluctuation is maintained at acceptable levels. This system has been successfully demonstrated on an 11m high riser facility at the Cranfield state of the art multiphase flow laboratory which is managed using Emerson's DeltaV plant management system.

It is reported that the new technology could allow a certain degree of fluctuation in the flow within an acceptable range and by recognising the capacity of the processing facility will minimise the controller impact on production. By doing this, it is claimed that the production could increase by 10% when compared to production obtained with the best case of manual choking in the same system.

Flow rate control

The flow rate out of the riser has also been considered for stabilizing severe slugging. The volumetric flow rate can be used as a controlled variable for stability. Storkaas [94] in his model based analysis concluded that using vol-

umetric flow rate as a controlled variable will give poor performance at low frequency. He also concluded that using volumetric flow rate in the inner loop of a cascade control design to control the flowrate out of the riser could give better performance. An improved slug catcher designed with dynamic choking and intelligent control system can be used to suppress severe slugging through flowrate control, as reported by Kovalev et al [57, 58] (see Figure 2.14).

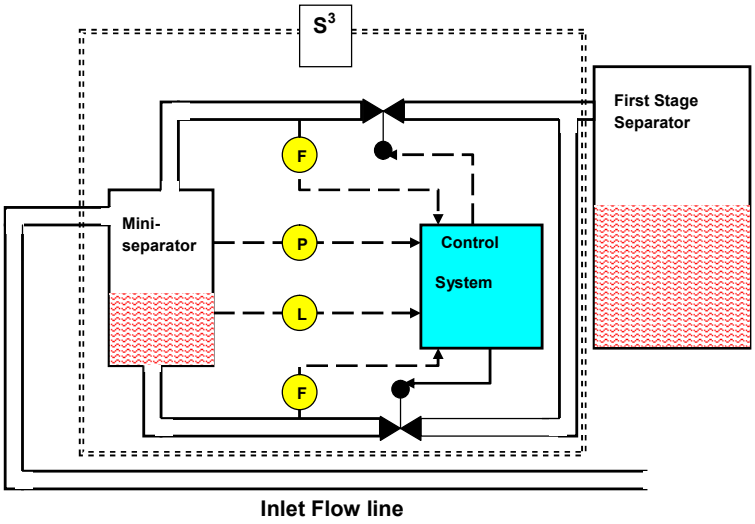

Figure 2.14: Schematic diagram of the S^3 control scheme

The slug suppression system (S^3) control strategy is based on total volumetric flow control and liquid flow control [57]. The measured variables include the liquid and gas volumetric flowrates, the separator pressure and separator liquid level, while the controlled variable is the total volumetric flowrate (the sum of the gas and liquid volumetric flowrate measured separately using flow meters). Under severe slugging conditions, the total volumetric flowrate control mode is not implemented, rather the liquid flow control mode operates to slow down slug velocity and prevent slug blow-out.

The operation of this system provides an improvement to the response time when compared to the use of multiphase flow control valves with large response time at the riser outlet. Due to the separated liquid and gas streams, the valve response time is faster. Also, because the slugs are either suppressed or decelerated, production deferment could be prevented in this system. For a non-linear system such as the riser-pipeline system, robust stability may not be guaranteed with a pre-tuned PID linear controller. The S^3 control scheme considers a single process variable, that is pressure. Other system variables (depending on the configuration) such as inlet flowrate, density and temperature should be incorporated and accounted for. A "vesseless" version of this system is also reported by Kovalev et al [58].

Recent industrial developments of slug control systems have also been reported with claims of increased production. An example of such a system is a patented slug mitigation, which was developed by Oram and Calvert of BP [78]. A schematic diagram of the system is shown in Figure 2.15.

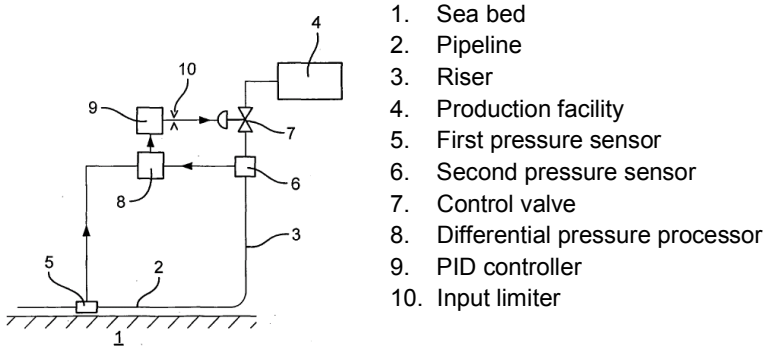

Figure 2.15: Schematic diagram of the slug mitigation system, [78]

The slug mitigation system has two pressure sensors, the first pressure sensor located at the riser base and the second pressure sensor located at the riser

top. The pressure difference between the two pressure sensors is processed by the differential pressure processor. Thus, the controller input is the differential pressure. The slug controller is a traditional PID controller whose integral time is set equal to zero, resulting to a PD controller. The controller output manipulates the control valve, whose upper and lower limit is set to about $\pm 20\%$ of its nominal value, to mitigate the severe slugging in the system. The differential pressure set point is determined by the operator. In another version of the system, a master PI controller with large integral time and small gain is used to automatically set the set point for the PD controller. The PD controller is considered as a slave, while the PI controller is considered as the master controller. The input to the master controller is pressure measurement from the first pressure (sea bed) sensor. The operator determines the pressure set point of the PI controller. Another version of the system is also presented, in which a dynamic valve constraint control is implemented. To achieve the dynamic constraint control, the upper and lower limits of the control valve is determined and set automatically from the process history. It is reported that the implementation of this slug control system on the Valhall production platform off the coast of Norway was successful, with claims that the slug control system increased production by 10% [14].

2.5 Conclusions

In conclusion, this chapter has presented a review of the severe slug control techniques, including their applications, limitations and challenges. Various forms of severe slug control techniques including modifying internal pipeline diameter, riser base gas injection, pipeline gas re-injection and manual and active choking of the riser top vales has been discussed. It can be deduced

that vast amount of work has been done to develop systems for severe slug control. However, the lack of adequate information on the performance of these systems is a challenge to deciding the direction for their further development. The conflicting report on the performance of similar techniques exposes the gap in the available knowledge of severe slug control. Thus, extensive amount of work is still required in order to gain sufficient knowledge and understanding of severe control and the sharing of available information could be the key to its success.

Chapter 3

Experimental facilities and procedure

3.1 Introduction

This chapter explains the experimental facilities and procedures used in the conduct of the experiment and in the acquisition of experimental data generated in the experiment. The experimental facility, which is located in the flow laboratory of the department of Process and Systems Engineering in Cranfield University consists of standard multiphase flow test rigs, including the riser-pipeline systems used in this work. The experimental facility is designed to continuously and safely process multiphase fluid under different operating conditions at real time. The chapter begins with the description of the multiphase flow facility and the operating conditions. The description of the different sections used for processing the flow in and out of the riser systems is also presented.

Also explained in this chapter is an industrial riser system, which is of a larger scale, when compared to the experimental facility. The industrial riser system

is not a physical experimental system, but a model based riser system, which is of industrial dimension. Thanks to the Scan Power Technology (SPT) Group for providing this system.

3.2 The multiphase flow facility

The multiphase flow test facility can be divided into three main sections. These include:

1. fluid supply and metering section
2. test section
3. phase separation section

The schematic diagram of the facility is shown in Figure 3.1.

3.2.1 Fluid supply and metering section

The fluid supply and metering section is the section that safely stores, supplies and provide measurement for the single phase fluid used in all the experiments. It is divided into three independent sources, each containing a single phase fluid. These include, air, water and oil sources. These three supply sources are discussed below.

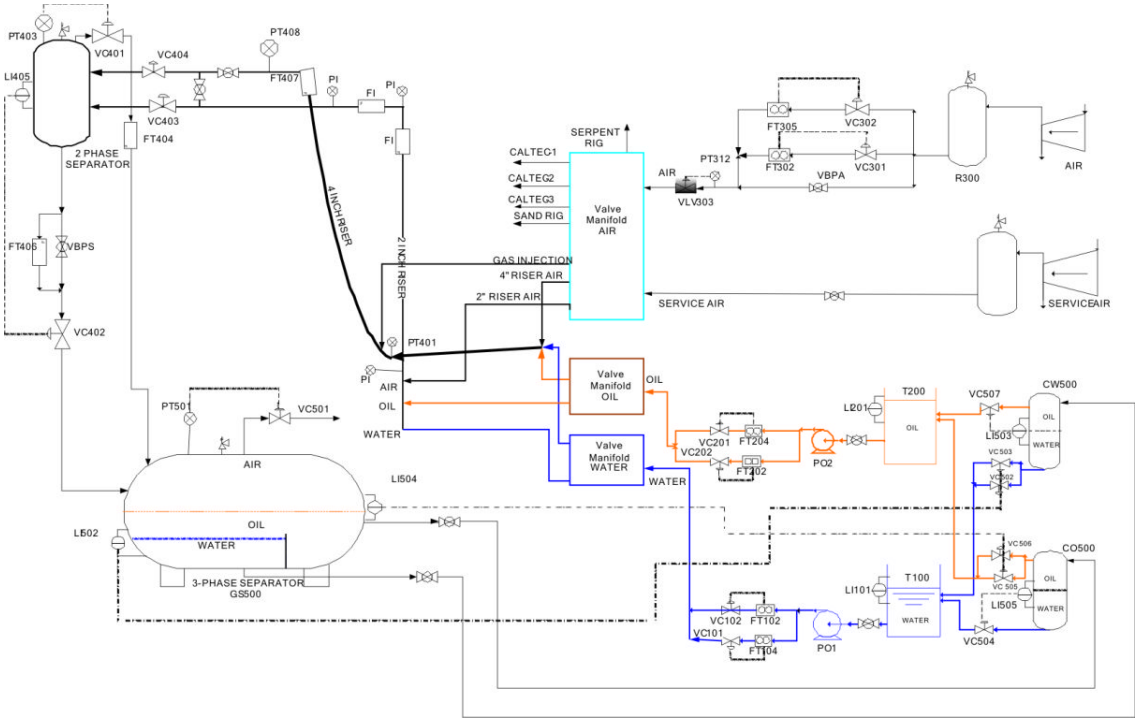

Figure 3.1: Multiphase facility at Cranfield University

3.2.1.1 Air supply

The air supply is obtained naturally from the atmosphere. The air is compressed and supplied from a bank of two compressors connected in parallel. This means that both compressors can run at the same time. When both compressors are run in parallel, a maximum air flow rate of 2550 m^3/hr FAD (free air delivery) at 7 barg can be supplied. Fluctuations are induced in the gas supply due to the compressors' loading and unloading processes. This fluctuations need to be reduced before the air reaches the test section, so as to inhibit its effect on the flow regime in pipeline and the riser. This is achieved by accumulating the air from the two compressors in a large air receiver. Air from the receiver passes through a bank of three filters (coarse, medium and fine) and then through a cooler where debris and condensates (present in the air) are stripped from the air before it goes into the flow meters.

3.2.1.2 Water and oil supply

Water is supplied from a 12.5 m^3 capacity water tank, and oil is supplied from a bunded oil tank of similar capacity. The water tank is situated inside the laboratory while the oil tank is located outdoors and has a bund with 110% (by volume) of the tank capacity.

The water and oil are supplied into the flow loop by two multistage Grundfos CR90-5 pumps. Both the water and oil pumps are identical and have a duty of 100 m^3/hr at 10 barg. The pictures of the water and oil pumps are shown in Figure 3.2. The pumps are operated remotely using the DeltaV control system.

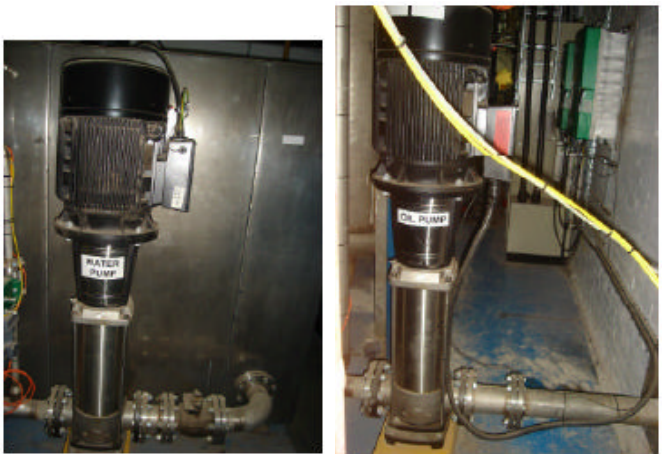

(a) Water pump (b) Oil pump

Figure 3.2: Water and oil pumps

In the water supply loop, there are two metering lines each comprising a control valve and a flow meter, which provides metering for the flow from 0-7.36 kg/s and 0-30 kg/s, respectively. The DeltaV system will accurately select the appropriate water metering flow loop when the desired flow rate is specified.

In the oil supply loop, there are also two metering lines, each comprising a control valve and a flow meter, which provides metering for the flow of 0-9.47 kg/s and 0-30 kg/s, respectively.

3.2.1.3 Flow metering

The flow rates of the air, water and oil are regulated using their respective control valves. These control valves are controlled by the supervisory control and data acquisition (SCADA) software, DeltaV. The water flow rate is measured by a 1 inch Rosemount 8742 Magnetic flow meter (up to 1 kg/s) and 3 inch Foxboro CFT50 Coriolis meter (up to 10 kg/s) while the oil flow rate is measured by a

1 inch Micro Motion Mass flow meter (up to 1 kg/s) and 3 inch Foxboro CFT50 Coriolis meter (up to 10 kg/s). The air is metered by a bank of two Rosemount Mass Probar flow meters of 0.5 inch and 1 inch diameter respectively. The smaller air flow meter measures the lower air flow rate (up to 120 Sm^3/h) while the larger one meters the higher air flow rate up to 4250 Sm^3/h (subject to compressor capacity).

3.2.2 The test section

Fluid supplied from the fluid supply section flows into the test section. The test section comprises of the riser systems, the two phase separator and the accompanying measuring instruments. There are two riser systems, which can run alternatively. The two riser systems are:

1. a 4 inch riser system and
2. a 2 inch riser system.

3.2.2.1 The 4 inch riser system

The 4 inch riser is a catenary riser with upstream pipeline length of 55m, which is inclined downwardly at 2°. The riser height is also about 10.5m. The upstream pipeline connects to the riser at the riser base. Fluid supply for the 4 inch riser system comes from the three independent single-phase sources for oil (dielectric 250), water and air. The supplied fluid mixes at a mixing point before flowing into the 55m pipeline, which connects to the riser at the base. A pressure transmitter, which is labeled PT401 in Figure 3.1 is installed at the

riser base, to measure pressure at the base of the riser. At the end of the riser, there is one Endress and Hauser (E+H) 4 inch Coriolis mass flow meter, which is labeled FT407 in Figure 3.1, installed in the vertical section before the two-phase separator. A pressure transmitter (PT408) is installed at the top of the riser to measure pressure at the riser top. A 4 inch automatic control valve, also labeled VC404 in Figure 3.1, is installed between the riser and the two-phase separator to regulate the riser outlet flow rate.

3.2.2.2 The 2 inch riser system

The 2 inch riser is a vertical riser with upstream pipeline length of 39m inclined downwardly at 2°. The riser height is about 10.5m. Fluid supply for the 2 inch riser system is supplied from three independent single-phase sources for oil (dielectric 250), water and air. The supplied fluid mixes at a mixing point before flowing into the 39m pipeline, which connects to the riser. At the end of the riser, there are two Endress and Hauser (E+H) 2 inch Coriolis mass flow meters, installed in the vertical and horizontal section before the two-phase separator. A 2 inch automatic control valve, labeled VC403 in Figure 3.1, is installed between the riser and the two-phase separator to regulate the riser outlet flow rate.

3.2.2.3 Two-phase separator

The two phase separator is located at the top of both riser. It is designed to receive and process fluid from both risers. It is approximately 1.2m high and 0.5m in diameter. It consists of a gas outlet automatic control valve labeled VC401

(see Figure 3.1), a liquid outlet automatic control valve (VC402), a pressure transmitter (PT403) and a liquid level transmitter (LI405).

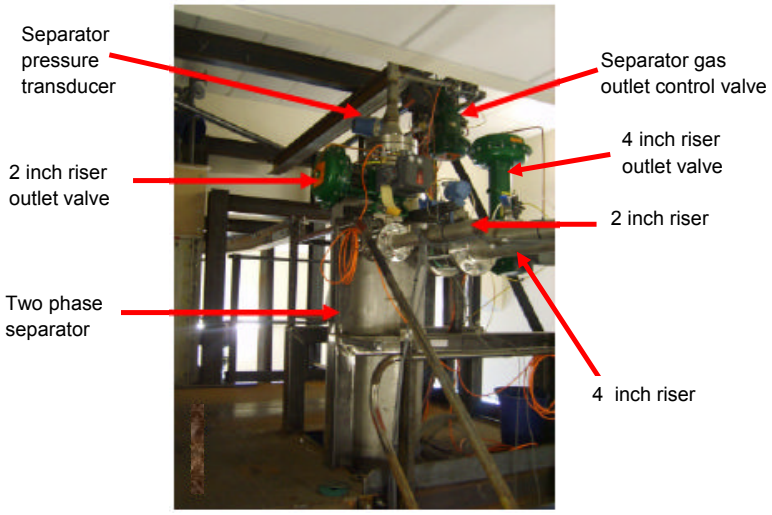

Figure 3.3: Two phase separator picture at the test section

The liquid flow out of the two phase separator is metered by a 2 inch Micro Motion Mass flow meter (FT406). A 3 inch bypass flow line with manual valve is also installed for liquid flow out of the separator. The bypass flow line is used for experiments with high liquid flow rate of about 7kg/s and above.

3.2.3 Phase separation section

The phase separation section receives the liquid and gas from the two phase separator. This section comprises of a 3-phase separator and two coalescers.

3.2.3.1 The three-phase separator

Gravity separation of the three phase flow into their single phases of oil, water and air is achieved in the three-phase separator. There are three sets of controllers, namely, pressure controller, oil-water interface level controller and gas-liquid level controller. The oil/water interface level is controlled by manipulating the control valves labeled VC502 and VC503 (see Figure 3.1), using a Split Range Control Module. For low flow rate out of the separator, the VC502 is used while for high flow rate VC503 is used. Also, the air/oil interface level is controlled by manipulating the control valves labeled VC505 and VC506, using a Split Range Control Module. For low flow rate out of the separator, the VC505 is used while for high flow rate VC506 is used. The oil and water released from the 3-phase separator flows in to the oil-water coalescer. The oil-water coalescer is used to achieve a more efficient separation of the oil and water phases. There are two coalescers. Each coalescer has an oil-water level controller. The oil and water released from the coalescers flow into their respective storage tanks.

3.3 Running the experiments

To run the experiment, firstly the manual control valves at the valve manifold are positioned in the right order for the riser system required for the experiment. This is very necessary to ensure that the liquid and gas flow through the required riser system safely. The compressor is then powered ON. The liquid pump is powered ON and controlled through the DeltaV control system. The desired liquid and air flow rates are set in the DeltaV flow metering environment. Each set flowrate is controlled to the set value by the DeltaV control system. The experimental data is obtained through the data acquisition system (see section 3.4).

3.3.1 Operating condition

Before commencing each experiment, the operating condition of the experimental facility is set to a suitable condition to ensure that the system can generate the required severe slugging flow regime. This is achieved by monitoring the system through the DeltaV system. The outlet pressure of the three phase separator is controlled at 1 barg for all the experiments. The temperature varies between 22^{o}C to 25^{o}C during the experiments. The liquid and air flow rate is controlled by the supervisory control and data acquisition (SCADA) software, DeltaV.

3.4 Data acquisition system

The multiphase test facility is controlled by a supervisory control and data acquisition (SCADA) software, DeltaV. This software is supplied by Emerson Process Management. The process data from the measuring instruments are connected to the DeltaV system in the control room. All pressure controllers, flow controllers, level controllers and safety interlocks are maintained and controlled by the DeltaV. The sampling rate of all the signals managed by DeltaV system is at 1 Hz rate. The recorded signals are stored in the DeltaV Historian database. The data can be downloaded from the DeltaV system for each variable after the experimental period.

3.5 Industrial riser system

The industrial riser system is an 8 inch riser-pipeline system consisting of a 5000m long pipeline, a 120m high riser and a pressure driven well of 69 barg. The reservoir temperature is 70^{o}C and the its production index is 10.12 Sm^3/d/bar (4.4 SBbl/d/psi). An additional gas lift source with a constant mass flowrate is applied to the well-head. The riser top has an 8 inch valve at the outlet. The schematic diagram of the generic riser system is shown in Figure 3.4. The industrial riser system is modelled using the commercial multiphase flow simulator OLGA, and the improved simplified riser model (ISRM). The development of the ISRM will be discussed in Chapter 4.

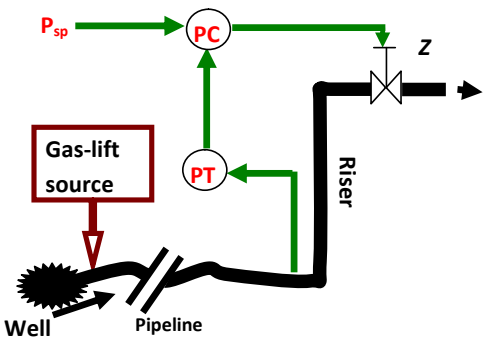

Figure 3.4: Schematic diagram of the industrial riser-pipeline system

3.6 Flow rate and operating conditions

The flow rate and pressure conditions used in all three riser-pipeline systems are summarised in Table 3.1.

Table 3.1: Flow rate and operating operating conditions

Riser Systems	Top separator pressure (barg)	Liquid source type	Liquid flow rate (kg/s)	Gas flow rate (kg/s)
2 inch	1	Constant flow rate	0.75	0.0033
4 inch	1	Constant flow rate	2	0.0067
Industrial riser (8 inch)	30	Well at 69 barg	Pressure dependent	0.525

Chapter 4

Plant-wide modeling for severe slugging prediction and control

4.1 Introduction

In this chapter, the modeling of the major system units of the riser-pipeline system for severe slug flow prediction and control performance analysis is discussed. In order to study the non-linear characteristics of severe slugging and design a robust control system for its suppression, a reliable model of the riser-pipeline system is required. Such a model should be able to predict the non linear characteristics of the severe slug flow. With slug control design in mind, such a model should, in addition to predicting severe slugging, be able to predict control performances required for slug controller design. Thus, a model that would be relevant for gaining the fundamental understanding of the severe slug control would be one that has the ability to:

1. predict severe slugging
2. estimate control performance

In order to ensure that the predicted flow characteristics are reliable and represents the real system behaviour, the modeling of the major system units of the riser-pipeline production system will be required.

4.2 Plant-wide model

In line with the objectives of this project, which is to study severe slugging control in a plant-wide scale, the modeling of the major system units of the riser production system and their performances is discussed in this section. The severe slug predicting model, which contains the models of the major system units of the riser-pipeline production system is known as a plant-wide model. To develop the plant-wide model, these major system units namely: the riser-pipeline, the topside separator and the pressure driven fluid source are modelled and linked together. Experimental studies have shown that the interaction between the process variables in these systems, such as pressure, affect the ability to control severe slugging [116].

4.2.1 The riser-pipeline model

The riser-pipeline model is a very important part of the plant-wide model. One major condition for the occurrence of severe slugging is the inclination of the pipeline, upstream of the riser inlet. A number of severe slug models have been developed using only the pipeline and the riser as a single unit [6, 67, 103]. The challenge with these models is their ability to accurately predict the nonlinear characteristics of severe slugging and the control performances of the system

without complex and unrealistic mathematical solutions. The suitability of some riser-pipeline models for severe slug control design will be briefly discussed.

4.2.1.1 Suitability of riser-pipeline models

A reliable slug controller is required for the study and the analysis of the control performance of the slug control system. In order to design a model based slug controller, a linearised model is normally desired. The linearisation of a nonlinear model requires that the internal equations of the nonlinear model should be readily accessible, and that the linearisation should be performed with the existing tools and methods. The two fluid model, the drift flux model and commercial multiphase flow simulators such as the OLGA models, are some of the exisiting models, which can predict severe slugging. However, there are some challenges with the application of these models in slug control design and performance analysis.

The two fluid model is based on mass and momentum balance for each phase while the drift flux model applies mass balance equation for each phase and a combined momentum balance for all the phases [46]. Both models are expressed in partial differential equations (PDEs) [102]. To obtain a model in ordinary differential equations (ODEs) for control design, the PDE model has to be transformed by space discretisation. However, the order of the model obtained from this process can be very high such that the numerical optimisation required for model based controller design gets complicated. This limits the application of both PDE models in model based design for severe slugging control. A model based on commercial simulators such as OLGA, cannot provide readily accessible internal equations due to commercial reasons, making

it unsuitable for linearisation. With these challenges, the need for a simplified severe slug model arises.

4.2.1.2 Simplified riser model (SRM)

An attempt to develop a simplified riser model (SRM), which can predict severe slugging as well as estimate relevant control performance, was made by Storkaas et al in 2005 [102]. The conservation equations of the SRM are described in this section. The simplified representation of the riser-pipeline system used to develop the SRM is shown in Figure 4.1.

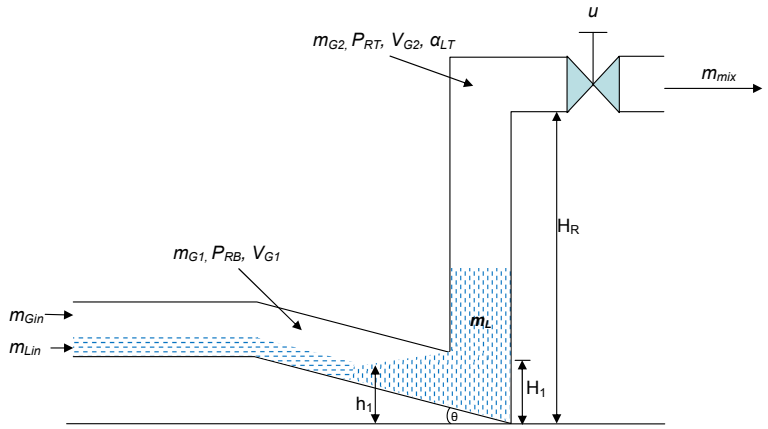

Figure 4.1: Riser-pipeline schematic diagram for the SRM

Based on Figure 4.1, the SRM was developed with three dynamical states, which account for the:

1. mass of gas in the pipeline, m_{G1}
2. mass of gas at the riser top, m_{G2}
3. mass of liquid in the riser, m_L

The corresponding conservation equations are given in (A.1), (A.2) and (A.3).

$$\frac{dm_{G1}}{dt} = m_{Gin} - m_G \tag{4.1}$$

$$\frac{dm_{G2}}{dt} = m_G - m_{Gout} \tag{4.2}$$

$$\frac{dm_L}{dt} = m_{Lin} - m_{Lout} \tag{4.3}$$

From Figure 4.1, it can be observed that severe slugging is initiated when $h_1 \geq H_1$, such that the riser base is blocked by liquid, where h_1 is the liquid height in the riser base and H_1 is the critical liquid height. In this condition, the gas mass flow rate, m_G, into the riser will be zero ($m_G = 0$). If $h_1 < H_1$, then the riser base is not blocked by the liquid, such that there is continuous flow of gas into the riser. Under this condition, the gas mass flow rate into the riser is dependent on the gas flow area, A, and the pressure drop at the riser base. The full description of the SRM, showing the state dependent equations, the flow equations and the entrainment model equations is given in Appendix A.

In order to design an efficient slug controller for the physical plant, a validation of the model's predictions against experimental results is required. Experimental result obtained from the riser systems in the Cranfield University multiphase flow lab showed that the capability of the SRM is limited due to some assumptions [77]. These assumptions and limitations are discussed below.

Limitations of the SRM

The assumptions that limit the performance of the SRM are highlighted below:

1. The riser outlet pressure (separator pressure), P_s, is assumed to be constant, which effectively means a separator with an infinite volume connected at the riser outlet. This does not represent any real system as the dynamics of the topside processing equipment (the separator) has a significant effect on the severe slugging behaviour as was demonstrated in previous work by Yeung et al [116].

2. The model does not account for the slug production stage, which occur in the severe slug cycle. The omission of this stage affects the prediction of liquid flow pattern out of the riser, and limits the application of the model in analysing the accumulated production over a production period, during severe slugging.

3. The assumption of constant pipeline gas volume (V_{G1}) in the pipeline, which implies constant liquid hold up, limits the prediction of the slug amplitude and frequency accurately simultaneously. According to Storkaas (2005, pp 47), *"..the simplified three state model predicts a slug frequency that, compared to the OLGA simulations, is about 10-20% too high for low-to-medium range valve openings and up to about 50% too high for large valve openings. The higher frequency probably comes from neglecting the liquid dynamics in the feed section. ...and when the upstream gas volume is fixed, we cannot achieve both frequency and amplitude simultaneously"*. Consequently, the model only offers the choice of predicting accurate slug amplitude or frequency at a time, not both.

4. The model assumes fixed liquid and gas inlet flow rates. Any change to the inlet flow rates will require re-tuning the model parameters. Therefore,

the inlet flow rates cannot be altered during a simulation. This limits the application of the model in analysing the impact of severe slugging control on production, with a pressure dependent fluid source.

In view of these limitations, a further mechanistic modeling effort is required to improve the performance and reliability of the SRM. This has led to the development of the improved simplified riser model (ISRM).

4.3 Improved simplified riser model (ISRM)

In this section, the development of the improved simplified riser model (ISRM), which is an improved model of the SRM is discussed. The simplified representation of the riser-pipeline system used to develop the ISRM is shown in Figure 4.2. This schematic diagram shows the riser-pipeline with the position of the separator and the linear well. In the ISRM, the assumptions made in the

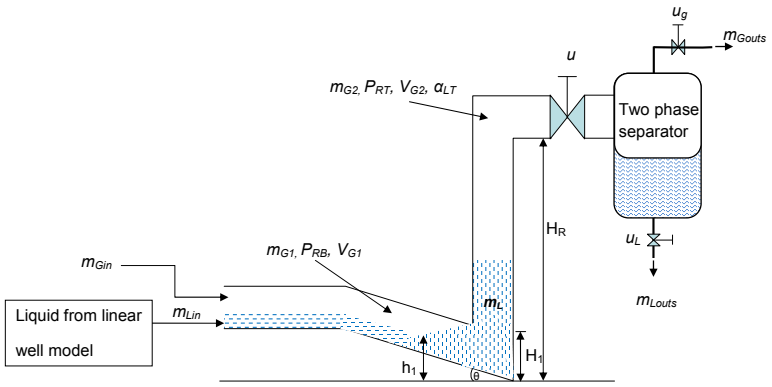

Figure 4.2: Riser-pipeline schematic diagram for the ISRM

SRM, as discussed above, are relaxed to eliminate the associated limitations.

The upstream gas volume, which is assumed constant in the SRM is modelled as a function of the dynamic pipeline pressure and fluid inlet flow rates, while the accumulated liquid upstream the riser inlet is modelled to enhance the prediction of the slug production stage. In addition, a topside two phase separator model and a linear well model are developed and linked to the ISRM to make up the ISRM with well and separator model.

4.3.1 Conservation equations of the ISRM

The ISRM consists of five dynamical state equations which account for:

1. mass of gas in the pipeline, m_{G1}
2. mass of gas at the riser top, m_{G2}
3. mass of liquid in the riser, m_L
4. separator top pressure, P_s
5. separator liquid height, h_L

The corresponding conservation equations for the m_{G1}, m_{G2} and the m_L are given in (4.4), (4.5) and (4.6) respectively.

$$\frac{dm_{G1}}{dt} = m_{Gin} - m_G \tag{4.4}$$

$$\frac{dm_{G2}}{dt} = m_G - m_{Gout} \tag{4.5}$$

$$\frac{dm_L}{dt} = m_{Lin} - m_{Lout} \tag{4.6}$$

The conservation equations for the P_s and the h_L, which are given in (4.7) and (4.8) result from the modeling of the two-phase separator to achieve dynamic riser outlet boundary condition. This eliminates the constant outlet boundary condition in the SRM. The two-phase separator modeling is presented in section 4.3.1.1.

$$\frac{dP_s}{dt} = \frac{P_s}{A_s(H_s - h_L)} \left[(Q_{Gins} - Q_{Gouts}) + A_s \frac{dh_L}{dt} \right] \tag{4.7}$$

In 4.7, A_s is the separator cross sectional area, H_s is the separator height and h_L is the liquid level in the separator, Q_{Gins} is the gas volume flow rate into the separator, and Q_{Gouts} is the gas volume flow rate out of the separator.

$$\frac{dh_L}{dt} = \frac{m_{Lins} - m_{Louts}}{A_s \rho_L} \tag{4.8}$$

In 4.8, m_{Lins} is the liquid mass flow rate into the separator, and m_{Louts} is the liquid mass flow rate out of the separator.

4.3.1.1 Dynamic riser outlet boundary condition - the separator model

In the SRM, the riser outlet pressure is assumed to be constant, which effectively means a separator with an infinite volume connected at the riser outlet. Thus, the dynamic effect of the topside separator on the performance, stability and productivity of the system is neglected. This will affect the ability of the model to accurately predict severe slugging and estimate control performances reliably. To eliminate this condition, a two phase separator model is developed to replace the constant pressure condition at the riser outlet. The schematic

diagram and dimension of the vertical two phase separator at the multiphase facility at Cranfield University is shown in Figure 4.3. The dimension of the separator can easily be changed in the model for different separator volumes. The

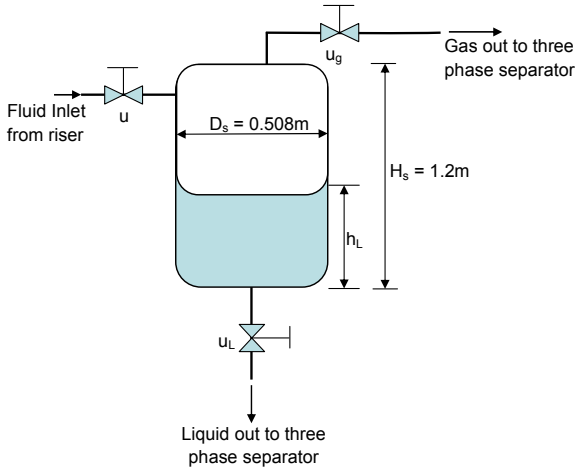

Figure 4.3: Two phase separator diagram

two phase separator model is a two state model, which accounts for the separator top pressure and the separator liquid level. The liquid level depends on the mass balance between the liquid flow rate into the separator, m_{Lins}, and the liquid flow rate out of the separator, m_{Louts}, as described by the conservation equation given by (4.9).

$$\frac{dh_L}{dt} = \frac{m_{Lins} - m_{Louts}}{A_s \rho_L} \tag{4.9}$$

where A_s is the separator cross sectional area, ρ_L is the liquid density, h_L is the liquid height.

The separator pressure depends on the gas mass balance and it is modeled based on the ideal gas law. Based on the ideal gas law given in (4.10), P_s is the separator pressure, V_G is the volume occupied by gas, R is the ideal gas constant, T is the separator temperature and n is the number of moles.

$$P_s V_G = nRT \tag{4.10}$$

The volume occupied by the gas V_G is given by:

$$V_G = A_s(H_s - h_L) \tag{4.11}$$

By taking the partial differential of (4.10), (4.12) is obtained.

$$P_s \frac{dV_G}{dt} + V_G \frac{dP_s}{dt} = RT \frac{dn}{dt} \tag{4.12}$$

The number of moles, n, is given by (4.13),

$$n = \frac{m}{M} \tag{4.13}$$

where m is the mass of gas in the separator and M is the molecular weight of the gas. By, substituting (4.13) into (4.12), (4.14) is obtained,

$$P_s \frac{dV_G}{dt} + V_G \frac{dP_s}{dt} = \frac{RT}{M} \frac{dm}{dt} \tag{4.14}$$

and

$$\frac{dm}{dt} = m_{Gins} - m_{Gouts} \tag{4.15}$$

where m_{Gins} is the gas mass flow rate of gas into the separator, and m_{Gouts} is the gas mass flow rate out of the separator. It is assumed that the pressure in the pipeline at the separator inlet will be approximately the same with the separator pressure. Thus, expressing (4.15) in terms of volumetric flow rate, (4.16) is obtained,

$$\frac{dm}{dt} = \rho_{Gs}(Q_{Gins} - Q_{Gouts}) \tag{4.16}$$

where ρ_{Gs} is the density of gas in the separator. By substituting (4.16) into (4.14), (4.17) is obtained.

$$P_s \frac{dV_G}{dt} + V_G \frac{dP_s}{dt} = P_s(Q_{Gins} - Q_{Gouts}) \tag{4.17}$$

By substituting (4.11) into (4.17), (4.18) is obtained.

$$P_s \frac{A_s d(H_s - h_L)}{dt} + A_s(H_s - h_L)\frac{dP_s}{dt} = P_s(Q_{Gins} - Q_{Gouts}) \tag{4.18}$$

Rearranging (4.18) for $\frac{dP_s}{dt}$, the dynamic equation for the separator pressure is obtained as given in (4.19).

$$\frac{dP_s}{dt} = \frac{P_s}{A_s(H_s - h_L)}\left[(Q_{Gins} - Q_{Gouts}) + A_s\frac{dh_L}{dt}\right] \tag{4.19}$$

4.3.2 State dependent variables

The state dependent variables such as the riser base pressure, P_{RB}, and riser top pressure, P_{RT}, are calculated using the ideal gas law, and are given by (4.20) and (4.21), where V_{G1} is the volume of gas in the pipeline, V_{G1}, and V_{G2} is the volume of gas at the riser top.

$$P_{RB} = \frac{m_{G1}RT}{V_{G1}M_G} \tag{4.20}$$

$$P_{RT} = \frac{m_{G2}RT}{V_{G2}M_G} \tag{4.21}$$

The volume of gas in the pipeline, V_{G1}, which was assumed constant in the SRM is modeled in the ISRM to achieve dynamic update of its value based on the flow rate into the pipeline.

4.3.2.1 Dynamic update of upstream gas volume

Slug growth and frequency is a function of the dynamic pipeline pressure, which in turn depends on the varying compressible gas volume in the pipeline [97, 109]. Consequently, with varying inlet flow rates, the SRM requires a dynamic upstream gas volume rather than a constant upstream gas volume for slug frequency tuning. Since the flow regime in the pipeline during severe slugging is stratified, the upstream gas volume in the pipeline, V_{G1}, can be calculated by determining the gas volume fraction, α_G, at the pipeline pressure. The pipeline pressure is approximated with the riser base pressure P_{RB}. Assuming constant temperature and no slip effect, the α_G is given by:

$$\alpha_G = \frac{Q_{Gin}}{Q_{Gin} + Q_{Lin}} = \frac{(\frac{m_{Gin}}{\rho_G})_{P_{RB}}}{(\frac{m_{Gin}}{\rho_G})_{P_{RB}} + (\frac{m_{Lin}}{\rho_L})} \tag{4.22}$$

where ρ_G is the gas density at the pipeline pressure, ρ_L is the liquid density, P_{RB} is the riser base pressure and m_{Gin} and m_{Lin} are the gas and liquid inlet mass flow rate respectively, while Q_{Gin} and Q_{Lin} are the gas and liquid inlet volumetric flow rate respectively. The upstream gas volume can be calculated based on these parameters as:

$$V_{G1} = A_p L \alpha_G \tag{4.23}$$

where A_p is the cross sectional area of the pipeline and L is the length of the inclined pipeline. Thus, the V_{G1} is dynamically calculated in the model as a function of the pipeline pressure. This eliminates the limitation imposed by fixed upstream gas volume, which requires a fixed fluid inlet flow rate, as obtained in the SRM.

4.3.2.2 Gas volume at the riser top

The volume of gas at the riser top, V_{G2}, is calculated as:

$$V_{G2} = V_T - V_{LR} \tag{4.24}$$

where V_{LR} is the volume of liquid in the riser, and the total volume, V_T, is given by 4.25, where L_h is the length of the horizontal pipe at the riser top, upstream the separator.

$$V_T = A_p(H_R + L_h) \tag{4.25}$$

4.3.2.3 Internal gas flow rate

From Figure 4.2, severe slugging is initiated when the liquid level upstream the riser inlet, h_1, is greater than or equal to the critical liquid height, H_1, ($h_1 \geq H_1$) such that the riser base is blocked by the liquid. In this condition, the gas mass flow rate, m_G, into the riser will be zero ($m_G = 0$). If $h_1 < H_1$, then the riser base is not blocked by the liquid, such that there is continuous flow of gas into the riser. Under this condition, the gas mass flow rate into the riser is dependent on the gas flow area, A, and the pressure drop at the riser base. Thus, the gas mass flow rate into the riser is given by:

$$m_G = v_{G1}\rho_{G1}A \tag{4.26}$$

where the gas density in the pipeline is given by (4.27), and the internal gas velocity v_{G1} is given by (4.28).

$$\rho_{G1} = \frac{m_{G1}}{V_{G1}} \tag{4.27}$$

$$v_{G1} = K_2 \frac{H_1 - h_1}{H_1} \sqrt{\frac{P_{RB} - P_{RT} - \rho_L g \alpha_L H_R}{\rho_{G1}}} \tag{4.28}$$

In (4.28), α_L is the liquid volume fraction in the riser, H_R is the riser height, H_1 is the critical liquid height, h_1 is the liquid level upstream the riser inlet, K_2 is the gas flow constant, $\frac{H_1 - h_1}{H_1}$ is the relative gas flow opening, which depends relatively on the liquid level.

4.3.3 Entrainment equation

The entrainment equation is also developed to model the distribution of fluid in the riser. This is achieved by modeling the volume fraction of the liquid that is exiting the riser top, α_{LT}. In the ISRM, this model includes the liquid volume in the pipeline upstream the riser base, which determine the occurrence of the slug production stage in the severe cycle. This was neglected in the SRM. The modeling of the liquid volume in the pipeline upstream the riser base is discussed in section 4.3.3.1 below.

4.3.3.1 Prediction of the slug production stage

The slug production stage observed in the severe slug cycle is an unstable steady state period with constant pressure at the riser base. This usually occurs when the riser column is filled with liquid, such that the static pressure head across the riser cannot increase further. This condition is sustained by the complete blocking of the riser inlet by liquid and the continuous liquid flow into the riser from the pipeline, with the overflow at the riser top. The sustenance

of this condition is dependent upon the liquid accumulated in the pipeline, upstream the riser inlet.

Thus, the slug production period in which the riser base pressure is constant, is the time it takes to push this liquid column into the riser by the compressed gas pressure (see section 1.1.2 and 1.1.2.1). Consequently, the slug production stage will contribute to the accumulated liquid production in each slug cycle. In order to predict the slug production stage in the severe slug model, this pipeline liquid column must be modelled.

In the modeling of the the liquid production at the top of the riser in the SRM this liquid volume in the pipeline upstream the riser inlet is neglected. Thus, the SRM cannot accurately predict the slug production stage in the severe slug cycle.

Figure 4.4 shows the schematic diagram of the riser with the accumulated liquid volume in the pipeline upstream the riser. The accumulated liquid volume can be approximated with the projected geometry from the pipeline, as shown in Figure 4.4.

In the projected geometry, the area of the circular part is the cross sectional area of the pipeline (A_p). The accumulated liquid height is given as h_1. The internal gas area (A) is the area through which gas can penetrate into the riser from the liquid top. If the riser inlet is completely blocked, such that h_1 is equal to the internal pipe diameter (D_p) then $A = 0$. In this condition, the effective area of the circular part is equal to A_p. However, if the $A \neq 0$, then the effective area of the circular part will be equal to $A_p - A$. Thus, the volume of the liquid accumulated in the pipeline, upstream riser inlet (V_{LP}), as represented by the above geometry can be obtained as:

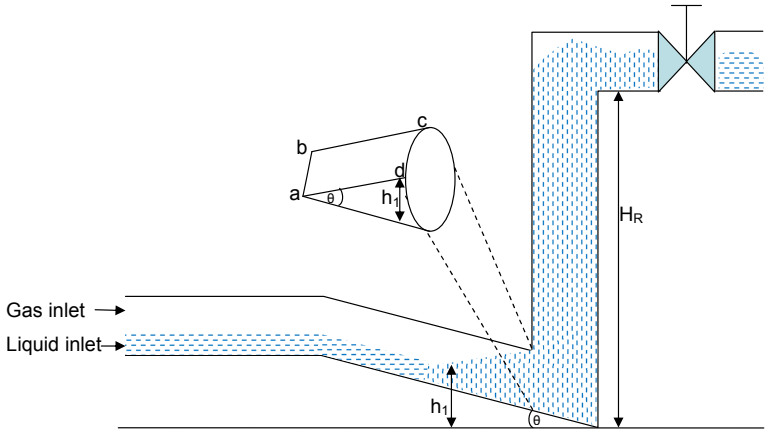

Figure 4.4: Riser base pressure from experiment

$$V_{LP} = \frac{(A_p - A)h_1}{\sin\theta} \tag{4.29}$$

Equation (4.29) is used as part of the model for the liquid production from the riser for each slug cycle, as shown in (4.30).

The total liquid fraction reaching the riser top, α_{LT}, is therefore modeled as given by (4.30),

$$\alpha_{LT} = \left(V_{LR} + \frac{h_1(A_p - A)}{\sin\theta} > V_T\right)\left[\frac{V_{LR} + (\frac{h_1(A_p-A)}{\sin\theta} - V_T}{A_p L_h}\right], \\ + \frac{w^n}{1+w^n}\left[\alpha_L - \left(V_{LR} + \frac{h_1(A_p - A)}{\sin\theta} > V_T\right)\left(\frac{V_{LR} + (\frac{h_1(A_p-A)}{\sin\theta}) - V_T}{A_p L_h}\right)\right] \tag{4.30}$$

where θ is the angle of inclination of the pipeline, w is the flow transition parameter which is given by (4.31), A_p is the pipe cross sectional area and L_h is the lenght of the riser top horizontal part.

$$w = \frac{K_3 \rho_{G1} v_{G1}^2}{\rho_L - \rho_{G1}} \tag{4.31}$$

4.3.4 Fluid flow out of the riser

Total fluid flow out of the riser, m_{mix}, is calculated using a simplified valve equation given by (4.32), where K_1 is the valve coefficient.

$$m_{mix} = K_1 u \sqrt{\frac{\rho_T (P_{RT} - P_s)}{g}} \tag{4.32}$$

The total fluid density, ρ_T, is given by (4.33), and gas density at riser top, ρ_{G2}, is given by (4.34).

$$\rho_T = \alpha_{LT}\rho_L + (1 + \alpha_{LT})\rho_{G2} \tag{4.33}$$

The gas density at the riser top, ρ_{G2}, is given by (4.34) and the total volumetric flow rate at the riser top is given by (4.35).

$$\rho_{G2} = \frac{m_{G2}}{V_{G2}} \tag{4.34}$$

$$Q_T = \frac{m_{mix}}{\rho_T} \tag{4.35}$$

The gas mass flow rate out of the riser is given by (4.36), while the liquid mass flow rate out of the riser is given by (4.37), where α_L^m is the liquid mass fraction.

$$m_{Gout} = (1 - \alpha_L^m) m_{mix} \tag{4.36}$$

$$m_{Lout} = \alpha_L^m m_{mix} \tag{4.37}$$

4.3.4.1 Pressure driven fluid source

The modeling of the pressure driven source is considered very important due to the dependency of the system stability and production on the pressure dynamics of the entire system. The use of constant flow rate source in slug control

analysis does not represent the actual operating condition of the riser-pipeline system in the offshore fields. Thus, the modeling of a pressure driven source whose fluid supply is dependent on the pressure interaction with the downstream processes will be discussed in this section. These pressure interactions and their effects on production will be discussed in detail in Chapter 6.

The pressure driven sources will differ in the environment of its application. In the laboratory application, such as the Cranfield multiphase flow laboratory, the pressure driven sources will be in the form of liquid pumps and gas compressors. However, in the offshore oil and gas field, the pressure driven source will be the oil and gas wells, and sometimes, a gas or liquid injection systems. From these systems, the pressure driven source can be classified into two main types, namely:

1. pressure driven liquid source
2. pressure driven gas source

In the offshore application, the pressure driven liquid source is the oil and water wells, while in the laboratory application, it is the liquid pumps. The pressure driven gas sources in the offshore application could be the gas wells and the gas injection systems, while in the laboratory application, it is the gas compressors. Among these systems, the focus will be on modeling the pressure driven liquid sources. Since the pump delivery flow rate is controlled, the focus will be on developing a linear liquid well model.

The linear well model as a pressure driven source

The linear well is modelled specifically to obtain the well liquid mass production rate, q_w. Detailed analysis of the properties of a linear well is given by Jamal et al [49]. The linear well production rate is given by:

$$q_w = \frac{G_f}{B\mu}(P_{res} - P_w) \tag{4.38}$$

where B is the formation volume factor (FVF), μ is the viscosity of the liquid, P_{res} is the reservoir pressure and P_w is the well bore hole pressure. G_f is the reservoir geometric factor defined by:

$$G_f = \frac{2\pi B_c K_h h_r}{\ln(\frac{R_{eq}}{R_w}) + s} \tag{4.39}$$

where B_c is the reservoir transmissibility factor, K_h is reservoir permeability, R_{eq} is the reservoir external radius, R_w is the reservoir inner radius, h_r is the reservoir thickness and s is the reservoir skin (damage, $0 < s < 1$).

The permeability, K_h is given by:

$$K_h = (K_x K_y)^{0.5} \tag{4.40}$$

while the R_{eq} is given by:

$$R_{eq} = 0.28\frac{\left[\left(\frac{K_y}{K_x}\right)^{0.5} L_x^2 + \left(\frac{K_x}{K_y}\right)^{0.5} L_y^2\right]^{0.5}}{\left(\frac{K_y}{K_x}\right)^{0.25} + \left(\frac{K_x}{K_y}\right)^{0.25}} \tag{4.41}$$

where K_x is the reservoir permeability in the x-direction, K_y is the reservoir permeability in the y-direction, L_x reservoir length in x-direction, L_y reservoir length in y-direction.

4.3.5 ISRM and SRM tuning parameters

The procedure for tuning the SRM was provided by the Storkaas [98]. However, the improvements provided by the ISRM has simplified the tuning procedure for the model. Figure 4.5 shows the flow chart, which summarises the tuning procedure for the two models.

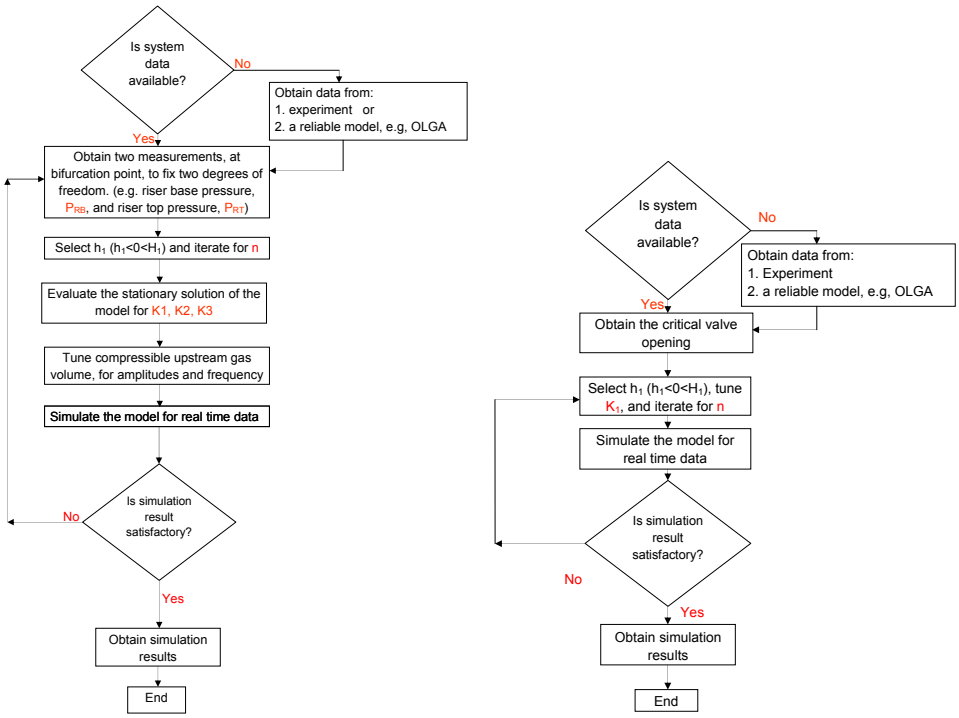

(a) SRM tuning (b) ISRM tuning

Figure 4.5: Model tuning flow chart

The SRM requires the tuning of six parameters including four empirical parameters, which include the riser top valve coefficient, K_1, the internal gas flow coefficient, K_2, the entrainment model parameters, K_3 and n, and some physical parameters such as the upstream gas volume, V_{G1}, and the average molecular weight of the gas, M_G. However, the ISRM requires the tuning of only

two parameters, which are the riser top valve coefficient and the entrainment model parameter, n. In the ISRM, other parameters tuned in the SRM are generated and updated dynamically as the inlet flow rate (condition) changes, consequently, they require no tuning in order to predict severe slugging.

The values of the tuning parameters used for the modeling of the 4 inch riser system in the SRM and the ISRM are shown in table 4.1.

Table 4.1: Tuning parameters for the SRM and the ISRM

		Value	
Parameter	Unit	SRM	ISRM
K_1	-	0.3	0.3
n	-	1.5	1.5
K_2	-	7.22	-
K_3	s^2/m^2	2.25	-
V_{G1}	m^3	0.24	-
M_G	kg/kmol	28.97	-

4.3.6 Performances of the ISRM with separator model

In this section, the performance of the ISRM is evaluated for relevant flow characteristics and compared with the performance of the SRM. The experimental results are used as a base case for this comparison. The experiments are performed with the 4 inch riser system.

4.3.6.1 Prediction of severe slugging flow with variable fluid inlet flow rate

Figure 4.6 compares the open-loop simulation results from the SRM and the ISRM against the experimental results.

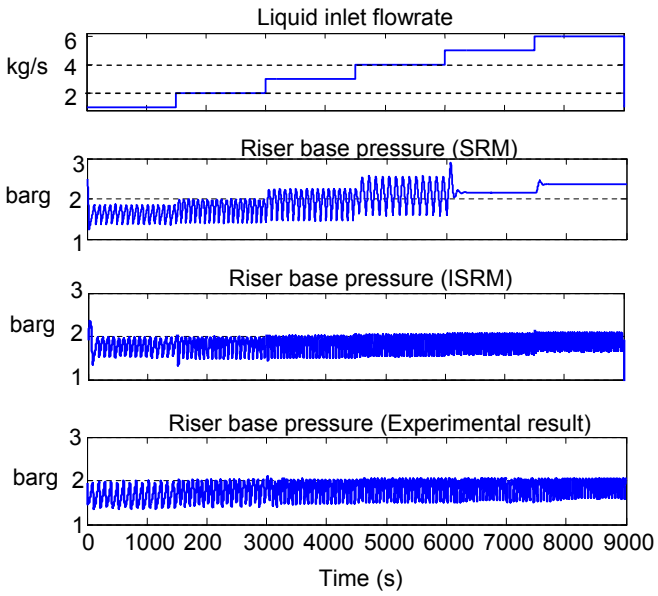

Figure 4.6: Comparison of SRM and ISRM with the experimental result

The simulations and the experiments are performed with the 4 inch riser system. The 4 inch riser system in the experimental facility has been described in section 3.2.2.1. The inlet flow condition is defined with increasing liquid inlet flow rates from 1 kg/s to 6 kg/s at a constant gas flow rate of 20 Sm^3/h. The riser top valve is at 100% opening. The P_{RB} profile is measured for each case and analysed.

The analysis showed that in the experimental result, the slug frequency and the P_{RB} increased from 0.013 Hz and 2 barg respectively at 1 kg/s of water

to 0.02 Hz and 2.08 barg respectively at 6 kg/s. The original SRM predicts reduced slug frequency from 0.013 Hz at 2 kg/s liquid flow rate to 0.007 Hz at 4 kg/s liquid flow rate, with a large increase in pressure. Maximum riser base pressure predicted at 4 kg/s water flow rate is 2.5 barg, about 25% higher than the experimental result. At 5 and 6 kg/s water flow rate, the model predicts that the system is stable. However, the ISRM predicts an increase in slug frequency from 0.013 Hz at 1 kg/s to 0.025 Hz at 6 kg/s of water, with slight and gradual increase in riser base pressure from 2 barg at 1 kg/s to 2.1 barg at 6 kg/s as observed in the experimental result. This shows that the ISRM predicts the severe slugging condition of the system at variable inlet flow rates closer to experimental result than the SRM does.

4.3.6.2 Prediction of severe slug frequency and pressure amplitude

The performance of the ISRM in severe slug frequency and pressure amplitude prediction is also evaluated and compared with that predicted with by the SRM. The simulation and experiment is performed with the 4 inch riser, with fluid inlet flow rate of 2kg/s of water and 20 Sm^3/h of gas. Figures 4.7 to 4.10 compares the simulation results obtained from the SRM and the ISRM against the experimental results.

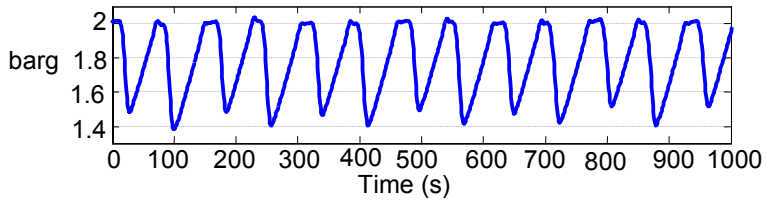

Figure 4.7: Riser base pressure from experiment

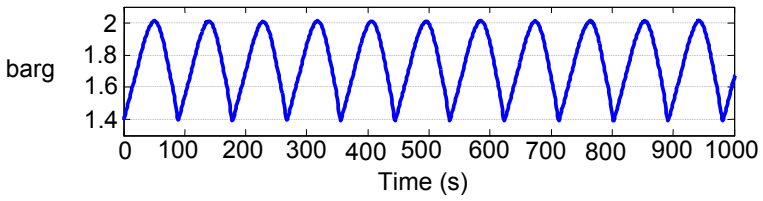

Figure 4.8: Riser base pressure of SRM with amplitude fitted

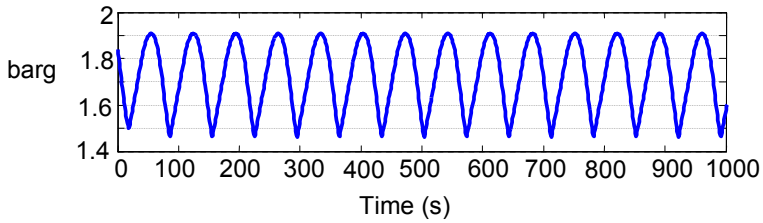

Figure 4.9: Riser base pressure of SRM with frequency fitted

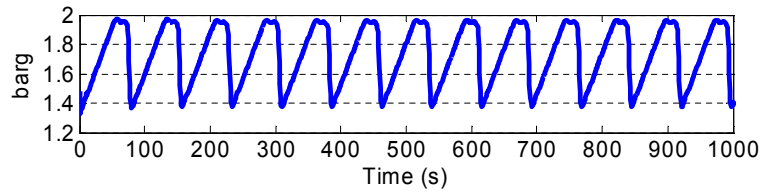

Figure 4.10: Riser base pressure of ISRM with amplitude and frequency fitted

Figure 4.7 shows the experimental data that gives a maximum P_{RB} of 2barg and minimum of 1.4 to 1.5barg and a slug frequency of 0.0133 Hz (1 slug/75 s). The SRM result in Figure 4.8 shows that the slug pressure amplitude is achieved, but the frequency is reduced to 0.011 Hz (1 slug/91 s), when compared to experimental result. In Figure 4.9, the SRM is re-tuned to achieve the right frequency of 0.0133 Hz, but the maximum pressure amplitude is reduces to 1.9 barg. This implies that the slug frequency and amplitude cannot be predicted simultaneously, as discussed in section 4.3. Figure 4.10 shows the ISRM result in which both the pressure amplitude and slug frequency match the experimental result correctly. This performance shows that the dynamic modeling of the pipeline gas volume and the included dynamics of the topside separator as part of the real plant in the ISRM has significantly improved the performance of the model and its ability to predict the severe slug characteristics (frequency and pressure amplitude) accurately.

4.3.6.3 Prediction of the slug production stage

Using the P_{RB}, a typical severe slug pressure profile will show the four stages that occur in the severe slug cycle, as shown in Figure 4.11.

These four stages generate three pressure sections namely: the pressure build up section (section ab), the constant pressure section (section bc) and the pressure drop section (section cd). The slug production stage occurs with a constant pressure at the riser base, which corresponds to section bc in Figure 4.11. The prediction of the slug production stage is very important due to its contribution to the analysis of the overall liquid accumulation in a slug production period.

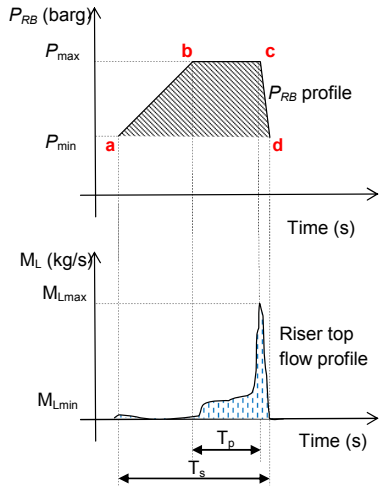

Figure 4.11: Typical severe slug profile

The performance of the ISRM is evaluated for predicting the slug production stage in the severe slug cycle. By using the constant flow rate condition specified for the 4 inch riser in Table 3.1, the experimental result shown in Figure 4.12 is obtained to shows that the slug production stage occur in the severe slug cycle in the system with the constant pressure section. The simulation of the ISRM as shown in Figure 4.13 shows that the slug production stage is also predicted by the model. However, Figure 4.14 shows that the slug production stage is not clearly predicted by the SRM.

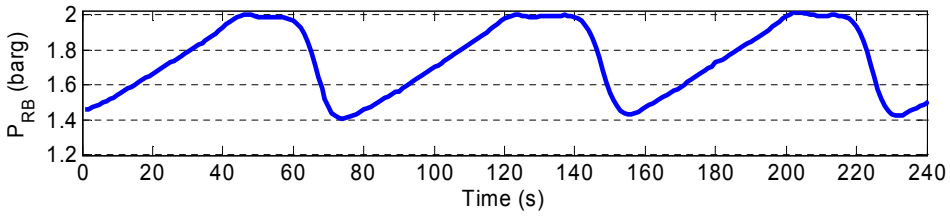

Figure 4.12: P_{RB} profile under severe slugging condition, experimental result

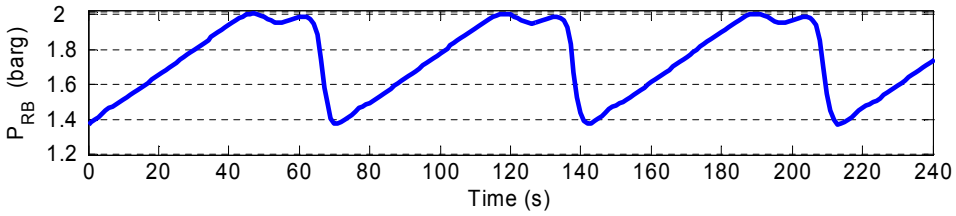

Figure 4.13: P_{RB} profile under severe slugging condition, ISRM

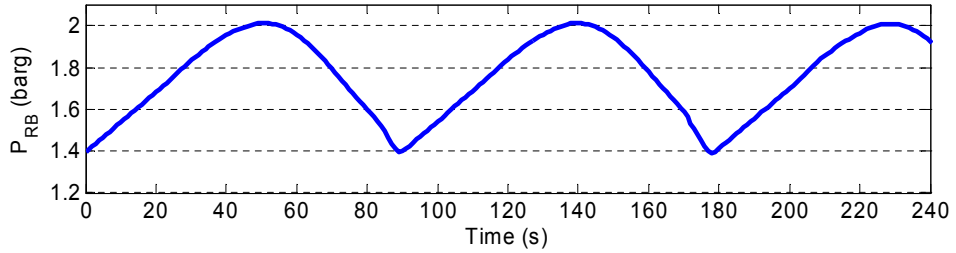

Figure 4.14: P_{RB} profile under severe slugging condition, SRM

This result shows the close agreement between the ISRM results and the experimental results. This makes the ISRM a more reliable model for severe slug characteristic prediction and control performance analysis.

4.3.6.4 Prediction of flow regime map

The performance of the ISRM shows that it can be used to predict severe slug flow regime for a riser-pipeline production system. Various flow combinations can be simulated continuously to predict the flow condition with relative accuracy when compared to experimental result. The prediction of severe slug flow regime map for the 4 inch riser at the multiphase flow laboratory of Cranfield University is carried out through experimental study and the ISRM simulation. About 194 test points for different liquid and gas combinations were simulated.

The test points for typical severe slugging response were identified and plotted in the flow regime map. The flow regime predicted by the ISRM is compared with that obtained from the system through experiments. Figure 4.15 shows the flow regime map obtained through experiment and the ISRM simulation at 1barg separator pressure.

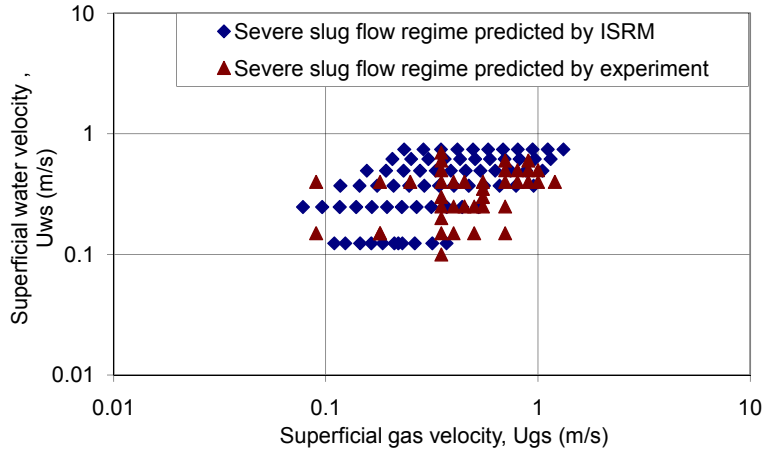

Figure 4.15: Flow regime map of 4 inch catenary riser

Comparing the two flow regime maps, it can be seen that the ISRM predicts a severe slugging locus, which closely agrees with that obtained experimentally. This result which is not possible to be obtained with the original SRM shows the suitability of the improved ISRM for predicting severe slugging for a wide range of flow conditions and for designing a robust control system for an open-loop unstable riser system.

4.4 Model nonlinear stability analyses

The ability of the severe slug model to estimate the nonlinear stability of the system is important in analysing controllability and designing slug controllers. The Hopf bifurcation map and root locus plot will be applied to study the nonlinear stability of the system. This nonlinear stability analyses will be performed using the riser top valve opening, u, on the industrial riser system and using the topside separator gas valve opening, u_g, on the 4 inch riser system as the manipulated variable. The schematic diagram of the riser-pipeline system with the riser top valve, u, and the separator gas valve, u_g, is shown in Figure 5.2.

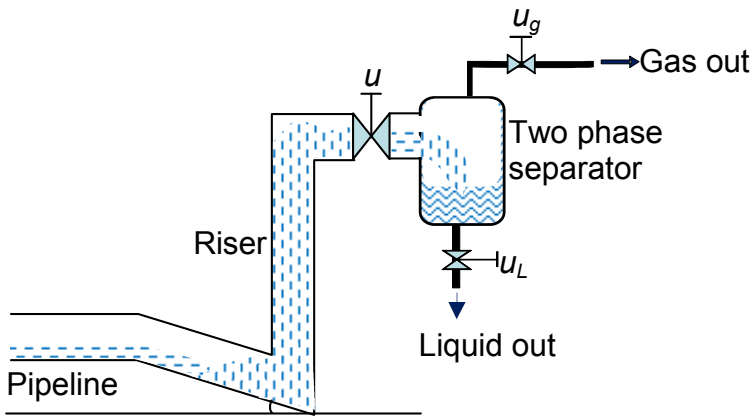

Figure 4.16: Riser pipeline system with u and u_g

4.4.1 Open-loop root locus

The open-loop roots, i.e. the roots of the denominator polynomial of the transfer function of a system can be obtained at any valve opening. These roots are called poles. The unstable response of the riser system gives an oscillatory

response corresponding to a pair of complex poles, $x + iy$, with $x > 0$. Poles can be plotted in the complex plane (s-plane), which has real axis (horizontal-axis) and imaginary axis (vertical-axis). The location of pole(s) obtained at a particular valve opening on the s-plane gives a clear indication on the stability of the plant at that operating point. A pair of complex poles with positive real parts indicates system instability and is located in the right half plane (RHP) of the s-plane. However, for a stable system, all the poles must be located in the left half plane (LHP). This implies that all the poles of a stable system must have a negative real part. Further explanations on why the presence of RHP poles will cause system instability can be found in literature [92, 94].

4.4.2 Hopf bifurcation map

The Hopf bifurcation is a type of bifurcation which occurs when a pair of complex poles crosses the imaginary axis from the left hand plane (LHP) to the right half plane (RHP) of the s-plane. Such crossing of a pair of complex poles across the imaginary axis of the s-plane leads to the vanishing of linear damping in the motion of an oscillator [111]. Thus, when Hopf bifurcation occurs in a system, there is a loss of stability in the system's controlled variable due to changes in an independent variable. For a nonlinear system like the riser-pipeline system, Hopf bifurcation can occur in the controlled variable if changes in an independent variable such as the valve opening causes the system to become unstable at any operating point. The Hopf bifurcation map of a riser-pipeline system can be generated through experimental and simulation studies. The ability of the ISRM to generate the bifurcation map is very important in the analysis of control performance of the riser-pipeline system.

4.4.3 Nonlinear stability analyses of the industrial riser system

Using these nonlinear stability analysis tools discussed in section 4.4.1 and 4.4.2, the ability to predict the stable and the unstable operating points of the industrial riser system using the ISRM can be evaluated. For these analyses, the manipulated variable in the system is the the riser top valve opening (u).

4.4.3.1 Open-loop root locus plot of the industrial riser system

Using the ISRM the open-loop transfer function of the industrial riser system can be obtained at desired operating points. The open-loop poles of the industrial riser model is obtained for the operating points $u = 100\%$ to $u = 12\%$. For each operating point, three poles are obtained. The three poles obtained include two complex poles and a negative real pole. The complex poles are plotted on the root locus plot shown in Figure 4.17.

At $u = 12\%$, the complex poles have negative real part. This indicates that the system is stable at this operating point. For $u > 12\%$, a pair of complex poles cross the imaginary axis into the RHP. Consequently, the poles for u between 100% and 20% all have positive real parts, and are plotted in the RHP as shown in Figure 4.17. This indicates that the system is unstable at these operating points. Thus, while stabilising control will be needed for $13\% \leq u \leq 100\%$, no stabilising control is needed for $u \leq 12\%$, where the system is open-loop stable.

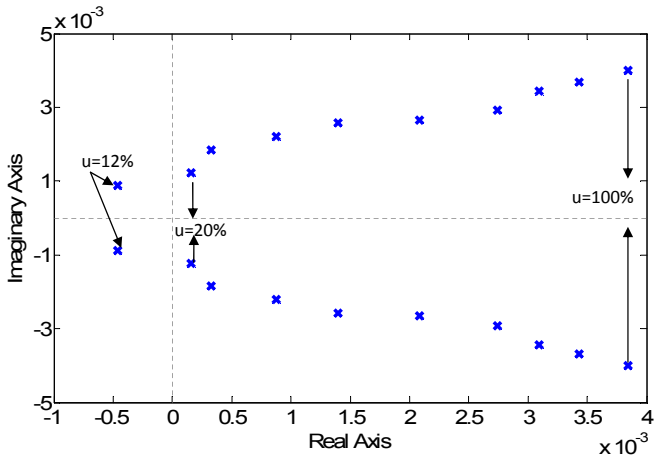

Figure 4.17: Open-loop root locus for the industrial riser system

4.4.3.2 Hopf bifurcation of the industrial riser system

Results from open-loop simulation of the industrial riser system using the OLGA software (solid line) are presented in the P_{RB} bifurcation map shown in Figure 4.18. Also the results from the open-loop simulation of the ISRM with well source (dashed line) are shown in the same figure.

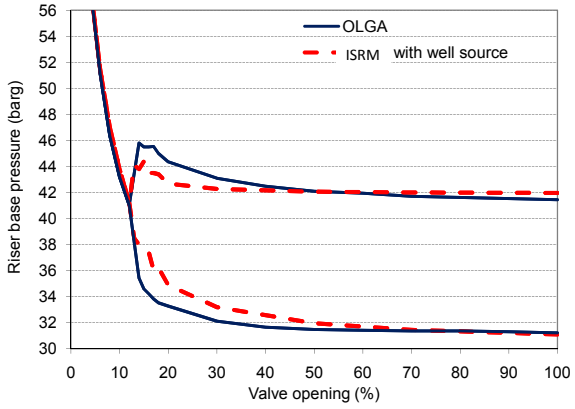

Figure 4.18: P_{RB} bifurcation map of the industrial riser system

The riser top valve, u is manually choked from the fully open position until the system becomes stable. For u between 100% and 13%, the industrial riser system is unstable and the P_{RB} oscillates between a minimum and a maximum pressure points. The desired stable non-oscillatory flow regime is obtained at a critical u of 12%. The corresponding P_{RB} is 41.05 barg. The critical value indicates the minimum P_{RB} and maximum u required to stabilise the system by manual choking. This is the bifurcation point. It can can observe that the P_{RB} bifurcation map predicted by the ISRM relatively agrees with that of the OLGA model. The same bifurcation point as the OLGA model of the industrial riser system is achieved by the ISRM. This result is consistent with the open-loop root locus shown in Figure 4.17.

4.4.4 Nonlinear stability analyses of the 4 inch riser system

The ability to predict the stable and the unstable operating points of the 4 inch riser system using the ISRM will be evaluated. For this analysis, the manipulated variable considered in the system is the topside separator gas valve (u_g).

4.4.4.1 Open-loop root locus plot of the 4 inch riser system

The open-loop root locus of the 4 inch riser system for control using the u_g is shown in Figure 4.19. The open-loop root locus is plotted for valve opening $10\% \leq u_g \leq 100\%$.

This open-loop root locus shows that for $u_g \leq 30\%$, the complex poles have negative real part. This indicates that the system is stable at this operating point. For $u_g \geq 40\%$, a pair of complex poles cross the imaginary axis into the

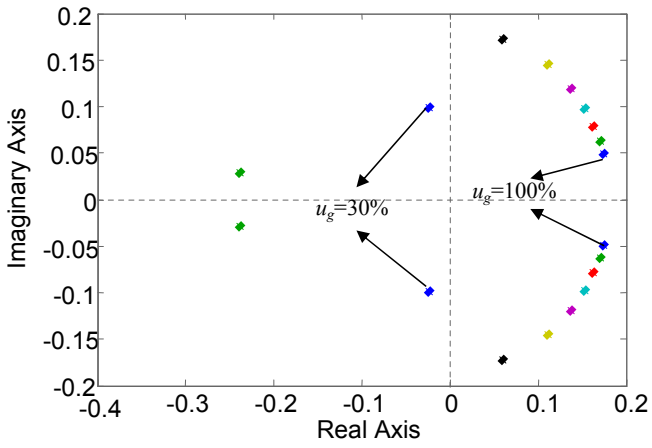

Figure 4.19: Open-loop root locus for the 4 inch riser system

RHP. Consequently, the poles for u_g between 100% and 40% all have positive real parts, and are plotted in the RHP as shown in Figure 4.19. This indicates that the system is unstable at these operating points. Thus, while stabilising control will be needed for $40\% \leq u_g \leq 100\%$, no stabilising control is needed for $u_g \leq 30\%$, where the system is open-loop stable.

4.4.4.2 Hopf Bifurcation of the 4 inch riser system

The Hopf bifurcation map of the 4 inch riser system for open-loop control using the u_g, on the ISRM and on the experimental facility is also evaluated. Figure 4.20 shows the P_{RB} Hopf bifurcation map obtained through open-loop simulation of the 4 inch riser system using the ISRM (solid line) and that obtained through experiment on the same system (dashed line).

The experimental results show that the system is unstable and the P_{RB} oscillates between minimum and maximum pressure points for $u_g \geq 40\%$. Also, the

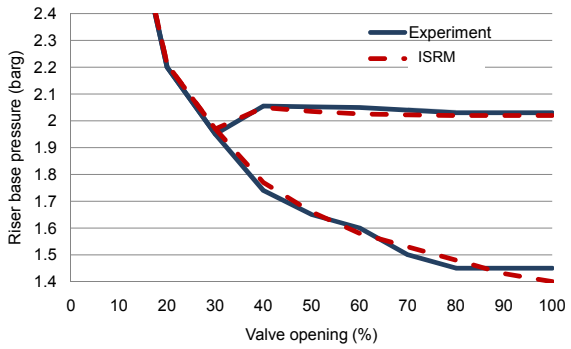

Figure 4.20: Pressure bifurcation map of the 4 inch riser system

Hopf bifurcation point occur at a critical valve opening of $u_g = 40\%$, such that the desired stable non-oscillatory flow regime is obtained. It can be observe that the bifurcation map predicted by the ISRM closely agree with the experimental result. The corresponding P_{RB} from the ISRM and from the experiment are 1.97 barg and 1.95 barg respectively. This result is consistent with the open-loop root locus presented in section 4.4.4.1.

These results show the ability of the ISRM to accurately predict relevant control properties required for slug controller design, for different control structures and riser-pipeline geometry.

4.5 Conclusions

In this chapter, the development of the plant-wide model for severe slug control is presented. The modeling of the riser slugging using a plant-wide model, which requires the modeling of the riser-pipeline system and its integration with the model of the two phase separator system and the pressure dependent well

model is achieved. Through the development of the plant-wide model, the ISRM is developed to eliminate some assumptions and limitations of the SRM in predicting severe slugging.

Simulation results from the SRM and the ISRM shows that the ISRM predicts severe slug characteristics, such as pressure amplitude and slug frequency more closely to the experimental result than the SRM. Also, the ability to predict severe slugging characteristics with changing inlet flow condition, which is not possible with the SRM is achieved with the ISRM. Improved performance is achieved with the ISRM in the prediction of the slug production stage in the severe slug cycle, when compared to the SRM, against the experimental results. The ability of the ISRM to predict relevant nonlinear stability is investigated using the industrial riser system and a 4 inch laboratory riser system. Its prediction of these nonlinear stabilities showed close agreement with experimental results.

Chapter 5

Controllability analysis of unstable riser-pipeline system

5.1 Introduction

In this chapter, the controllability analysis of an unstable riser-pipeline system is presented. The focus of the controllability analysis in this work is on the input-output controllability concept. Thus, the aim of the controllability analysis is to verify to what extent the system can achieve the desired performance objectives. In the input-output controllability analysis concept, a system is described as controllable if there exists a controller that can stabilise the system and provide acceptable system performance(s) [94]. As was pointed out by Skogestad and Postlethwaite, [94], input-output controllability differs from the state controllability analysis, which was introduced by Kalman [54, 55]. In the state controllability theory, a system is considered to be controllable if every desired transition of the plants state from a given initial state to any final state can be effected in a finite time by some unconstrained control inputs [54, 55]. In view of this, state controllability analysis does not consider the quality of the

response between the two states, and the input magnitude required could be large. Thus, in this work, the focus is on the input-output controllability concept. The input-output controllability will simply be called controllability, since it is clear that the state controllability is not considered.

The controllability of a system will depend on a number of system related factors, including the choice of control structure, the operating condition(s) and the system (riser-pipeline) design. A system's controllability analysis can be performed with focus on all or one of these factors. In each case, certain (relevant) control objectives are imposed on the system and the ability of the system to achieve them is analysed using relevant control theories.

In the controllability analysis of the riser-pipeline-system presented in this work, the control objectives are focused on the core operational targets and the direct benefits that are required from the control of an unstable riser-pipeline system. These direct benefits include, the ability to stablise the system as well as maximise (increase) oil production. The interdependency between a stable valve opening and the accumulated production is explored as the fundamental basis for the controllability analysis. The system related factors such as the choice of control structure and the operating conditions which affect the system's ability to achieve these control objectives are considered in the course of this controllability analysis.

Control strategies which are considered particularly relevant to the riser-pipeline system are considered. The system's nonlinearity, which affects its characteristics and ability to achieve stability at any desired valve opening is considered. Relevant control theories which provide key insights in the closed-loop control performance of a system are applied in the analysis of the control performance of the nonlinear model in a feedback loop.

The chapter begins with an overview of the existing controllability analysis approach and its limitations. This is followed with the description of the controllability analysis tools applied in the work. The rest of chapter presents a controllability analysis approach that focuses on achieving stability as well as increase oil production in an unstable riser-pipeline system.

5.1.1 Limitations of the riser-pipeline controllability analysis

In order to appreciate the relevance of the controllability analysis results presented in this work, it is necessary to discuss the limitations of the existing results in the riser-pipeline controllability analysis. The only published work on the controllability of the riser-pipeline system was reported by Storkaas et al [100], which was based on general system controllability theories, developed to establish the ability to achieve perfect control using different controlled variable [94]. It was based on the perfect control ideology in which steady state error, e, is theoretically required to be zero as shown in the basic feedback control structure in Figure 5.1.

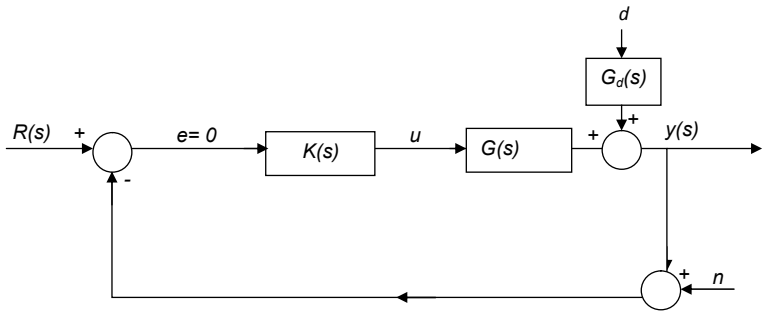

Figure 5.1: Feedback control structure with set point

Based on the concept of perfect control, certain control objectives were imposed on the riser system. These control objectives include:

1. perfect disturbance rejection (disturbances due to the topside separator pressure and the liquid and gas flow rate)

2. perfect tracking of controlled variable set point

3. suppressing measurement noise

Some conclusions based on their controllability analysis pointed out that certain controlled variables such as the riser top pressure, P_{RT}, will not be suitable for slug control of the unstable riser-pipeline system, while the riser base pressure P_{RB} will be the most suitable controlled variable.

In view of the desired performance required from the control of unstable riser-pipeline system, it is clear that these control objectives does not reflect the real needs required by a practical slug control system. Practically, the controllability analysis of the unstable riser-pipeline should indicate the extent to which the control system is able to stablise the unstable riser-pipeline with maximised production. Thus, it is important to consider a more appropriate control strategy to analyse the controllability of the unstable riser-pipeline system. This will require:

1. defining the control objectives of the system that are relevant to the oil and gas production

2. implementing an appropriate control strategy which can achieve the control objectives

By adopting more appropriate control objectives, the analyses of the ability to stabilise the unstable riser-pipeline system and maximise production, using various controlled variables, including the P_{RT} which had been considered unsuitable for slug control of the unstable riser-pipeline system will be carried out.

5.2 Controllability analysis tools

The focus of the controllability analysis presented in this work is on the ability to achieve closed-loop stability with maximised oil production. The analysis of these controllability issues requires using relevant control theories. Firstly, the description of the control objectives that are relevant to the riser-pipeline system is presented.

5.2.1 Control objectives

A suitable approach in the controllability analysis of the riser-pipeline system is to define the control objectives to reflect and address the core operation targets of an unstable riser-pipeline system. These will be system specific and differ from the general control objectives mentioned earlier in section 5.1.1. From the riser-pipeline production system point of view, the slug control objectives should focus on:

1. achieving stable operation

2. maximising (increasing) production

In view of these objectives, the perfect control of the controlled variable set point in riser pipeline system will not be necessary, as it does not provide any benefit to the oil production system operation. The relevant basic control structure which is practically relevant for achieving these objectives will be discussed and implemented in section 5.5.2. Next, the relationship between valve opening and production will be briefly discussed.

5.2.2 Valve opening and production

The ability to maximise production using the result based on the stability performance of the system is analysed. Depending on the control structure, a number of controlled variables including the riser base pressure (P_{RB}), riser top pressure (P_{RT}), total volumetric flowrate at the riser outlet (Q_T) and the topside separator pressure (P_s), could be used for the unstable riser-pipeline system control. Whichever controlled variable is used, the fundamental objective should be the ability to stabilise the system at a valve opening that is large enough to ensure maximum production. The analysis of production dependency on the flow line pressure is discussed in Chapter 6, where it will be shown that, an increase in the production rate can be achieved by reducing P_{RB}, which depends on a number of system related factors including the pressure loss across the valve, (DP_u).

Assuming a linear valve characteristics, the relationship between the DP_u and the valve opening, u, can approximately be defined as:

$$DP_u \propto \frac{1}{u^2} \tag{5.1}$$

Equation 5.1 shows that relatively small valve opening will result in high DP_u and consequently high P_{RB}. Conversely, relatively large valve opening will re-

sult in low DP_u and consequently low P_{RB}. Thus, in order to reduce the P_{RB}, we are required to achieve system stability at a relatively large valve opening.

5.2.3 Lower bound on the input magnitude

The analysis of the lower bound on the input usage will be employed to evaluate the ability of the control system to achieve closed-loop stability at large valve opening as required in the control objectives discussed in section 5.2.1. The unstable riser system cannot be stabilised at any open-loop operating point if the control input saturates, such that the scaled control input magnitude required to stabilise the system at that operating point is greater than or equal to 1 ($|u| \geq 1$). Thus, the analysis of the input magnitude, $|u|$, which is required to stabilise the system at any open-loop unstable valve opening is very important.

The previous work by Glover [31] showed that the input magnitude required to stabilise the system at each open-loop unstable valve opening can be obtained by evaluating lower bound on KS, which is defined as a function of the minimum Hankel Singular Value of the plant, as given in (5.2), (see also Skogestaad and Postlethwaite [94]).

$$\|KS\|_\infty \geq \frac{1}{\underline{\sigma}_H(U(G))} \tag{5.2}$$

where $U(G)$ is the unstable part of G, K is the controller and S is the sensitivity function defined as $S = (1 + GK)^{-1}$.

Equation 5.2 gives the lower bound of the input magnitude which is required to stabilise the system. This implies that by evaluating the right-hand-side (RHS) of (5.2), the minimum input magnitude required to stabilise the system will be

obtained. Thus, the required input magnitude will therefore be greater than or equal to the RHS of (5.2).

5.2.4 Scaling

In order to evaluate the lower bound on the input usage given in (5.2), the model must be scaled such that the maximum magnitude is less than one [94]. The scaling of the system is achieved by evaluating the relationship given in (5.3).

$$G(s) = \frac{\hat{G}(s)D_u}{D_y} \tag{5.3}$$

In (5.3), $\hat{G}(s)$ is the unscaled system transfer function, D_u is the maximum input deviation, D_y is the maximum allowed output deviation. The value of D_u can be evaluated with the relationship given in (5.4) [94].

$$D_u = \min(|u_{max} - u|, |u_{min} - u|) \tag{5.4}$$

In (5.4), $u_{max} = 1$, $u_{min} = 0$ and u is the nominal valve opening where the analysis is performed. By evaluating (5.4), the values of D_u will be obtained for $0 < u < 1$ as shown in Table 5.1.

Table 5.1: Calculated D_u values

u	0.2	0.3	0.4	0.5	0.6	0.7	0.8	0.9
D_u	0.2	0.3	0.4	0.5	0.4	0.3	0.2	0.1

The value of D_y can be evaluated with relationship given in (5.5) [94].

$$D_y = \min(|r - y_{max}|, |r - y_{min}|) \tag{5.5}$$

In (5.5), y_{max} and y_{min} are the maximum and minimum values of the controlled variable at each operating point defined by the valve opening respectively. Also, r is the set point of the controlled variable, which is desired at steady state. For an open-loop unstable operating point, the value of r will be equal to the value of the controlled variable at the corresponding unstable equilibrium point. Thus, the D_y can be calculated by evaluating the maximum allowed deviation from the value of the controlled variable at the unstable equilibrium point at each valve opening. This analysis can easily be performed using the Hopf bifurcation map of the controlled variable. This will be explained in details in section 5.3.1.

The first step to performing these controllability analyses is to obtain the linear model transfer function of the system at the open-loop unstable valve openings. These linear model transfer functions can be defined in a general form as a function of the unstable steady state valve opening for each controlled variable.

5.2.5 Linear model transfer functions

Consider a hypothetical three state unstable system with the linear model transfer function as given in (5.6).

$$G(s) = \frac{b_0}{s^3 + a_2 s^2 - a_1 s + a_0} \tag{5.6}$$

The value of the coefficients a_2, a_1, a_0 and b_0 will depend on the steady state valve opening (u_e) in which the linear model is obtained. For a set of steady state valve openings (u_{ei}), a set of linear system models, $G_i(s, u_e)$, will be obtained for each u_e, for $i = 1, 2, ..., n$, where n is the number of linear model transfer functions obtained from the system. If the coefficients a_2, a_1, a_0 and b_0

in (5.6) are defined as nonlinear functions as given in (5.7), the general form of the linear model, $G(s, u_e)$, can be defined as given in (5.8). Thus, for a given u_e, the corresponding linear model of the system is obtained by evaluating the nonlinear functions in (5.7) and substituting in (5.8).

$$a_2 = f_2(u_e), \qquad a_1 = f_1(u_e), \qquad a_0 = f_0(u_e), \qquad b_0 = g_0(u_e) \tag{5.7}$$

$$G_i(s, u_e) = \frac{g_0(u_e)}{s^3 + f_2(u_e)s^2 - f_1(u_e)s + f_0(u_e)} \tag{5.8}$$

The linear model transfer function of the riser-pipeline system can be defined in this general form, with the numerator and the denominator coefficients defined by nonlinear functions. The system's linear model transfer function can then be obtained at any desired steady state valve opening in the open-loop unstable region, if the relationship for the nonlinear functions are defined as a function of the steady state valve opening. Next, the methods which can be applied to derive these nonlinear functions will be discussed.

5.2.5.1 Deriving the nonlinear functions

Consider a nonlinear system represented by a general state space form given by (5.9) and (5.10)

$$\dot{x} = f(x, u) \tag{5.9}$$

$$y = g(x, u) \tag{5.10}$$

where x is the state variable, y is the output and u is the input variable (valve opening). A linear model of (5.9) and (5.10) can be obtained at an unstable steady state operating point defined by, (x_e, u_e), such that:

$$0 = f(x_e, u_e) \tag{5.11}$$

$$y_e = g(x_e, u_e) \tag{5.12}$$

and the obtained linear model in terms of the deviation terms is given as:

$$\delta\dot{x} = A\delta x + B\delta u \tag{5.13}$$

$$\delta y = C\delta x + D\delta u \tag{5.14}$$

In (5.13) and (5.14), δx can be replaced by x, and δu can be replaced by u. Also in (5.14), δy can also be replaced by y, such that x, y and u denotes the deviation from the equilibrium. Thus, (5.13) and (5.14) can be simplified as given in (5.15) and (5.16) respectively,

$$\dot{x} = Ax + Bu \tag{5.15}$$

$$y = Cx + Du \tag{5.16}$$

where A is the state matrix, B is the input matrix, C is the output matrix and D is the input-output direct coupling matrix. The matrices of the linearised model are obtained as partial derivatives of the dynamical state equations and are given as:

$$A = \left|\frac{\partial f}{\partial x}\right|_{x_e,u_e}, \quad B = \left|\frac{\partial f}{\partial u}\right|_{x_e,u_e}, \quad C = \left|\frac{\partial g}{\partial x}\right|_{x_e,u_e}, \quad D = \left|\frac{\partial g}{\partial u}\right|_{x_e,u_e} \tag{5.17}$$

From (5.17), the linear system transfer function from the input, u, to the output, y, can be obtained as:

$$\frac{y(s)}{u(s)} = C(Is - A)^{-1}B + D \tag{5.18}$$

In order to determine the linear model transfer function as given in (5.18), the state matrix (A), the input matrix (B), the output matrix (C) and the input-output direct coupling matrix (D), could be defined as a function of the physical system variables. However, for high order and multi-variable systems, this method can become complicated. A less complicated method is a numerical solution which can be achieved by determining a nonlinear empirical function that approximates the value of the coefficients in the linear model. To achieve this, a basic knowledge of the system's transfer functions is required. This can be obtained by using any suitable system identification method. However, for a system whose mechanistic model has been developed, such as the ISRM of the industrial riser system, the transfer function at any valve opening can easily be obtained by using the technical computing softwares such as Matlab®. The coefficients of all the transfer functions obtained at all relevant valve openings are collected and plotted against the corresponding steady state valve openings. An empirical function is obtained to define their trend of the plot.

The advantage of applying these nonlinear functions is that the stability analysis of the system using them will provide a general understanding as to which coefficient the stability of the system depends upon. Also, the linear model transfer functions of the system can be easily obtained by substituting the desired unstable steady state valve opening, without having the ISRM of the system.

In the next section, controllability of the industrial riser system for stability and

maximum production will be presented. For the description of the industrial riser system, please see section 3.5. This controllability analysis will focus on the use of two manipulated variables for slug control. These variables include the riser top valve opening (u) and the topside separator gas outlet valve opening (u_g). The schematic diagram of the riser-pipeline system showing the position of the two variables is shown in Figure 5.2.

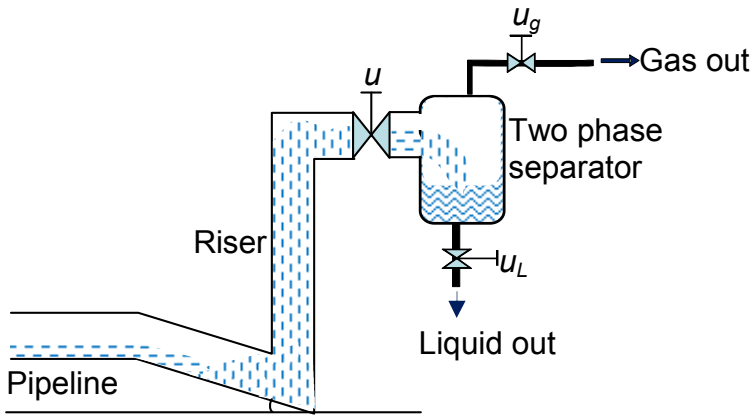

Figure 5.2: Riser pipeline system with u and u_g

5.3 Controllability analysis with the riser top valve opening, u

In this section, the controllability analysis of the industrial riser system using the riser top valve opening, u, is presented. The controllability of the system with three controlled variables, which are the P_{RB}, the P_{RT} and the Q_T is analysed. The ISRM had been discussed in Chapter 4. For each controlled variable, (5.2) is evaluated to determine the minimum input magnitude required to stabilise

the system at all open-loop unstable valve openings. This analysis requires that the linear model transfer function be obtained.

The linear model transfer function of the riser-pipeline system is obtained from the ISRM (with well model), for the industrial riser system for the P_{RB}, the P_{RT} and the Q_T. The transfer functions that are obtained are of third order, consisting of two unstable pole and one stable pole. The evaluation of $\|KS\|_\infty$ using the Hankel Singular Value analysis in (5.2) requires only the unstable projection of the linear model transfer function. Thus, the third order transfer functions can be reduced to second order form, such that the important system dynamics and the unstable poles in the transfer functions are preserved. This model reduction can easily be performed using the $balancmr$ command in Matlab®. The general form of the second order linear model transfer functions, which are obtained for the P_{RB}, the P_{RT} and the Q_T are given in (5.19), (5.20) and (5.21) respectively.

$$G(s,u_e)_{P_{RB}} = \frac{-g_1(u_e)s - g_0(u_e)}{s^2 - f_1(u_e)s + f_0(u_e)} \tag{5.19}$$

$$G(s,u_e)_{P_{RT}} = \frac{g_1(u_e)s - g_0(u_e)}{s^2 - f_1(u_e)s + f_0(u_e)} \tag{5.20}$$

$$G(s,u_e)_{Q_T} = \frac{g_2(u_e)s^2 + g_1(u_e)s + g_0(u_e)}{s^2 - f_1(u_e)s + f_0(u_e)} \tag{5.21}$$

The nonlinear functions for the P_{RB}, the P_{RT} and the Q_T, which are obtained using the method described in section 5.2.5.1 are given in Appendix B.1, B.2 and B.3 respectively. By evaluating and substituting these nonlinear functions, the linear model transfer function of the system will be obtained at the required steady state valve opening for each controlled variable. For example, by evaluating the nonlinear functions, which are given in Appendix B.1 for the P_{RB}

at $u_e = 20\%$, and substituting the values into (5.19), the linear model transfer function given in (5.22) is obtained, and by evaluating it at $u_e = 30\%$, (5.23) is obtained.

$$G_{20\%}(s) = \frac{-0.03227s - 0.000053}{s^2 - 0.0003225s + 1.509 \times 10^{-6}} \tag{5.22}$$

$$G_{30\%}(s) = \frac{-0.03s - 0.000071}{s^2 - 0.0006534s + 3.472 \times 10^{-6}} \tag{5.23}$$

The linear model transfer function can be obtained for each controlled variable. These linear model transfer functions are then applied to analyse the input magnitude required to stabilise the system using each controlled variable, at the open-loop unstable valve openings.

5.3.1 Lower bound on KS analysis

The linear model transfer functions that are required to evaluate the lower bound on $\|KS\|_\infty$ for each controlled variable is obtained as discussed in section 5.2.5. These linear models must be scaled before they are applied in the analysis. The model scaling is achieved by applying the scaling procedure, which had been discussed in section 5.2.4. The values for the maximum input deviation, D_u, required for the scaling had been given in Table 5.1. The maximum allowed output deviation, D_y, can be calculated by evaluating the maximum deviation from the desired steady state value of the controlled variable.

Consider the riser base pressure (P_{RB}) Hopf bifurcation map of the industrial riser system, which is given in Figure 5.3, the steady state value in the open-loop unstable region is presented by the unstable equilibrium pressure line, P_{RBc}. This Hopf bifurcation map and the P_{RBc} are obtained using OLGA. To obtain P_{RBc} using OLGA, firstly, the steady state option must be turned on in the case definition/options on the property bar. Also, the initial valve opening should be specified for each operating point. The P_{RBc} is obtained in the pressure trends as the initial steady state value at t=0.

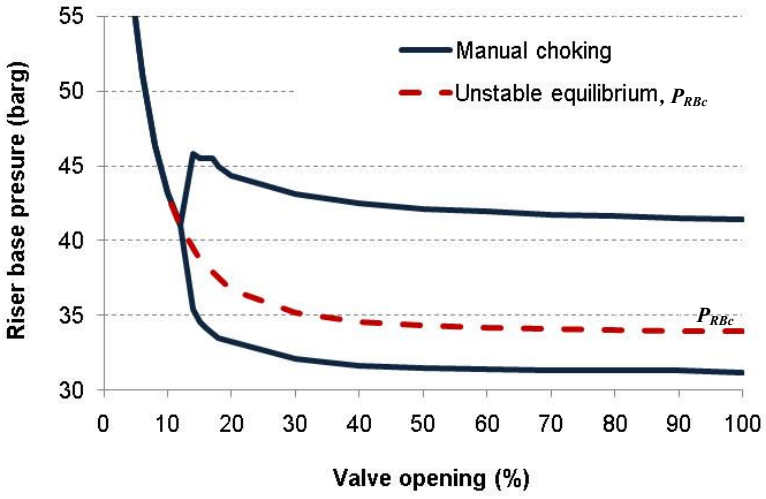

Figure 5.3: Riser base pressure Hopf bifurcation map

The D_y from this unstable equilibrium line can be calculated using (5.24), which is deduced from (5.5), where P_{RBmax} is the maximum riser base pressure and P_{RBmin} is the minimum riser base pressure, which is obtained at each valve opening.

$$D_y = \min(|P_{RBc} - P_{RBmax}|, |P_{RBc} - P_{RBmin}|) \tag{5.24}$$

The value of P_{RBc} for each valve opening is given in Table 5.2. By evaluating (5.24) at each valve opening, the values of D_y, which are required to scale

Table 5.2: D_y values for P_{RB}

u_e	0.2	0.3	0.4	0.5	0.6	0.7	0.8	0.9
P_{RBc}(barg)	36.76	35.15	34.6	34.33	34.18	34.09	34.03	33.96
D_y (barg)	3.26	2.15	2	2.21	2.16	1.94	2.03	2.16

the system are obtained and presented in Table 5.2. Similarly, for the P_{RT} and the Q_T, the D_y required to scale the systems for each valve opening can also be obtained from their Hopf bifurcation maps. The unstable equilibrium values P_{RTc} and Q_{Tc} obtained for each valve opening are given in Tables 5.3 and 5.4 respectively . By evaluating (5.24) for the P_{RT} and Q_T at each valve opening, the values of D_y, which are required to scale the systems are obtained and presented in Tables 5.3 and 5.4 respectively.

Table 5.3: D_y values for P_{RT}

u_e	0.2	0.3	0.4	0.5	0.6	0.7	0.8	0.9
P_{RTc} (barg)	32.806	31.63	30.74	30.47	30.33	30.24	30.19	30.15
D_y (barg)	3.8	3.6	2.94	2.47	1.33	1.24	1.19	1.15

Table 5.4: D_y values for Q_T

u_e	0.2	0.3	0.4	0.5	0.6	0.7	0.8	0.9
Q_{Tc} (m^3/s) $\times 10^{-2}$	2.24	2.35	2.4	2.41	2.43	2.43	2.44	2.45
D_y (m^3/s) $\times 10^{-2}$	0.24	0.35	0.4	0.41	0.43	0.43	0.44	0.44

Next, the lower bound on $\|KS\|_\infty$ is evaluated using (5.2). For each controlled variable, the lower bound of $\|KS\|_\infty$ is obtained for the valve openings, $20\% <$

u <100%, and summarised in Table 5.5. From the analysis of the $\|KS\|_\infty$, the valve opening where closed-loop stability is possible without input saturation, for each variable is predicted.

Table 5.5: Calculated values of $\|KS\|_\infty$

u_e		0.2	0.3	0.4	0.5	0.6	0.7	0.8	0.9
$\|KS\|_\infty$	P_{RB}	0.2	0.23	0.49	0.77	0.93	3	5.4	10.96
	P_{RT}	0.22	0.35	1.06	1.69	3.7	8.2	13.78	27.4
	Q_T	0.18	0.19	0.369	0.47	0.85	1.44	2.11	4

The results shown in Table 5.5 indicate that the minimum input magnitude required to stabilise the system increases as the valve opening is increased for all the controlled variables.

For the P_{RB}, $\|KS\|_\infty < 1$ is obtained for valve openings 20% $\leq u \leq$60%. Also for the P_{RT}, $\|KS\|_\infty < 1$ is obtained for valve openings 20% $\leq u \leq$30% and for the valve openings Q_T, $\|KS\|_\infty < 1$ is obtained for 20% $\leq u \leq$ 60%. The minimum input magnitude required to stabilise the system is less than one at these valve openings for each controlled variable. This implies that theoretically, the system can be stabilised at these valve openings without input saturation. However, $\|KS\|_\infty > 1$ is obtained at 70% $\leq u \leq$ 100% for the P_{RB}, at 40% $\leq u \leq$100% for the P_{RT} and at 70% $\leq u \leq$100% for the Q_T. The minimum input magnitude required to stabilise the system is greater than one at these valve openings for each of these variables. This implies that theoretically, the system cannot be stabilised at these valve openings.

It can be deduced from these analyses that theoretically, all the three controlled variables can stabilise the unstable riser system at some open-loop unstable

valve opening without input saturation. However, the important issue resulting from the controllability analysis of these variables is that the maximum stable valve opening, which they can each achieve is different. Generally, it can be observed that the P_{RB} and the Q_T are able to stabilise the system at a larger valve opening than the P_{RT}. This is important as it reflects the production that is achievable with each controlled variable, under stable operating condition.

Having analysed the controllability of the unstable riser-pipeline system with riser top valve as the manipulated, next the controllability analysis is performed with the topside separator gas valve as the manipulated variable.

5.4 Controllability analysis with the topside separator gas valve u_g

In this section, the controllability analysis of the industrial riser system (with well and separator models) using the topside separator gas valve opening is presented (see Figure 5.2). The topside separator is modeled with the dimension of the two phase separator given in Figure 4.3. The focus of the controllability analysis will be on four controlled variables, which include the P_{RB}, the separator pressure (P_s), the P_{RT} and the volumetric gas flowrate out of the separator, Q_{Gouts}. For a better understanding of the stability behaviour of the system with u_g, firstly, the nonlinear stability analysis of the system will be presented.

5.4.1 Nonlinear stability analysis

The nonlinear stability analysis of the industrial riser system will be presented using the Hopf bifurcation map and the open-loop root locus, which had been discussed in sections 4.4.2 and 4.4.1 respectively.

5.4.1.1 Open-loop root locus plot

The open-loop root locus plot of the industrial riser system with u_g as the manipulated variable is presented in Figure 5.4. The open-loop root locus is plotted for valve opening 23% $\leq u_g \leq$100%.

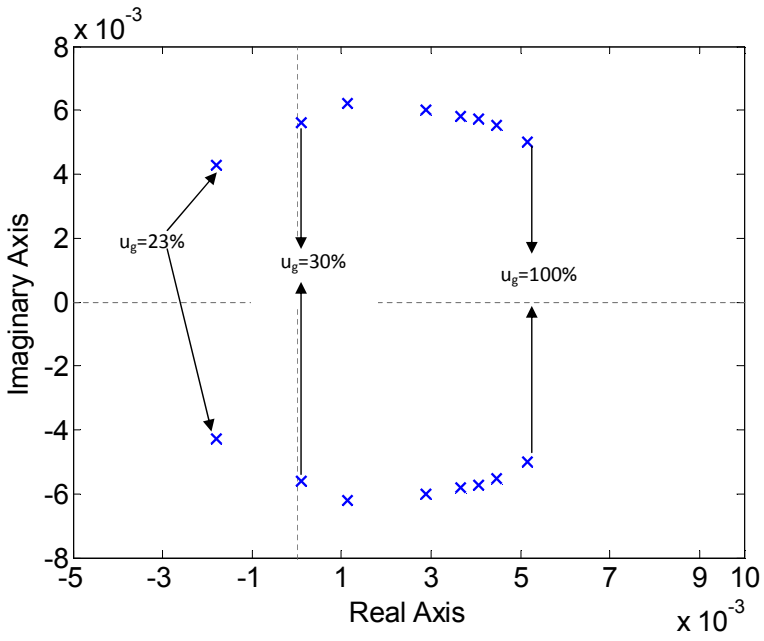

Figure 5.4: Open-loop root locus plot with u_g

This open-loop root locus shows that for $u_g \leq$23%, the complex poles have negative real part. This indicates that the system is stable at these valve openings. For $u_g \geq$30%, a pair of complex poles cross the imaginary axis into the RHP. Consequently, the poles for u_g between 100% and 30% all have positive real parts, and are plotted in the RHP as shown in the Figure. This indicates that the system is unstable at these valve openings. Thus, while stabilising control will be needed for 30$\leq u_g \leq$100% , no stabilising control is needed for $u_g \leq$23%, where the system is open-loop stable.

5.4.1.2 Hopf bifurcation map

The open-loop control of the industrial riser system requires the manual choking of the valves in order to transform the unstable flow condition in the system to a stable flow condition. The result of the manual choking is presented using Hopf bifurcation map which has been discussed in section 4.4.2. Figure 5.5 shows the bifurcation map obtained from the open-loop control of the industrial riser model using separator outlet gas valve u_g and the rise top valve. Each valve is manually choke from a fully open position where the system is unstable until stability is achieved at the bifurcation point.

The difference in the maximum open-loop stable valve opening achieved by using each valve opening can be easily observed. As was shown in Figure 4.18, with the riser top valve, the system can be stabilised at a valve opening of $u =$12%, corresponding to a P_{RB} of about 41.05 barg. However, with the separator gas valve, the system can be stabilised at a valve opening of $u_g =$23%, corresponding to a P_{RB} of about 38.1 barg. This shows that open-loop control with the separator gas valve stabilised the system at a relatively larger valve opening, with a corresponding P_{RB} that is lower than using the riser top valve.

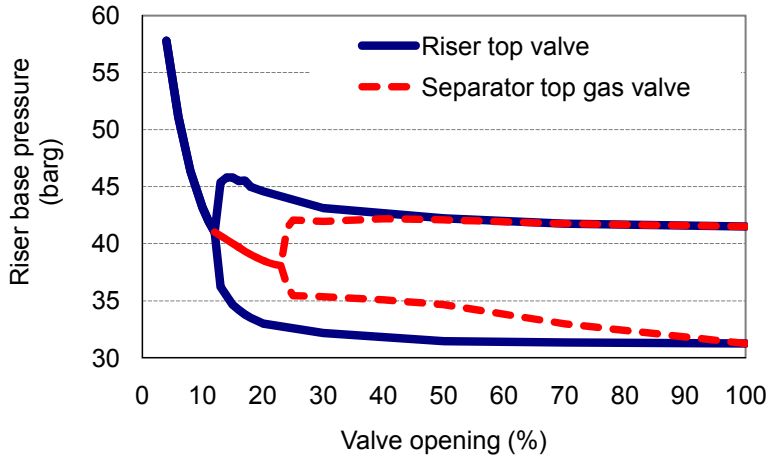

Figure 5.5: Hopf bifurcation map

The controllability analysis of the system with the u_g will be performed at the open-loop unstable valve openings, which corresponds to $30\% \leq u_g \leq 100\%$.

5.4.2 Linear model transfer functions

The first step in performing this controllability analysis is to obtain the linear model transfer function of the system at all relevant open-loop unstable valve openings. As it was discussed in section 5.2.5, the linear model transfer functions of the system can be defined by its general form at the open-loop unstable valve openings for each controlled variable. With separator model added to the ISRM with well model, the system becomes a five order system. The general form of the industrial riser system's linear model transfer function from u_g to P_{RB}, P_s, P_{RT} and Q_{Gouts} are given in (5.25), (5.26), (5.27) and (5.28) respectively. The steady state value of u_g is denoted by u_{ge}.

$$G_{P_{RB}}(s,u_{ge}) = \frac{-g_2(u_{ge})s^2 - g_1(u_{ge})s - g_0(u_{ge})}{s^5 + f_4(u_{ge})s^4 + f_3(u_{ge})s^3 - f_2(u_{ge})s^2 + f_1(u_{ge})s + f_0(u_{ge})} \tag{5.25}$$

$$G_{P_s}(s,u_{ge}) = \frac{-g_4(u_{ge})s^4 - g_3(u_{ge})s^3 + g_2(u_{ge})s^2 - g_1(u_{ge})s - g_0(u_{ge})}{s^5 + f_4(u_{ge})s^4 + f_3(u_{ge})s^3 - f_2(u_{ge})s^2 + f_1(u_{ge})s + f_0(u_{ge})} \tag{5.26}$$

$$G_{P_{RT}}(s,u_{ge}) = \frac{-g_3(u_{ge})s^3 + g_2(u_{ge})s^2 - g_1(u_{ge})s - g_0(u_{ge})}{s^5 + f_4(u_{ge})s^4 + f_3(u_{ge})s^3 - f_2(u_{ge})s^2 + f_1(u_{ge})s + f_0(u_{ge})} \tag{5.27}$$

$$G_{Q_{Gouts}}(s,u_{ge}) = \frac{g_5(u_{ge})s^5 + g_4(u_{ge})s^4 + g_3(u_{ge})s^3 + g_2(u_{ge})s^2 + g_1(u_{ge})s + g_0(u_{ge})}{s^5 + f_4(u_{ge})s^4 + f_3(u_{ge})s^3 - f_2(u_{ge})s^2 + f_1(u_{ge})s + f_0(u_{ge})} \tag{5.28}$$

These linear models will be applied for stability analyses of the system using the Routh stability criterion procedure in section 5.5.4. For this purpose, a lower order model will be required to avoid complication in the analysis. Also for the purpose of evaluating the $\|KS\|_\infty$ as was discussed in section 5.3, only the unstable projection of the transfer function is required. Thus, model reduction method is also applied to find less complex lower order approximation of these transfer functions, such that the important system dynamics in the transfer functions and the unstable poles are preserved. Thus, using the $balancemr$ command in Matlab®, (5.25) to (5.28) can be reduced to equivalent second order transfer functions given in (5.29) to (5.32).

$$G_{P_{RB}}(s,u_{ge}) = \frac{-g_1(u_{ge})s - g_0(u_{ge})}{s^2 - f_1(u_{ge})s + f_0(u_{ge})} \tag{5.29}$$

$$G_{P_s}(s, u_{ge}) = \frac{g_1(u_{ge})s - g_0(u_{ge})}{s^2 - f_1(u_{ge})s + f_0(u_{ge})} \tag{5.30}$$

$$G_{P_{RT}}(s, u_{ge}) = \frac{g_1(u_{ge})s - g_0(u_{ge})}{s^2 - f_1(u_{ge})s + f_0(u_{ge})} \tag{5.31}$$

$$G_{Q_{Gouts}}(s, u_{ge}) = \frac{g_2(u_{ge})s^2 + g_1(u_{ge})s + g_0(u_{ge})}{s^2 - f_1(u_{ge})s + f_0(u_{ge})} \tag{5.32}$$

It can be observed that the general form of the P_{RT} and the P_s are similar.

5.4.3 Lower bound on KS analysis

The lower bound on $\|KS\|_\infty$, which is given in (5.2) will be evaluated to analyse the input magnitude required to stabilise the system with each variable. The system models given in (5.29) to (5.32) are defined by evaluating their respective nonlinear functions and substituting them accordingly. The system model obtained for each variable is applied in (5.2) to evaluate the lower bound on $\|KS\|_\infty$. These nonlinear functions are provided in Appendix B.4, B.5, B.6 and B.7 for the P_{RB}, the P_s, the P_{RT} and the Q_{Gesp} respectively. The nonlinear functions are derived by implementing the method described in section 5.2.5.1 on the industrial riser system, at all required valve opening of 30$\% < u_g <$100$\%$.

These linear model transfer functions must be scaled before they are applied in the analysis. The model scaling is achieved by evaluating (5.3) for each variable. The values for the maximum input deviation (D_u) required for the scaling is obtained from Table 5.1. The value of the maximum allowed output deviation (D_y) for the P_{RB}, the P_s, the P_{RT} and the $G_{Q_{Gouts}}$ are calculated from their respective Hopf bifurcation maps as discussed in section 5.2.4 and 5.3.1.

By evaluating (5.24) for the P_{RB}, the P_{RT}, the P_s and the Q_{Gouts}, the values of D_y are obtained and are given in Tables 5.6, 5.7, 5.8 and 5.9 respectively.

Table 5.6: D_y values for P_{RB}

u_{ge}	0.3	0.4	0.5	0.6	0.7	0.8	0.9
P_{RBc}(barg)	36.11	35.46	35.18	35	34.79	34.73	34.7
D_y (barg)	0.25	0.36	0.51	1.62	1.79	2.63	3.35

Table 5.7: D_y values for P_{RT}

u_{ge}	0.3	0.4	0.5	0.6	0.7	0.8	0.9
P_{RTc} (barg)	32	31	30.67	30.53	30.44	30.39	30.35
D_y (barg)	3	2.3	1.97	1.83	1.74	1.69	1.65

Table 5.8: D_y values for P_s

u_{ge}	0.3	0.4	0.5	0.6	0.7	0.8	0.9
P_{sc} (barg)	31.5	30.5	30.27	30.33	30.23	30.18	30.14
D_y (barg)	2.5	2	1.97	1.83	1.74	1.69	1.65

Table 5.9: D_y values for Q_{Gouts}

u_{ge}	0.3	0.4	0.5	0.6	0.7	0.8	0.9
$Q_{G_{outs_c}}$ (m^3/s) $\times 10^{-2}$	2.08	2.07	2.06	2.056	2.053	2.051	2.05
D_y (m^3/s) $\times 10^{-2}$	0.8	0.7	0.6	0.56	0.53	0.51	0.5

For each controlled variable, $\|KS\|_\infty$ is obtained for the valve openings, $30\% < u_{ge} < 90\%$, and summarised in Table 5.10. The results shown in Table 5.10,

shows that the minimum input magnitude required to stabilise the system increase as the valve opening is increased for each of the controlled variable. If $\|KS\|_\infty < 1$, then theoretically, the system can be stabilised at that valve opening without input saturation. For the P_{RB}, $\|KS\|_\infty < 1$ is obtained for valve openings 30$\% \leq u_{ge} \leq$50$\%$. Thus, with the P_{RB}, the system can be stabilised at a valve opening within this range. For the P_s and the P_{RT}, $\|KS\|_\infty < 1$ is obtained only for 30$\% \leq u_{ge} \leq$ 40$\%$. For the Q_{Gouts}, $\|KS\|_\infty < 1$ is obtained for 30$\% \leq u_{ge} \leq$60$\%$, which also indicate the valve opening at which the system can be stabilised.

Table 5.10: Calculated $\|KS\|_\infty$ values

u_{ge} (%)		30	40	50	60	70	80	90
$\|KS\|_\infty$	P_{RB}	0.06	0.12	0.75	1.8	4.3	12	36.5
	P_s	0.06	0.9	5.4	18	49.9	150	648.7
	P_{RT}	0.04	0.57	2.3	6.13	13.6	33.4	117.4
	Q_{Gouts}	0.01	0.11	0.35	0.83	1.7	3.9	13

With these results, the controllability analyses of the system for stability at large valve opening, which is necessary for maximising oil production is obtained. It can be observed that theoretically, all the four variables can stabilise the unstable riser system at some open-loop unstable valve opening without input saturation. However, as was observed in the controllability analysis with the riser top valve, the clear issue resulting from the controllability analyses for these variables is that the maximum stable valve opening which they can achieve are different. Generally, the P_{RB} and the Q_{Gouts} are able to stabilise the system at a larger valve opening than the P_s and the P_{RT}. This is an important factor as it will reflect the production that is achievable with each variable.

5.5 Simulations and results analyses

In the controllability analysis with the riser top valve opening (u), it was found generally that the P_{RB} and the Q_T are able to stabilise the system at a larger valve opening than the P_{RT}. Also, in the controllability analysis with the separator gas valve (u_g), it was found that generally the P_{RB} and the Q_{Gouts} are able to stabilise the system at a larger valve opening than the P_s and the P_{RT}. In the practical implementation of slug control system, the ability to achieve closed-loop stability at the predicted valve opening will depend on a number of factors, including the appropriateness of the slug control structure. In this section, a feedback control structure with derivative controller (D controller) is applied on the industrial riser system to validate the general prediction of the controllability analyses results.

5.5.1 The simulation model

The controller parameters are designed with linear model transfer function, which is obtained from the ISRM of the industrial riser system. The industrial riser system was described in section 3.5. The controller is then implemented on the industrial riser system, which is modeled in the OLGA multiphase flow simulator software. The OLGA model of the industrial riser system is nonlinear. The implementation of the controller is achieved using the OLGA-Matlab link, which is established by using the OLGA-Matlab toolbox. The controller is configured in the Matlab® software. Through OLGA-Matlab link, the results (controlled variable data) from dynamic multiphase flow simulations performed by OLGA becomes available in MATLAB, and the control input from Matlab become available in OLGA.

5.5.2 Control structure with derivative controller

The control structure that allows the practical application of the slug control system to focus on stabilising the system at a reference valve opening, will be discussed and applied on the industrial riser system. A feedback control structure with derivative controller (D controller) is proposed for this purpose. Consider the general relationship for a derivative controller in which the controller input is the control error (e), as shown in (5.33).

$$u(t) = K_c \tau_d \frac{de(t)}{dt} \tag{5.33}$$

In (5.33), K_c is the controller gain, $e(t)$ is the control error and τ_d is the derivative time. Fundamentally, the control action of the derivative controller is obtained by taking the derivative of the control error, which is the controller input. If the control error becomes constant (not necessarily zero), the derivative controller output will be zero. For a stable riser system, the controlled variable will be fairly constant. Thus, if the controller input is equal to the measured value of the controlled variable, then, the derivative controller can be applied to stabilise the system, such that, for a stable system (steady state), the controller output will be equal to zero. In this case, the controlled variable set point can be set equal to zero, such that the controller input will be equal to the measured value of the controlled variable, as shown in Figure 5.6. This slug control strategy eliminates the requirement for perfect tracking of the controlled variable as a slug control objective, which does not provide any benefit to the slug control of the oil and gas production system.

Since the controller output will be approximately equal to zero ($u_k \approx 0$) for a constant value of the controlled variable (at steady state), then a reference

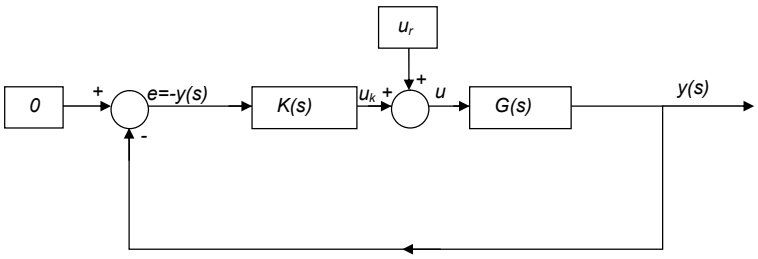

Figure 5.6: Feedback control structure with set point equal to zero

valve opening, (u_r), is required to be defined as the desired system's valve opening at steady state. Thus, the derivative controller action will be required to stabilise the system at the reference valve opening (u_r). The advantage of this approach is that it allows the practical application of the slug control system to focus on stabilising the system at a large reference valve opening, which is necessary for maximising oil production. Also, the valve opening is a more suitable variable to define and manipulate than any other controlled variable, since its value is bounded within 0% and 100% for all system structures and operating conditions. With the controller output obtained from the derivative of the controlled variable, the controller equation will be as given in (5.34).

$$u(t) = K_c\tau_d\frac{dy(t)}{dt} \tag{5.34}$$

The controller (K(s)) can be defined in Laplace transform as given in (5.35),

$$K(s) = K_c\tau_d s = K_D s \tag{5.35}$$

where $K_D = K_c\tau_d$.

The practical implementation of this controller will require multiplying it with a filter, to obtain a proper controller transfer function. Equation (5.35) will be written as shown in (5.36). In (5.36), τ_f is the filter time constant.

$$K(s) = \frac{K_D s}{\tau_f s + 1} \tag{5.36}$$

The implementation of this controller will first require the determination of its parameters. In order to determine the values of K_D and τ_f for which the system is stable, a system stability analysis method is applied. One of such methods is the Routh stability criterion. The Routh stability criterion is discussed briefly in the next section.

5.5.2.1 Routh stability criterion

In this section, the a popular system stability analysis tool, known as the Routh stability criterion will be introduced. The Routh stability criterion states that the number of polynomial roots in the right-half-plane (RHP) (i.e RHP poles) of the S-plane is equal to the number of sign changes in the first column of the Routh array table [81]. It is known that the presence of RHP poles indicates unstable system [74]. Thus, any sign change in the first column of the Routh array table would indicate that the system is unstable. The Routh stability criterion can be used to evaluate the limits of the magnitude of the controller parameters for which the element in the first column of the Routh array table would be positive. The Routh stability criterion is applied to the characteristic equation of a closed-loop transfer function of the system defined by, $1 + G(s)K(s) = 0$, where $G(s)$ is the system transfer function and $K(s)$ is the controller. The coefficients of this closed-loop transfer function are applied to create the Routh array table from which the analysis is performed. The mathematical steps for analysing the Routh array table is defined in the literature [74, 81].

5.5.3 Simulation with riser top valve (u) as manipulated variable

The simulation analyses with the riser top valve as the manipulated variable is presented in this section. In line with the controllability analysis, simulation analyses for three controlled variables namely the P_{RB}, the P_{RT} and the Q_T are presented. The derivative controller will be designed for each controlled variable using the linear model transfer function obtained from the ISRM. The controller is then implemented on the nonlinear model of the industrial riser system in OLGA as described in section 5.5.1.

5.5.3.1 Simulation procedure

For each controlled variable, the following procedure is followed in performing the simulation to implement the controller.

1. The valve opening is initially set to a fixed position (manually) corresponding to the open-loop unstable valve opening of u =20$\%$.

2. The controller is switched on after open-loop simulation period that is greater than 2 hours and the system is allowed to be stabilised by the controller action.

3. Once the system is stabilised, the reference valve opening (u_r) is gradually increased and the system is allowed to be stabilise by the controller action for each step increase.

4. The gradual increase in the u_r is continued until the valve opening at which the controller cannot stabilise the system is reached. At this valve opening, the system becomes unstable.

5. The maximum stable valve opening, the minimum P_{RB} and the accumulated liquid achieved is then recorded.

It will be observed that based on this simulation procedure, in each simulation result, the system oscillates at the beginning of the simulation because the system is open-loop unstable and also oscillates at the end because the system is closed-loop unstable. This simulation procedure applies to all the simulation results presented in sections 5.5.3.2, 5.5.3.3, 5.5.3.4 and 5.5.4.

5.5.3.2 P_{RB} control

To obtain the bounds for the values of K_D and τ_f for which the system is stable at any valve opening, the Routh stability analysis will be applied using the system's model given in (5.19). With the P_{RB}, the closed-loop characteristic equation of the system is obtained as $1 - G(s, u_e)K(s) = 0$. With the $K(s)$ given as the derivative controller in (5.36), the characteristic equation is be obtained as shown in (5.37).

$$\tau_f s^3 + s^2[g_1(u_e)K_D - f_1(u_e)\tau_f + 1] + s[g_0(u_e)K_D - f_1(u_e) + \tau_f f_0(u_e)] + f_0(u_e) = 0 \tag{5.37}$$

From (5.37), the Routh array table, which is shown in Table 5.11 is created.

where $S^{11} = \frac{AK_D^2 + BK_D + C}{g_1(u_e)K_D - f_1(u_e)\tau_f + 1}$ and

Table 5.11: Routh array table for stability analysis

S^3	τ_f	$g_0(u_e)K_D - f_1(u_e) + \tau_f f_0(u_e)$
S^2	$g_1(u_e)K_D - f_1(u_e)\tau_f + 1$	$f_0(u_e)$
S^1	S^{11}	
S^0	$f_0(u)$	

$A = g_0(u_e)g_1(u_e)$,

$B = f_0(u_e)g_1(u_e)\tau_f - f_1(u_e)g_1(u_e) - f_1(u_e)\tau_f g_0(u_e) + g_0(u_e)$,

$C = f_1(u_e)[-f_0(u_e)\tau_f^2 + f_1(u_e)\tau_f - 1]$.

From the analysis of the Routh array table, three conditions for stability, which are given in (5.38), (5.39) and (5.40) are obtained.

$$\tau_f > 0 \tag{5.38}$$

$$K_D > \frac{\tau_f f_1(u_e) - 1}{g_1(u_e)} \tag{5.39}$$

and

$$AK_D^2 + BK_D + C > 0 \tag{5.40}$$

Equation (5.40) is a quadratic polynomial which can be solved by using a common quadratic solution method, which is given in (5.41). By solving (5.41), two solutions for K_D say Y_1 and Y_2 are obtained.

$$K_{D(1,2)} > \frac{-B \pm \sqrt{B^2 - 4AC}}{2A} \tag{5.41}$$

The solution for K_D from (5.41) will be obtained by evaluating (5.42).

$$K_D > \max(Y_1, Y_2) \tag{5.42}$$

Through the numerical evaluation of these conditions using the nonlinear functions, which are given in (B.1) to (B.4) in Appendix B.1, the solutions from (5.39) and (5.42) are combined to obtained (5.43), which gives the combined solution for the value of K_D for which the system will be stable.

$$K_D > Y_1, \qquad Y_1 = \frac{-B + \sqrt{B^2 - 4AC}}{2A} \tag{5.43}$$

Stability condition analyses

For robust stability of the system, it is desired that the controller be designed at the valve opening which require small control input to achieve stability. By analysing (5.43) for the P_{RB}, it is observed that generally, the lower bound of K_D required to stabilise the system will increase with increasing values of $f_1(u_e)$ and decreasing value of the product of the open-loop transfer function numerator coefficients, $g_1(u_e)$ and $g_0(u_e)$. Thus, for large values of $f_1(u_e)$ and small values of $g_1(u_e)g_0(u_e)$, the control input required to stabilise the system will be large, a condition which is not suitable for achieving robust stability in the system. Small value of K_D can be achieved at a valve opening with relatively small values of $f_1(u_e)$ and large values of $g_1(u_e)g_0(u_e)$, when compared to other valve openings. With this insight, the operating condition of the system and the system design can be defined to satisfy these condition in the open-loop transfer function.

Controller synthesis and simulation results

By evaluating the nonlinear functions and applying them on (5.43), the lower bound of the value of K_D for which the system will be stable for each valve opening is evaluated. The value of the filter time constant (τ_f) is defined to be equal to 0.9. The obtained values are summarised in Table 5.12.

Table 5.12: Calculated K_D values for the P_{RB}

u_e (%)	20	30	40	50	60	70	80	90	100
K_D(s/barg)(>)	6.1	9.2	25.4	38.7	56.3	73.1	74.6	75.4	76.8

From Table 5.12, the effect of the system's valve opening on the magnitude of K_D required for stability can be observed. Generally, the magnitude of K_D required to achieve stability increases as the valve opening increases. This reflects the increasing magnitude of the control input that is required to stabilise the system as the open-loop valve opening increases. This agrees with the result of the controllability analysis (see Table 5.5). For a small value of u_e, the K_D is relatively small, indicating that relatively small control input will be required to stabilise the system at this valve opening, a condition which is necessary for achieving robust stability in the system.

The controller designed at $u = 20\%$ is therefore implemented and the simulation results obtained is analysed. The controller value implemented in the simulation is obtained by multiplying the minimum value, which is given in Table 5.12 by a factor of 2(6dB). The value of the filter time constant (τ_f) is defined to be equal to 0.9.

During the simulation the following steps are taken in line with the procedure explained in section 5.5.3.

1. The valve opening is initially set to a fixed position corresponding to the open-loop unstable valve opening of u =20%.

2. The controller is then switched on after a simulation period of 4 hours. It is observed that the system is stabilised when the controller is switched on.

3. Once the system is stabilised, the reference valve opening (u_r) is gradually increased and the system is allowed to stabilise for each step increase.

4. The gradual increase in the u_r is continued until the valve opening at which the controller cannot stabilise the system is reached at 29 hours.

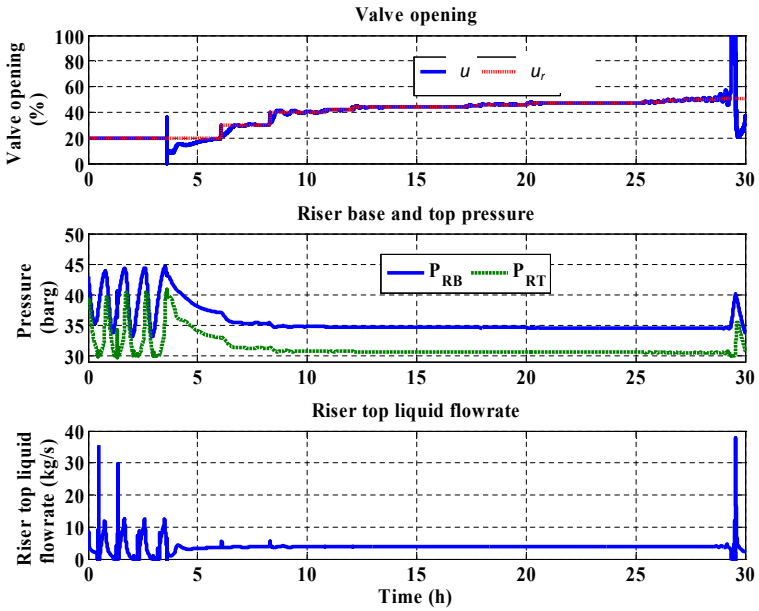

Figure 5.7: Simulation result for the P_{RB}

From this simulation result, it can be observed that the system was stabilised at a maximum valve opening of 49$\%$. Next, the control of the system with P_{RT} will be presented.

5.5.3.3 P_{RT} control

The simulation result obtained by implementing the P_{RT} as the controlled variable is also presented. The Routh stability analysis, which is similar to that performed for the P_{RB} can be also be applied for the P_{RT} to obtain the condition for stability. The resulting conditions for evaluating the value of K_D for which the system will be stable are given in (5.44), (5.45) and (5.46).

$$\tau_f > 0 \tag{5.44}$$

$$K_D < -\frac{\tau_f f_1(u_e) - 1}{g_1(u_e)} \tag{5.45}$$

$$AK_D^2 + BK_D + C > 0 \tag{5.46}$$

where $A = -g_1(u_e)g_0(u_e)$

$B = f_1(u_e)g_1(u_e) - f_0(u_e)g_1(u_e)\tau_f - f_1(u_e)\tau_f g_0(u_e) + g_0(u_e),$

$C = f_1(u_e)(f_1(u_e)\tau_f - f_0(u_e)\tau_f^2 - 1)$

Equation (5.46) is a quadratic equation, whose solution will give two conditions for K_D, say Y_1 and Y_2. The combined solution for K_D will be better obtained

by factorising the solution numerically. Through the analysis of the numerical solution, the combined solution for the value of K_D for which the system will be stable is obtained as given in (5.47).

$$Y_1 < K_D < -\frac{\tau_f f_1(u_e) - 1}{g_1(u_e)} \tag{5.47}$$

where $Y_1 = \frac{-B+\sqrt{B^2-4AC}}{2A}$.

Controller synthesis and simulation result

By inserting the nonlinear functions, which are given in Appendix B.2 into equation (5.47) the values of K_D for which the closed-loop system will be stable can easily be evaluated for each valve opening. The analysis of (B.5) and (B.7) shows that the value of $f_1(u_e)$ will increase while the value of $g_1(u_e)$ will decrease with increasing valve opening. This implies that the minimum upper and lower bound on K_D will be obtained at the open-loop unstable valve opening of u =20%, which is the smallest open-loop unstable valve opening considered.

The lower and upper bound on K_D, which is obtained at valve opening u_e =20% with the filter time constant (τ_f) equal to 1 is 7.5$<$ K_D $<$28.8. The value of K_D implemented in the system is obtained by multiplying the lower bound by a factor of 2(6dB). During the simulation, the valve opening is initially set to a fixed position corresponding to the open-loop unstable valve opening of u =20%. The controller is then switched on after a simulation period that is greater than 2 hours. The simulation result obtained by implementing this controller is shown in Figure 5.8.

The interpretation of this simulation result follows the steps explained in section 5.5.3. From this simulation result, it can be observed that the controller

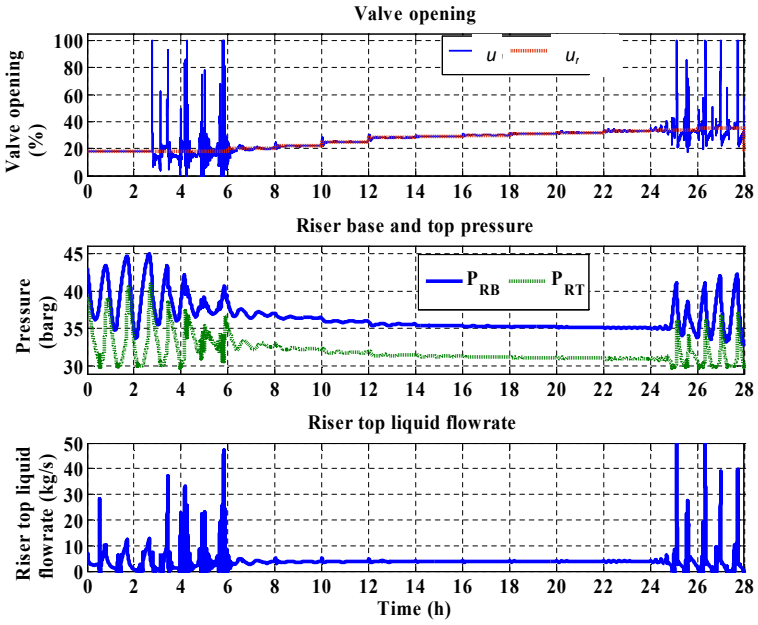

Figure 5.8: Simulation result for the P_{RT}

was switched on after more than 2 hours of open loop simulation. The system was stabilised at about 3 hours after the controller was switched on. This large settling time, which is not observed with the P_{RB} and the Q_T, could indicate a limitation in achieving quick stabilisation of the system with the P_{RT} as a controlled variable, when the controller is implemented with certain degree of severity of the severe slugging in the system. The system was stabilised at a maximum valve opening of 33% at 24 hours. Next, the control of the system with Q_T as the controlled variable will be presented.

5.5.3.4 Q_T control

The simulation result obtained by implementing the Q_T as the controlled variable is also presented. The Routh stability analysis, which is similar to that performed for the P_{RB} and the P_{RT} can be also be applied for the Q_T to obtain the condition for stability. Three conditions with which the value of K_D can be evaluated are given in (5.48), (5.49) and (5.50).

$$\tau_f > -K_D g_2(u_e) \tag{5.48}$$

$$K_D > \frac{\tau_f f_1(u_e) - 1}{g_1(u_e)} \tag{5.49}$$

$$AK_D^2 + BK_D + C > 0 \tag{5.50}$$

where $A = g_1(u_e)g_0(u_e)$

$B = g_1(u_e)f_0(u_e)\tau_f - g_0(u_e)\tau_f f_1(u_e) + g_0(u_e) - f_1(u_e)g_0(u_e) - f_0(u_e)g_2(u_e))$

$C = f_1(u_e)(f_1(u_e)\tau_f - f_0(u_e)\tau_f^2 - 1)$

Equation (5.50) is a quadratic equation, whose solution will give two conditions for K_D, say Y_1 and Y_2. The combined solution would be obtained by evaluating (5.51). The combined solution for K_D will be better obtained by factorising the solution numerically. From the numerical solution analysis, the combined solution for the value of K_D for which the system will be stable is obtained as given in (5.52).

$$K_D > \max(Y_1, Y_2) \tag{5.51}$$

$$K_D > (Y_1), \qquad Y_1 = \frac{-B + \sqrt{B^2 - 4AC}}{2A} \tag{5.52}$$

Controller synthesis and simulation results

By applying the nonlinear functions, which are given in Appendix B.3 to evaluate equation (5.52), the values of K_D for which the closed-loop system will be stable with Q_T as the controlled variable can easily be evaluated for each valve opening. The condition $K_D > 31378$ s^2/m^3, is obtained at valve opening u_e =20% with the filter time constant (τ_f) equal to 1. The value of K_D implemented in the system is obtained by multiplying this minimum value by a factor of 2(6dB). The simulation result obtained is shown in Figure 5.9.

The interpretation of this simulation result also follows the simulation procedure explained in section 5.5.3. From this simulation result, it can be observed that the system was stabilised at a maximum valve opening of 39%. Next, the analyses and the comparison of these simulation results will be presented.

5.5.3.5 Analyses and comparison of simulated results

From the simulation results shown in Figures 5.7 - 5.9, it can be observed that the unstable riser system was stabilised using all the three controlled variables, at some open-loop unstable valve opening. Firstly, this shows that by applying the control strategy implemented in this controllability analysis, any of these

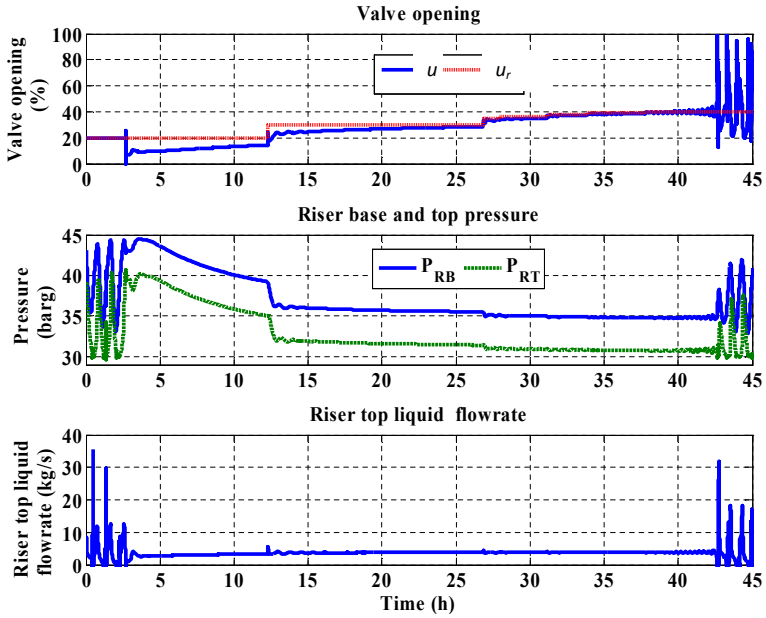

Figure 5.9: Simulation result for the Q_T

variables can stabilise the unstable riser system at an open-loop unstable operating. Unlike the conclusion from the Storkaas' controllability analysis [100] in which the P_{RT} is considered to be unsuitable for slug control, and the Q_T is considered to be suitable if it is used in the inner feedback loop in a cascade control, this result shows that slug control with P_{RT} and the Q_T is possible if perfect set point tracking of the controlled variable is avoided in the system such that a derivative controller is applied to stabilise the system at a reference valve opening. With this control strategy, the controller input does not need to be zero to stabilise the system at the reference valve opening.

However, as was discussed in section 5.3.1, the important insight from these controllability analyses is the difference in the maximum stable valve opening which each variable can achieve. This will reflect the production that is achievable. It was predicted in the controllability analysis in section 5.3.1 that gener-

ally, the P_{RB} and the Q_T will stabilise the system at larger valve opening than the P_{RT}. From the simulation results, the P_{RB} achieved stability at the maximum valve opening of 49$\%$. This is higher than that achieved with the P_{RT}, which is 33$\%$. Also the Q_T achieved stability at the maximum valve opening of 39$\%$, which is still higher than that achieved with the P_{RT}. Thus, these simulation results confirm the general trend of the ability of these variables to stabilise the unstable riser system at large valve opening, as predicted in the controllability analysis.

Also, the corresponding production achieved with each variable showed that the maximum production is achieved with the P_{RB}, while the minimum is achieved with the P_{RT}. These results are summarised in Table 5.13.

Table 5.13: Simulation performance table

Controlled variable	u ($\%$)	P_{RBmin} (barg)	Production (m^3/day)
P_{RB}	49	34.54	348
Q_T	39	34.7	344.7
P_{RT}	33	35.58	334.5

5.5.4 Simulation with topside separator gas valve (u_g) as manipulated variable

The implementation of the P_{RB}, the P_s, the P_{RT} and the Q_{Gesp} as controlled variables to stabilise the unstable riser system with the topside separator gas valve (u_g) as manipulated variable is presented in this section. The Routh stability criterion is also applied for each variable as in the case of control with

the riser top valve as the manipulated variable. The system's linear transfer function, which is required for the Routh stability analysis, is obtained for each variable at the relevant valve openings by using their general form. The general form of the linear model transfer function for each controlled variable had been provided in section 5.4.2.

From the Routh stability analysis, the combined solution for the stability of the system is obtained as a function of the valve opening. For the P_{RB}, it can be observed that the general form of the linear model transfer function given in (5.29) is similar to the general form of the P_{RB} model given in (5.19). Thus, the solution obtained for the P_{RB} in (5.43) can be applied to evaluate the values of K_D for which the system is stable with P_{RB} as the controlled variable and u_g as the manipulated variable.

For the P_s and P_{RT}, it can also be observed that the general form of the linear model transfer function given in (5.30) and (5.31) are similar to the general form of the P_{RT} model given in (5.20). Thus, the solution obtained for the P_{RT} in (5.47) can be applied to evaluate the values of K_D for which the system is stable with P_s and P_{RT} as the controlled variables. Also, the solution obtained in (5.52) will also be applied to evaluate K_D for Q_{Gouts}, since its general form, which is given in (5.32) is the same with that obtained for the Q_T, which is given in (5.21). The calculation of the controller values for each controlled variables can easily be done using the corresponding conditions. The general trend of the value of K_D showed that the controller magnitude required to stabilise the system increased as the valve opening u_g increased. This agrees with the magnitude required to stabilise the system as obtained in section 5.4.3. Table 5.14 provides the lower bound of K_D obtained at u_g =30%. The controller value implemented for each controlled variable is obtained by multiplying the minimum by a factor of 2(6dB).

Table 5.14: K_D values for controller designed at $u_g = 30\%$

	P_{RB}	P_s	P_{RT}	Q_{Gouts}
K_D	$K_D > 11.1$ (s/barg)	$1.8 < K_D < 16.6$ (s/barg)	$0.85 < K_D < 12.7$ (s/barg)	$K_D > 27000$ (s^2/m^3)

5.5.5 Simulation results analyses and comparison

In this section, the simulation result obtained from the implementation of the controller designed for each of the controlled variable; P_{RB}, P_s, P_{RT} and Q_{Gouts}, is presented. For each controlled variable, the simulation results is obtained by implementing the controller designed at $u_g = 30\%$.

The valve opening is initially set to a fixed opening corresponding to the open-loop unstable valve opening of u_g =30%. The controller is then switched on after a simulation period when the system is open-loop unstable. Once the system is stabilised, the reference valve opening (u_r) is gradually increased and the system is allowed to stabilise for each step increase. The gradual increase in the u_r is continued until the valve opening at which the controller cannot stabilise the system is reached. The simulation results are presented in Figure 5.10 - 5.13.

From these simulation results it can be observe that the system was stabilised with all the four controlled variables when the controller was switched on. This shows that by implementing an appropriate control strategy, any of these controlled variables can stabilise the unstable riser system at an open-loop unstable operating. Thus, the key focus of the controllability analysis should be to evaluate the maximum closed-loop stable valve opening, which each controlled variable can achieve, since stability at a relatively large valve opening will be

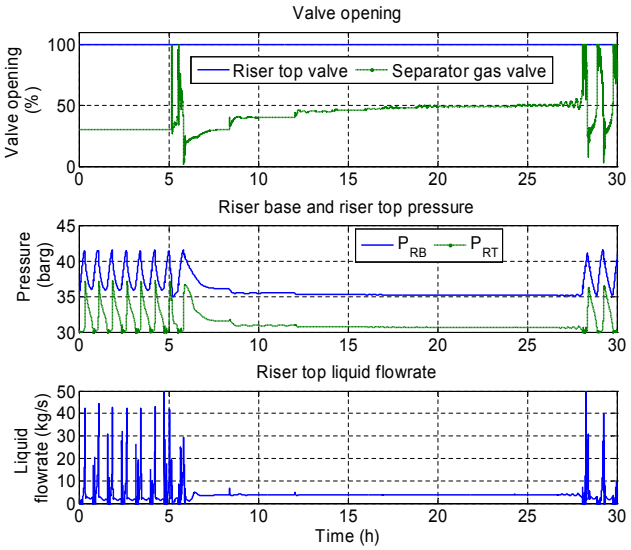

Figure 5.10: Simulation result with the P_{RB}

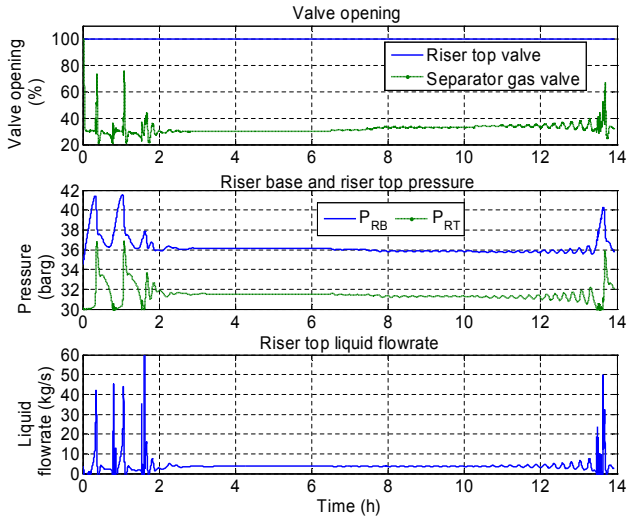

Figure 5.11: Simulation result with the P_s

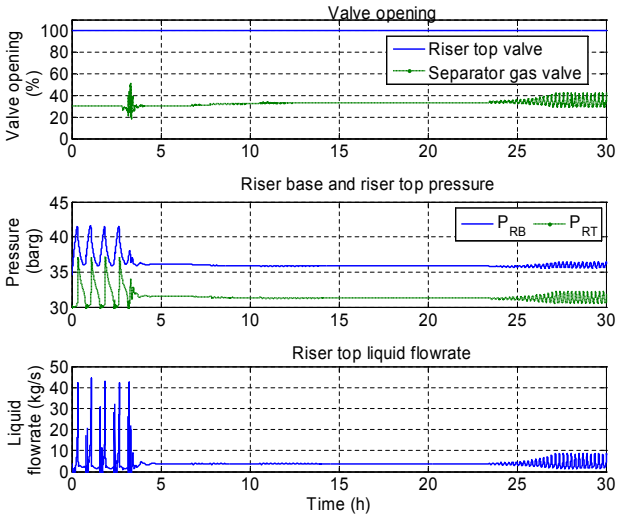

Figure 5.12: Simulation result with the P_{RT}

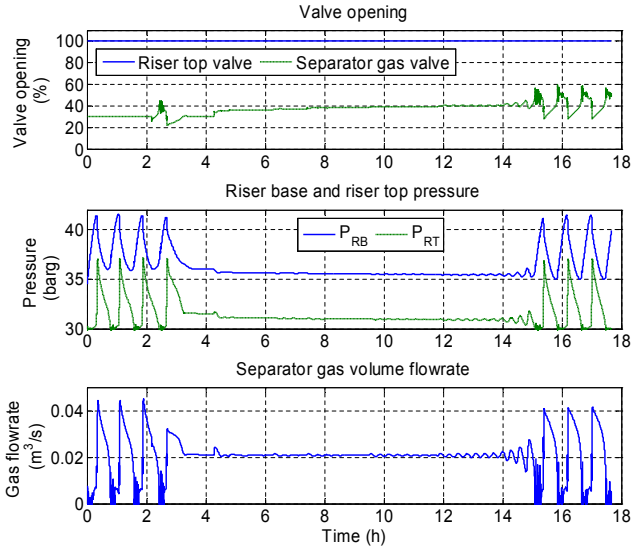

Figure 5.13: Simulation result with the Q_{Gouts}

required to maximise oil production (see section 5.2.2).

From the controllability analysis of the P_{RB}, the Q_{Gouts}, the P_s and the P_{RT} in section 5.4.3, the general prediction of the ability to stabilise the system at large valve opening indicates that the P_{RB} and the Q_{Gouts} are able to stabilise the system at a larger valve opening than the P_s and the P_{RT}. The simulation results are analysed against this prediction. From Figure 5.10, it can be observed that the maximum stable valve opening achieved by the P_{RB} is 50$\%$. This is larger than that achieved by the P_s and the P_{RT}, which achieved maximum stable valve opening at 32$\%$ and 33$\%$ respectively. Also, the maximum stable valve opening achieved by the Q_{Gouts} is 40$\%$. This valve opening is also larger than that achieved by the P_s and the P_{RT}, although, it is smaller than the valve opening achieved by the P_{RB}. These results are also summarised in Table 5.13. It is clear that the simulation results agree with the general predictions of the controllability analysis. The liquid production achieved by each of the controlled variable is also summarised in Table 5.15. The maximum production is achieved with the P_{RB}, while the minimum is achieved with the P_s.

Table 5.15: Simulation performance table

Controlled variable	u_g ($\%$)	P_{RBmin} (barg)	Production (m^3/day)
P_{RB}	50	35.18	339.2
P_s	32	35.88	331
P_{RT}	33	35.85	331.5
Q_{Gouts}	40	35.58	334.5

5.6 Comparison of the controllability with u and u_g

In this section, a general comparison of the controllability of the industrial riser system using the u and the u_g is presented. Firstly, it can be observed that the riser-pipeline system can be controlled by using either u or u_g as the manipulated variable. Generally, the controllability analysis showed that both u and u_g have the ability to stabilise the system at large valve opening with the riser base pressure and the gas volumetric flow rate as the controlled variables. For the P_{RT}, the controllability analysis showed its limited ability to stabilise the system at a large valve opening for the two manipulated variables.

From the simulation result analysis, the control with u_g showed the ability to stabilise the system at a slightly higher valve opening than control with the u. However, due to the differences in the individual valve characteristics in the industrial riser system, it is observed that although the control with u_g achieved stability at a slightly higher valve opening, the control with u achieved lower P_{RB}, when compared to an equivalent valve opening with the u_g. This is shown in Table 5.16, which shows the maximum stable valve opening (u_{ms}), the P_{RBmin}, and the production obtained through simulation for the P_{RB} and the P_{RT}.

Table 5.16: Controllability with u and u_g comparison table

	u_{ms} (%)		P_{RBmin} (barg)		Production (m^3/day)	
Variable	u	u_g	u	u_g	u	u_g
P_{RB}	49	50	34.54	35.18	348	339.2
P_{RT}	33	33	35.58	35.85	334.5	331.5

As will be discussed in Chapter 6 and 7, in order to maximise oil production it

is necessary to operate the system such that the flowline pressure is reduced under stable operating condition. Although it is desired to stabilise the system at a large valve opening in order to maximise oil production, this controllability analysis also reveals that when analysing the controllability of the riser-pipeline system for different valves as the manipulated variable, the minimum P_{RB} obtained, which can be affected by the individual valve characteristics must be evaluated. This has been achieved through simulation analysis. It is shown that for the industrial riser system used in this work, closed-loop control with u will give a lower P_{RB} than with u_g for the same value of the valve opening.

5.7 Conclusions

In this chapter, the controllability analysis of the unstable riser-pipeline system for stability and production has been presented. The control objectives are defined to reflect the core operational targets of the riser-pipeline production system, which are the ability to ensure system stability and achieve maximum oil production. The interdependency between a stable valve opening and the accumulated production was explored as the fundamental basis for the controllability analysis. It is shown that, the larger the stable valve opening achieved in the system, the higher the ability to maximise oil production.

The ability of a slug control system to achieve these desired control objectives are evaluated with focus on the choice of the controlled variables, using two manipulated variables, which include the riser top valve opening and the topside separator gas valve opening. The controllability analysis was focused on applying the Hankel singular value analysis of the system linear model to eval-

uate the minimum control input magnitude required to stabilise the system at each open-loop unstable valve opening.

The controllability analysis of the industrial riser system using u as the manipulated variable showed that theoretically, all the three controlled variables considered, namely: the P_{RB}, the P_{RT} and the Q_T, has the ability to stabilise the system at some open-loop unstable operating points without input saturation. Also, the controllability analysis of the same industrial riser system using the u_g as the manipulated variable, showed that all the four controlled variables considered namely: the P_{RB}, the P_s, the P_{RT} and the Q_{Gesp}, has the ability to stabilise the system at some open-loop unstable operating point without input saturation. Interestingly, this controllability analysis also revealed the varying ability of each controlled variable to stabilise the system at a large valve opening.

Generally, using u as the manipulated variable, it was observed that the P_{RB} and the Q_T are able to stabilise the system at a larger valve opening than the P_{RT}. Also, by using u_g as the manipulated variable, it was observed that the P_{RB} and the Q_{Gouts} are able to stabilise the system at a larger valve opening than theP_s and the P_{RT}. These results are important as they reflect the production that is achievable with each controlled variable, under stable operating condition.

A more suitable slug control strategy in which the unstable riser-pipeline system is stabilised at a reference valve opening using a derivative controller action is implemented to perform closed-loop simulation for each controlled variable. In this controlled strategy, perfect tracking of the controlled variable set point was neglected in the system such that the controlled variable set point is set equal to zero, and the derivative controller input is the measured value of the controlled

variable, which is not necessarily zero. The derivative controller parameters are obtained using the Routh stability criterion.

The closed-loop simulations in OLGA confirmed the general predictions of this controllability analysis. In the simulation using u as the manipulated variable, it was observed that the P_{RB} and the Q_T are able to stabilise the system at a larger valve opening than the P_{RT}, as was predicted. However, it was also observed that the P_{RB} achieved stability at a slightly larger valve opening than the Q_T. Also, in the simulation using u_g as the manipulated variable, it was confirmed that the P_{RB} and the Q_{Gouts} are able to stabilise the system at a larger valve opening than theP_s and the P_{RT}. Simulation results also showed that accumulated production increased with the ability to stabilise the system at a large valve opening. In the simulation with the u, the maximum accumulated production was obtained with the P_{RB} and the minimum with the P_{RT}. Also, in the simulation with the u_g, the maximum accumulated production was obtained with the P_{RB} and the minimum with the P_s.

Interestingly, this controllability analyses has shown that most controlled variables including the P_{RT} which was considered to be unsuitable for slug control, and the Q_T which was considered to be suitable if it is used in the inner feedback loop in a cascade control, can be used for slug control if an appropriate slug control strategy, such that presented in this chapter is implemented.

Chapter 6

Production potential of severe slug control system

6.1 Introduction

The primary objective of a slug control system which is to eliminate slugging and ensure stable system operation has guided the common approach to slug control systems design and implementation. One of the proven solutions to slug control is the choking of the riser top valve. Choking transforms the unstable flow in the riser to stable flow. However, due to the additional pressure drop across the valve, it induces extra back pressure on the pipeline. Active feedback, feed forward and cascade control systems have been applied to dynamic choking for slug control [23, 32, 42, 51, 71, 75, 76, 101, 99].

Although the implementation of a slug controller in the active choking solution has shown its potential to successfully eliminate severe slugging with some benefits, it can also adversely affect the overall production of the system if it is implemented inappropriately. As a result of this, the emphasis on the performance of slug control systems has recently shifted from just achieving a stable

system condition to also maximizing production [76].

However, the method for analysing the potential of a slug control system to maximise production and how this potential can be achieved have remained unclear. Most slug control systems are implemented without proper systematic assessment of its potential to maximise production in the system. In this work, a systematic method based on the pressure bifurcation map of the riser system is proposed to analyse the production and pressure loss relationship, and to reveal the potential of a slug control system to maximise production.

It is shown that for an unstable riser-pipeline system with known inlet and outlet boundary conditions, production loss or gain due to operation in stable or unstable operating conditions could be predicted using a pressure dependent dimensionless variable known as the Production Gain Index (PGI). The chapter starts with the description of the pressure and production dependency followed by production estimation using the PGI and finally a case study.

6.2 Pressure and production

The ultimate aim of stabilising severe slugging flow conditions is to achieve smooth and productive operation. Therefore, a slug control system should not only consider stability but also maximise oil production. For this purpose, it is necessary to analyse the effect of pressure loss associated with choking on the oil production. For simplicity, linear relations are assumed in the analysis below. Firstly, the pressure and production relationship of a linear well will be discussed.

6.2.1 Linear well productivity

The relationship for determining oil production rate from a linear well can be derived generally from Darcy's law [49] as given in (6.1), where q_w is the well production rate, B is the production index, P_{res} is the reservoir pressure and P_{WH} is the well-head pressure. The production index, B, is a function of the reservoir geometric factor and the formation volume factor, which are dependent on the reservoir dynamic characteristics (see section 4.3.4.1). In this analysis, it is assumed that the reservoir dynamic characteristics and pressure do not change significantly over a reasonable period. Thus, the production index, B, and the P_{res} will be assumed as constants.

$$q_w = B(P_{res} - P_{WH}) \tag{6.1}$$

The relationship in (6.1) shows that $q_w \propto (P_{res} - P_{WH})$. Therefore, an increase in the production rate can be achieved by reducing P_{WH}, which depends on a number of system related factors including the downstream separator pressure, and pressure loss across the pipeline and the riser. Here, the P_{WH} dependency on the valve opening including the pressure loss across the valve, the riser and the pipeline will be consider. For a specific valve opening, the system can either be stable or unstable. This will be analysed correspondingly as follows.

For a stable operating condition, the P_{WH} can be fairly constant, while for an unstable system, P_{WH} will oscillate significantly. For both conditions, the total production over a certain period T, is given as follows,

$$J_W = \int_0^T q_w dt = B(P_{res} - \bar{P}_{WH})T = J_0 - J_p \tag{6.2}$$

where $J_0 = BP_{res}T$ is constant, $J_p = B\bar{P}_{WH}T$ is pressure dependent production loss and $\bar{P}_{WH} = \frac{1}{T}\int_0^T P_{WH}dt$ is the average pressure over T.

6.2.2 Unstable systems

For an unstable riser-pipeline system, the average well-head pressure ($\bar{P}_{WH}$) is calculated based on the prevalent pressure profile that is obtained from the system. The prevalent pressure profile, which is obtained from the unstable system could be described as irregular.

An irregular slug pressure profile can take any shape, sometimes a dome shape. For an irregular (dome) shaped slug pressure profile as shown in Figure 6.1, the $\bar{P}_{WH}$ can be calculated by taking the mean integral of the pressure points within the slug period.

This would require dividing the pressure profile into N-number of segments. Equation (6.3) gives the relationship for calculating the $\bar{P}_{WH}$ for the irregular slug pressure profile.

$$\bar{P}_{WH} = \frac{1}{N}\sum_{i=1}^{N} P_{WH}(t_0 + i\tau) \tag{6.3}$$

where N is the number of segments, t_0 is the starting time, τ is the sampling time and $P_{WH}(t_0 + i\tau)$ is the instantaneous pressure value at $t_0 + i\tau$. With this equation, the $\bar{P}_{WH}$ in the system for any resulting pressure profile at any valve opening can be calculated.

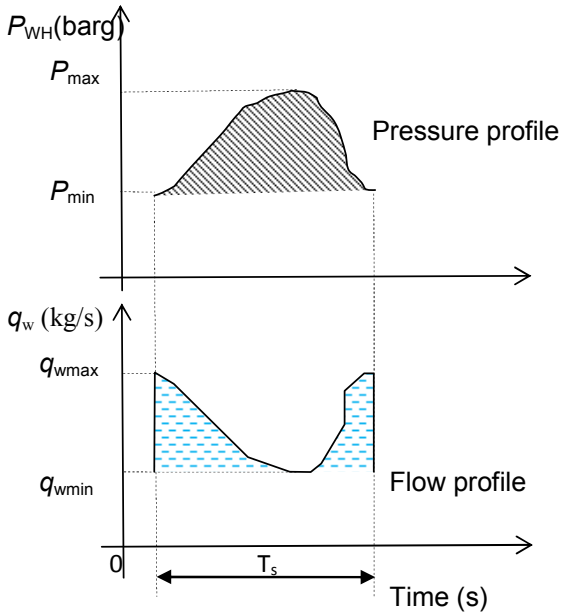

Figure 6.1: Irregular dome slug profile

6.2.3 Stable systems

For stable systems, the P_{WH} is constant at steady-state, hence it is the same as $\bar{P}_{WH}$. However, for unstable flow conditions, such as severe slugging flows, steady-state is never reachable and the corresponding equilibrium is referred to as the unstable equilibrium. Assume that such an unstable system is represented by a differential equation as follows:

$$\dot{x} = f(x, u), \qquad P_{WH} = g(x, u) \tag{6.4}$$

where x is the state of the system, u is the opening of choking valve and P_{WH} is the well-head pressure, then, the unstable equilibrium, x_e and the corresponding well-head pressure for a given valve opening, u_e is determined by the

algebraic equations, which are given in (6.5).

$$f(x_e, u_e) = 0, \qquad P_{WHe} = g(x_e, u_e) \tag{6.5}$$

If such an unstable system is stabilised by a feedback control, $u = k(P_{WH})$, then the steady-state of the stable closed-loop system, x_c, P_{WHc} and u_c are determined as follows.

$$0 = f(x_c, u_c), \qquad P_{WHc} = g(x_c, u_c), \qquad u_c = k(P_{WHc}) \tag{6.6}$$

Therefore, if $u_e = u_c$, then $x_e = x_c$ and $P_{WHe} = P_{WHc}$, *i.e.* the steady-state of the stable closed-loop system must be equal to the unstable equilibrium condition in accordance with the same valve opening. The values of $P_{WHc} = P_{WHe}$ at the unstable equilibrium point corresponding to a particular valve opening can be calculated using an accurate model of the system. However, it can also be obtained using the multiphase flow simulator such as OLGA.

For the riser system, u is the valve opening, which determines the operating point of the system. For a set of input values, say $u = (u_1, u_2, ...u_n)$, the corresponding equilibrium values $x = (x_1, x_2, ...x_n)$ are determined by (6.5). These values can then be used for production analysis of active slug control.

6.3 Production Gain Index (PGI)

For a riser system stabilised by a slug controller operating at a valve position, u_c, the production gain when compared to an unstable slugging condition corresponding to an open-loop valve opening, u, is $J_p(u) - J_p(u_c)$. In order to analyse the production potential of the slug control system, a dimensionless variable, the Production Gain Index (PGI) is introduced as the ratio of the production gain, $J_p(u) - J_p(u_c)$ against $J_p(u_c)$ as follows.

$$\xi(u, u_c) = \frac{J_p(u) - J_p(u_c)}{J_p(u_c)} = \frac{\bar{P}_{WH}(u)}{P_{WHc}(u_c)} - 1 \tag{6.7}$$

The PGI as a function of u and u_c can be represented as contours in the (u, u_c) plane. Amongst these contours is the zero PGI (ZPGI) contour, which is defined as $\xi(u, u_c) = 0$. The ZPGI contour divides the (u, u_c) plane into two areas, namely: the positive PGI (PPGI) area, which is located above the ZPGI line and the negative PGI (NPGI) area, which is located below the ZPGI line. A typical example of this ZPGI contour is shown in Figure 6.4 for a case study, which will be discussed in section 6.4.

According to the definition of the PGI in (6.7), the PPGI area corresponds to production gain operating points, *i.e.* for any point (u, u_c) in this area, if a slug controller can stabilise the system at the valve opening, u_c, then the corresponding production will be larger than the one obtained when the valve opening is fixed at u without any control. Similarly, the NPGI area indicates production loss operating conditions, *i.e.* for a point (u, u_c) in this area, if a slug control stabilises the system with valve opening u_c, the resulting production will be less than the one corresponding to the valve opening fixed at u without control.

6.4 Case study - the industrial riser system

To illustrate the application of the PGI analysis method to reveal the production potential of a riser-pipeline system, the industrial riser system, which is described in section 3.5 will be used. The open-loop stability of this system can be analysed using the Hopf bifurcation map presented in Figure 4.18. The Hopf bifurcation map indicates that the maximum open-loop valve opening cor-

responding to a stable system is $u = 12\%$. For $u > 12\%$, the system becomes unstable, and oscillates between the maximum and minimum pressure values. The $\bar{P}_{WH}(u)$ and $P_{WHc}(u_c)$ of the system for $12\% < u, u_c \leq 100\%$ will be calculated.

6.4.1 The $\bar{P}_{WH}$ and the P_{WHc} for the industrial riser system

In this section, the $\bar{P}_{WH}$ and P_{WHc} for the industrial riser system for each of the open-loop unstable valve opening will be calculated.

6.4.1.1 Calculating the $\bar{P}_{WH}$

To calculate the $\bar{P}_{WH}$ for the industrial riser system for $12\% < u \leq 100\%$, the system is simulated using the OLGA model to obtain the P_{WH} profile. The P_{WH} profile obtained at four different valve openings are shown in Figure 6.2.

From Figure 6.2, it can be observed that these P_{WH} profiles are almost irregular in shape, with varying slug period and the minimum and maximum pressure values. Thus, using (7.19), the $\bar{P}_{WH}$ can be calculated for each valve opening (u). The values of $\bar{P}_{WH}$ obtained for each u are plotted in the solid line with the square marks in the bifurcation map shown in Figure 6.3.

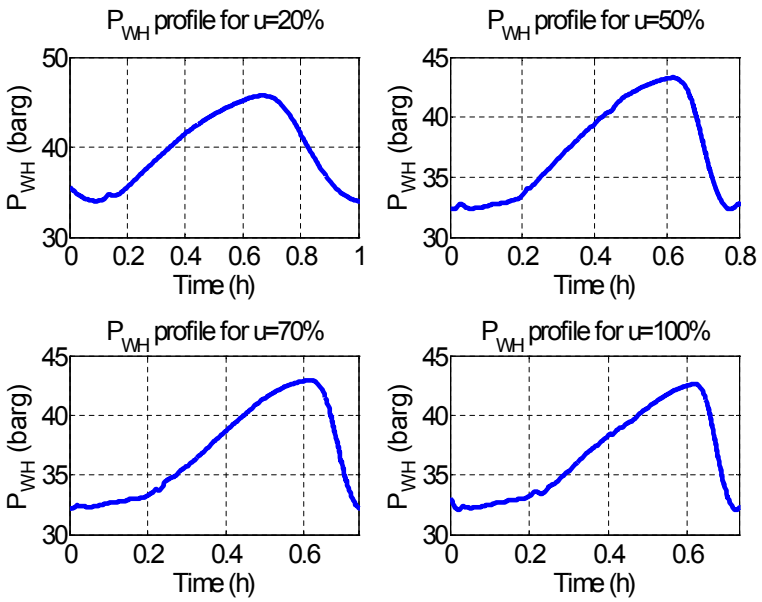

Figure 6.2: Well-head pressure profile

6.4.1.2 Calculating the P_{WHc}

The OLGA model of the industrial riser system is used to calculate the P_{WHc} with the following procedures. Firstly, the steady state option must be turned on in the case definition/options on the property bar. Also, the initial valve opening should be specified for each operating point. The P_{WHc} is obtained in the pressure trends as the initial steady state value at t=0. The P_{WHc} obtained using the OLGA model is plotted with the dashed line as shown in Figure 6.3.

From Figure 6.3, it can be observed that the P_{WHc} is less than the $\bar{P}_{WH}$ at each operating point where $u = u_c$. However, this is not the case when the P_{WHc} corresponding to a particular valve opening, u_c, is compared across the $\bar{P}_{WH}$ for all the operating points, $12\% \leq u \leq 100\%$ as shown by the base line in Figure 6.3. The crossing point of the base line with P_{WHc} indicates that

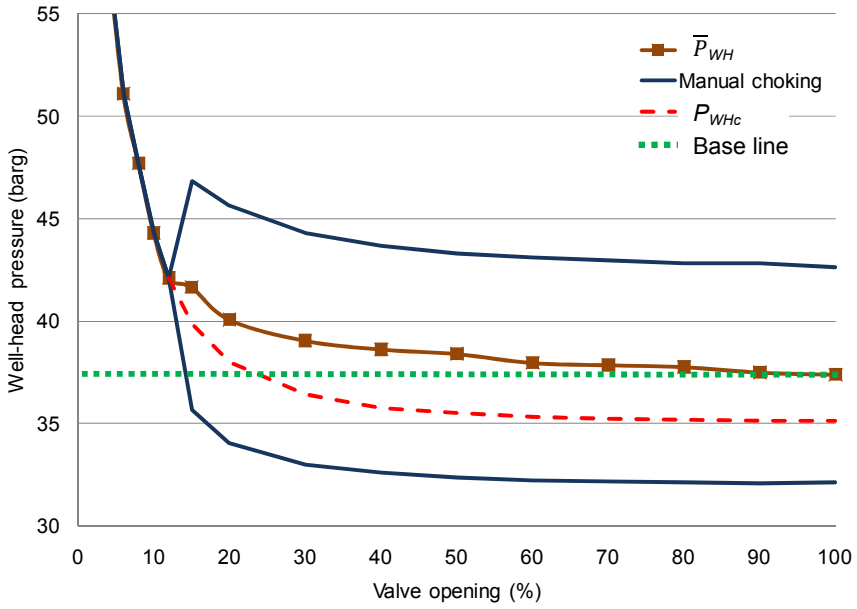

Figure 6.3: Well-head pressure Hopf bifurcation map of the industrial riser system with $\bar{P}_{WH}$ and P_{WHc}

the corresponding u_c together with u =100% is a point of the (u, u_c) plane on the zero-PGI curve. The P_{WHc} points on the right of this u_c correspond to positive PGI values for any 12% $\leq u \leq$100%. This indicates that implementing a feedback controller to stabilise the system at a P_{WHc} may not provide the most suitable operating point for maximum oil production. To systematically analyse the system for the suitable operating point for maximum oil production, the PGI analysis will be applied, as discussed in section 6.3.

6.4.2 PGI analysis

By using the data points in Figure 6.3, the ZPGI values will be obtained using (6.7). For each u, the ZPGI value is obtained where $\xi(u, u_c) = 0$, i.e where the $\bar{P}_{WH}(u)$ is equal to the $P_{WHc}(u_c)$. With the ZPGI points, the plot of $\xi(u, u_c) = 0$ (ZPGI line) is generated, with a plot of u_c against u, as shown in Figure 6.4.

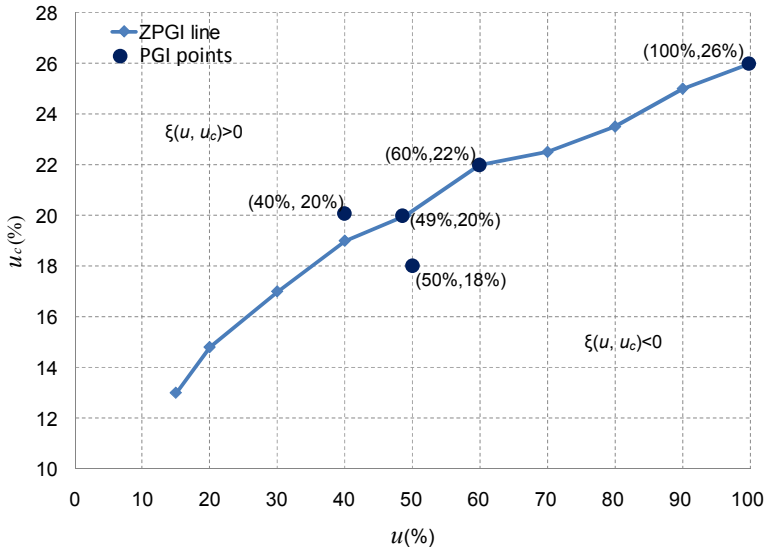

Figure 6.4: Plot of the ZPGI for the industrial riser system

From Figure 6.4, the points on the ZPGI line defines the operating points (u, u_c) where the production obtained at the point defined by u (with no control) will be the same with that obtained at the corresponding u_c (with controller). For example, for the ZPGI point defined by (60%,22%), it can be predicted that the production obtained without a slug controller at u =60% will be the same with that obtained with a slug controller at u_c =22%, since $\xi(60\%, 22\%) = 0$. Thus, a slug controller operating at u_c =22% has zero production gain or loss over operation at u =60%.

For any operating point on the ZPGI line defined by (u, u_c), a PPGI will be obtained with reference to the u_c, for all open-loop valve openings less than the corresponding u. From the reference u_c, the open loop valve openings less than the corresponding u will be traced above the ZPGI line. Thus, any operating point defined by (u, u_c) above the ZPGI line, corresponds to a PPGI point, where the $\xi(u, u_c) > 0$. The production obtained with a slug controller, which stabilises the system at u_c, will be higher than that obtained with the system operating at u without control.

For example, for the PPGI point defined by (40$\%$,20$\%$) in Figure 6.4, it can be predicted that the production obtained with a slug controller at u_c =20$\%$ will be higher than that obtained without a slug controller at u =40$\%$, since $\xi(40\%, 20\%) > 0$. Also, for the ZPGI point defined by $(49\%, 20\%)$, it can be predicted that the production obtained with a slug controller at u_c =20$\%$ will be higher than that obtained for all open-loop valve openings u <49$\%$.

Furthermore, for any point on the ZPGI line defined by (u, u_c), a NPGI will be obtained with reference to the u_c for all open-loop valve openings larger than the corresponding u. From the reference u_c, the open loop valve openings larger than the corresponding u will be traced below the ZPGI line. Thus, any operating point defined by (u, u_c) below the ZPGI line corresponds to a NPGI point, where the $\xi(u, u_c) < 0$. This implies that the production obtained with a slug controller, which stabilises the system at u_c, will be less than that obtained with the system operating at u without control.

For example, for the NPGI point defined by (50$\%$,18$\%$) in Figure 6.3, it can be predicted that the production obtained with a slug controller at u_c =18$\%$ will be less than that obtained without a slug controller at u =50$\%$, since $\xi(50\%, 18\%) < 0$. Thus, for the ZPGI point defined by (49$\%$,20$\%$), it can be predicted that the

production obtained with a slug controller at $u_c = 20\%$ will be less than that obtained for all open-loop operating points u >49$\%$. From these analyses, it can also be deduced that for the ZPGI point defined by (100$\%$,26$\%$), the production obtained with a slug controller at u_c >26$\%$ will be higher than that obtained for all open-loop valve openings $u \leq$100$\%$.

These analyses provide a very useful insight into the production potential of this industrial riser system, using a slug controller. The PGI analysis reveals that the extent to which a feedback controller can assure increased production depends on the maximum closed-loop operating point the feedback controller can achieve. Since the ZPGI line is independent of the control design but dependent on the riser-pipeline system design, the operating condition and the flow condition, the decision on whether to implement a feedback controller or not in order to stabilise the riser system as well as maximise production can easily be made without rigorous simulations or costly trial and error method.

6.4.3 Simulated production

In this section, the actual production obtained from a 24 hour simulation of the industrial riser system under closed-loop and open-loop operating condition will be analysed and compared with the predictions of the PGI analysis.

6.4.3.1 The simulation model and controller

Open-loop simulation is performed for several operating points in the range of $15\% \leq u \leq 100\%$ and the accumulated production for a 24 hour period is recorded. Unlike the open-loop simulation, the closed-loop simulation will

require a stabilising controller. To meet this requirement, two slug controllers namely:

1. relay tuned slug controller
2. robust PID slug controller

are implemented and analysed. The design of the relay tuned slug controller and the robust PID slug controller will be discussed in details in Chapter 7. Both the open-loop and closed-loop simulations are carried out on the nonlinear model of the industrial riser system in OLGA. The closed-loop simulation is carried out using the OLGA-Matlab link, which is established by using the OLGA-Matlab toolbox (see section 5.5.1).

6.4.3.2 Implementation of the relay tuned slug controller

The implemented relay tuned slug controller (K_1) is a PI controller. The relay is designed using process parameters obtained from the system response which is determined by the shape factor analysis. The controller transfer function is given in (6.8).

$$K_1 = \frac{-4.02s - 0.18}{22.4s} \tag{6.8}$$

This controller when implemented on the industrial riser system can stabilise the system to a maximum closed-loop operating point of u_c =28.3$\%$. The open and closed-loop simulated productions are shown in Figure 6.5

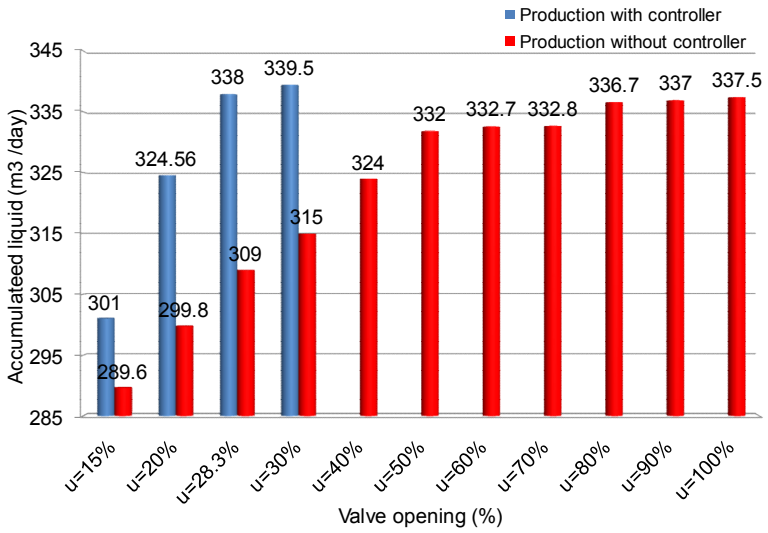

Figure 6.5: Accumulated production, with and without relay tuned controller

6.4.3.3 Implementation of the robust PID slug controller

The implemented robust PID slug controller (K_2) is also a slug controller which has been reported in a previous work [76]. The controller is designed based on a number of robust stability and performance criteria. The controller transfer function is given in 6.9.

$$K_2 = \frac{-16s^2 - 3200s - 4}{800s} \tag{6.9}$$

This controller when implemented on the industrial riser system can stabilise the system to a maximum closed-loop operating point of u_c =57.6%. The open and closed-loop simulated productions are shown in Figure 6.6.

The comparison of these simulated productions with the PGI predictions is presented in the next section.

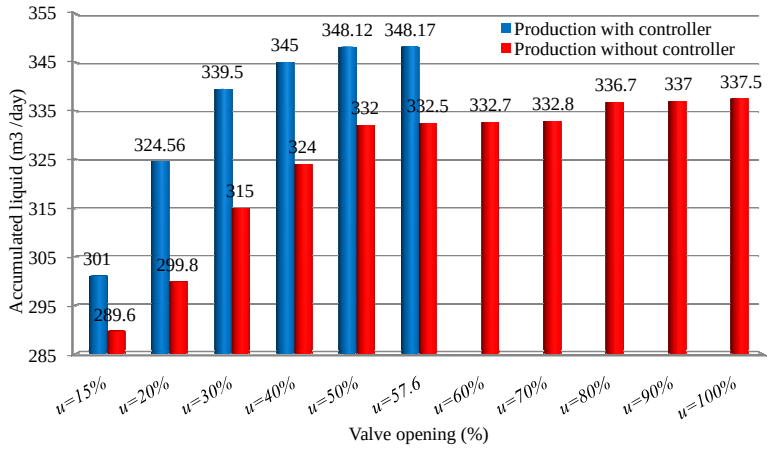

Figure 6.6: Accumulated production, with and without robust PID controller

6.4.4 Simulated production comparison

From the simulated production obtained using the two slug controllers, it is observed that the production at u_c =20% is 3% and 0.17% higher than the open-loop production at u =30% and u =40% respectively. However, the open-loop production at u=50% is 2.29% higher than the closed-loop production at u_c =20%.

Comparing these productions to the PGI predictions in section 6.4.2, which predicted that closed-loop production at u_c =20% will be higher than the open-loop production at any operating point of u <49%, and that closed-loop production at u_c =20% will be less than the open-loop production at any operating point of u >49%, it can be observed that the simulated production at u_c =20% agrees with the PGI predictions. When similar comparison is done for the closed-loop production at u =15%, the simulated production also agrees with the prediction of the PGI analysis.

Also, it can be observed from the simulated production that the closed-loop production at $u_c \geq$30$\%$ is higher than the open-loop production for all the open-loop operating points, 15$\% \leq u \leq$ 100$\%$. Thus, the production of the relay tuned slug controller at $u_c =$28.3$\%$ is higher than the production at all the open-loop operating points, 15$\% \leq u \leq$ 100$\%$. This is also the case for the robust PID controller at $u_c =$57.6$\%$. This agrees with the PGI prediction defined by the point (100$\%$,26$\%$) in Figure 6.4.

Thus, the above analysis confirms that the production potentials of the riser-pipeline system predicted by the PGI analysis agrees with all the actual simulated production results. Hence, at this point, it is clear that with proper PGI analysis of a riser-pipeline system, the production potential of the system at any operating point can be predicted.

6.4.5 PGI analysis for different reservoir pressures

With the industrial riser system, the PGI analysis can be performed for different reservoir pressures. This analysis can reveal the potential of the slug control system to maximise oil production for a declining reservoir pressure. To perform this analysis, the ZPGI line is plotted for three reservoir pressures namely: 79 barg, 69 barg and 59 barg. The obtained ZPGI line plots are shown in Figure 6.7.

From this Figure 6.7, it can be observed that for a given u, the corresponding u_c, which defines the ZPGI point decreases as the reservoir pressure decreases. Thus, the ZPGI line of a reservoir with lower pressure is located within the NPGI region of a reservoir with higher pressure. For example, the ZPGI line of the 59 barg reservoir is located below the ZPGI line of the 69 barg reservoir. Thus,

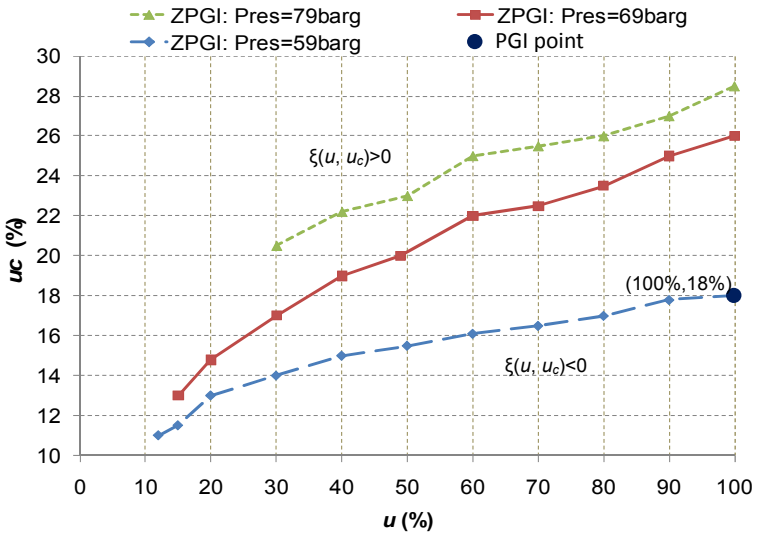

Figure 6.7: ZPGI line plot for different reservoir pressures

the NPGI region ($\xi(u, u_c) < 0$) reduces while the PPGI region ($\xi(u, u_c) > 0$) is increases with decreasing reservoir pressure. The increase in the PPGI region and decrease in the NPGI region with decreasing reservoir pressure indicates that the potential of the slug controller to maximise production over no control will increase even with decreasing reservoir pressure.

For the ZPGI point defined by (100%, 18%) for the 59 barg reservoir ZPGI line, it can be predicted that the production at relatively small valve opening of $u_c >$18% (with slug control) will be higher than the production at $u \leq 100\%$ (with no control). This implies that the PPGI region of the 59 barg reservoir includes with the NPGI region of the 69 barg and the 79 barg reservoir. This indicates that with the 59 barg reservoir, the slug controller has the potential to increase production in the NPGI region of the 69 barg reservoir and the 79 barg reservoir. The result of this is the significant potential of the slug control system to ensure significant increase in production at low reservoir pressure, when compared to

no control production. This has the potential to extend the operation life of the oil field. This potential will be discussed in details with simulation results in section 7.5.2, where the stability and production in declining reservoir pressure condition is discussed.

6.5 Conclusions

In conclusion, this chapter has presented a new concept known as the PGI analysis, for accurately predicting the production potential of the unstable riser-pipeline system. The PGI analysis reveals the potential of gaining or loosing production due to the system's operating point and operating condition. The application of the PGI analysis employs a systematic analysis of the pressure and production relationship in a riser-pipeline system, using a bifurcation map.

By using the PGI analysis, suitable operating point(s) for maximising production with or without a slug controller can be predicted. The ZPGI contours which is defined as $\xi(u, u_c) = 0$, divides the (u, u_c) plane into two areas namely: the positive PGI (PPGI) area, which is located above the ZPGI line and the negative PGI (NPGI) area, which is located below the ZPGI line. Operating point on the ZPGI line defined by (u, u_c) indicates the operating point where the production with a slug controller at u_c will be equal to production without a slug controller (unstable system) at u. Any operating point, (u, u_c), located above the ZPGI line corresponds to production gain operating point known as the PPGI, while any operating point located below the ZPGI line corresponds to a production loss operating point, known as the NPGI.

In order to achieve production gain at the predicted operating point, the designed slug controller must be able to stabilise the system at the predicted operating point. If the slug controller cannot achieve stability at the predicted operating point, then the potential to achieve production gain is undermined.

The implementation of the PGI analysis on the industrial riser system shows that the prediction of the PGI analysis agrees with the actual simulated production. The ZPGI line plot for different reservoir pressures shows that the NPGI region decreases, while the PPGI region increases with decreasing reservoir pressure. This showed that the potential of the slug controller to maximise production will increase even with decreasing reservoir pressure. These results are very significant when planning control strategy for stability and production, especially for brown fields.

Chapter 7

Design and characterisation of slug controllers for maximising oil production

7.1 Introduction

The primary objective of a slug control system is to stabilise the riser-pipeline system by suppressing severe slugging. In addition to the requirement for a slug control system to achieve stability, the emphasis on the system productivity has become of interest. The interest on the performance of slug control systems has recently shifted from just achieving a stable operating condition to also maximising production [76].

In Chapter 6, the systematic method for determining the production potential of slug control of an unstable riser-pipeline system, using the production gain index (PGI) was presented. It was explained that by using the production gain index (PGI), the closed-loop valve opening where maximum oil production can be achieved can be predicted. Once this suitable closed-loop valve opening

is predicted, it is required that a stabilising slug controller, which can achieve closed-loop stability at the predicted valve opening be designed. If the designed stabilising controller cannot achieve closed-loop stability at the predicted valve opening, then the expected benefit for implementing the slug controller could be undermined.

Thus, the knowledge of the slug controller design technique and the characterisation of their performance will be useful in achieving the desired slug control objectives. Systematic methods for designing and analysing the performance of the active slug controller at the open-loop unstable valve opening in order to maximise oil production is presented in this chapter. The basic approach of the slug controller design presented in this chapter is to design and implement the slug controller at the open-loop unstable valve opening, where the system would be unstable without feedback control. The controller design and implementation is carried out for two controlled variables, namely: the riser base presure (P_{RB}) and the total volumetric flowrate (Q_T). Figure 7.1 gives a schematic diagram of the offshore riser-pipeline system with an active feedback control structure, for P_{RB} control.

The body of this chapter commences with the analysis of the principle of determining the ability of the slug controller to achieve closed-loop stability at large valve opening in an unstable riser-pipeline system. This is followed by slug controllers design using three different slug controller design techniques. The implementation of the slug controllers on the relevant riser-pipeline system is presented. The analysis of the achieved closed-loop stability and the accumulated liquid production are also presented.

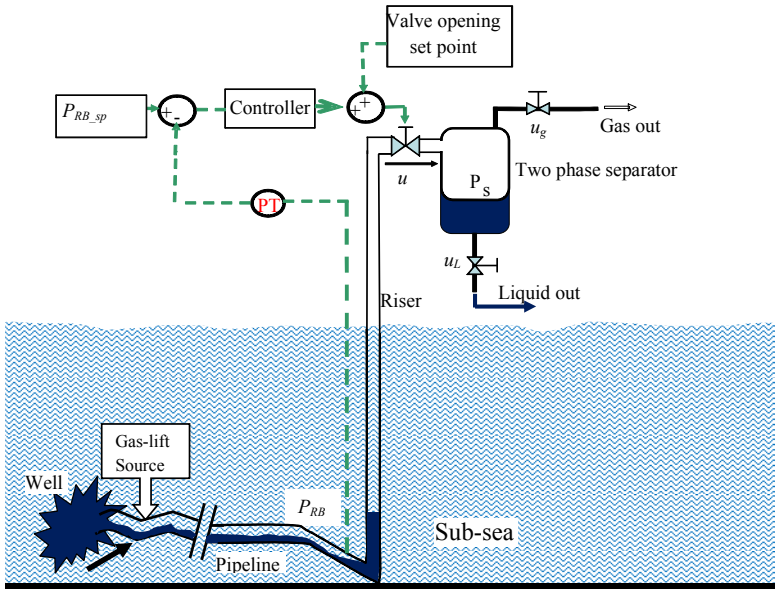

Figure 7.1: Schematic diagram of the industrial riser-pipeline system

7.2 Characterisation of slug controllers

In this section, the principle for determining the ability of a slug controller to stabilise a riser-pipeline system at a large valve opening will be discussed. The ability of a slug controller to stabilise the riser-pipeline system at operating points corresponding to large valve openings can be characterised based on its robustness.

A slug controller designed with a linear model obtained at a given operating point, corresponding to an open loop unstable valve opening can be applied to stabilise the system at a larger valve opening. From the non-linear stability analysis of the riser-pipeline system presented in section 4.4, it was observed that the stability characteristics of the system will vary with the operating point, defined by the valve opening at which it operates. This variation in the sys-

tem's characteristics at different valve openings requires that a slug controller must be robust in order to stabilise the system at a wide range of valve openings. Therefore, the robustness of the slug controller will determine its ability to stabilise the system at other valve openings other than that at which it was designed.

Consider a detailed block diagram of the general control problem as was introduced by Doyle [21, 22] shown in Figure 7.2, where P is the general plant, K is the controller.

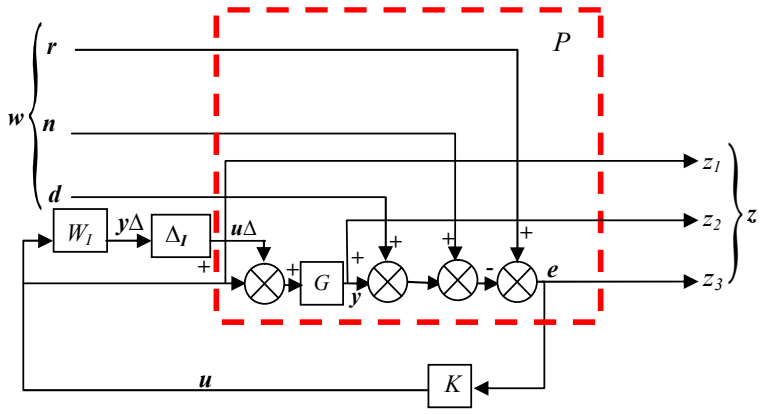

Figure 7.2: Detailed block diagram of a generalised control system

Signals linking the blocks include the measured output, y, the manipulated (control) input, u, the exogenous output, z and the exogenous inputs, w, which include the system disturbances, d, the measurement noise, n, and the references (set point), r. In the riser-pipeline system, d is identified as the inlet liquid and gas flow disturbance, and the topside separator pressure disturbance at the riser outlet.

From Figure 7.2, the closed loop transfer function of the partitioned P, from w to z, can be obtained as N, which is given in (7.1), where $T = GK(1 + GK)^{-1}$

and $S = (1 + GK)^{-1}$.

$$N = \begin{bmatrix} 0 \\ 0 \\ 1 \end{bmatrix} + \begin{bmatrix} 1 \\ G \\ G \end{bmatrix} K(1 + GK)^{-1}(-1) = \begin{bmatrix} -KS \\ -T \\ S \end{bmatrix} \tag{7.1}$$

The closed-loop transfer function of the system from r to y can easily be derived to show that $y = rT$. With a focus on robust stability of the slug control system, N can be simplified to obtain the closed-loop transfer function from w to z, for $w = r$ and $z = y$, such that $N = [-T]$. In order to achieve the robust stability of the control system, the requirement would be to synthesis a slug controller, K, that minimises the H_∞ norm of T as shown in (7.2) [94].

$$\min_K \|N(K)\|_\infty \triangleq \min_\omega \|T(j\omega)\|_\infty \tag{7.2}$$

Given, a set of slug controllers, K_i, (for $i = 1, 2, 3...n$), it will be expected that a slug controller which achieves the least value of $\|T(j\omega)\|_\infty$ will be the most robust slug controller and will be able to achieve stable system operation at larger valve openings. Thus, the valve opening for a slug controller to stabilise the riser-pipeline system can be characterised using the corresponding $\|T(j\omega)\|_\infty$.

7.3 Slug controller design techniques

In this section, the design of three slug controllers using three different slug control design techniques is presented. The three slug controller design techniques are:

1. Relay auto tuned slug controller
2. Robust PID slug controller
3. H_∞ robust slug controller

For each slug controller design technique, the fundamental principle behind it is firstly discussed. Each slug controller design is performed using two different controlled variables namely: the P_{RB} and the Q_T. The obtained slug controller is implemented on a corresponding riser-pipeline system. The robust stability of each controller is characterised and predicted using the principle described in section 7.2. The predicted robust stability of the controllers is validated using the analysis of the maximum valve opening for a stable closed-loop system, and the corresponding accumulated production obtained by implementing the controller.

7.3.1 Relay auto-tuned slug controller

In this section, the principle of the relay based system identification method for slug controller design is presented. Due to the complexity of the real riser-pipeline system, the ISRM may still not be suitable for all the systems due to the complexity of the real system. As a result, it will be appropriate to get an

approximate model of the open-loop unstable riser-pipeline system using the relay based system identification approach. In line with the control performance objectives applied in this work, the performance of the relay auto-tuned slug controller is evaluated for its ability to achieve stability and maximise production. However, this approach has an added advantage because it can be applied online (on the plant) and offline (through simulation).

The basic control structure for relay auto-tuned controller design and implementation is shown in the block diagram in Figure 7.3. Firstly, the controller parameters are designed by connecting the plant $G(s)$ to the relay and taking appropriate design procedures, which will be discussed later. Once the controller parameters are obtained, the controller is configured with the controller parameters and the plant is switched to the controller output. Further details of the relay auto-tuning and its control design principles can be found in many literatures [4, 80, 112]. Next, the riser-pipeline process indentification using the relay feedback shape factor will be discussed.

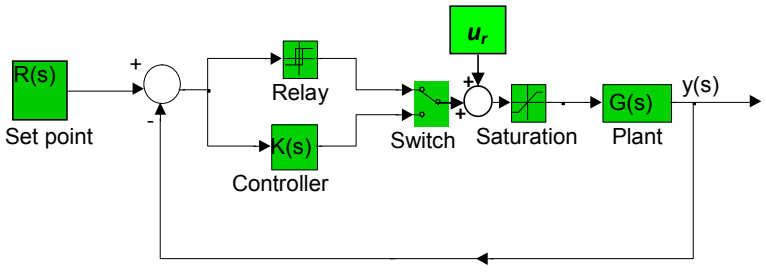

Figure 7.3: Relay auto-tuning feedback control structure

7.3.1.1 Process identification using relay feedback shape factor

The first step in the relay auto-tuned controller design for the riser-pipeline system is to identify the riser-pipeline process model by approximation, using the relay feedback shape factor. To achieve this, the riser-pipeline system, $G(s)$, is first connected to the relay. The system is configured by defining a reference valve opening, u_r, which corresponds to an open-loop unstable condition. Also, the controlled variable set point is defined at a suitable operating point, which corresponds to the unstable equilibrium point in the open-loop unstable region.

The relay is then configured by defining the switch on and off point (a), which is specified around the output variable set point, and defining the relay height, h (relay output when on and off), which is specified around the reference valve opening.

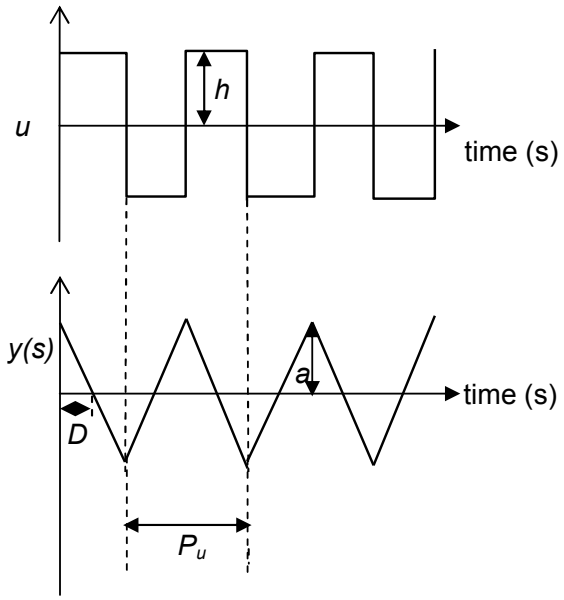

Figure 7.4: Relay test feedback response

Having configured the relay, the required relay feedback response is obtained by running the system. At first, the system input, u, is increased by $+h$ and the output $y(s)$ decreases, (for P_{RB} control). As the output decreases below the switch off point (a), the input decreases by $-h$, such that the output increases again. This results to a limit cycle feedback response, known as the relay feedback response, with period, P_u, which is known as the ultimate period. The shape of the resulting relay feedback response, which is used to approximate and identify the process type can vary, depending on the ratio of the dead time D to the process time constant τ [112].

In this application, the riser-pipeline process is identified as a first-order-plus-dead-time (FOPDT) process. In order to identify this process, the feedback response of the riser-pipeline system must satisfy certain characteristics based on the shape of the response. These characteristics as reported by Thyagarajan and Yu [112] states that an unstable system whose relay feedback response has sharp edges at the peak amplitude with a sustained oscillation can be approximated by a first-order-plus-dead-time (FOPDT) system. Figure 7.4 shows a schematic diagram of the nature of this response. Three important parameters D, a and P_u are obtained from the relay feedback response, where D is the dead time, a is the peak amplitude and P_u is the ultimate period.

An unstable FOPDT system is defined by the process transfer function given in (7.3), where τ is the time constant, k_P is the process gain. The model parameters obtained from the relay feedback response are used to calculate the parameters of the process transfer function.

$$G(s) = \frac{k_p e^{-Ds}}{\tau s - 1} \tag{7.3}$$

A stabilising slug controller can be designed based on the identified process parameters.

7.3.1.2 Process and controller parameters

To design the controller parameters, the D, a and P_u obtained from the relay feedback response are used to calculate the process time constant, τ, and the process gain, k_P, using (7.4) and (7.5). The mathematical derivation of (7.4) and (7.5) is based on the analytical expressions of the feedback response shown in Figure 7.4 [112].

$$\tau = \frac{0.5P_u}{\ln\left[\frac{1}{(2e^{-D/\tau}-1)}\right]} \tag{7.4}$$

$$k_p = \frac{a}{h(e^{D/\tau}-1)} \tag{7.5}$$

For the unstable FOPDT, the PI controller parameters can be calculated using a set of conditional relationships based on the integral time average error (ITAE) controller tuning rules [112]. The ratio of D to τ defines a dimensionless variable, ε, given in (7.6).

$$\varepsilon = \frac{D}{\tau} \tag{7.6}$$

The value of ε defines the condition to evaluate the PI controller parameters, namely: the controller gain, k_c and the controller integral time, τ_i, using (7.7) - (7.12).

for $\varepsilon < 0.1$:

$$k_c = \frac{K_u}{3.2} \tag{7.7}$$

$$\tau_I = 2.2P_u \tag{7.8}$$

for $0.1 \leq \varepsilon \leq 1$:

$$k_c = \frac{0.586}{k_p}\left(\frac{\tau}{D}\right)^{0.916} \tag{7.9}$$

$$\tau_I = \frac{\tau}{1.03 - 0.165\left(\frac{D}{\tau}\right)} \tag{7.10}$$

for $\varepsilon > 1$: $\lambda = \max(1.7D, 0.2\tau)$

$$k_c = \frac{0.586}{k_p}\left(\frac{\tau}{D}\right)^{0.916} \tag{7.11}$$

$$\tau_I = \frac{\tau}{1.03 - 0.165\left(\frac{D}{\tau}\right)} \tag{7.12}$$

Once the controller parameters are obtained, the controller can be implemented on the system. Next, this slug control design technique will be implemented on the 2 inch riser and on the industrial riser systems.

7.3.1.3 Relay auto-tuned controller design for P_{RB} control of the 2 inch riser

The relay auto-tuning method is implemented on the control system for the 2 inch riser-pipeline system in the experimental facility in the flow laboratory. The 2 inch riser system has been described in Chapter 3. It is also implemented on the SRM and on the ISRM of the 2 inch riser system. The controlled variable is the P_{RB} and the manipulated variable is the riser top valve opening u. In each case, the relay is configured with $h = 10\%$ and on and off point$=$ 0.05 barg.

The Hopf bifurcation map of this system obtained through open-loop simulation of the 2 inch riser system using the ISRM (solid line) and that obtained through experiment on the same system (dashed line) is shown in Figure 7.5. This result is obtained with the inlet liquid and gas flow rate controlled at 0.75kg/s and 0.0033kg/s respectively.

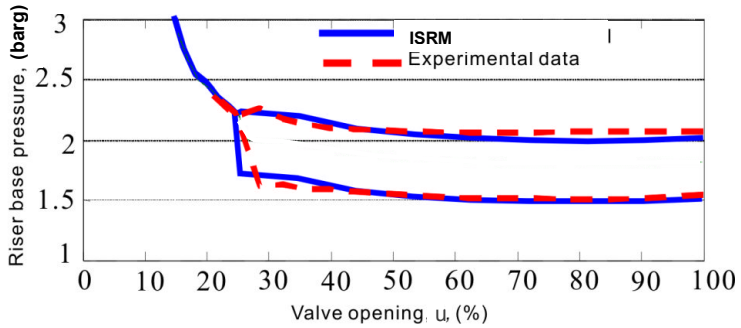

Figure 7.5: Riser base pressure bifurcation map of the 2 inch riser

It shows that the P_{RB} oscillates between minimum and maximum pressure points for u >25%. Both ISRM and the experimental results show that at a critical valve opening of u=25%, the desired stable non-oscillatory flow regime is obtained. The corresponding P_{RB} from the ISRM and from the experiment are 2.25 barg and 2.27 barg respectively.

From the result of this bifurcation map, stabilising the system at the open-loop unstable region where u >25% will be aimed. The feedback response is obtained at an unstable valve opening of u=30% and a P_{RB} set point of 1.9 barg. Figures 7.6, 7.7 and 7.8 shows that the relay responses obtained from the experiment, the SRM and the ISRM respectively.

From each relay response, the relay response parameters are obtained and the corresponding process parameters are calculated. The relay design and

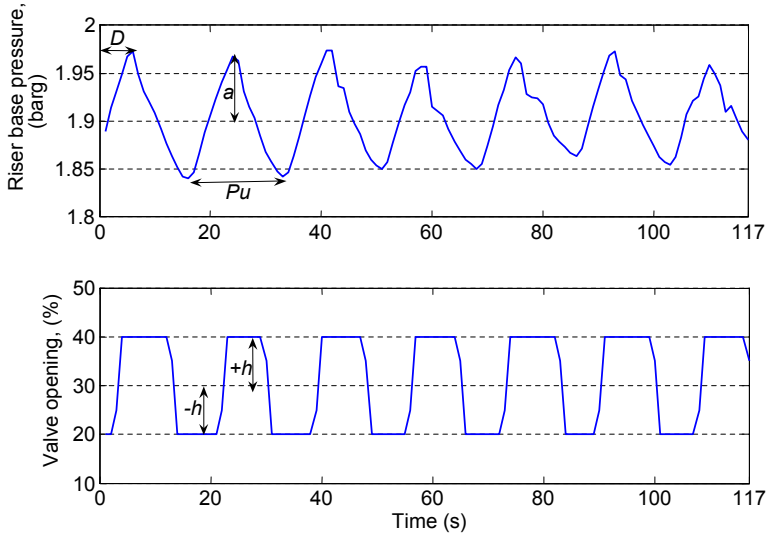

Figure 7.6: Relay feedback response of the 2 inch riser (Experimental result)

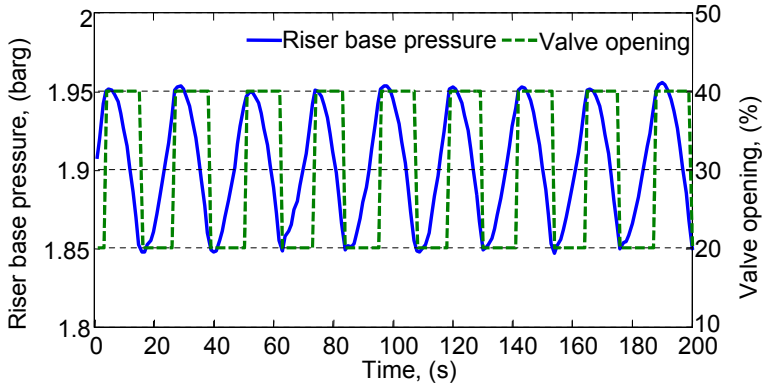

Figure 7.7: Relay feedback response of the 2 inch riser using the SRM

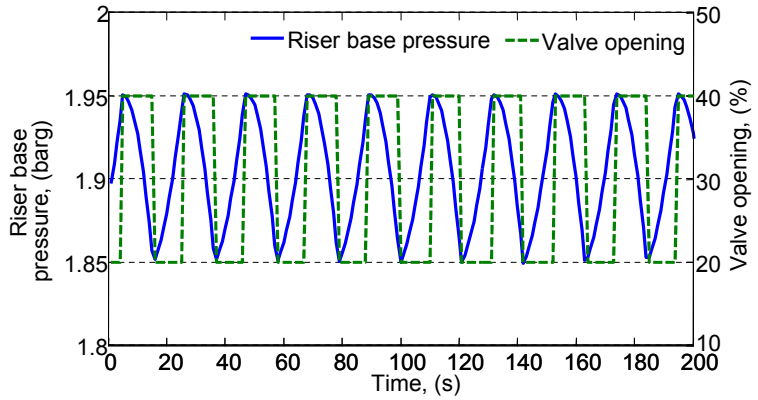

Figure 7.8: Relay feedback response of the 2 inch riser using the ISRM

the response parameters are summarised in Table 7.1, while the process parameters and the designed controller parameters are summarised in Table 7.2. The controller parameters are calculated using (7.9) and (7.10).

Table 7.1: Relay design and response parameters

	Relay design parameters		Relay response parameters		
2 inch riser system	h	On and off point	a (barg)	$P_u(s)$	D(s)
Experiment	± 0.1	± 0.05	0.057	20	4
ISRM	± 0.1	± 0.05	0.05	20	4
SRM	± 0.1	± 0.05	0.052	22.56	6

Table 7.2: Process and controller parameters

	Process parameters		Controller parameters	
2 inch riser system	τ	k_p(barg)	K_c(barg^{-1})	$\tau_I(s)$
Experiment	7.11	0.43	2.3	7.6
ISRM	7.9	0.34	3.25	8.35
SRM	6.3	0.83	0.71	7.17

Controller implementation

The designed controllers are implemented on the corresponding system, using the feedback control structure that is shown in Figure 7.3. The result obtained by implementing the controller on the plant is shown in Figure 7.9. This result shows that the system is unstable at fixed valve opening of u=30%. The system is stabilised to a P_{RB} of 1.85 barg at u=32% when the controller was switched on after 1200 s. This result shows the ability of the relay auto-tuned controller to stabilise the unstable riser-pipeline system at the open-loop unstable valve opening, with a lower riser base pressure compared to manual choking, as shown in Figure 7.1.

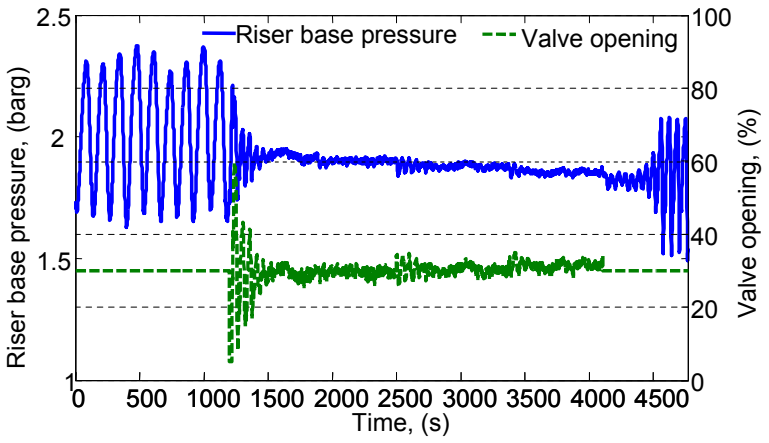

Figure 7.9: Relay tuned controller implementation (Experimental result)

The result of implementing the controller on the ISRM shown in Figure 7.10. This result shows that the system is stabilised at a P_{RB} set point of 1.81 barg and u=30%. It is observed that the system gradually became unstable (severe slugging) again when the valve opening was returned to 30% fixed valve position at 4000s.

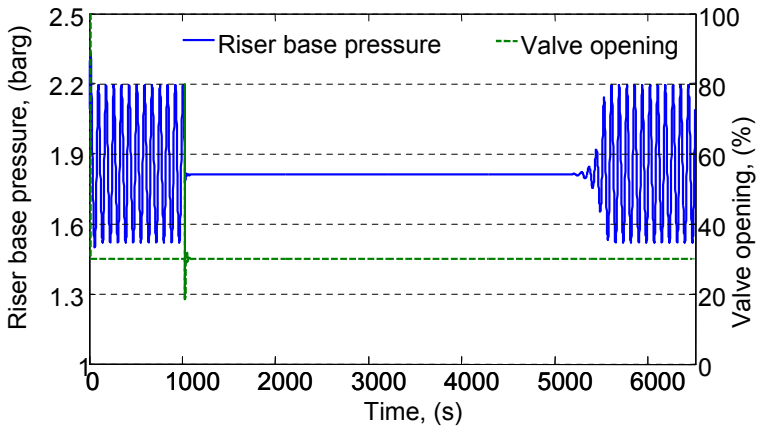

Figure 7.10: Relay tuned controller implementation on the ISRM

From Table 7.2, it can be observed that a low controller gain is obtained for the SRM, when compared to the controller gains that are obtained for the ISRM and the experimental facility. The simulation result from the SRM shows that this controller parameters cannot stabilise the system. This is because the SRM predicts a slug frequency that is less than the actual system slug frequency, resulting in a higher dead time, D. This gives a proportional gain that is too small to stabilise the system. This shows the improved performance of the ISRM in predicting severe slug characteristics, which is necessary for designing robust controllers that is capable of stabilising the system.

One key aim of the our slug controller design and implementation is to analyse the ability to maximise oil production from the unstable riser-pipeline system. A suitable system for this analysis should have a pressure dependent source at the inlet. Since the inlet flow rate of the 2 inch and 4 inch riser systems are always controlled to a fixed value, further controller design and analysis will focus on the industrial riser, which has a well source.

7.3.1.4 Relay auto-tuned slug controller design for an industrial riser

To evaluate the performance of the relay auto-tuned active controller on severe slugging control of larger scale riser-pipeline systems and on oil production, the relay auto-tuned controller is implemented on the industrial riser system in the OLGA software. With the industrial riser system, the production, which can be achieved using the relay-tuned controller, can be evaluated since the industrial riser system has a pressure driven well source. The relay auto-tuned controller design is implemented for control using two controlled variables namely, the P_{RB} and the Q_T. The controller performance is analysed for each of the controlled variable. With the flow condition given in Table 3.1, it is shown in Figure 4.18 that the industrial riser system is open-loop stable at u=12$\%$ and open-loop unstable at $u >$13$\%$.

Riser base pressure (P_{RB}) control

In the relay auto-tuned slug controller design for P_{RB} control, the system is configured by setting the reference valve opening to the open-loop unstable valve opening of u=20$\%$. The relay is then designed using the relay design parameters shown in Table 7.3. The feedback response obtained from the relay test is shown in Figure 7.11, and the response parameters are summarised in Table 7.3.

Table 7.3: Relay design and response parameters

	Relay design parameters		Relay response parameters		
Valve opening ($\%$)	h	On and off point	a (barg)	$P_u(s)$	$D(s)$
20$\%$	$\pm$0.11	$\pm$0.5	0.52	486	14.2

From this response, the system response parameters are obtained and the process parameters calculated using (7.4) and (7.5). The controller parameters

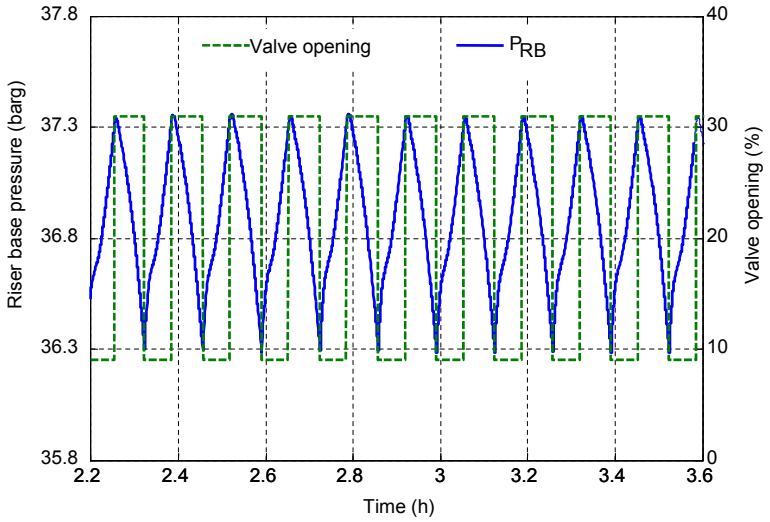

Figure 7.11: Relay feedback response for P_{RB} control

are calculated using (7.9) and (7.10). The process and the designed controller parameters are summarised in Table 7.4.

Table 7.4: Process and controller parameters

	Process parameters		Controller parameters	
Valve opening (%)	τ	k_p(barg)	K_c(barg^{-1})	$\tau_I(s)$
20%	20.5	4.72	0.18	22.4

Riser top total volumetric flow rate (Q_T) control

Using the relay auto-tuned slug controller design principle discussed in section 7.3.1, a slug controller can also be designed with Q_T as the controlled variable. This controller design is also implemented at the open-loop unstable valve opening of 20%. The relay configuration parameters are shown in Table 7.5.

Table 7.5: Relay design and response parameters

	Relay design parameters		Relay response parameters		
Valve opening (%)	h	On and off point	a (m^3/s)	$P_u(s)$	$D(s)$
20%	±0.11	±0.005	0.02	39.6	7.2

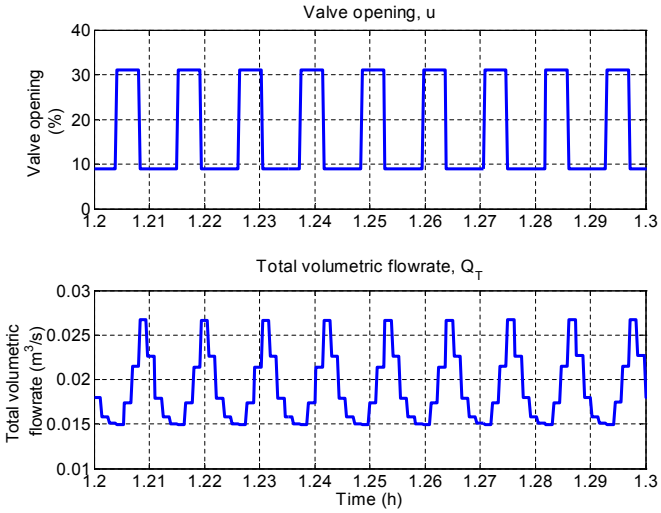

Figure 7.12: Relay feedback response for Q_T control

The relay feedback response obtained from the relay test is shown in Figure 7.12. From this feedback response, the system response parameters are obtained and the process parameters calculated using (7.4)and (7.5). The controller parameters are calculated as described using (7.9) and (7.10). The relay response parameters are summarised in Table 7.5, while the process and the designed controller parameters are summarised in Table 7.6.

Table 7.6: Process and controller parameters

	Process parameters		Controller parameters	
Valve opening (%)	τ	k_p(m^3/s)	K_c((m^3/s)$^{-1}$)	$\tau_I(s)$
20%	10.4	0.045	18	11

The result of the implementation of these controllers will be presented in section 7.5.1.1. Next, the robust PID controller design technique will be considered.

7.3.2 Robust PID slug controller

Another active slug controller design technique, which can be implemented on an unstable riser-pipeline system is the robust PID controller. Since the multiphase riser-pipeline system is extremely nonlinear, to ensure the stability of the control system for a wide operating range of open-loop unstable operating points, a PID controller could be designed based on a number of robust performance and stability criteria. As a result, a robustly designed PID controller will be able to achieve closed-loop stability at a relatively large valve opening. This could ensure further reduction of the slug controller impact on oil production and under the right conditions could lead to increased production.

The design of a robust PID controller presented in this work requires a linear model of the system obtained at an open-loop unstable valve opening. This linear model can be obtained using the ISRM of the relevant riser-pipeline system. The principle of design of the robust PID controller is based on synthesising a stabilising controller, which satisfy a number of relevant robust stability and performance criteria. These robust performance and stability criteria are described in the next section with a brief introduction of the feedback control structure.

7.3.2.1 Controller design criteria

Figure 7.13 gives a basic feedback control structure, which can be used to synthesis the controller design criteria and implement the controller.

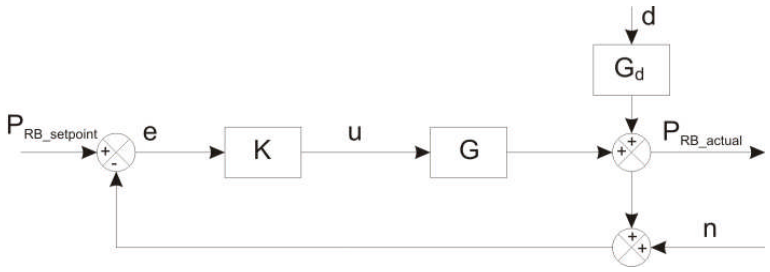

Figure 7.13: Feedback control loop diagram for severe slug control

In Figure 7.13, G is the transfer function of the riser-pipeline system obtained through linearisation of the ISRM at the desired open-loop operating point, K is the PID controller with transfer function given as:

$$K = K_c \left(1 + \frac{1}{\tau_i s} + \tau_D s\right) \tag{7.13}$$

where K_c is the controller gain, τ_I is the controller integral time and τ_D is the controller derivative time. n represents uncertainties due to measurement noise and modeling errors. G_d is the transfer function from disturbances to P_{RB}, where disturbances, d, include the liquid and gas flowrate variations, well pressure and downstream (topside separator) pressure fluctuations. From Figure 7.13, the P_{RB} of the riser-pipeline control system can be represented as:

$$P_{RB\_actual} = Gu + G_d d \tag{7.14}$$

Thus, the closed-loop response can be derived as:

$$P_{RB\_actual} = TP_{RB\_setpoint} + SG_d d - Tn \tag{7.15}$$

Where $S = (1 + GK)^{-1}$ is known as the sensitivity function and $T = GK(1 + GK)^{-1}$ is known as the complementary sensitivity function. These sensitivity functions are used to define the criteria for robust PID controller design as summarised below. The criteria used in determining suitable PID parameters for robust stability are:

1. the upper bound on sensitivity function, $|S|$, which requires that $S \approx 0$ or $T \approx 1$

2. the lower and upper bound on the loop gain, GK, which requires that $|G(j\omega)K(j\omega)| > 1$ at lower frequencies below the cross over frequency (ω_c), and that $|G(j\omega)K(j\omega)|$ is small, that is $|G(j\omega)K(j\omega)| < 1$ at higher frequencies above the cross over frequencies

3. the lower bound on bandwidth, ω_B^*, which requires that for a pair of complex-conjugate unstable poles expressed as $p = x + jy$, at the open-loop unstable operating point, the lower bound on bandwidth is given as:

$$\omega_B^* > 0.67(x + \sqrt{4x^2 + 3y^2}) \tag{7.16}$$

The cross over frequency ω_c is the frequency where $|G(j\omega)K(j\omega)|$ crosses 1 from above and the ω_B^* the frequency where the $|S(j\omega)|$ crosses 0.707 (-3dB) from below. A suitable controller design parameter(s), must satisfy these criteria. The $|S(j\omega)|$ and the $|G(j\omega)K(j\omega)|$ are obtained using the bode plot. Further details on these criteria can be found in the literatures [77, 94].

7.3.2.2 Robust PID controller design for the industrial riser system

In this section, the design of the robust PID controller for the control of the industrial riser system using the P_{RB} and Q_T as controlled variable is presented. The robust PID slug controller is designed with linear model transfer function, which is obtained from the ISRM of the industrial riser system. The controller is implemented on the nonlinear OLGA model of the industrial riser system. This implementation is carried out using the OLGA-Matlab link as discussed in section 5.5.1.

Riser base pressure (P_{RB}) control

Thus, the transfer function of the linear model obtained at $u = 20\%$ valve opening with u as input and P_{RB} as output is given as:

$$G_{20}\%(s) = \frac{-0.258s - 0.0004248}{s^3 + 7.994s^2 - 0.002577s + 1.206e-005}$$

(7.17)

From the plant model shown in (7.17), a pair of complex conjugate poles, $0.00016 \pm 0.0012i$ is obtained. From (7.16), the lower bound of ω_B^* is obtain as 0.00156rad/s. The $\|S\|_\infty$, the $|G(j\omega)K(j\omega)|$ and the actual ω_B^* are evaluated by analysing the bode plot of $|S(j\omega)|$ and $|G(j\omega)K(j\omega)|$ at various controller parameters, K_c, τ_i, τ_D.

We can determine the margin of the stable controller gain, K_c, for which the system is stable using stability criteria analysis method such as the Routh-Hurwitz stability criterion. The Routh-Hurwitz stability criterion is applied to the characteristic equation of a closed-loop system defined by: $1 + G_{(20\%)}(s)K = 0$. Where $G_{(20\%)}(s)$ is the plant transfer function defined by (7.17). The Routh stability criterion was introduced in Chapter 5.

Table 7.10 shows the PID controller design parameters and the corresponding $\|S\|_\infty$, ω_B^* and $|G(j\omega)K(j\omega)|$ obtained from the bode diagram.

Table 7.7: PID controller tuning parameters

Controller parameter				Stability parameter			
$K_c(barg^{-1})$	τ_i	τ_D	$\|S\|_\infty$	ω_c	ω_B	$\|G(j\omega)K(j\omega)\|$	
						$\omega \leq \omega_c$	$\omega > \omega_c$
-0.05	500	0.005	14	0.0025	0.002	158	$5.7e^{-7}$
-0.1	500	0.005	2.6	0.0034	0.0241	316	$1.1e^{-6}$
-2	500	0.005	1	0.0392	0.0353	6309	$2.7e^{-5}$
-5	500	0.005	1.02	0.603	0.093	16788	$2.4e^{-7}$
-10	500	0.005	1.03	0.813	0.187	30902	$5.6e^{-7}$
-15	500	0.005	1.05	0.906	0.278	47836	$7.9e^{-7}$

From table 7.10, it can be observed that the parameters with K_c=-2 are the best satisfying the stability criteria.

Riser top total volumetric flow rate (Q_T) control

The design of the robust PID controller for Q_T control of the industrial riser system using the robust PID controller design principle is implemented with the transfer function of the linear model obtained at u=20% given as:

$$G_{20\%}(s) = \frac{0.1232s^3 + 0.9659s^2 + 0.001434s + 2.016 \times 10^{-7}}{s^3 + 7.994s^2 - 0.002577s + 1.206 \times 10^{-5}} \tag{7.18}$$

The lower bound of ω_B^* is the same as calculated for the P_{RB} since the open-loop poles are the same for the same operating point. With the condition for the $|G(j\omega)K(j\omega)|$ satisfied, the $\|S\|_\infty$, and the actual ω_B^* are also obtained by analysing the Bode plot of $|S(j\omega)|$ at various controller parameters, K_c, τ_i, τ_D. By solving the Routh stability criteria for this system, a condition for stability defined by $K_c > 0$, which will serve as a guide to our choice of K_c can be obtained.

Table 7.8 shows the PID controller design parameters and the corresponding $\|S\|_\infty$, and ω_B^* obtained from the Bode diagram.

From Table 7.8, it can be observed that the minimum $\|S\|_\infty$ and the ω_B greater than 0.00156 is obtained with the controller parameters corresponding to K_c=32. Thus, these controller parameters are the best satisfying the stability criteria, and will be implemented on the system.

Table 7.8: PID controller tuning parameters

Controller parameter			Stability parameter	
K_c (barg^{-1})	τ_i	τ_D	$\|S\|_\infty$	ω_B
2	80	0.005	10.8	0.00132
4	80	0.005	1.5	0.00137
8	80	0.005	0.97	0.00141
16	80	0.005	0.78	0.00147
32	80	0.005	0.65	0.00157

7.3.3 H_∞ robust slug controller

In this section, the principle of design the H_∞ robust controller design for an unstable riser-pipeline system is presented. A robust control system is insensitive to the model uncertainties, Δ , which arise due to the differences between the actual system and the system model. In the ISRM, these uncertainties arise partially due to some neglected (un-modelled) dynamics of the multiphase flow in the riser-pipeline system. In robust control design, this model mismatch can be represented as an un-modelled dynamic uncertainty in the frequency domain. This will be discussed later in section 7.3.3.3.

7.3.3.1 Control configuration

A general control problem shown in Figure 7.14, which was introduced by Doyle [21, 22] can be used to structure the riser slugging control system. From Figure 7.14, the block P is the general plant and the block K is the controller. Signals linking the blocks include y, which is the measured output, u, which is the manipulated (control) input, and w, which is the exogenous input. The

exogenous input, w, includes the system disturbances, d, noise, n, and the references (set point), r. The exogenous output, z, is the measured output deviation from the set point (error). In the riser-pipeline system, d is identified as the inlet liquid and gas flow disturbance, and the separator pressure disturbance at the riser outlet, n the measurement noise, and r the set-point of the controlled variable.

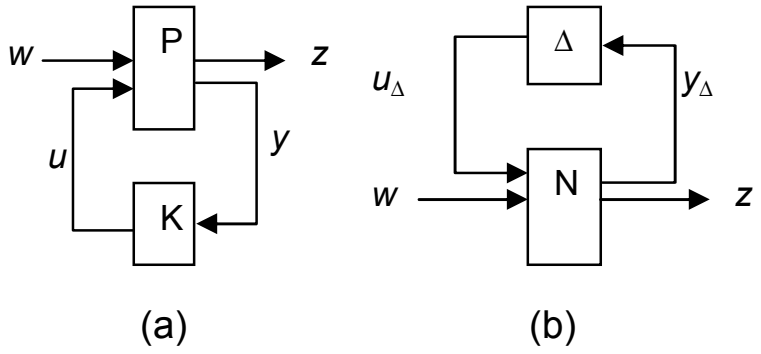

Figure 7.14: Generalised control system (GCS) diagram

From Figure 7.14(a), the transfer matrix, P of the generalised plant is partitioned to be compatible with K according to the inputs and outputs as:

$$P = \begin{bmatrix} P_{zw} & P_{zu} \\ P_{yw} & P_{yu} \end{bmatrix}$$

The closed-loop transfer function of the system from the exogenous input, w, to the exogenous output, z can obtained as:

$$N = P_{zw} + P_{zu}K(1 - P_{yu}K)^{-1}P_{yw} \triangleq F_l(P, K) \tag{7.19}$$

where $F_l(P, K)$ is the lower linear fraction transformation (LFT) of P with K. A general control configuration with model uncertainty is obtained by closing the upper loop round N as shown in Figure 7.14(b). The detailed generalised

control structure was shown in Figure 7.2. Considering the system uncertainty, the close loop transfer function from w to z results in an upper LFT, F, given as:

$$F = F_u(N, \triangle) := N_{zw} + N_{zu_\triangle} \triangle (1 - N_{y_\triangle u_\triangle} \triangle)^{-1} N_{y_\triangle w} \tag{7.20}$$

From Figure 7.2, the partitioned generalised plant,P, from the inputs $[u_\triangle\ r\ n\ d\ u]^T$ to the outputs $[y_\triangle\ z_1\ z_2\ y]^T$ is derived as:

$$P = \begin{bmatrix} 0 & 0 & 0 & 0 & W_I \\ -W_pG & W_pR & -W_pN_s & -W_pG_d & -W_pG \\ 0 & 0 & 0 & 0 & W_u \\ -G & R & -N_s & -G_d & -G \end{bmatrix}$$

Thus, from (7.19), N, which is the transfer function from w to z is derived as:

$$\begin{bmatrix} -W_IKSG & W_IKSR & -W_IKSN_s & -W_IKSG_d \\ -W_pSG & W_pSR & -W_pSN_s & -W_pSG_d \\ -W_uKSG & W_uKSR & -W_uKSN_s & -W_uKSG_d \end{bmatrix}$$

Controller synthesis based on this generalised control configuration can be applied to an open-loop unstable robust controller design for severe slug mitigation.

7.3.3.2 Controller design criteria

The control objective in terms of quantitative performance criteria is to minimise various norms of the system, such as the H_∞ norm from w, to z [12]. The H_∞ optimal control problem aims to find a stabilising controller, K, such that $\|F_l(P,K)\|_\infty = \max_\omega \bar{\sigma}(F_l(P,K)(j\omega))$ is minimised. If $\min \|F_l(P,K)\|_\infty = \gamma_{\min}$, then usually, a theoretically simpler design is to obtain a sub-optimal controller with $\gamma > \gamma_{\min}$.

Thus, the control problem would be to find a stabilizing controller such that $\|F_l(P,K)\|_\infty < \gamma$. Such controllers should satisfy the performance and robust stability conditions as described below.

Robust performance

The sensitivity function of the perturbed system, $S_p(s) = (1 + G_p(s)K(s))^{-1}$ is typically a good indicator of closed-loop performance of a system. The maximum peak amplitude of S_p is usually selected such that $\|S_p\|_\infty \leq 2$. This performance specification can be represented by a performance weight, W_p, which places an upper bound, $\frac{1}{|W_p(s)|}$, on the magnitude of S_p. Thus, the performance requirement becomes $|S_p(j\omega)| < 1/|W_p(j\omega)|, \forall\omega$ such that $\|W_p(j\omega)S_p(j\omega)\|_\infty$. In terms of the H_∞ norm, this performance requirement demands from (7.20) that, $F \leq 1, \forall\triangle, \|\triangle\|_\infty \leq 1$ [76]. $W_p(s)$ is defined as $W_p(s) = \frac{s/M+\omega_B^*}{s+\omega_B^* A}$ where ω_B^* is the bandwidth requirement. $|S(j\omega)| \leq M$ is required for high frequency performance above the bandwidth and $|S(0)| \leq A$ is the steady state offset required for low frequency performance.

Robust stability

To evaluate robust stability of a system, we determine if the system is stable for all plants in the uncertainty set, that is, $F = F_u(N, \triangle)$ is stable $\forall\triangle, \|\triangle\|_\infty \leq 1$. Nominal stability, NS, is required as a prerequisite for robust stability of F. NS demands that N is internally stable, so that the only source of instability in F is the feedback loop $(1 - N_{y_\triangle u_\triangle}\triangle)^{-1}$ introduced by the uncertainty, $\triangle$ as shown in (7.20). $N_{y_\triangle u_\triangle}$ is the closed-loop transfer function from $u_\triangle$ to $y_\triangle$, which is obtained as $-W_I KSG = -W_I T$ from N . By analysing the Nyquist plot of the loop transfer function with uncertainty, L_p , the robust stability condition is, $\frac{|W_I(j\omega)L(j\omega)|}{|1+L(j\omega)|} < 1, \forall\omega \Leftrightarrow |W_I(j\omega)T(j\omega)| < 1, \forall\omega$. Thus, from N, it is required that $|N_{y_\triangle u_\triangle}| = |W_I(j\omega)T(j\omega)| < 1, \forall\omega, \forall\triangle, \|\triangle\|_\infty \leq 1$, to achieve robust stability.

7.3.3.3 Un-modelled dynamic uncertainty

The un-modelled complexity of flow dynamics in the real system can introduce an un-modelled dynamic uncertainty in the controller design. This un-modelled dynamic uncertainty is evaluated as a multiplicative input uncertainty in the manipulated input variable, u. The multiplicative (relative) input uncertainty structure is applied such that the perturbed plant $G_p(j\omega)$ is obtained as $G_p(j\omega) = G(j\omega)(1 + \Delta W_I(j\omega))$, where Δ is a normalised perturbation such that $\|\Delta\|_\infty \leq 1$. The un-modelled uncertainty is usually represented by a simple multiplicative input uncertainty weight given by:

$$W_I(s) = \frac{\tau_w s + r_0}{\left(\frac{\tau_w}{r_\infty}\right) s + 1} \tag{7.21}$$

where r_0 is the relative uncertainty at steady state, $1/\tau_w$ is the approximate frequency at which the relative uncertainty is 100% and r_∞ is the magnitude of the uncertainty at high frequency [94]. For a suitable uncertainty weight, it is required that $|W_I(j\omega)| \geq l_I(\omega)$, $\forall\omega$, where

$$l_I(\omega) = \left|\frac{G_p(j\omega) - G(j\omega)}{G(j\omega)}\right| \tag{7.22}$$

7.3.3.4 H_∞ robust slug controller design for the industrial riser

In this section, the design of the H_∞ robust slug controller for the industrial riser is presented. The Industrial riser system had been described in section 3.5. The H_∞ robust slug controller is designed with linear model transfer function,

which is obtained from the ISRM of the industrial riser system. The controller is implemented on the OLGA model of the industrial riser system, which is nonlinear. The controller implementation is achieved by using the OLGA-Matlab link as discussed in section 5.5.1.

The industrial riser system is open-loop unstable at $u >$12$\%$ with manual choking, where u is the valve opening (see Figure figbifurcation). Thus, the synthesis of a stabilising H_∞ robust slug controller at the open-loop unstable valve opening of u=20$\%$ is carried out. The transfer function of the linear model at u=20$\%$ valve opening with u as input and P_{RB} as given in (7.17). Equation (7.18) also gives the transfer function of the system from u to Q_T. For this controller design, the model transfer functions must be scaled using the method discussed in section 5.2.4. Table 7.9 gives the value of the maximum allowed change in the input, D_u, and the maximum allowed output deviations required to scale (7.17) and (7.18) for the P_{RB} and the Q_T respectively.

Table 7.9: D_u and D_y for model scaling

Controlled variable	D_u	D_y
P_{RB}(barg)	0.2	3.26
Q_T(m^3/s)	0.2	0.0024

The sensitivity weight, Wp, is given as:

$$W_p = \frac{s + 0.01}{s + 4 \times 10^{-5}} \tag{7.23}$$

$G_d(s)$ is the disturbance transfer function from inlet gas and liquid mass flowrate and topside separator pressure to the outputs. The $G_d(s)$ for the P_{RB} is given as:

$$G_{dP_{RB}}(s) = \begin{bmatrix} \frac{3.292s^3+26.15s^2-0.03762s+2.77\times10^{-5}}{s^3+7.994s^2-0.002577s+1.206\times10^{-5}} \\ \frac{-18.74s^3-148.8s^2+0.2908s-0.0001033}{s^3+7.994s^2-0.002577s+1.206\times10^{-5}} \\ \frac{8.492e-008s+1.398\times10^{-10}}{s^3+7.994s^2-0.002577s+1.206\times10^{-5}} \end{bmatrix}$$

while the $G_d(s)$ for the Q_T is given as:

$$G_{dQ_T}(s) = \begin{bmatrix} \frac{0.0008888s^3+0.1025s^2+4.208\times10^{-5}s+7.77\times10^{-9}}{s^3+7.994s^2-0.002577s+1.206\times10^{-5}} \\ \frac{-0.006525s^3-0.5876s^2-0.0005147s+3.315\times10^{-7}}{s^3+7.994s^2-0.002577s+1.206\times10^{-5}} \\ \frac{-4.055e-008s^3-3.179e-007s^2-4.718e\times10^{-10}s-6.634\times10^{-14}}{s^3+7.994s^2-0.002577s+1.206\times10^{-5}} \end{bmatrix}$$

For disturbance rejection, it is required that $|G_d(j\omega)/G(j\omega)| < 1, \forall\omega$ [77], and the set-point weight, $R(s)$, is estimated to satisfy the condition $|R(j\omega)/G(j\omega)| < 1, \forall\omega \leq \omega_r$, which is required for acceptable control with good reference tracking [94]. The $R(s)$ for the P_{RB} is as given in (7.24), while that for the Q_T is given in (7.25).

$$R_{P_{RB}}(s) = \frac{0.22(s+1)}{s^3+0.73s^2+0.14s+8.8\times10^{-4}} \tag{7.24}$$

$$R_{QT}(s) = \frac{0.2381s^2+0.001677s+7\times10^{-8}}{s^2+0.00235s+1.05\times10^{-6}} \tag{7.25}$$

To estimate the model uncertainty weight, a perturbed plant model with $\|l_I(j\omega)\|_\infty = 2.08$, at high frequency is considered, such that the uncertainty weight is calculated as shown in (7.26).

$$W_I(s) = \frac{2.2s+0.0009}{s+0.0015} \tag{7.26}$$

The H_∞ controller is synthesised by using the $hinfsyn$ function in Matlab®. The synthesised controller, K obtained for the P_{RB} is shown in (7.27), while that obtained for the Q_T is shown in (7.28). Balanced realisation method has been applied to reduce the order of these controllers.

$$K = \frac{\begin{array}{r}-0.9s^6 - 1.17s^5 - 0.28s^4 - 0.0028s^3 - \\ -2.7 \times 10^{-6}s^2 - 6.79 \times 10^{-9}s - 3.43 \times 10^{-}12\end{array}}{\begin{array}{r}s^7 + 3.22s^6 + 1.27s^5 + 0.14s^4 + 1.4 \times 10^{-3} + \\ +3.39 \times 10^{-6}s^2 + 2.52 \times 10^{-9}s + 5.48 \times 10^{-13}\end{array}}, \tag{7.27}$$

$$K = \frac{\begin{array}{r}13.36s^7 + 420s^6 + 9.83s^5 + 0.072s^4 + 0.000171s^3 + \\ +1.52 \times 10^{-7}s^2 + 8.293 \times 10^{-11}s + 7.9 \times 10^{-15}\end{array}}{\begin{array}{r}s^7 + 31.64s^6 + 0.5884s^5 + 0.003359s^4 + 7.14 \times 10^{-6}s^3 + \\ +2.388 \times 10^{-9}s^2 + 2.6 \times 10^{-13}s + 1.2 \times 10^{-20}\end{array}}, \tag{7.28}$$

7.4 Characterisation of the slug controllers for closed-loop stability at large valve opening

The ability of each of the slug controllers designed for the industrial riser system to achieve closed-loop stability at a large valve opening can be predicted by using the robust stability criteria based on the magnitude of the $\|T\|_\infty$ obtained for each controller, as discussed in section 7.2. The synthesis of the H_∞ robust controller, which is done using the technical computing software, Matlab®, automatically generates the $\|T\|_\infty$, when enabled.

7.4.1 Characterisation of P_{RB} controller

The $\|T\|_\infty$ calculated for the three controllers using the technical computing software, Matlab®, is summarised in Table 7.10. From Table 7.10, it can be observed that the highest $\|T\|_\infty$ is obtained for the relay tuned controller while the smallest is obtained for the H_∞ robust controller.

Table 7.10: Summary of $\|T\|_\infty$ with P_{RB} control

	Relay tuned slug controller	Robust PID slug controller	Robust H_∞ slug controller
$\|T\|_\infty$	4.45	1.06	0.79

From these results, it can be predicted that the H_∞ robust controller will achieve closed-loop stability at valve opening that is larger than that which the robust PID controller and the relay tuned controller can achieve. Also, the robust PID controller will achieve closed-loop stability at a valve opening that is larger than that which the relay tuned controller can achieve.

7.4.2 Characterisation of Q_T controller

From Table 7.11, it can observed that for controller design using Q_T as the controlled variable, the highest $\|T\|_\infty$ is still obtained for the relay auto-tuned slug controller, while the smallest is obtained for the H_∞ robust controller. From this results, it can also predicted that using the Q_T as the controlled variable, the H_∞ robust controller will achieve closed-loop stability at a valve opening that is larger than that which the relay tuned controller and the robust PID controller can achieve.

Table 7.11: Summary of $\|T\|_\infty$ for Q_T control

	Relay tuned slug controller	Robust PID slug controller	Robust H_∞ slug controller
$\|T\|_\infty$	1.2	1.06	1

Also, for this application, the robust PID controller will achieve closed-loop stability at a valve opening that is larger than that which the relay auto tuned controller can achieve.

To validate these predictions, each of the controller is implemented on the industrial riser system and subsequently the simulation results are analysed.

7.5 Slug controller implementation and simulated production analysis

The performances of the controllers are analysed by implementing them on the industrial riser system, which is modeled in the OLGA multiphase flow simulator software. For the description of the industrial riser system, see section 3.5. The controller is configured in Matlab in an OLGA-Matlab link structure, which is established by using the OLGA-Matlab toolbox. Through OLGA-Matlab link, the results from dynamic multiphase flow simulations performed by OLGA becomes available in MATLAB, and the control input from Matlab become available in OLGA. The analysis of the obtained results is focused on evaluating the maximum closed-loop stable valve opening achieved and the accumulated production. The implementation for the P_{RB} control is presented first, followed by that of the Q_T control.

7.5.1 Slug controller implementation with P_{RB} control

The implementation of the relay auto-tuned controller is presented first, followed by the robust PID controller and then the H_∞ robust controller. The comparison and validation of the predicted ability to achieve stability at a large valve opening in the open-loop unstable region and the analysis of the accumulated oil production across the three controllers with respect to their respective $\|T\|_\infty$ are presented.

7.5.1.1 Implementation of the relay auto-tuned slug controller

The simulation result obtained by implementing the relay auto-tuned controller designed in section 7.3.1.4 is shown Figure 7.15.

This simulation result shows that at fixed valve opening of 20$\%$ (open-loop), the system is unstable, and the riser base pressure, P_{RB}, oscillates. When the controller is switched on after 5 hours, with the P_{RB} set point at 36.8 barg, severe slugging is suppressed (system stabilised). By reducing the P_{RB} set point further, the controller maintained system stability to a minimum riser base pressure of 35.5 barg with valve opening increasing to a maximum value of 28.3$\%$. This result indicates that this controller achieved closed-loop stability at minimum P_{RB} of 35.5 barg and a maximum valve opening of 28.3$\%$. Below this pressure at T=47 hours, the valve opening saturates and the system becomes unstable. Thus, the controller cannot stabilise the system beyond this valve opening.

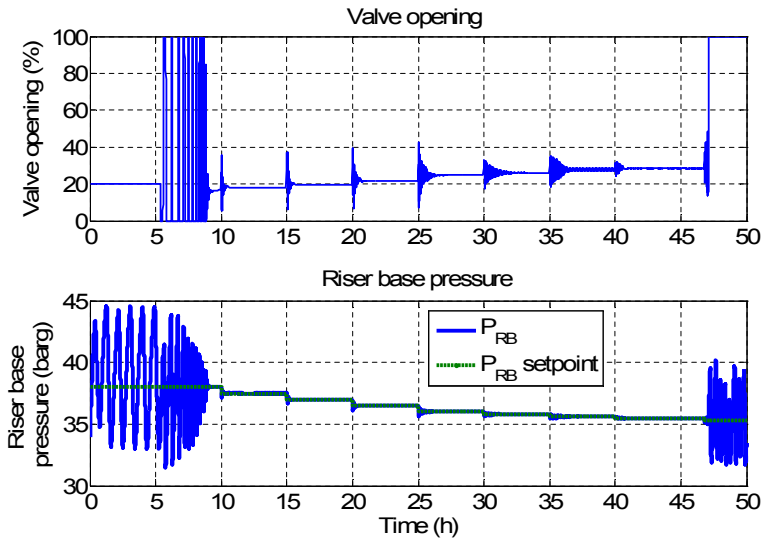

Figure 7.15: Slug control with relay tuned controller

Simulated production analysis

Figure 7.16 shows that the implementation of the relay controller at u=20% yielded an accumulated oil production of 324.6 m^3/day and 338 m^3/day at u=28.3%. This implies that with this controller, a 15% increase in production at u=20%, and a 19.5% increase in production at u=28.3% can be achieved, when compared to production obtained using manual choking.

Comparing this to the accumulated production with no control (severe slugging) at u=20%, it can be observed that there is a 7% increase in production with the controller. It is evident that with the open-loop unstable controller tuning method, the relay tuned active slug control can meet the two fundamental objectives of slug control, namely: stabilising the system (at a higher valve opening other than the open-loop stable valve opening), and increasing oil production.

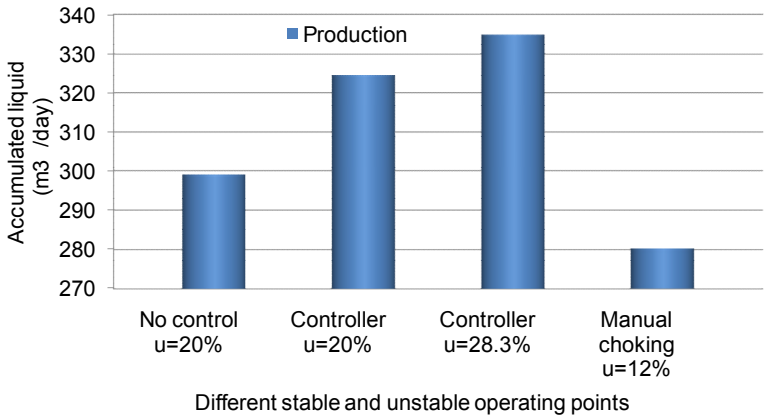

Figure 7.16: Accumulated oil flow at different operating condition

7.5.1.2 Implementation of the robust PID slug controller

The simulation result obtained by implementing the robust PID controller designed in section 7.3.2.2 is shown in Figure 7.17. This simulation result shows that at fixed valve opening of 20% (open-loop), the system is unstable, and the riser base pressure, P_{RB}, oscillates. When the controller is switched on at 2.5 hours, with the P_{RB} set point at 36.8 barg, severe slugging is suppressed (system stabilised) with u at 20%. By reducing the P_{RB} set point further, the controller maintained system stability to a minimum riser base pressure of 34.4 barg with valve opening increasing to a maximum value of 57.6%.

Beyond this point at 35 hours, the controller is not able to stabilise the system. However, if the valve opening was returned to 20% fixed valve opening (open-loop), the system gradually returned to a completely unstable condition. This was also observed in the result from ISRM with well source as shown in Figure 7.18.

Comparing this performance to that achieved with the relay tuned controller, it

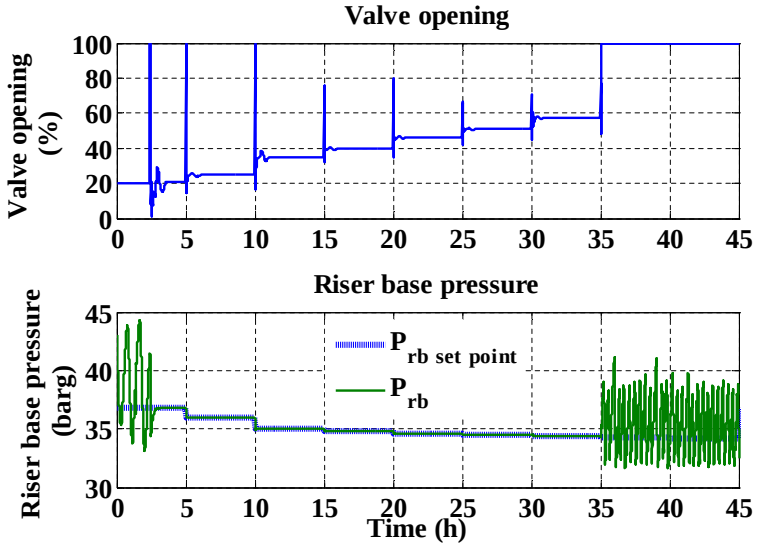

Figure 7.17: Slug control with robust PID controller - OLGA simulation

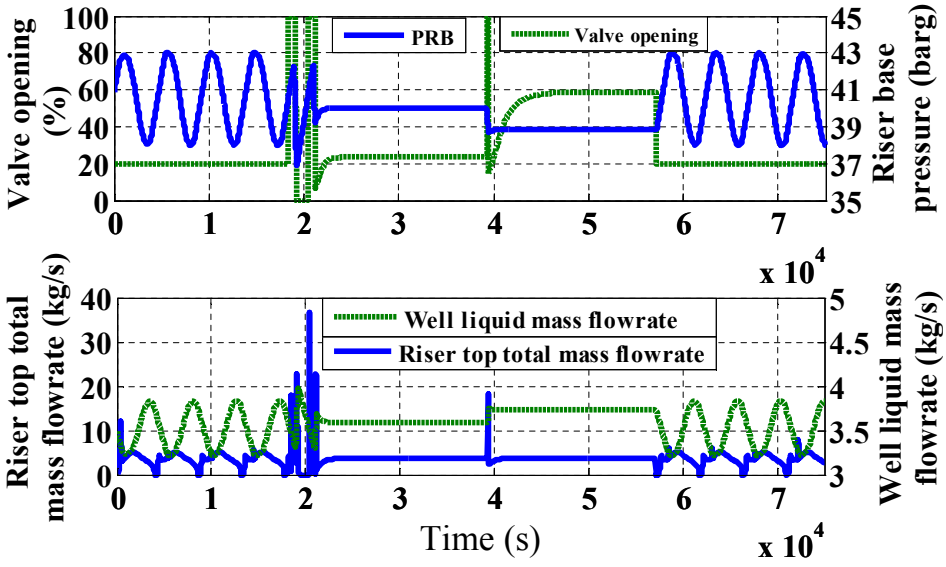

Figure 7.18: Slug control with robust PID controller - ISRM simulation

can be observed that robust PID controller achieved closed-loop stability at a larger valve opening that is larger than that of the relay tuned controller. This agrees with the prediction based on the analysis of their $\|T\|_\infty$ as presented in section 7.4.1.

The accumulated production, which the robust PID controller achieved at the maximum closed-loop stable valve opening will be analysed. This will be compare with that achieved by the relay tuned controller, and the robust H_∞ controller, in section 7.5.1.4.

Simulated production analysis

The accumulated production in a 24hr simulation period is analysed to assess the impact of robust PID controller tuned at open-loop unstable valve opening with P_{RB} control. Comparison is performed with production under manual choking condition and severe slugging for corresponding stable valve opening and at 100$\%$ valve opening condition.

Figure 7.19 show the simulated production under severe slugging condition and with the controller. The accumulated production under severe slugging condition at the valve opening of u=20$\%$ is 299.7 m^3/day. By stabilising the system with the controller designed at u = 20$\%$, the simulated production obtained is 324.6 m^3/day. This implies that by implementing the robust PID controller at this valve opening (u=20$\%$), production is increased by 8.3$\%$ when compared to the production under severe slugging condition at the same fixed valve position. By implementing the controller at the maximum stable valve opening of u=57.6$\%$, the production obtained is 348.17 m^3/day. This implies that by stabilising the system with the controller at u=57.6$\%$, production is increased by 4.7$\%$ when compared to the production under severe slugging condition at the same valve opening.

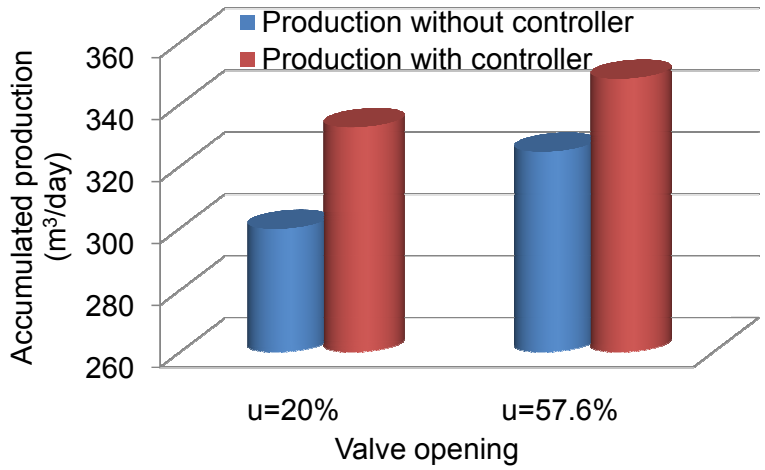

Figure 7.19: Simulated production comparison I: severe slug production

With manual choking control, the system is stabilised at u=12% as shown in Figure 4.18, and the simulated production is 280.25 m^3/day, as shown in Figure 7.20. This shows that production is increased by 15% when compared to simulated production with active controller at u=20%.

By implementing the controller at the maximum stable valve opening of u = 57.6%, the production obtained is 348.17 m^3/day as shown in Figure 7.20. This implies that by stabilising the system with the robust PID controller at u=57.6%, production is increased by 24.3% when compared to manual choking control at u=12%. Analysis of the production with the valve fully open (u=100%) shows that the production with severe slugging occurring at this condition is 337.5 m^3/day. This indicates that the production achieved by the robust PID controller operating at u=57.6% is even 1.4% higher than that with the valve fully open.

It can be observed that for the flow and operating conditions applied, higher percentage increase in production is obtained with comparison to manual choking, which reflects the high reduction in production from the unstable condition if

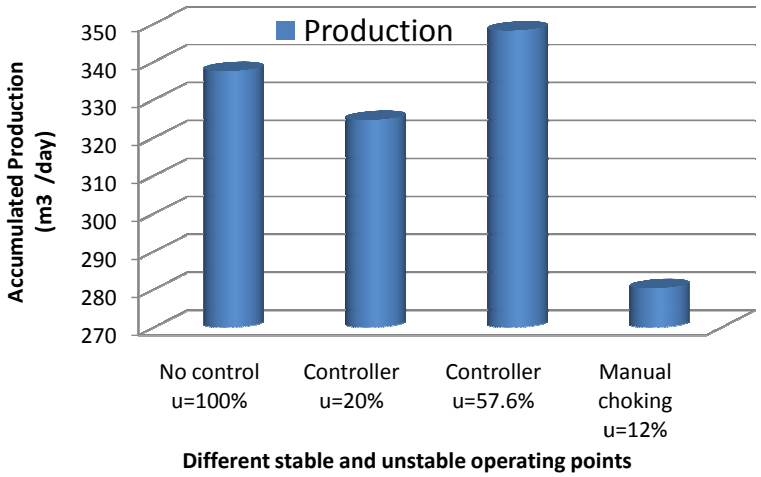

Figure 7.20: Simulated production comparison II: manual choking and no control

manual choking control method is implemented. Thus, manual choking control will adversely reduce production, while active slug control at open-loop unstable operating points will not reduce production, but will under suitable condition increase production.

7.5.1.3 Implementation of H_∞ robust slug controller

The simulation result obtained by implementing the H_∞ robust controller designed in section 7.3.3.4 is shown in Figure 7.21. This result indicates that the controller's closed-loop stability is limited to minimum P_{RB} of 34.3 barg corresponding to a maximum valve opening of 65.5%. Beyond this point, the input saturates and the system cannot be stabilised. The comparison of this result with other controllers' results is presented in section 7.5.1.4.

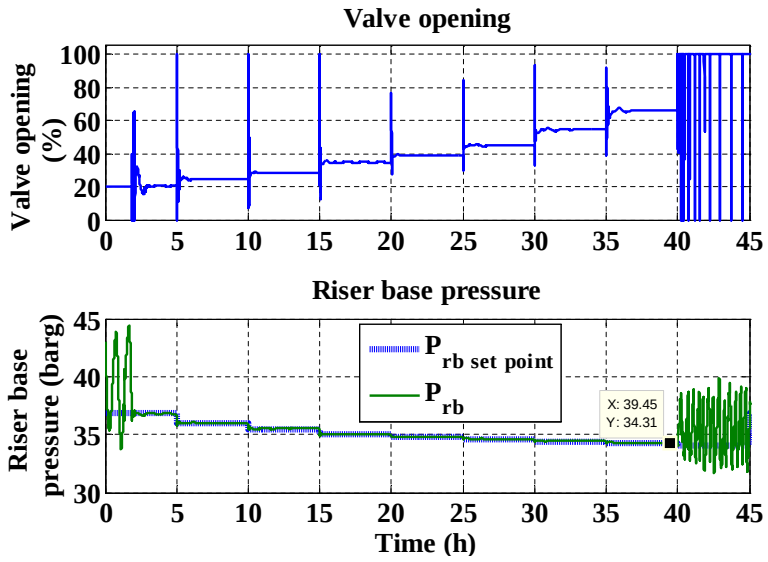

Figure 7.21: Slug control with H-infinity controller

Simulated production analysis

The accumulated liquid production achieved with the H_∞ robust controller is summarised in Figure 7.22. We observe that the accumulated liquid production of 351.6 m^3/day is achieved by implementing the robust H_∞ controller.

It can be calculated from Figure 7.22 that production is increased by 25.5% when compared to manual choking control at u=12%. Analysis of the production with the valve fully open (u=100%) indicates that the production achieved by the H_∞ controller operating at u=65.5% is even 1.8% higher than that with the valve fully open.

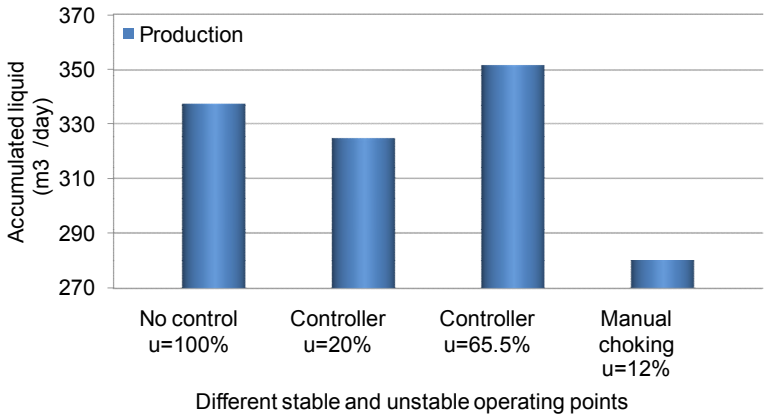

Figure 7.22: Accumulated oil at different operating points

7.5.1.4 Comparison of maximum stable valve opening and simulated production

From Figures 7.15, 7.17 and 7.21 it can be observed that the closed-loop stable riser system becomes unstable when the valve opening, u, saturates continuously. The maximum valve opening at which the system become unstable differs for the three controllers. In section 7.4.1, it was predicted that the stable closed-loop valve opening, which the H_∞ robust controller will achieve will be larger than that of the relay tuned controller and the robust PID controller, based on the value of their $\|T\|_\infty$. Comparing the controller performances as summarised in pressure bifurcation map shown Figure 7.23, it is clear that the H_∞ robust controller achieved closed-loop stability with the least value of P_{RB}, corresponding to the largest valve opening, when compared to the robust PID controller and the relay tuned controller. These results are also summarised in Table 7.12, with the corresponding H_∞ shown.

These performances confirms the analysis, that the slug controller with the

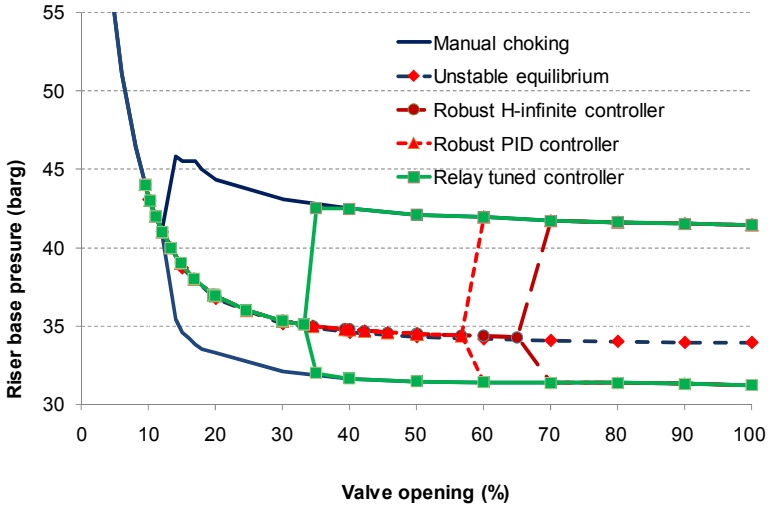

Figure 7.23: Pressure bifurcation map showing controller's maximum closed-loop stable valve openings

Table 7.12: Controllers' performance table

	Relay tuned slug controller	Robust PID slug controller	Robust H_∞ slug controller
$\|T\|_\infty$	4.45	1.06	0.79
$P_{RBmin}(barg)$	35.5	34.4	34.3
$u(\%)$	28.5	56.7	65.5

least value of $\|T\|_\infty$ is less more robust and will achieve closed-loop stability at a larger valve opening in the open-loop unstable region. This makes it most suitable for implementation on an unstable riser pipeline system whose control performance objectives is focused on achieving stability as well as maximising production. Therefore, for a number of available slug controllers, it is useful to characterise their ability to stabilise the unstable riser system at large valve opening in the open-loop unstable region using the $\|T\|_\infty$. This will provide useful prediction of their performance and provide a guide to achieving the PGI prediction of the system (see Chapter 6).

The effect of the P_{RBmin} achieved by of the slug controllers is obvious since lower P_{RB} would reflect reduction in the flow line pressure, which will result to increased oil production. The effect of the controller performances on the oil production can be analysed by measuring the accumulated liquid over a given period at the maximum stable valve opening as shown in Figure 7.24.

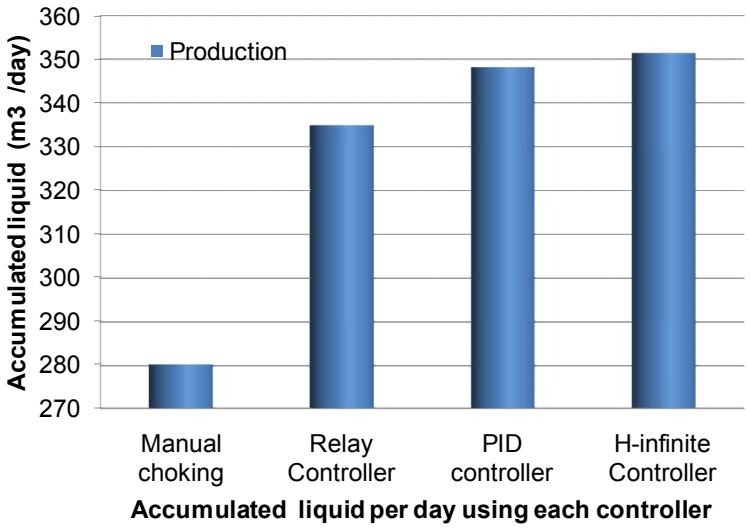

Figure 7.24: Accumulated oil per day using each controller

From Figure 7.24, it can be observed that the maximum daily oil production of 351.6 m^3/day is achieved by implementing the robust H_∞ controller, while the minimum daily oil production of 338 m^3/day is achieved by the relay tuned controller. By relating this result to the information shown in Table 7.10 and Table 7.12, it can be observed that the choice for a stable slug controller for maximum oil production can be made by analysing the $\|T(s)\|_\infty$ and choosing the controller with the minimum value. The worst case will be the conventional and widely used manual choking method, which gives production of 280.25 m^3/day resulting to a 25.5$\%$ loss in production when compared to production using robust H_∞ controller.

7.5.2 Stability and production in declining reservoir pressure condition

As the well pressure declines (as oil fields mature), the differential pressure between the topside pressure set point and the well source decreases and the fluid flow rate is reduced. This would impose further disturbance (instability) on the riser system such that further action is required to stabilise the system. With topside valve choking control, this further action would imply reducing the valve opening further. Implementing manual choking or the robust PID controller in this condition could have serious impact on production.

Figure 7.25 shows the minimum riser base pressure and the maximum valve opening required to stabilise the generic (industrial) riser model at declining reservoir pressure (from 69 barg to 45.3 barg) by using manual choking and using the open-loop unstable tuned controller. To stabilise the system with manual choking, the maximum valve opening is reduced from 12$\%$ at 69 barg

to 7% at 45.3 barg. However, with the robust PID controller, the system is stabilised at a wider maximum valve opening of 57% at 69 barg and 42% at 45 barg.

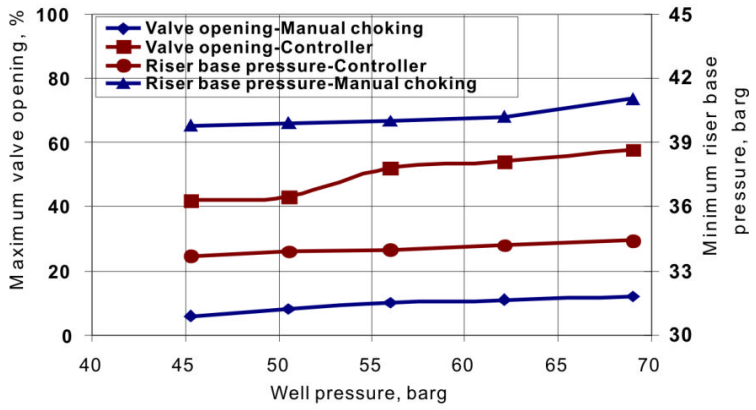

Figure 7.25: Stability at declining well pressure

This result shows that with the manual choking, the minimum pressure drop across the riser is much higher than the maximum pressure drop across the riser obtained with the controller implementation for the range of the well pressures. The impact of this on production is illustrated in Figure 10 below.

Figure 7.26 shows that implementing a robust slug controller can extend the operation life of an unstable offshore riser-pipeline system. With the robust PID controller, significant proportional production increase is maintained while with manual choking, production is further reduced with declining well pressure.

Consider an offshore riser system, which requires a minimum production around 200 m^3/day to break even and remain in operation, it can be observed from Figure 7.26 that with manual choking, the system cannot operate beyond a reservoir pressure around 62 barg. The daily production for this system with reservoir pressure below 62 barg is less than 200 m^3/day. However, with the

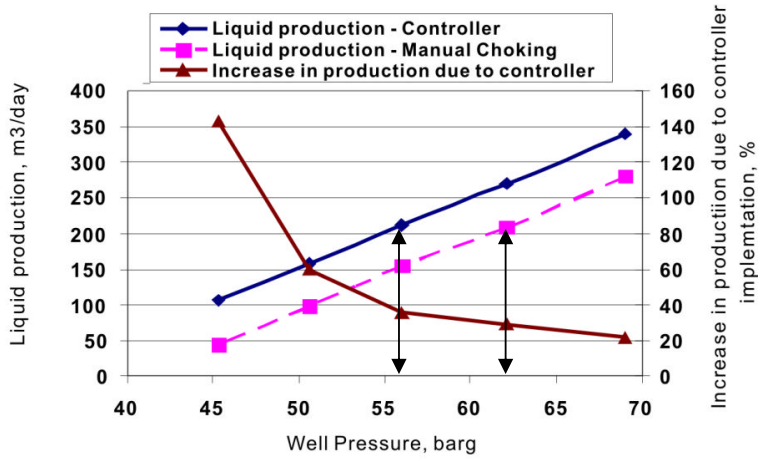

Figure 7.26: Percentage of production increase against well pressure

implementation of the robust PID controller, this system will still be in operation and producing until the reservoir pressure is as low as 56 barg. Thus, the operational life of the unstable offshore riser-pipeline system is extended. It should be pointed out that this result is based on a linear well model. If the reservoir model is nonlinear, the trend of the impact of slug control on production may behave differently.

7.5.3 Slug controller implementation with Q_T control

The result of the implementation of the slug controllers for Q_T control is analysed in this section. The simulation result obtained from the implementation of the relay auto-tuned controller is presented in Figure 7.27. This results shows that the controller achieved closed-loop stability at a maximum valve opening of u=45.6%, which corresponds to a P_{RB} of 34.62 barg.

The simulation result obtained from the implementation of the robust PID slug

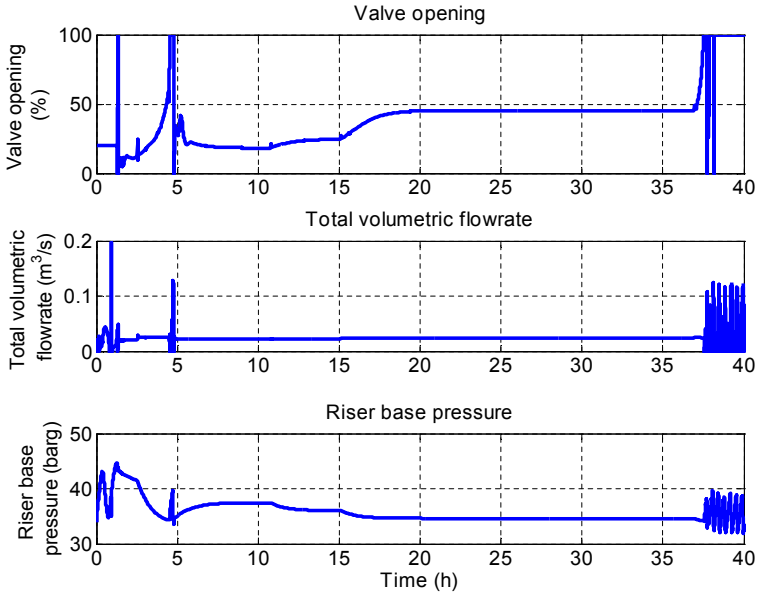

Figure 7.27: Simulation result of the relay tuned slug controller

controller is also presented in Figure 7.28. This results shows that the controller achieved closed-loop stability at a maximum valve opening of u=58.6%, which corresponds to a P_{RB} of 34.38 barg.

Also the simulation result obtained from the implementation of the H_∞ robust slug controller is also presented in Figure 7.29. This result shows that the controller achieved closed-loop stability at a maximum valve opening of u=60%, which corresponds to a P_{RB} of 34.36 barg.

The comparison of the results shows that these simulation results also agrees with the analysis of the robust stability of the system presented in section 7.4.2. The H_∞ robust controller with the least value of the $\|T\|_\infty$, achieved closed-loop stability at the largest valve opening, while the relay auto-tuned controller with the highest value of the $\|T\|_\infty$, achieved closed-loop stability at the smallest valve opening. The accumulated oil production also shows that the H_∞ robust

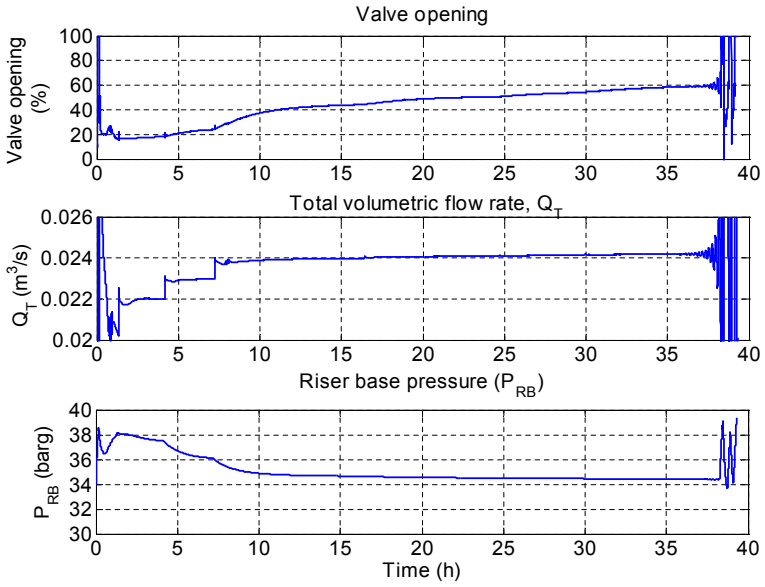

Figure 7.28: Simulation result of the robust PID slug controller

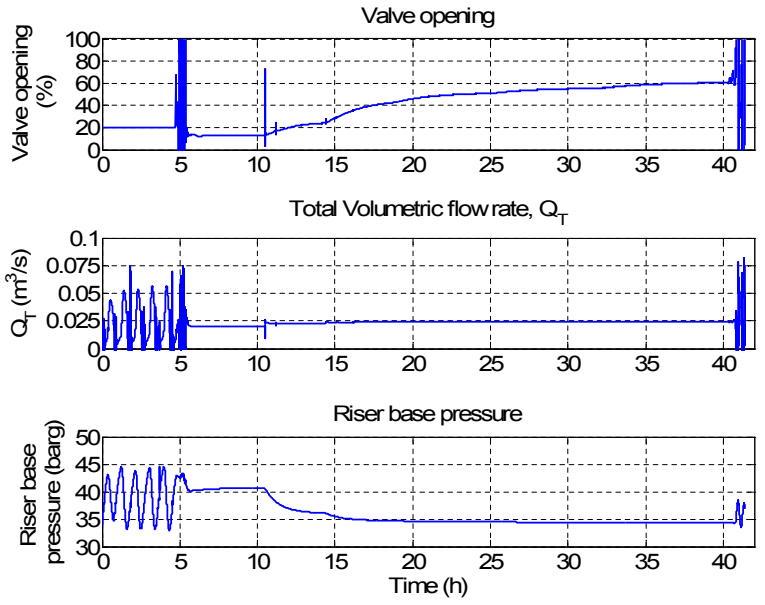

Figure 7.29: Simulation result of the H_∞ robust slug controller

controller achieved the maximum oil production for 24 hour simulation period. These results are summarised in Table 7.13.

Table 7.13: Controllers' stability performance

	Relay tuned slug controller	Robust PID slug controller	Robust H_∞ slug controller
$\|T\|_\infty$	1.2	1.06	1
$P_{RBmin}(barg)$	34.62	34.38	34.36
$u(\%)$	45.6	58.6	60
Accumulated production (m^3/day)	346.5	349.3	349.5

7.6 Conclusions

In conclusion, this chapter has presented the design, implementation and the performance analysis of active slug controllers for maximising oil production. The severe slug control design has focused on achieving two important objectives. These include: eliminating severe slugging and maximising oil production.

From the results of the active control of severe slugging presented in this chapter, it can be concluded that active feedback control designed and implemented at open-loop unstable valve opening is effective in eliminating severe slugging and maximise oil production in an unstable riser-pipeline system. For a number of available slug controllers, the ability of any slug controller to achieve closed-loop stability at large valve opening in the open-loop unstable operating point can be assessed by the analysis of their $\|T\|_\infty$. A slug controller, which

achieves the lowest value of the $\|T\|_\infty$, will achieve closed-loop stability at a larger valve opening than a slug controller with highest $\|T\|_\infty$.

Three active slug controllers namely: the relay auto-tuned controller, the robust PID controller and the H_∞ robust controller has been designed, evaluated and implemented under the same operating condition for two controlled variables, the P_{RB} and the Q_T. The performance evaluation of this set of active slug controllers has been done by analysing their $\|T\|_\infty$. The analysis revealed that the H_∞ robust controller has the least value of the $\|T\|_\infty$ followed by the robust PID controller, while the relay auto-tuned controller has the maximum value. Simulation results obtained from the two controlled variables showed that H_∞ robust controller achieved closed-loop stability at the maximum valve opening in the open-loop unstable region, while the relay tuned controller achieved closed-loop stability at the minimum valve opening.

The maximum liquid production achieved by each controller also differed, reflecting the difference in the maximum closed-loop stable valve opening achieved by each controller. By this, the liquid production achieved by the H_∞ robust controller is the maximum for the three controllers.

It was also shown through the analysis of the stability of an unstable offshore riser system with a declining linear well pressure condition, that the implementation of a robust slug controller can extend the operational life of such a system.

Chapter 8

Improved relay auto-tuned slug controller design for increased oil production

8.1 Introduction

The application of the relay auto-tuned slug controller using the relay shape factor has some significant advantages, in that it can be applied both online (with the plant) and offline (through simulation), and its application method does not require detailed modeling of the system. The plant model can be approximated from the shape of the relay feedback response as was discussed in Chapter 7. However, these advantages are undermined by the poor robustness of the slug controller when it is implemented in the real system. From the performance of the three slug controllers designed in Chapter 7, it is observed that the relay auto tuned controller achieved the smallest closed-loop stable operating point which corresponds to the highest P_{RB}, resulting to the least achieved production. This performance reveals the poor robustness of the relay auto tuned slug

controller. Consequently, the relay tuned controller lacks the ability to handle plant uncertainties.

Thus, the improvement of the relay auto-tuned slug controller will be necessary to make it attractive. An approach to achieve this improvement is presented in this chapter. The chapter begins with the analysis of the perturbed (uncertain) FOPDT model. This is followed by the development of the improved controller design algorithm, the controller implementation and the performance analysis.

8.2 The perturbed (uncertain) FOPDT model

By using the shape of the relay feedback response, the riser-pipeline system model can be identified as the FOPDT process. The process of identifying this FOPDT process for the riser-pipeline system which had been discussed in section 7.3.1.1, does not consider the system uncertainties which could affect the model's performance in controller design. The model uncertainties occur due to the difference between the true system and the system model. These differences often occur due to neglected and unmodeled system dynamics in the system model [94].

The model uncertainties can be defined with respect to the process parameters such as the process gain, k_p, the process dead time, D, and the process time constant, τ, which define the model. Consider a nominal (without uncertainty) unstable FOPDT model of a riser-pipeline system given by:

$$G_0(s) = \frac{k_p e^{-Ds}}{\tau s - 1} \tag{8.1}$$

The model mismatch between the identified FOPDT model and the real system can be represented in any of these process parameters. We will consider the pole uncertainty in the identified FOPDT model, since the stability of the system will depend on its pole location. The pole of (8.1) is $1/\tau$, which shows that the pole is a function of the time constant τ. We will define an uncertain time constant of the FOPDT model in (8.1) as τ_u. With τ_u, (8.1) will become a perturbed (uncertain) FOPDT model $G_p(s)$, and can be defined as given in (8.2).

$$G_p(s) = \frac{k_p e^{-Ds}}{\tau_u s - 1} \tag{8.2}$$

The uncertain time constant, τ_u, can be defined as given in (8.3).

$$\tau_u = \tau(1 + r_\tau \Delta) \tag{8.3}$$

In (8.3), τ is the system's identified time constant, r_τ is the relative magnitude of the time constant uncertainty and Δ is the system perturbation, whose magnitude is defined by $\|\Delta\|_\infty < 1$. By substituting (8.3) into (8.2), a perturbed FOPDT model, which is given in (8.4) is obtain.

$$G_p(s) = \frac{k_p e^{-Ds}}{\tau s + r_\tau \tau s \Delta - 1} \tag{8.4}$$

The term $r_\tau \tau s$ can be defined as a function of an uncertainty weight, $w_I(s)$, such that

$$r_\tau \tau s = w_I(s)(\tau s - 1) \tag{8.5}$$

By substituting (8.5) into (8.4), and factorising it, (8.6) is obtained. Equation 8.6 is a perturbed plant with inverse multiplicative uncertainty.

$$G_p(s) = \frac{k_p e^{-Ds}}{(\tau s - 1)(1 + w_I(s)\Delta)} \tag{8.6}$$

The inverse multiplicative uncertainty is known to be suitable for analysing pole uncertainty [94]. The uncertainty weight, w_I, can be defined by a simple frequency dependent multiplicative weight term. A typical form of this uncertainty weight which is provided in the literature by Skogestad and Postlethwaite [94], is given in (8.7).

$$w_I(s) = \frac{\tau_0 s + r_0}{(\tau_0/r_\infty)s + 1} \tag{8.7}$$

In (8.7), r_0 is the relative uncertainty of the system as steady state, $1/\tau_0$ is the frequency for which the relative uncertainty is 100%, and r_∞ is the magnitude of the weight at high frequency. The $w_I(s)$ can be estimated by defining its parameters to satisfy the condition given in (8.8),

$$|w_I(j\omega)| \geq l_I(\omega), \forall\omega \tag{8.8}$$

where $l_I(\omega)$ is the error between the nominal plant $G_0(j\omega)$ and the perturbed plant, $G_p(j\omega)$.

$$l_I(\omega) = \left| \frac{G_p(j\omega) - G_0(j\omega)}{G_0(j\omega)} \right|$$

Having derived the perturbed FOPDT model of the system, the relay auto-tuned slug controller algorithm is synthesised based on this perturbed FOPDT model given in (8.6).

8.3 Relay auto-tuned controller synthesis

In this section, the synthesis of the controller algorithm for the perturbed FOPDT model given in (8.6) is presented. The simplified closed-loop block diagram for our controller synthesis is shown in Figure 8.1.

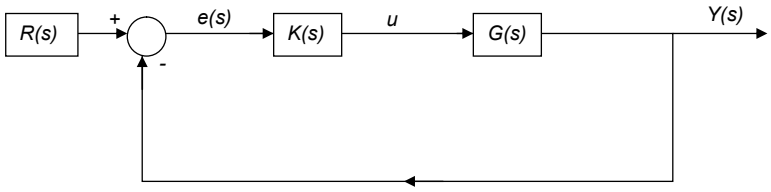

Figure 8.1: Block diagram for controller synthesis

The closed-loop transfer function from $R(s)$ to $Y(s)$ in Figure 8.1 can be obtained as given in (8.9).

$$\frac{Y(s)}{R(s)} = \frac{G(s)K(s)}{1 + G(s)K(s)} \tag{8.9}$$

From (8.9), the equation of the controller, $K(s)$, can be solved to obtain:

$$K(s) = \frac{1}{G(s)} \left(\frac{Y(s)/R(s)}{1 - Y(s)/R(s)} \right) \tag{8.10}$$

The expression for $Y(s)/R(s)$ can be obtained by considering the simplest closed-loop response form of the FOPDT system as proposed by Dahlin [20] and Smith and Corripio [95], which is given below in (8.11).

$$\frac{Y(s)}{R(s)} = \frac{e^{-Ds}}{\tau_c s + 1} \tag{8.11}$$

where τ_c is the closed-loop response time constant and D is the dead time of the identified FOPDT process. By substituting (8.11) into (8.10) and simplifying it, the expression for $K(s)$ is obtained as given in (8.12).

$$K(s) = \frac{1}{G(s)} \left(\frac{e^{-Ds}}{\tau_c s + 1 - e^{-Ds}} \right) \tag{8.12}$$

For the purpose of our controller synthesis, the plant model $G(s)$ in (8.12) will be substituted with the perturbed FOPDT model, $G_p(s)$, given in (8.6). Thus, by substituting (8.6) into (8.12) and simplifying, the expression for $K(s)$ is obtained as:

$$K(s) = \frac{(\tau s + 1)(1 + w_I(s)\Delta)}{k_p(\tau_c s + 1 - e^{-Ds})} \tag{8.13}$$

The delay term, e^{-Ds}, in the denominator can be approximated using the first order Pad$\acute{e}$ approximation [95], which is given by (8.14).

$$e^{-Ds} = \frac{1 - \frac{D}{2}s}{1 + \frac{D}{2}s} \tag{8.14}$$

By substituting (8.14) into (8.13), the resulting expression can be simplified to obtain the algorithm for the PI controller parameters, the controller gain, k_c and the integral time, τ_I, as given in (8.15) and (8.16)

$$k_c(s) = \frac{\tau(1 + w_I(s)\Delta)}{k_p(\tau_c + D)} \tag{8.15}$$

$$\tau_I = \tau(1 + w_I(s)\Delta) \tag{8.16}$$

Equation 8.15, can be further simplified by considering that a closed-loop response with 5% overshoot of the set point change is a desired response [95]. For this type of response, it was recommended by Martin et al [65], that the τ_c be made equal to the dead time, D, of the FOPDT system. Following this, (8.15) can be simplified to obtain:

$$k_c(s) = \frac{\tau(1 + w_I(s)\Delta)}{2Dk_p} \tag{8.17}$$

For an unstable riser system, at this point, it can be assumed that the model uncertainty will be dominated by the uncertainty at high frequency. Thus, the $w_I(s)$ in (8.17) can be defined specifically for the uncertainty at high frequency such that for $\omega \to \infty$, the uncertainty weight will be equal to the relative uncertainty at high frequency as given in (8.18).

$$w_I(j\infty) = r_\infty \tag{8.18}$$

By substituting (8.18) into (8.16) and (8.17), the k_c and τ_I given in 8.19 and 8.20 will obtained.

$$k_c = \frac{\tau(1 + r_\infty\Delta)}{2Dk_p} \tag{8.19}$$

$$\tau_I = \tau(1 + r_\infty\Delta) \tag{8.20}$$

A systematic method for determining the uncertainty weight parameters will be explained in the controller design, presented in the next section.

8.4 Controller design and implementation

In Chapter 7, the relay auto-tuned slug controller method was implemented to design slug controllers for P_{RB} and Q_T control using the riser top valve as the manipulated variable. The performance of these controllers in achieving closed-loop stability at large valve opening were not very satisfactory, when compared to the robust PID and the H_∞ robust controller. In this section, the improved relay design controller algorithm will be implemented to improve the performance of these controllers on the industrial riser system.

8.4.1 Controller design and implementation with P_{RB} control

The relay auto-tuned controller design for P_{RB} control of the industrial riser system was carried out in section 7.3.1.4. From the relay feedback response, the dead time $D = 14.2s$ is obtained and the process gain, $k_p = 4.72$ and time constant, $\tau = 20.5$ are calculated. Using these parameters, the nominal FOPDT model $G_0(s)$ is defined as given in (8.21).

$$G_0(s) = \frac{4.72e^{-14.2s}}{20.5s - 1} \tag{8.21}$$

From this nominal plant model, the perturbed plant, $G_p(s)$, is defined as given in (8.22), by considering the uncertainty of the time constant, τ.

$$G_p(s) = \frac{4.72e^{-14.2s}}{\tau_u s - 1} \tag{8.22}$$

The range of uncertain time constants, τ_u, is assume to be $\pm$ 90% around the nominal valve. Using the $ureal$ command in Matlab® Robust Control Toolbox, a set of 11 samples of the uncertain time constant was obtained. Each sample

of τ_u within the uncertainty set corresponds to a perturbed plant. Thus, based on (8.22), a set of perturbed plants, Π_p, are defined, as given by (8.23).

$$\Pi_p = \{G_p(s, \tau_u) | \tau_u \in R^+\} \tag{8.23}$$

Given this set of perturbed plant from (8.23), the maximum model error is obtained by evaluating (8.24), for a set of model errors, Π_{l_I}, defined by (8.25), where $l_{I(i)}(\omega)$ is given by (8.26).

$$l_I(\omega) = \max_{G_p \in \Pi_p} \{\Pi_{l_I}\} \tag{8.24}$$

$$\Pi_{l_I} = \{l_{I(i)}(\omega) | i \in Z^+\} \tag{8.25}$$

$$l_{I(i)}(\omega) = \left| \frac{G_{p(i)}(j\omega) - G_0(j\omega)}{G_0(j\omega)} \right| \tag{8.26}$$

For clarity, the model errors are also plotted in Figure 8.2. The plotted model errors are obtained by evaluating (8.26), for $i = (1, 2, 3, ...n)$, where $n = 11$ is the number of perturbed FOPDT plant in the set Π_p.

For the maximum error obtained by evaluating (8.24), it can be observed from Figure 8.2 that $|l_I(\omega)|$ is 0.022 at low frequency and 10 at high frequency. With these values, the uncertainty weight $w_I(j\omega)$ that will account for all the possible model errors considered, can be designed such that the condition $|w_I(j\omega)| \geq |l_I(\omega)|, \forall\omega$ as given in (8.8) is satisfied. Thus, the uncertainty weight is defined as shown in (8.27), and plotted by the first line in Figure 8.2.

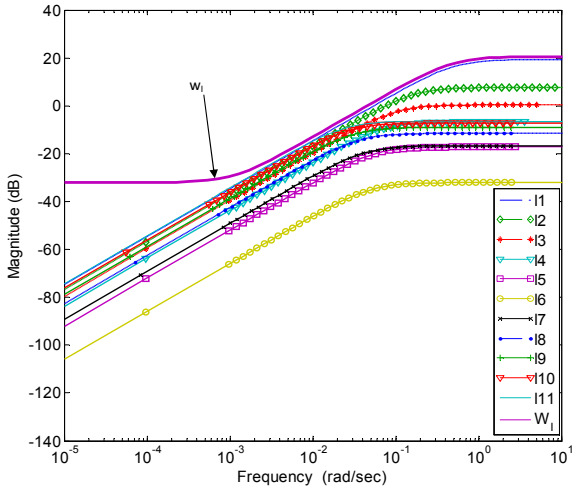

Figure 8.2: Error and uncertainty weight plot

$$w_I(s) = \frac{22.2s + 0.025}{(22.2/10.7)s + 1} \tag{8.27}$$

From this (8.27), the values $\tau_0 = 22.2$, $r_0 = 0.025$ and $r_\infty = 10.7$ are obtained, which are required values in the controller algorithm. The perturbed FOPDT model parameters are summarised in Table 8.3. The PI controller parameters are then calculated from (8.19) and (8.20) and the values are also shown in Table 8.3.

Table 8.1: Process and controller parameters for P_{RB} control

	Perturbed process parameters					Controller parameters	
Valve opening (%)	τ	k_p(barg)	r_∞	r_0	τ_0	k_c(barg^{-1})	τ_I (s)
20	20.5	4.72	10.7	0.025	22.2	1.8	240

8.4.1.1 Controller implementation

This controller parameters are then implemented on the industrial riser system in the OLGA software and the result obtained is shown in Figure 8.3.

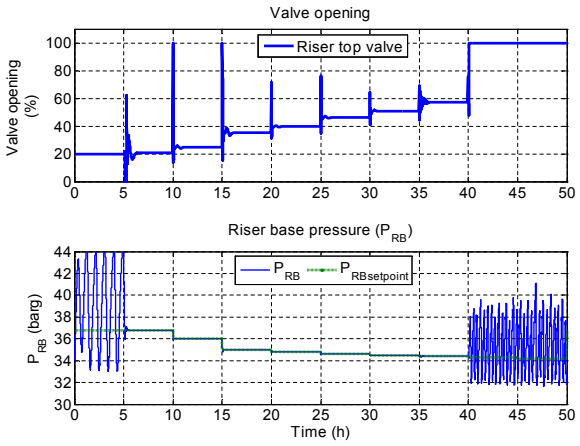

Figure 8.3: OLGA model simulation result with improved relay auto-tuned controller

During the simulation the following steps are taken.

1. The valve opening is initially set to a fixed position corresponding to the open-loop unstable valve opening of u =20%.

2. The controller is then switched on after a simulation period of 5 hours. It is observed that the system is stabilised when the controller is switched on.

3. Once the system is stabilised, the P_{RB} set point is gradually reduced and the system is allowed to stabilise for each step reduction.

4. The gradual reduction in the P_{RB} set point is continued until the P_{RB} at which the controller cannot stabilise the system is reached at 40 hours.

From this result, it is observed that the controller achieved closed-loop stability at a maximum valve opening of u =57.6$\%$, corresponding to $P_{RB} = 34.4$ barg. Comparing this performance to that obtained with the original relay auto-tuning controller algorithm shown in Figure 7.15, it is clear that there is a significant improvement in the performance of the improved controller. From the performance results summarised in Table 8.2, it can be observe that the improved controller algorithm achieved accumulate production of 348.17 m^3/day.

Table 8.2: Comparison of relay auto-tuned controller performance

Relay Controller	maximum u ($\%$)	P_{RBmin} barg	Accumulated liquid (m^3/day)	$\|T\|_\infty$
Original	28.3	35.5	335	4.45
Improved	57.6	34.4	348.17	1.08

This indicates a 4$\%$ increase in production when compared to the production obtained from the original relay auto-tuned controller design presented in Chapter 7. This is as a result of its ability to achieve closed-loop stability at a larger valve opening and reduced P_{RB}. From Table 8.2, it can also be observe that $\|T\|_\infty$ obtained with the improved controller algorithm is much lower than that obtained in Chapter 7. This also shows that the slug controller with a lower value of $\|T\|_\infty$ has a better ability to achieve closed-loop stability at a larger valve opening in the open-loop unstable region.

Next the improved controller algorithm is implemented for the Q_T control of the industrial riser system.

8.4.2 Controller design and implementation with Q_T control

The improved relay controller algorithm can also be applied to improve the performance of the Q_T control in the control of the unstable industrial riser system. Firstly, the nominal system transfer function $G_0(s)$ has to be defined. We can recall from section 7.3.1.4 that the process gain, k_p, and the time constant, τ, was obtained as 0.045 barg and 10.4 respectively for the Q_T control. The dead time, D, obtained from the relay feedback response is 7.2 s. Using these parameters, the nominal FOPDT model of the system as given in (8.28), can be defined.

$$G_0(s) = \frac{0.045e^{-7.2s}}{10.4s - 1} \tag{8.28}$$

From this nominal plant model, the perturbed plant, $G_p(s)$, is defined as given in (8.29), by considering the uncertainty of the time constant, τ_u.

$$G_p(s) = \frac{0.045e^{-7.2s}}{\tau_u s - 1} \tag{8.29}$$

The range of uncertain time constants, τ_u, is assumed to be $\pm$60% around the nominal valve. Using the $ureal$ command in Matlab® Robust Control Toolbox, a set of 7 samples of the uncertain time constant was obtained. Each sample of τ_u within the uncertainty set corresponds to a perturbed plant. Thus, based on (8.29), a set of perturbed plants, Π_p, are defined, in the form given by (8.23).

The maximum model error is obtained by evaluating (8.23) using (8.28) and (8.29). Figure 8.4 shows a plot of the model errors, which is obtained by evaluating (8.26), for $i = (1, 2, 3...n)$, where $n = 7$ is the number of perturbed plants in the set.

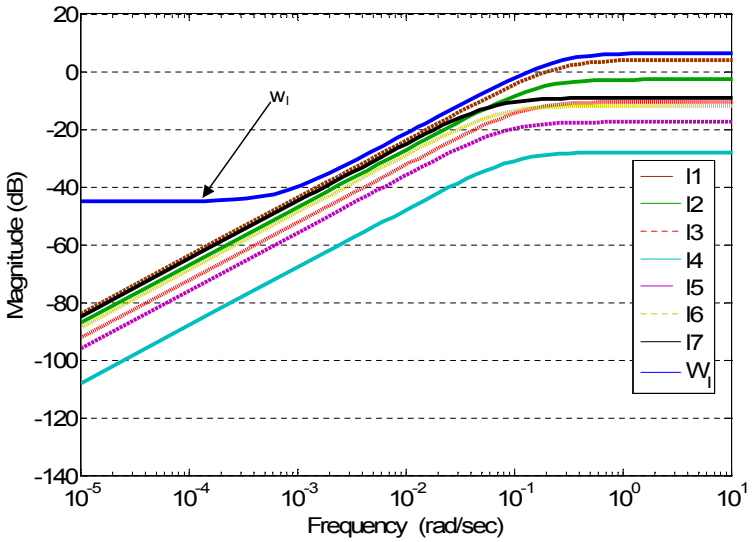

Figure 8.4: Error and uncertainty weight plot

For the maximum error obtained by evaluating (8.24), it can be observed from Figure 8.4 that $|l_I(\omega)|$ is 0.007 at low frequency and and 1.6 at high frequency. The uncertainty weight parameters will be obtained from this error plot in Figure 8.4. The uncertainty weight, $w_I(j\omega)$, is then designed such that the condition $|w_I(j\omega)| \geq |l_I(\omega)|, \forall\omega$ is satisfied. The uncertainty weight is as shown in (8.30), and the uncertainty weight plot is given by the first line from top in Figure 8.4.

$$w_I(s) = \frac{8.3s + 0.008}{(8.3/2)s + 1} \tag{8.30}$$

Table 8.3: Process and the PI controller parameters for Q_T

	Perturbed process parameters					Controller parameters	
Valve opening (%)	τ	k_p(barg)	r_∞	r_0	τ_0	k_c(m^3/s^{-1})	τ_I (s)
20	10.5	0.045	2	0.008	8.3	35.6	23

8.4.2.1 Controller implementation

These controller parameters are then implemented on the industrial riser system in the OLGA software, using the OLGA-Matlab link structure (see section 5.5.1). The result obtained is shown in Figure 8.5. From this result, it can

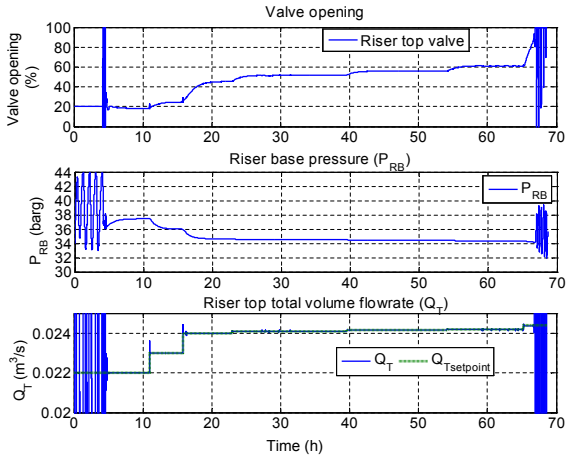

Figure 8.5: OLGA model simulation result with improved relay auto-tuned controller

be observed that the controller achieved closed-loop stability at a maximum valve opening of u =60%, corresponding to P_{RB} =34.36 barg. Comparing this performance to that obtained with the relay auto-tuned controller algorithm shown in Figure 7.27, it is clear that there is a significant improvement in the performance of this controller. From the performance results summarised in Table 8.4, we observe that the improved controller algorithm achieved accumulate production of 349.5 m^3/day.

This indicates about 1% increase in production when compared to the production obtained from the original relay auto-tuned controller design presented in

Table 8.4: Comparison of relay auto-tuned controller performance

Relay Controller	maximum u (%)	P_{RBmin} barg	Accumulated liquid (m^3/day)	$\|T\|_\infty$
Original	45.6	34.62	346.5	1.2
Improved	60	34.36	349.5	1

Chapter 7. This is as a result of its ability to achieve closed-loop stability at a larger valve opening and reduced P_{RB}. From Table 8.4, it is also observed that $\|T\|_\infty$ obtained with the improved controller algorithm is lower than that obtained with the original controller algorithm. This also shows that the slug controller with a lower value of $\|T\|_\infty$ has a better ability to achieve closed-loop stability at a larger valve opening in the open-loop unstable region.

8.5 Control with topside separator gas valve, (u_g)

Another control structure which can be implemented for the control of unstable riser system is the control with the topside separator gas valve (u_g) as the manipulated variable. The schematic diagram of a riser system with this control structure for P_{RB} control is shown in Figure 8.6.

In this control structure, the topside separator gas valve is manipulated using the controller output, to stabilise the system. We will consider the implementation of this control structure using the riser base pressure, P_{RB}.

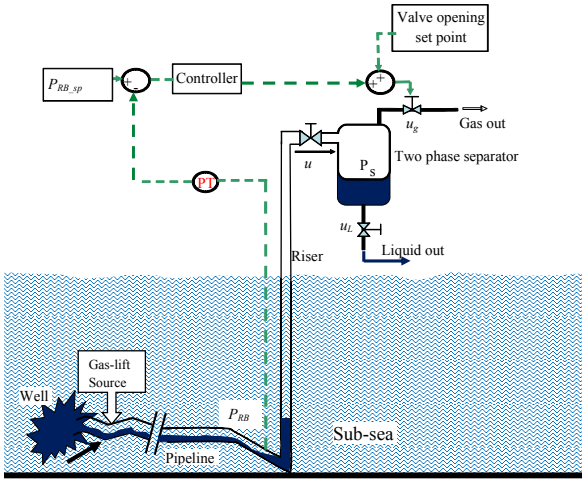

Figure 8.6: Schematic diagram of the industrial riser-pipeline system

8.5.1 Control with the P_{RB}

The performance of the improved relay auto-tuned controller can be assessed by using u_g opening as the controlled input and the P_{RB} as the controlled variable on the industrial riser system. The controller design using the relay auto-tuning method presented in Chapter 7 is first presented. Then the controller with the improved method relay-auto tuning method presented in this chapter is implemented and the results compared.

From the analysis of the unstable industrial riser-pipeline system control using the u_g presented in Chapter 5, it was obtained that the industrial riser-pipeline with separator volume of 0.25 m^3 is unstable for u_g >23%. Thus, the relay auto-tuned controller will be designed at the open-loop unstable operating point of u_g =30%, with this separator volume. The relay design parameters and the feedback response parameters obtained from the feedback response shown in Figure 8.7 are summarised in Table 8.6.

Table 8.5: Relay design and response parameters

	Relay design parameters		Relay response parameters		
Valve opening (%)	h	On and off point	a (barg)	$P_u(s)$	$D(s)$
30%	± 0.2	± 0.5	0.5	388	14.3

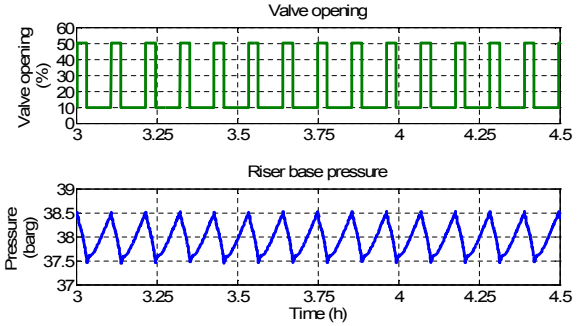

Figure 8.7: Relay feedback response for P_{RB} control with u_g

From this feedback response, the system response parameters are obtained and the process parameters calculated using (7.4) and (7.5) from Chapter 7. The controller parameters are calculated as described using (8.20) and (8.19). The process and the designed controller parameters are summarised in Table 8.6.

Table 8.6: Process and controller parameters

	Process parameters		Controller parameters	
Valve opening (%)	τ	k_p(barg)	K_c(barg^{-1})	$\tau_I(s)$
30%	20.2	2.5	0.32	22

The controller parameters are then implemented on the industrial riser system in OLGA, using the OLGA-Matlab link structure (see section 5.5.1). The simulation result obtained by implementing the controller is shown in Figure 8.8.

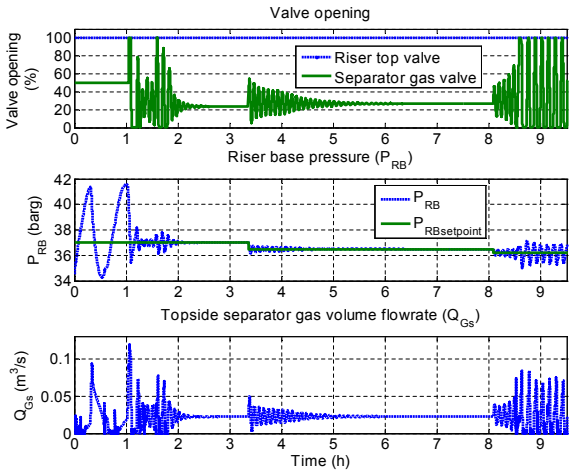

Figure 8.8: Simulation result for P_{RB} control with u_g

From this result, it is observed that the controller stabilised the system at maximum closed-loop operating point of 26.8%, corresponding to the P_{RB} of 36.5%. Below this pressure, the system will become unstable. The settling time of the closed-loop response is about 1 hour when the controller is switched on after 1 hour of the simulation time. The accumulated liquid for a 24 hour simulation is 328 m^3/day.

Next, the improved relay auto-tune controller design method is applied on the system. From the process parameters of the nominal plant shown in Table 8.6, the nominal FOPDT process is defined as

$$G_0(s) = \frac{2.5e^{-14.3s}}{20.2s - 1} \tag{8.31}$$

By determining the set of possible errors for the set of the uncertain τ, similar to that discussed in section 8.4.1 and 8.4.2, the perturbed plant parameters

given in Table 8.7, is obtained. The controller parameters k_c and τ_I which are calculated using (8.19) and (8.20) are also presented in Table 8.7.

Table 8.7: Process and the PI controller parameters

	Perturbed process parameters					Controller parameters	
Valve opening (%)	τ	k_p(barg)	r_∞	r_0	τ_0	k_c(barg^{-1})	τ_I (s)
30	20.2	2.5	8	0.008	20	2.1	150

The designed PI controller parameters are implemented on the system in the OLGA software and the simulation result obtained is shown in Figure 8.9.

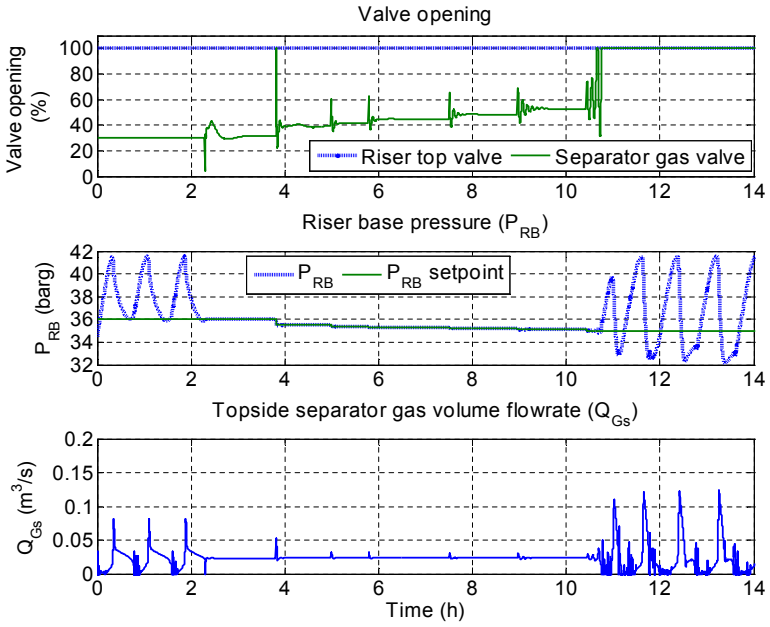

Figure 8.9: Improved relay controller simulation result for P_{RB} control with u_g

This simulation shows that the improved relay auto-tuned controller achieved closed-loop stability at a valve opening of u_g =53%. This corresponds to a P_{RB}=35.1 barg and the accumulated liquid is equal to 339 m^3/day. Thus, with

the improved controller, a 3.4% increase in production is achieved, when compared with to the production achieved previously. This result clearly shows a significant improvement when compared to the performance of the original relay tuning method.

8.6 Conclusions

In this chapter, the development, implementation and the performance analysis of an improved relay auto-tuned slug controller algorithm has been presented. The developed controller algorithm is based on a perturbed FOPDT model of the riser system, obtained through relay shape factor analysis.

The developed controller algorithm is implemented on the industrial riser system, for PRB control using the riser top valve and the topside separator gas valve as the manipulated variable. The controller is also implemented for Q_T control using the riser top valve as the manipulated variable on the industrial riser model.

The performance of the improved relay auto-tuned controller showed that the controllers has the ability to stabilise the unstable riser system at a valve opening that is larger than that achieved with the original (conventional) design algorithm implemented in Chapter 7. About 4% increase in production is achieved with the improved controller algorithm presented in this chapter, when compared to the the conventional design algorithm implemented in Chapter 7.

Chapter 9

Conclusions and further work

9.1 Conclusion

The conclusions from the work presented in this thesis are presented in this section. This thesis has presented a comprehensive approach to severe slugging control with focus on achieving stable operation and maximising production. The body of the thesis contains seven chapters and the conclusions are drawn from the last six chapters.

A review of the severe slug control techniques, including their applications, limitations and challenges was presented in Chapter 2. Various forms of severe slug control techniques including modifying internal pipeline diameter, riser base gas injection, pipeline gas re-injection and manual and active choking of the riser top vales were discussed. The dearth of sufficient information on the performance of existing slug control systems is identified as a challenge to deciding the direction for their further development. Also the conflicting report on the performance of similar techniques exposed the gap in the available knowledge of severe slug control. Extensive amount of work is still required in order to gain sufficient knowledge and understanding of severe slugging control.

The development of the plant-wide model for severe slug control is achieved with an improved simplified riser model (ISRM) developed to eliminate some assumptions and limitations of the simplified riser model (SRM) in predicting severe slugging. The model of the two phase separator system and the pressure dependent well model is developed and linked to the ISRM. Simulation results from the ISRM shows that it predicts severe slug characteristics, such as pressure amplitude and slug frequency more closely to the experimental result than the SRM. Also, the ability to predict severe slugging characteristics with changing inlet flow condition which is not possible with the SRM is achieved with the ISRM. Improved performance is also achieved with the ISRM in the prediction of the slug production stage in the severe slug cycle, when compared to the SRM, against the experimental results. The ability of the ISRM to predict relevant nonlinear stability is investigated using an industrial riser system and a 4 inch laboratory riser system. Its prediction of these nonlinear stabilities showed close agreement with experimental results.

The controllability analysis of the unstable riser-pipeline system for stability and production was presented in Chapter 4 to show that by implementing appropriate control strategy on the riser-pipeline system, both topside and subsea variables can be used for stabilising control of the riser pipeline system. The analysis of the input magnitude required to stabilise the unstable system at the open-loop unstable valve openings is achieved by evaluating the lower bound on the transfer function KS. The controllability analysis of an industrial riser system using the riser top valve, u, as the manipulated variable showed that all three controlled variables, namely the P_{RB}, the P_{RT} and the Q_T has the ability to stabilise the system. However, the controllability analysis showed that generally, the P_{RB} and the Q_T has the ability to stabilise the riser system at a larger valve opening than the P_{RT}. Also the controllability analysis of the system using the topside separator gas outlet valve, u_g, as the manipulated variable showed

that all four variables namely, the P_{RB}, the P_s, the P_{RT} and the Q_{Gouts} has the ability to stabilise the system. However, it is shown that generally, the P_{RB} and the Q_{Gouts} has the ability to stabilise the riser system at a larger valve opening than the P_s. The difference in their ability to stabilise the system at large valve opening also revealed their corresponding ability maximise production. The controllability analysis also showed through simulation that the P_{RT} which was previously considered to be unsuitable for slug control, and the Q_T which is considered to be suitable if it is used in the inner feedback loop in a cascade control, can be used for slug control if perfect set point tracking of controlled variable is neglected in the system such that a derivative controller is applied to stabilise the system at a reference valve opening, with the controller input equal to the measured value of the controlled variable.

A new concept known as the Production Gain Index (PGI) analysis was introduced in Chapter 5 for systematic analysis of the production potential of a severe slug control system. The application of the PGI analysis employed a systematic analysis of the pressure and production relationship in a riser-pipeline system, using a bifurcation map. The PGI is introduced as the ratio of the production gain, $J_p(u) - J_p(u_c)$ against the pressure dependent production at steady state $J_p(u_c)$. By applying the PGI analysis on an unstable rise-pipeline system, suitable operating point(s) for maximising production with or without a slug controller is predicted. Thus, the PGI analysis reveals the potential of a feedback control system to maximise production in a riser-pipeline system. The ZPGI contours which is defined as $\xi(u, u_c) = 0$, divides the (u, u_c) plane into two areas; the positive PGI (PPGI) area which is located above the ZPGI line and the negative PGI (NPGI) area which is located below the ZPGI line. Operating point on the ZPGI line defined by (u, u_c) indicates the valve openings where the production with a slug controller at u_c will be equal to production without a slug controller (unstable system) at u. In applying a feedback control, any

operating point, (u, u_c), located above the ZPGI line corresponds to production gain operating point known as the PPGI, while any operating point located below the ZPGI line corresponds to a production loss operating point, known as the NPGI. The implementation of the PGI analysis on an industrial riser system shows that the prediction of the PGI analysis agrees with the actual simulated production.

The design of three active slug controllers was presented in Chapter 6 to show that the $\|T\|_\infty$ can be used to characterise the slug controllers' ability to achieve closed loop stability at larger valve opening. The three active slug controllers include the relay auto-tuned controller, the robust PID controller and the H_∞ robust controller. A slug controller which achieved a low value of the $\|T\|_\infty$, will achieve closed loop stability at a larger valve opening than a slug controller with high $\|T\|_\infty$. The evaluation of the $\|T\|_\infty$ of these three active slug controllers revealed that the H_∞ robust controller has the least value of the $\|T\|_\infty$ followed by the robust PID controller, while the relay auto-tuned controller has the maximum value for the two controlled variables considered, namely: the P_{RB} and the Q_T. Simulation results obtained from the two controlled variables using an industrial riser system in OLGA confirmed that the H_∞ robust controller achieved closed loop stability at the maximum valve opening, while the relay tuned controller achieved closed loop stability at the minimum valve opening. The difference in the maximum closed loop stable operating point achieved by each controller also reflected in the liquid production achieved, with the H_∞ robust controller achieving the maximum production among the three controllers.

A new improved relay auto-tuned PI controller algorithm was developed and implemented in Chapter 7 to improve the performance of the relay tuned slug controller. The developed controller algorithm is based on a perturbed FOPDT model of the riser system, obtained through relay shape factor analysis. The

developed controller algorithm is implemented for severe slug control on an industrial riser system. Its performance indicates that it has the ability to stabilise the unstable riser system at a valve opening that is larger than that achieved with the original (conventional) controller algorithm applied, with about 4% increase in production achieved.

9.2 Future work

This work has presented a comprehensive analysis of the systematic approach to achieving stability and maximising production from an unstable riser-pipeline system. However, there are still a number of issues which are necessary for further work, in order to achieve further improvement on this subject.

Currently, the plant-wide model is developed only for severe slugging prediction. Considering its simplified approach, the model can be extended to predict other forms of slugging such as the hydrodynamic slugging. Also, the model can be improved further with focus on modelling the pipeline geometry more accurately so as to account for the pipeline pressure losses in the model. This can improve the ability of the model to represent the real system more accurately, and could improve the performance of the slug controller designed for slug control using the model.

Since the current plant-wide model can only simulate two phase oil-gas or water-gas flow, the model can also be further developed to be able to simulate three phase oil-water-gas flow. Also, the well model can be extended to include the nonlinear model

The PGI concept can be further applied on larger and more complex industrial riser systems under relevant ideal conditions. This will be relevant to improving the concept and its understanding, and advancing it for industrial application.

The ability of the controlled variables, such as the P_{RT} and P_s to stabilise the system at larger valve opening can be further improved. There may exist some control structures or variable combination which could improve the ability of these variables to stabilise the system at larger valve openings.

The effectiveness of other control design and analysis methods such as structured singular value and μ-analysis in slug control can be investigated.

The transfer of the knowledge gained in this research for industrial application can be achieved through the knowledge transfer partnership program.

Appendix A

Simplified riser model (SRM) equations

The equations of the SRM are presented in this Appendix.

A.1 Conservation equations

Based on the riser-pipeline diagram shown in Figure 4.1, the SRM was developed with three dynamical states, which account for the:

1. mass of gas in the pipeline, m_{G1}
2. mass of gas at the riser top, m_{G2}
3. mass of liquid in the riser, m_L

The corresponding conservation equations are given in (A.1), (A.2) and (A.3).

$$\frac{dm_{G1}}{dt} = m_{Gin} - m_G \tag{A.1}$$

$$\frac{dm_{G2}}{dt} = m_G - m_{Gout} \tag{A.2}$$

$$\frac{dm_L}{dt} = m_{Lin} - m_{Lout} \tag{A.3}$$

A.2 State dependent variables

The riser base pressure, P_{RB}, and the riser top pressure, P_{RT}, are state dependent variables and are given in (A.4) and (A.5) respectively, where M_G is the gas molecular weight, R is the gas constant and T is the system temperature.

$$P_{RB} = \frac{m_{G1}RT}{V_{G1}M_G} \tag{A.4}$$

$$P_{RT} = \frac{m_{G2}RT}{V_{G2}M_G} \tag{A.5}$$

In (A.4), the volume of gas in the pipeline, V_{G1}, is assumed to be constant and the volume of gas at the riser top, V_{G2}, is calculated using (A.6),

$$V_{G2} = V_T - V_{LR} \tag{A.6}$$

where V_T is the total riser volume and V_{LR} is the liquid volume in the riser.

If $h_1 \geq H_1$, then the gas mass flow rate into the riser is equal to zero, $m_G = 0$, and severe slugging is initiated. If $h_1 < H_1$, then the gas mass flow rate into the riser is given by:

$$m_G = v_{G1}\rho_{G1}A \tag{A.7}$$

where v_{G1} is the gas velocity given by (A.8), and the gas density, ρ_{G1}, is given by (A.9).

$$v_{G1} = K_2\frac{H_1 - h_1}{H_1}\sqrt{\frac{P_{RB} - P_{RT} - \rho_L g\alpha_L H_R}{\rho_{G1}}} \tag{A.8}$$

$$\rho_{G1} = \frac{m_{G1}}{V_{G1}} \tag{A.9}$$

In (A.8), α_L is the liquid volume fraction in the riser, H_R is the riser height, K_2 is the gas flow constant, $\frac{H_1-h_1}{H_1}$ is the relative gas flow opening, which depends relatively on the liquid level. In (A.9), V_{G1} is assumed to be constant.

A.3 Fluid flow equations

The fluid flow rate across the riser top valve (flow out of the riser) is derived as shown in (A.10),

$$m_{mix} = K_1 u\sqrt{\frac{\rho_T(P_{RT} - P_s)}{g}} \tag{A.10}$$

where the separator pressure, P_s, is assumed to be constant, u is the valve opening, K_1 is the valve coefficient and ρ_T is the total fluid density is given by (A.11).

$$\rho_T = \alpha_{LT}\rho_L + (1 + \alpha_{LT})\rho_{G2} \tag{A.11}$$

The gas mass flow rate out of the riser is given by (A.12), while the liquid mass flow rate out of the riser is given by (A.13), where α_L^m is the liquid mass fraction.

$$m_{Gout} = (1 - \alpha_L^m) m_{mix} \tag{A.12}$$

$$m_{Lout} = \alpha_L^m m_{mix} \tag{A.13}$$

A.4 Entrainment equation

The entrainment equation is developed to model the distribution of fluid in the riser. This is achieved by modeling the volume fraction of the liquid that is exiting the riser top, α_{LT}. The total liquid fraction reaching the riser top, α_{LT}, is therefore modeled as given by (A.14).

$$\begin{aligned} \alpha_{LT} = (V_{LR} > H_R A_p)[\frac{V_{LR} - H_R A_p}{A_p L_h}], \\ + \frac{w^n}{1 + w^n}[\alpha_L - (V_{LR} + > H_R A_p)(\frac{V_{LR} - H_R A_p}{A_p L_h})] \end{aligned} \tag{A.14}$$

where w is the flow transition parameter which is given by (A.15), A_p is the pipe cross sectional area and L_h is the lenght of the riser top horizontal part.

$$w = \frac{K_3 \rho_{G1} v_{G1}^2}{\rho_L - \rho_{G1}} \tag{A.15}$$

Appendix B

Nonlinear functions for evaluating system linear transfer functions

B.1 Nonlinear functions for the P_{RB} with u

Equations (B.1) to (B.4) give the nonlinear functions of the transfer function coefficients against the valve opening for the P_{RB} as the controlled variable. By evaluating these functions, the linear model transfer function of the system will be defined at any unstable the steady state valve openings.

$$f_1(u_e) = -0.0491u_e^4 + 0.1365u_e^3 - 0.1303u_e^2 + 0.0393u_e - 0.004 \tag{B.1}$$

$$f_0(u_e) = 3 \times 10^{-5}u_e^2 + 5 \times 10^{-6}u_e - 6 \times 10^{-7} \tag{B.2}$$

$$g_1(u_e) = -0.1371u_e^4 + 0.3107u_e^3 - 0.2101u_e^2 + 0.023u_e + 0.034 \tag{B.3}$$

$$g_0(u_e) == -0.0206u_e^6+0.0733u_e^5-0.105u_e^4+0.0774u_e^3-0.0309u_e^2+0.0063u_e-0.0005 \tag{B.4}$$

B.2 Nonlinear functions for the P_{RT} with u

Equations (B.5) to (B.8) give the nonlinear functions of the transfer function coefficients against the valve opening for the P_{RT} as the controlled variable. By evaluating these functions, the linear model transfer function of the system will be defined at any unstable the steady state valve openings.

$$f_1(u_e) = -0.0491u_e^4 + 0.1365u_e^3 - 0.1303u_e^2 + 0.0393u_e - 0.004 \tag{B.5}$$

$$f_0(u_e) = 3 \times 10^{-5}u_e^2 + 5 \times 10^{-6}u_e - 6 \times 10^{-7} \tag{B.6}$$

$$g_1(u_e) = 8.7583u_e^6 - 30.837u_e^5 + 43.13u_e^4 - 30.537u_e^3 + 11.481u_e^2 - 2.148u_e + 0.1203 \tag{B.7}$$

$$g_0(u_e) == -0.0146u_e^6+0.0523u_e^5-0.0756u_e^4+0.0563u_e^3-0.0228u_e^2+0.0048u_e-0.0003 \tag{B.8}$$

B.3 Nonlinear functions for the Q_T with u

Equations (B.9) to (B.13) give the nonlinear functions of the transfer function coefficients against the valve opening for the Q_T as the controlled variable. By evaluating these functions, the linear model transfer function of the system will be defined at any unstable the steady state valve openings.

$$f_1(u_e) = -0.0491u_e^4 + 0.1365u_e^3 - 0.1303u_e^2 + 0.0393u_e - 0.004 \tag{B.9}$$

$$f_0(u_e) = 3 \times 10^{-5}u_e^2 + 5 \times 10^{-6}u_e - 6 \times 10^{-7} \tag{B.10}$$

$$g_2(u_e) = -0.454u_e^4 + 1.123u_e^3 - 0.8458u_e^2 + 0.138u_e - 0.122 \tag{B.11}$$

$$g_1(u_e) = -0.0038u_e^4 + 0.0102u_e^3 - 0.0093u_e^2 + 0.0035u_e - 0.0002 \tag{B.12}$$

$$g_0(u_e) = -1 \times 10^{-6}u_e^4 + 3 \times 10^{-6}u_e^3 - 3 \times 10^{-6}u_e^2 + 1 \times 10^{-6}u_e - 1 \times 10^{-7} \tag{B.13}$$

B.4 Nonlinear functions for the P_{RB} with u_g

Equation B.14 to B.17 gives the nonlinear functions which define the coefficients of the open loop transfer function for each operating point for the P_{RB}.

By evaluating these functions, the linear model transfer function of the system will be defined at any unstable the steady state valve openings.

$$f_1(u_{ge}) = 1.5415u_{ge}^5 - 5.0628u_{ge}^4 + 6.3911u_{ge}^3 - 3.8341u_{ge}^2 + 1.0633u_{ge} - 0.1094 \quad \text{(B.14)}$$

$$f_0(u_{ge}) = 8 \times 10^{-5}u_{ge}^3 - 0.0002u_{ge}^2 + 0.0002u_{ge} - 1 \times 10^{-5} \quad \text{(B.15)}$$

$$g_1(u_{ge}) = 0.0003u_{ge}^3 - 0.0011u_{ge}^2 + 0.0013u_{ge} - 0.0005 \quad \text{(B.16)}$$

$$g_0(u_{ge}) = -3\times10^{-15}u_{ge}^5 + 2\times10^{-14}u_{ge}^4 - 4\times10^{-14}u_{ge}^3 + 3\times10^{-14}u_{ge}^2 - 1\times10^{-14}u_{ge} + 2\times10^{-15} \quad \text{(B.17)}$$

B.5 Nonlinear functions for the P_s with u_g

Equation B.18 to B.21 gives the nonlinear functions which define the coefficients of the open loop transfer function for each operating point for the P_s. By evaluating these functions, the linear model transfer function of the system will be defined at any unstable the steady state valve openings.

$$f_1(u_{ge}) = 1.5415u_{ge}^5 - 5.0628u_{ge}^4 + 6.3911u_{ge}^3 - 3.8341u_{ge}^2 + 1.0633u_{ge} - 0.1094 \quad \text{(B.18)}$$

$$f_0(u_{ge}) = 8 \times 10^{-5} u_{ge}^3 - 0.0002 u_{ge}^2 + 0.0002 u_{ge} - 1 \times 10^{-5} \quad \text{(B.19)}$$

$$g_1(u_{ge}) = -0.8562 u_{ge}^4 + 2.7509 u_{ge}^3 - 3.3051 u_{ge}^2 + 1.7697 u_{ge} \quad \text{(B.20)}$$

$$g_0(u_{ge}) = 0.0012 u_{ge}^4 - 0.0041 u_{ge}^3 + 0.0052 u_{ge}^2 - 0.0029 u_{ge} + 0.0006 \quad \text{(B.21)}$$

B.6 Nonlinear functions for the P_{RT} with u_g

Equation B.22 to B.25 gives the nonlinear functions which define the coefficients of the open loop transfer function for each operating point for the P_{RT}. By evaluating these functions, the linear model transfer function of the system will be defined at any unstable the steady state valve openings.

$$f_1(u_{ge}) = 1.5415 u_{ge}^5 - 5.0628 u_{ge}^4 + 6.3911 u_{ge}^3 - 3.8341 u_{ge}^2 + 1.0633 u_{ge} - 0.1094 \quad \text{(B.22)}$$

$$f_0(u_{ge}) = 8 \times 10^{-5} u_{ge}^3 - 0.0002 u_{ge}^2 + 0.0002 u_{ge} - 1 \times 10^{-5} \quad \text{(B.23)}$$

$$g_1(u_{ge}) = 0.4505 u_{ge}^3 - 1.1103 u_{ge}^2 + 0.9234 u_{ge} - 0.2678 \quad \text{(B.24)}$$

$$g_0(u_{ge}) = -0.0013 u_{ge}^4 + 0.0024 u_{ge}^3 - 0.0004 u_{ge}^2 - 0.0012 u_{ge} + 0.0006 \quad \text{(B.25)}$$

B.7 Nonlinear functions for the Q_{Gsep} with u_g

Equation B.26 to B.29 gives the nonlinear functions which define the coefficients of the open loop transfer function for each operating point for the Q_{Gsep}. By evaluating these functions, the linear model transfer function of the system will be defined at any unstable the steady state valve openings.

$$f_1(u_{ge}) = 1.5415u_{ge}^5 - 5.0628u_{ge}^4 + 6.3911u_{ge}^3 - 3.8341u_{ge}^2 + 1.0633u_{ge} - 0.1094 \quad \text{(B.26)}$$

$$f_0(u_{ge}) = 8 \times 10^{-5}u_{ge}^3 - 0.0002u_{ge}^2 + 0.0002u_{ge} - 1 \times 10^{-5} \quad \text{(B.27)}$$

$$g_1(u_{ge}) = -0.2366x3 + 0.6218x2 - 0.5445x + 0.147 \quad \text{(B.28)}$$

$$g_0(u_{ge}) = 0.0049u_{ge}^5 - 0.0175u_{ge}^4 + 0.0242u_{ge}^3 - 0.0165u_{ge}^2 + 0.0055u_{ge} - 0.0006 \quad \text{(B.29)}$$

References

[1] AL-KANDARI, A. H., AND KOLESHWAR, V. S. Overcoming slugging problems in a long-distance multiphase crude pipeline. In *Procedings SPE Annual Technical Conference and Exhibition, Paper SPE 56460* (3-6 October 1999).

[2] AL-SHEIKH, J., SAUNDERS, D., AND BRODKEY, R. Prediction of flow patterns in horizontal two-phase pipe flow. *Can. J. of Chemical Engineering 48* (1970), 21–29.

[3] ALVAREZ, C. J., AND AL-MALKI, S. S. Using gas injection for reducing pressure losses in multiphase pipelines. In *Procedings SPE Annual Technical Conference and Exhibition, Paper SPE 84503* (5-8 October 2003).

[4] ÅSTRÖM, K. J., AND HAGGLUND, T. Automatic tuning of simple regulators with specifications on phase and amplitude margins. *Automatica 20* (1984), 645–651.

[5] BAKER, O. Simultaneous flow of oil and gas. *Oil and Gas Journal 54* (1954), 185–195.

[6] BALINO, J., BURR, K., AND NEMOTO, R. Modeling and simulation of severe slugging in airwater pipelineriser systems. *Int. J. of Multiphase Flow 36* (2010), 643–660.

[7] BARBUTO, F., AND CAETANO, E. On the occurrence of severe slugging phenomenon in pargeo-1 platform, campos basin, offshore brazil. *Proceedings 5th International Conference on Multiphase Production, BHRg* (1991), 491–503.

[8] BEGGS, H., AND BRILL, J. A study of two phase flow in inclined pipes. *J. of Petroleum. Technology 25* (1973), 607–617.

[9] BENDIKSEN, K., MALNES, D., AND NULAND, R. M. S. The dynamic two-fluid model olga: Theory and application. *SPE Prod. Eng. 6* (1991), 171–180.

[10] BØE, A. Severe slugging characteristics, part i, flow regime for severe slugging. *Presented at Special Topics in Two-Phase Flow, Trondheim, Norway* (1981).

[11] BONNACAZE, R., ERSKINE, W., AND GRESKOVICH, E. Holdup and pressure drop for two-phase slug flow in inclined pipelines. *AIChE J. 17* (1971), 1109–1113.

[12] BOYD, S., GHAOUI, L. E., FREON, E., AND BALAKRISHNAM, V. Linear matrix inequalities in system and control theory. *Society for Industrial and Applied Mathematics, 3600 University City Science Center, Philadelphia, Pennsylvania USA* (1994).

[13] BRENNEN, C. *Fundamentals of Multiphase Flows*, 1st edition ed. Cambridge University Press, UK, 2005.

[14] BROWN, M. From chaos to calm. Frontier, www.bp.com/liveassets/bp_internet/globalbp/globalbp_uk_english/reports_and_publications/frontiers/STAGING/local_assets/pdf/bpf24_06-10_slugging.pdf, December 2010.

[15] CAO, Y., YEUNG, H., AND LAO, L. Inferential slug control system. Report Report No. 09/YC/533, Cranfield University, Cranfield UK, Department of Offshore, Process and Energy Engineering, Cranfield University, Cranfield UK, 2009.

[16] CORNELIUSSEN, S., COUPUT, J.-P., DAHL, E., DYKESTEEN, E., FROYSA, K.-E., MALDE, E., MOESTUE, H., MOKSNES, P., SCHEERS, L., AND TUNHEIM, H. Handbook of multiphase flow metering. Technical report, Norwegian Society for Oil and Gas Measurement, The Norwegian Society of Chartered Technical and Scientific Professionals, Solli, OSLO, March, 2004.

[17] COSTIGAN, G., AND WHALLEY, P. Slug flow regime identification from dynamic void fraction measurement in vertical air-water flows. *Int. J. Multiphase Flow 23*, 2 (1997), 263–283.

[18] COURBOT, A. Prevention of severe slugging in the dunbar 16" multiphase pipeline. *OTC 8196, Offshore Technology Conference* (1986), 445–452.

[19] COUSINS, A. R., AND JOHAL, K. S. Multi-purpose riser. *European Patent, No. 00300126.0, Mentor subsea technology services Inc., Houston Texas* (2002).

[20] DAHLIN, E. B. Designing and tuning digital controllers. *Instruments and Control Systems 41*, 77 (June, 1968).

[21] DOYLE, J. C. Synthesis of robust controllers and filters. In *IEEE Conf. on Decision and control* (San Antonio, Texas, 1983), pp. 109–114.

[22] DOYLE, J. C. Advances in multivariable control. *Lecture notes, ONR/Honeywell Workshop, Minneapolis, USA* (October, 1984).

[23] DRENGSTIG, T., AND MAGNDAL, S. Slug control of production pipeline. Tech. Rep. N-4091, Stavanger University College, School of Science and Technology, Ullandhaug, 2001.

[24] DURET, E., AND TRAN, Q. Gas injection controlling liquid slugs in pipeline riser. *UK Patent, No: 02062826* (2002).

[25] ESPEDAL, M., AND BENDIKSEN, K. Onset of instabilities and slugging in horizontal and near-horizontal gas liquid flow. *European Two-Phase Flow Group Meeting, Paris Paper G4* (May 1989), 1–30.

[26] FABRE, J., PERESSON, L., ODELLO, R., AND ROMANET, T. Severe slugging in pipeline/riser systems. *SPE 16846, Presented at Society of Petroleum Engineers Annual Technical Conference 19* (1987), 113–129.

[27] FAN, Z., LUSSEYRAN, F., AND HARRANTY, T. Initiation of slugs in horizontal gas-liquid flows. *AICHE J. 39* (1993), 1741–1753.

[28] FAN, Z., RUDER, Z., AND HARRANTY, T. Pressure profile for slugs in horizontal pipes. *Int. J. Multiphase Flow 19* (1993), 421–437.

[29] FARGHARLY, M. A. Study of severe slugging in real offshore pipeline riser-pipe system. In *Procedings SPE Middle East Oil Show, Paper SPE 15726* (7-10 March 1997).

[30] FUCHS, P. The pressure limit for terrain slugging. *Proceedings 3rd International Conference on Multiphase Production, BHRg* (1987), 65–71.

[31] GLOVER, K. Robust stabilization of linear multivariable systems: relations to approximation. *Int. J. of Control 43*, 3 (1986), 741–766.

[32] GODHAVN, J. M., MEHRDAD, P. F., AND PER, H. F. New slug control strategy, tuning rules and experimental results. *Journal of Process Control 15*, 5 (2005), 547–557.

[33] GOLDZBERG, V., AND MCKEE, F. Model predicts liquid accumulation, severe terrain-induced slugging for two phase lines. *Oil and Gas Journal 19* (August 1987), 105–109.

[34] GOULD, T., TEK, M., AND KATZ, D. Two-phase flow through vertical, inclined or curved pipes. *J. of Petroleum. Technology 26* (1974), 915–926.

[35] GOVIER, G., AND OMER, M. The horizontal pipeline flow of air-water mixtures. *Can. J. of Chemical Engineering 40* (1962), 93–104.

[36] GRESKOVICH, E. Holdup prediction for stratified downflow of gas-liquid mixtures. *Ind. Engng Chem., Process Design Development 11* (1972), 81–85.

[37] GROUP, S. P. T. Engineering and operation of production system. *www.sptgroup.com/upload/documents/Brochures/olga5_dec07.pdf* (April, 2010).

[38] GUET, S., AND OOMS, G. Fluid mechanical aspects of the gas-lift technique. *Annual Review of Fluid Mechanics 38*, 1 (2006), 225–249.

[39] HASSANEIN, T., AND FAIRHURST, P. Challenges in the mechanical and hydraulic aspects of riser design for deep water developments. In *Procedings IBC UK Conf. Ltd. Offshore Pipeline Technology Conference* (29 September - 2 October 1998).

[40] HAVRE, K., AND DALSMO, M. Active feedback control as a solution to severe slugging. In *Procedings SPE Annual Technical Conference and Exhibition, Paper SPE 79252* (2002).

[41] HAVRE, K., STORNES, K., AND STRAY, H. Taming slug flow in pipelines. Tech. rep., ABB, 2002.

[42] HENRIOT, V., COURBOT, A., HEINTZ, E., AND MOYEUX, L. Simulation of process to control severe slugging: application to the dunbar pipeline. In *Procedings SPE Annual Technical Conference and Exhibition, Paper SPE 56461* (3-6, October 1999).

[43] HILL, T. Multiphase flow field trials on bp's magnus platform. *Journal of Energy Resources Technology 109* (1987), 142–147.

[44] HILL, T., AND WOOD, D. Slug flow: Occurrence, consequences, and prediction. In *Procedings SPE Annual Technical Conference and Exhibition, Paper SPE 27960* (1994).

[45] HOOGENDOORN, C. Gas liquid flow in horizontal pipes. *Chemical Enginnering Science 9* (1959), 205–217.

[46] ISHII, M., AND MISHIMA, K. Two-fluid model and hydrodynamic constitutive relations. *Nucl. Eng. Des.* (1984), 107–126.

[47] ISSA, R., AND KEMPF, M. Simulation of slug flow in horizontal and nearly horizontal pipes with the two-fluid model. *Int. J. Multiphase Flow 29*, 1 (2003), 69–95.

[48] ISSA, R., AND WOODBURN, P. Numerical prediction of instabilities and slug formation in horizontal two-phase flows. *3rd International Conference on Multiphase Flow, ICMF98, Lyon, France* (1998).

[49] JAMAL, H. A., ALI, S. M. F., AND ISLAM, M. R. *Petroleum Reservior Simulation, A Basic Approach*, 1st edition ed. Gulf Publishing Company, Houston TX USA, 2006.

[50] JANSEN, F. E., AND O., S. Method of eliminating pipeline-riser flow instability. In *Procedings SPE Western Regional Meeting, Paper SPE 27867* (23-25, March 1994).

[51] JANSEN, F. E., SHOHAM, O., AND TAITEL, Y. The elimination of severe slugging - experiments and modeling. *Int. J. of Multiphase Flow 22*, 6 (1996), 1055–1071.

[52] JAYANTI, S., AND HEWITT, G. Prediction of the slug-to-churn flow transition in vertical two-phase flow. *Int. J. Multiphase Flow 18*, 6 (1992), 847–860.

[53] KADRI, U., ZOETEWEIJ, M., MUDDE, R., AND OLIEMANS, R. A growth model for dynamic slugs in gasliquid horizontal pipes. *Int. J. Multiphase Flow 35* (2009), 439–449.

[54] KALMAN, R. E. On the general theory of control systems. *Proc. 1st International Congress on Automatic Control 1* (1961), 481–492.

[55] KALMAN, R. E., HO, Y., AND NARENDRA, K. Controllability of linear dynamic systems. *Contrib. Differential Equations 1* (1962), 189–213.

[56] KORDYBAN, E., AND RANOV, T. Mechanism of slug formation in horizontal two-phase flow. *J. Bas. Engineering 92* (1970), 857–864.

[57] KOVALEV, K., CRUICKSHANK, A., AND PURVIS, J. The slug suppression system in operation. In *Procedings SPE Annual Technical Conference and Exhibition, Paper SPE 84947* (2003).

[58] KOVALEV, K., SEELEN, M., AND HAANDRIKMAN, G. Vessel-less s3: Advanced solution to slugging pipelines. In *Procedings SPE Annual Technical Conference and Exhibition, Paper SPE 88569* (2004).

[59] LARSEN, M., AND HEDNE, P. Three phase slug tracking with petra. *Proceedings 2nd North American Conference on Multiphase Production, BHRg* (2000), 170–192.

[60] LIN, P., AND HANRATTY, T. Prediction of the initiation of slug with linear stability theory. *Int. J. Multiphase Flow 12* (2003), 79–98.

[61] LINE, A., AND LOPEZ, D. Two-fluid model of wavy seperated two-phase flow. *Int. J. Multiphase Flow 23*, 6 (1997), 1131–1146.

[62] LIOMBAS, J., PARAS, S., AND KARABELAS, A. Co-current stratified gasliquid downflowinfluence of the liquid flow field on interfacial structure. *Int. J. Multiphase Flow 31*, 8 (2005), 869–896.

[63] MAKOGAN, T. Y., AND BROOK, G. J. Device for controlling slugging, world intellectual property organization, 2007/034142 a1, 2007.

[64] MANDHANE, J., GREGORY, G., AND AZIZ, K. A flow pattern map for gas-liquid flow in horizontal pipes. *Int. J. Multiphase Flow 1* (1974), 537–553.

[65] MARTIN, J. J., CORRIPIO, A. B., AND SMITH, C. How to select controller modes and tuning parameters from simple process models. *ISA Transactions 15*, 4 (1976), 314–319.

[66] MCQUILLAN1984, K., AND WHALLEY, P. Flow patterns in vertical two-phase flow. *Int. J. Multiphase Flow 11*, 2 (1985), 161–175.

[67] MENG, W., AND ZHANG, J. J. Modeling and mitigation of severe riser slugging: a case study. In *Procedings SPE Annual Technical Conference and Exhibition, Paper SPE 71564* (30 September - 3 October 2001).

[68] MISHIMA, K., AND ISHII, I. Flow regime transition criteria for two-phase flow in vertical pipes. *Int. J. Heat Mass Transfer 27*, 5 (1984), 723–737.

[69] MOE, J., LINGELEM, M., HOLM, H., AND OLDERVIK, O. Severe slugging in offshore gas-condensate flowline-riser systems. *Proceedings 4th*

International Conference on Multiphase Production, BHRg (1989), 527–560.

[70] MOKHATAB, S., AND TOWLER, B. Severe slugging in flexible risers: Review of experimental investigations and olga predictions. *Petroleum Science and Technology 25*, 7 (2007), 867–880.

[71] MOLYNEUX, P. D., AND KINVIG, J. P. Method of eliminating severe slugging in a riser of a pipeline includes measuring pipeline pressure and operating a valve. *UK Patent No. 0013331.4., 2000* (2000).

[72] MONTGOMERY, J. Severe slugging and unstable flows in an s-shaped riser. Ph.d thesis, Cranfield University, Cranfield University, Befordshire, England, 2002.

[73] MUKHERJEE, H., AND BRILL, J. Emprical equations to predict flow pattern in two-phase inclined flow. *Int. J. Multiphase Flow 11*, 3 (1985), 299–315.

[74] OGATA, K. *Mordern Control Engineering*, 4th int. edition ed. Prentice Hall, Upper Saddle River, New Jersey, 2002.

[75] OGAZI, A. I., CAO, Y., YEUNG, H., AND LAO, L. Robust control of severe slugging to maximising oil production. In *International Conference on System Engineering* (Conventry,UK, 2009), 2009 Conference.

[76] OGAZI, A. I., CAO, Y., YEUNG, H., AND LAO, L. Slug control with large valve opening to maximising oil production. In *SPE Offshore Europe Conference and Exhibition* (Aberdeen ,UK, 2009), Paper SPE 124883.

[77] OGAZI, A. I., OGUNKOLADE, S., CAO, Y., LAO, L., AND YEUNG, H. Severe slugging control through open loop unstable pid tuning to increase

oil production. In *14th International Conference on Multiphase Technology* (Cannes, France, June 2009), BHR Group, pp. 17 – 32.

[78] ORAM, P., AND CALVERT, P. Slug mitigation, world intellectual property organization, wo 2009/133343 a1, 21(3), 5 Nov. 2009.

[79] OZAWA, M., AND SAKAGUCHI, T. Note on modeling of transient slug flow in multiphase flow system. *Memoirs of the Faculty of Engineering, Kobe University 32* (1985), 25–44.

[80] PANDA, R. C., AND YU, C.-C. Shape factor of relay response curves and its use in autotuning. *Journal of Process Control 15* (2005), 893–906.

[81] PHILIPS, C. L., AND HARBOR, R. D. *Feedback Control Systems*, 4th edition ed. Prentice Hall International, Upper Saddle River, New Jersey, 1988.

[82] POTS, B., BROMILOW, I., AND KONIJN, M. Severe slug flow in offshore flowline/riser systems. *Society of Petroleum Engineers, Middle East Technical Conference and Exhibition* (March 1985), 347–356.

[83] POTS, B. F. M., BROMILOW, I. G., AND KONIJN, M. J. W. F. Severe slug flow in offshore flow-line/riser systems, spe-13723-pa. *SPE Prod. Eng. 2*, 4 (1987), 319–324.

[84] ROGER, D. B. Report, Department of Chemistry, The impact of declining major North Sea oil fields upon Norwegian and United Kingdom oil production, Northern Kentucky University, Highland Heights, KY 41099-1905, 2000.

[85] SARICA, C., AND SHOHAM, O. A simplified transient model for pipeline-riser systems. *Chemical Engineering Science 46*, 9 (1991), 2167–2179.

[86] SARICA, C., AND TENGESDAL, J. A new technique to eliminate severe slugging in pipeline/riser systems. *SPE 63185, SPE Annual Technical Conference and Exhibition, Dallas, TX* (2000), 633–641.

[87] SCHICHT, H. Flow patterns for an adiabatic two-phase flow of water and air within a horizontal tube. *Verfahrenstechnik 3*, 4 (1969), 153–161.

[88] SCHMIDT, Z., BRILL, J. P., AND BEGGS, H. D. Choking can eliminate severe pipeline slugging. *Oil and Gas Journal 12* (1979), 230–238.

[89] SCHMIDT, Z., BRILL, J. P., AND BEGGS, H. D. Experimental study of severe slugging in a two-phase-flow pipeline riser pipe system, spe-8306-pa. *SPE Journal 20*, 3 (1980), 407–414.

[90] SCHMIDT, Z., DOTY, D. R., AND DUTTA-ROY, K. Severe slugging in offshore pipeline riser pipe systems. *Society of Petroleum Engineers Journal* (1985), 27–38.

[91] SHARMA, Y., IHARA, M., AND MANABE, R. Simulating slug flow in hilly-terrain pipelines. In *SPE Offshore Europe Conference and Exhibition* (Villahermosa, Mexico, 10-12 Feb., 2002), Paper SPE 74359.

[92] SIDI, M. *Design of Robust Control Systems*, 1st edition ed. Krieger Publishing Company, Malabar, Florida, 2001.

[93] SINGH, G., AND GRIFFITH, P. Determination of the pressure drop and optimum pipe size for a two-phase slug flow in an inclined pipe. *TRASME, J. Engng Ind 92* (1970), 717–726.

[94] SKOGESTAD, S., AND POSTLETHWAITE, I. *Multivariable Feedback Control*, 2nd edition ed. John Wiley and Sons, UK, 2005.

[95] SMITH, C. A., AND CORRIPIO, A. B. *Principles and Pracice of Automatic Process Control*, 2nd edition ed. John Wiley and Sons, Inc, Canada, 1997.

[96] SPEDDING, P., WOODS, G., RAGHUNATHAN, R., AND WATTERSON, J. Vertical two-phase flow, part i: Flow regimes. *IChemE 76* (July, 1998), 612–629.

[97] STAPLEBERG, H. H., AND MEWES, D. The pressure loss and slug frequency of liquid-liquid-gas flow in horizontal pipes. *Int. J. of Multiphase Flow 20*, 2 (April, 1994), 285–303.

[98] STORKAAS, E. Stabilising control and controllability: control solutions to avoid slug flow in riser-pipeline systems. Thesis, Norwegian University of Science and Technology, Department of Chemical Engineering, Norwegian University of Science and Technology, 2005.

[99] STORKAAS, E., AND SKOGESTAD, S. Cascade control of unstable systems with application to stabilization of slug flow. *Technical report, Department of Chemical Engineering, Norwegian University of Science and Technology, Trondheim, Norway* (2004).

[100] STORKAAS, E., AND SKOGESTAD, S. Controllability analysis of two-phase pipeline-riser systems at riser slugging conditions. *Control Engineering Practice 15*, 5 (May, 2007), 567–581.

[101] STORKAAS, E., SKOGESTAD, S., AND ALSTAD, V. Stabilisation of desired flow regimes in pipelines. In *AIChE annual meeting* (Reno, Nevada, 2001), Paper 287d.

[102] STORKAAS, E., SKOGESTAD, S., AND GODHAVN, J. A low dimensional dynamic model of severe slugging for control design and analysis. Tech.

rep., Statoil ASA, R&D, Process Control, Arkitekt Ebells vei 10, Rotvoll, N-7005, Trondheim, Norway, 2005.

[103] TAITEL, Y. Stability of severe slugging. *Int. J. of Multiphase Flow 12*, 2 (1986), 203–217.

[104] TAITEL, Y., AND BARNEA, D. Two phase slug flow. *Advances in Heat Transfer, Academic Press* (1990), 83–132.

[105] TAITEL, Y., BARNEA, D., AND DUKLER, A. Modelling flow pattern transition for steady upward gas-liquid flow in vertical tubes. *AICHE J. 26* (1980), 345–354.

[106] TAITEL, Y., BARNEA, D., SHOHAM, O., AND DUKLER, A. E. Flow pattern transition for gas-liquid flow in horizontal and inclined pipes. *International Journal of Multiphase Flow 6* (1979), 217–225.

[107] TAITEL, Y., BARNEA, D., SHOHAM, O., AND DUKLER, A. E. Gas-liquid flow in inclined tubes: Flow patterns transitions for upward flow. *Chemical Engineering Science 40*, 1 (1985), 131–136.

[108] TAITEL, Y., AND DUKLER, A. A model for predicting flow regime transition in horinzontal and near horizontal gas-liquid flow. *AICHE J. 22* (1976), 47–55.

[109] TAITEL, Y., AND DUKLER, A. E. A model for frequency during gas-liquid flow in horizontal and near horizontal pipes. *Int. J. of Multiphase Flow 3*, 6 (December, 1977), 585–596.

[110] TENGESDAL, J. O., SARICA, C., AND THOMPSON, L. Severe slugging attenuation for deepwater multiphase pipeline and riser systems. In *Procedings SPE Annual Technical Conference and Exhibition, Paper SPE 87089* (29 September - 2 October 2002).

[111] THOMPSON, J. M. T., AND STEWART, H. B. *Nonlinear Dynamics and Chaos*, 1st edition ed. John Wiley and Sons Ltd, Chichester Great Britain, 1986.

[112] THYAGARAJAN, T., AND YU, C. C. Improved auto tuning using the shape factor from relay feedback. *Industrial and Engineering Chemistry Research 42*, 20 (February 2003), 4425–4440.

[113] UJANG, M. P., LAWRENCE, C. J., HALE, C. P., AND HEWITT, G. F. Slug initiation and evolution in two-phase horizontal flow. *Int. J. Multiphase Flow 32* (2006), 527–552.

[114] WEISMAN, J. *Two-phase Flow Patterns - Chapter 15 in Handbook of Fluids in Motion*, 1st edition ed. Ann Arbor Science Publisher, Michigan, USA, 1983.

[115] WEISMAN, J., AND KANG, S. Flow pattern transitions in vertical and upwardly inclined lines. *International Journal of Multiphase Flow 7*, 27 (1969), 271–291.

[116] YEUNG, H., CAO, Y., AND ADEDIGBA, G. The importance of downstream conditions on riser behaviour. In *5th North American Conference on Multiphase Technology* (Banff, Canada, June, 2006), 2006 Conference.

[117] ZHENG, G., BRILL, J., AND TAITEL, Y. Slug flow behavior in a hilly terrain pipeline. *Int. J. Multiphase Flow 20* (1994), 63–79.